GEOLOGICAL SURVEY OF CANADA

OPEN FILE 5644

A lithogeochemical assessment of the Lower Cretaceous sediments of the Scotian Basin

G. Pe-Piper, S. Triantafyllidis, D.J.W. Piper, B. Moulton, R.F.Hubley

2007

Natural Resources Canada Ressources naturelles Canada

Canada

GEOLOGICAL SURVEY OF CANADA

OPEN FILE 5644

A lithogeochemical assessment of the Lower Cretaceous sediments of the Scotian Basin

G. Pe-Piper, S. Triantafyllidis, D.J.W. Piper, B. Moulton, R.F.Hubley

2007

Available from
Geological Survey of Canada, Atlantic
1 Challenger Drive
Dartmouth, Nova Scotia B2Y 4A2

Pe-Piper, G., Triantafyllidis, S., Piper, D.J.W., Moulton, B., Hubley, R.F.
2007: A lithogeochemical assessment of the Lower Cretaceous sediments of the Scotian Basin. Geological Survey of Canada, Open File 5644,138 p.

Open files are products that have not gone through the GSC formal publication process.

Preface:

This Open File is one of a series on detrital and diagenetic mineralogy of the Lower Cretaceous rocks of the Scotian basin and their on-land equivalent, the Chaswood Formation, resulting from a collaborative program between Saint Mary's University and the Geological Survey of Canada. The work was funded principally by Petroleum Research-Atlantic Canada (PR-AC) and an NSERC Collaborative R&D project grant. The report presents lithogeochemical data from a series of wells representing an east-west transect of the Scotian Basin and provides a preliminary interpretation.

Acknowledgments:

We thank the staff of the Canada-Nova Scotia Offshore Petroleum Board for access to cores and cutting samples and Dr Philip Frahlick for manuscript review.

Authors' addresses:

Georgia Pe-Piper, Stavros Triantafyllidis, Ben Moulton, Robert F. Hubley
Department of Geology, Saint Mary's University, Halifax, Nova Scotia, B3H 3C3, Canada
gpiper@smu.ca

David J.W. Piper
Geological Survey of Canada (Atlantic), Bedford Institute of Oceanography, P.O. Box 1006, Dartmouth, Nova Scotia, B2Y 4A2, Canada
dpiper@nrcan.gc.ca

ESS Project ECOSEA Y-54

Abstract

Whole rock geochemical analyses have been made from conventional core samples of Lower Cretaceous sandstones and shales from the wells: Naskapi N-30, Alma K-85, Alma F-67, Glenelg N-49, Glenelg E-58, North Triumph B-52, Peskowesk A-99 and Dauntless D-35; and from picked cuttings samples from the wells: Sambro I-29, Dauntless D-35, Fox I-22, Crow F-52, and Argo F-38. Samples with abnormal abundances of P, Mg, Ca and Fe result from important amounts of carbonate or phosphate cement; after removing these samples, 79 reliable analyses were obtained.

Published geochemical discrimination diagrams for clastic sediments were evaluated. These diagrams aim to identify effects of source-area weathering, hydraulic sorting during transport, and the character of the source area rocks (and hence by inference, their tectonic setting). The chemical effects of source area weathering are difficult to interpret because they may be mirrored by the effects of burial diagenesis. However, there is petrographic evidence for rapid erosion and transport from the source area. Source area rocks were identified as predominantly of intermediate to felsic composition, characteristic of a continental island arc or passive margin. This is consistent with the petrographically identified source areas predominantly within the Appalachian orogen. Some discrimination diagrams suggest that the sources to the western Scotian basin were more mafic and those to the east more felsic, consistent with petrographic evidence for important K-feldspar supply to the east and predominant plagioclase supply to the west. Chemical discrimination diagrams did not provide unambiguous characterization of the predominant source rocks for different parts of the basin.

Nevertheless, there are significant changes in elemental abundances in different parts of the basin that are interpreted to represent supply from different source rocks. In the east, Peskowesk (and generally also Fox and Dauntless) sandstones are lower in Ti and have a high K/Rb ratio. Sandstones from the Glenelg and North Triumph fields have distinctively high Hf and Th/U ratios and low La/Sm ratios compared with wells both to the east and west. Mudrocks show an increase from west to east in Nb and Y and a decrease in Sr and Hf. There are systematic variations in Th content of mudrocks between the western (Naskapi and Alma), central (Glenelg and North Triumph) and eastern (Fox, Peskowesk and Dauntless) areas. Data are insufficient in most wells except Alma and Peskowesk to document stratigraphic variation in key elements.

Systematic variation in the chemical composition of sediment in the Scotian Basin is consistent with published petrographic evidence for supply from several different rivers. Regional variation in some elements such as Ti and K may have important consequences for diagenesis. More samples will be needed to evaluate hypotheses proposed in this report.

1. Introduction

The Lower Cretaceous rocks of the offshore Scotian Basin (Fig. 1) comprise fluvial, deltaic and shelf sediments of the Mississauga and Logan Canyon formations (Wade and MacLean, 1990) that host most of the gas and oil discoveries of the Scotian basin. The equivalent fluvial rocks on land are known as the Chaswood Formation (Stea and Pullan, 2001). The sandstone-rich Missisauga Formation is of Berriasian to Barremian age (Williams et al., 1990) and passes seaward into the shales of the Verrill Canyon Formation. The overlying Aptian to Cenomanian Logan Canyon Formation is also predominantly deltaic, comprising two shale units (Naskapi and Sable members), separated by two sandier units (Cree and Marmora members). Previous paleogeographic reconstructions (e.g. Jansa and Wade, 1975) have shown a major "Sable delta" on the east Scotian Shelf, supplied by a river flowing through Cabot Strait. The general deltaic character of the deposits has been confirmed by many subsequent studies (e.g. Drummond, 1992), but both seismic data (Cummings et al., 2006) and detrital petrology (Pe-Piper and MacKay, 2006; Pe-Piper et al. 2006a) suggest that the Lower Cretaceous was deposited by a series of small steep rivers draining reactivated upland areas of Atlantic Canada. The size and provenance of these rivers are significant issues for understanding the dispersal of sand and the sedimentological and diagenetic evolution of sandstone bodies in the Mississauga and Logan Canyon formations.

Whole rock geochemistry of sedimentary rocks has the potential to provide important information about both diagenesis and sediment provenance. Systematic variation in lithogeochemistry may influence early diagenetic processes: Gould et al. (2007) inferred a relationship between the abundance of detrital Ti and the development of early diagenetic berthierine in the Venture field. Later diagenesis may also be affected by lithogeochemistry: for example the development of illite on burial in some cases is influenced by the availability of K in the host rock (Chuhan et al., 2000, 2001). However, in the literature much of the use of lithogeochemistry has been in determining sediment provenance. This is an important issue in the Scotian Basin, where different fluvial inputs may result in different diagenetic histories in different parts of the basin.

One approach to interpreting lithogeochemical data is to use binary or ternary elemental plots from the literature that purport to distinguish between sediment sources or between processes such as sorting that detrital sediments undergo. Some of these geochemical discrimination diagrams may also be strongly influenced by diagenetic processes.

The purpose of this study is: (1) to present representative lithogeochemical data from the Lower Cretaceous of the Scotian Basin; (2) to document regional variability in lithogeochemistry

in the basin and (3) to explore the use of geochemical discrimination diagrams in understanding this variability and the provenance of Scotian Basin sediments.

2. Previous work

2.1 Sedimentological setting of the analysed samples

Lithofacies in this study have been interpreted using previous published criteria, notably the work of Drummond (1992) and reports by MacRae and Jauer (2001) and Reimer (2002), as further summarized by Piper et al. (2004). Most deltaic facies in the logged wells comprise well-sorted shoreface sandstone (lithofacies 2) and wave-dominated prodelta mudstone and siltstone (lithofacies 1), with local sideritic transgressive lags (lithofacies 3) (Table 1). In some wells, more proximal deltaic facies are also present. These proximal facies show strong tidal influence and include lithofacies interpreted by MacRae and Jauer (2001) as sandy tidal flats (lithofacies 5), muddy tidal flats (lithofacies 6), coastal swamps (lithofacies 7) and transgressive sequences in lagoons or interdistributary bays (lithofacies 8). Sediment was delivered through deep tidally-influenced fluvial channels (lithofacies 4), that in places contain coarse sandstone.

Sedimentological logs of the sampled wells are presented in previous publications and reports, namely Pe-Piper and Piper (2007) for Naskapi and Sambro; Piper et al. (2004) and Pe-Piper et al. (2004a) for Alma, Glenelg, North Triumph; Pe-Piper et al. (2006a) for Peskowesk; Shannon (2002) for Dauntless; and Weir-Murphy (2004) for wells of the Orpheus Graben. Stratigraphic picks are those of MacLean and Wade (1993) and have been derived from the BASIN database.

2.2 Detrital petrology

Previous work of the detrital petrology of the Chaswood Formation in Nova Scotia and New Brunswick has shown that these deposits had a local supply of lithic clasts from bedrock of the southern Appalachians (Pe-Piper et al. 2004a,c, 2005b; Gobeil et al. 2006; Piper et al. 2007), with some diagnostic minerals reworked from Carboniferous sedimentary rocks. This region developed a horst and graben topography in response to strike-slip motion along the Cobequid-Chedabucto fault zone and NE-trending splays (Pe-Piper and Piper, 2004). U-Pb monazite dating shows that source rocks to the Chaswood Formation were principally of Taconic age, likely from northern New Brunswick and three discrete rivers are recognised as having deposited the Chaswood Formation (Pe-Piper and MacKay, 2006). Ilmenite is the predominant detrital heavy mineral in the Chaswood Formation, but its chemical composition indicates it is

not derived from the Meguma terrane, but rather from the Avalon and more inboard terranes of the Appalachians (Pe-Piper et al., 2005a). Lithic clasts and dating of detrital muscovite suggest that Carboniferous sedimentary rocks were an important source of sediment to the Chaswood Formation (Pe-Piper et al., 2004c; Gobeil et al. 2006).

The Lower Cretaceous sandstones of the southwestern Sable sub-basin in the Alma, Glenelg and North Triumph fields include marker minerals such as chromite and paragonite not known from the Chaswood Formation, together with Proterozoic detrital monazite. These data point to a source farther east than the most easterly Chaswood Formation (Diogenes Brook in Cape Breton Island) (Fig. 1), likely from uplifted Grenville basement and ophiolites of western Newfoundland. This sediment might have been transported either by an ancestral St Lawrence river, with tributaries draining western Newfoundland, or from a smaller river draining only western Newfoundland.

Sandstones from the Peskowesk A-99 well (Pe-Piper et al. 2006a) are quite different from those of the southwestern Sable sub-basin (Pe-Piper et al. 2004b). This is seen most clearly in feldspar compositions, with subequal abundances of K-feldspar and plagioclase in the southwestern Sable sub-basin, but dominance of K-feldspar (perthite) at Peskowesk. The predominant rhyolite - syenite - microgranite lithic clasts at Peskowesk are absent in the southwestern Sable sub-basin, where the most prominent lithic clasts are foliated (metamorphic) rock fragments, present in sandstones in the Missisauga Formation. Spessartine garnet is common in the southwestern Sable sub-basin, but was not detected at Peskowesk. Tourmaline is much less common at Peskowesk and the single analysed grain was derived from granite, compared with a metasedimentary source for tourmaline in the southwestern Sable sub-basin. Rutile from the southwest Sable sub-basin includes about 10% with high Mn content, which appears absent from Peskowesk. Ilmenite is more abundant at Peskowesk than in the southwest Sable sub-basin. The abundance of both biotite and muscovite is greater at Peskowesk than in the southwest Sable sub-basin, where modal abundance of muscovite is < 2% and of biotite <0.2 %, even though most sandstones analysed there are finer grained than at Peskowesk.

The river supplying sediment to Peskowesk thus appears to have been quite distinct from that which provided sediment to the southwestern Sable sub-basin. It must have lain to the southeast of the river draining western Newfoundland that supplied sediment to the southwestern Sable sub-basin. Furthermore, these distinct rivers with distinct sediment supply to the southwestern and northeastern Sable sub-basin persisted from the Mic Mac Formation at least to the Cree Member of the Logan Canyon Formation. The variations in sediment supplied to Peskowesk through time are much less than the variations between Peskowesk and the wells of the southwest Sable sub-basin.

Less comprehensive data from Dauntless D-35 in the east suggests that it received rather different sediment than did Peskowesk A-99. Likewise, Naskapi N-30 and Sambro I-29 in the west have a very different detrital petrography and may have been sourced from one of the Chaswood Formation rivers.

A preliminary scoping study of the geochemistry of shales from the Scotian basin showed that they are unusually rich in TiO_2 compared with average shales world-wide (Pe-Piper et al., 2005a), likely as a result of the break-down products of detrital ilmenite. Such silt-sized material is an important source of labile Fe for the formation of early chlorite rims that preserve porosity in the Sable sub-basin (Gould et al., 2007).

3. Materials and methods

3.1 Sample selection

Eight wells containing conventional core were sampled to cover the geographic range of the basin, from west to east (Fig. 1). In addition, a few cuttings samples were examined from four additional more proximal wells. The stratigraphic position of samples was dependant on the position of conventional cores: most samples are from the Missisauga Formation, with some from Logan Canyon Formation and rare samples from the MicMac Formation (Fig. 2).

The samples analysed are summarised in Table 1. Samples from conventional core include sandstones, shales, and mudstones with siltstone laminae. The necessary large samples for analysis were commonly obtained from intervals of rubbly core recovery, so as to minimise sampling in high-quality core.

3.2 Preparation of samples

Conventional cores were logged and samples were collected from the Logan Canyon, Missisauga and in one case from the Mic-Mac formations fron the wells: Naskapi N-30, Alma K-85, Alma F-67, Glenelg N-49, Glenelg E-58, North Triumph B-52, Peskowesk A-99 and Dauntless D-35. These cores are stored at the Canada-Nova Scotia Offshore Petroleum Board (CNSOPB) Core Lab. Samples were taken from shale/mudstone and sand(stone) intervals. These samples were cut from the outside of conventional cores and lightly brushed and washed to remove any drilling mud. Small pieces were broken off from the shale samples to be used for scanning electron microscopy and a very thin slab from the sandstone samples for polished thin sections. Whatever was left was used for whole rock geochemistry. Only a few samples from each well had enough material left for whole rock analyses, especially from the sandstones.

Representative sub-samples of archived cutting samples from the CNSOPB Core Lab were taken from the Logan Canyon and Missisauga formations of the wells: Sambro I-29, Dauntless D-35, Fox I-22, Crow F-52, and Argo F-38. These cutting samples were washed with warm tap water through a 63 μm sieve to remove any unwanted material (mud and oil from the drilling). Samples that were either too old or included excess debris had to be soaked in soapy water for a short period of time to facilitate the washing procedure. Samples were then sieved at 2 mm, allowing the separation of the grains into two classes: >63 μm to <2 μm and >2 mm.

Cuttings larger than 2 mm were identified using a binocular microscope and were separated based on lithology/mineralogy, grain size, colour or apparent cement. Each group of cuttings was placed into separate vials and labelled with the corresponding well, depth and lithology. Representative unidentified cuttings were used to make polished thin section mounts and analysed under a polarized reflected light petrographic microscope and an electron microprobe. Representative lithologies that had enough cuttings for whole rock analysis were further processed for lithogeochemical analysis.

3.3 Analytical procedures

Depending on the size of sample available the samples were either crushed by hand using an agate pestle and mortar (for small samples) or were crushed using a shatterbox with an iron bowl (for larger samples).

Major and trace elements were determined by Activation Laboratories according to their Code 4Lithoresearch and Code 4B1 packages, which combine lithium metaborate/tetraborate fusion ICP rock analyses with a trace element ICP-MS package.

4. Results and preliminary data analysis

4.1 Analytical results

Analytical results are provided in Table 2. A preliminary check that lithologies were correctly identified was made by plotting Al_2O3 vs. SiO_2 (Fig. 3), which allowed distinction of sorted sandstones and siltstones with > 75% SiO_2 and mudrocks with < 75% SiO_2.

4.2 Chemical Index of Alteration - CIA

The degree of alteration of feldspars to clays indicates both the degree of weathering of the source rocks and that of the diagenesis that the sediments suffered since deposition. Quantitatively, using the molecular proportions of $Al_2O_3 - CaO^* + Na_2O - K_2O$, a chemical

index of alteration (CIA)

$$CIA = \{Al_2O_3/(Al_2O_3+CaO^*+Na_2O+K_2O)\}x100$$

was developed by Nesbitt and Young (1982) to numerically express the degree of alteration (where CaO* is the amount of CaO incorporated in the silicate fraction of the rock). The CIA values of average shales range from 70 to 75 (Taylor and McLennan, 1985).

The sample set chosen to be plotted for initial geochemical diagrams was based on their values of the calculated chemical index of alteration (CIA), with no correction of CaO for the amount present in cement. The following samples with CIA values >82 or <25 have been omitted:

North Triumph B-52	3784.17	6.05
Peskowesk A-99	2940.48	5.37
Peskowesk A-99	3806.51	[very low]
Peskowesk A-99	3812.64	[very low]
Glenelg N-49	3628.43A	87.43
Alma F-67	2884.3	7.83
Argo F-38	579	[very low]
Crow F-52	600	[very low]

Samples with low CIA values likely have diagenetic changes leading to enrichment in Ca in cement. Samples with very high CIA values may have lost alkalis during diagenetic processes. Samples from Fox I-22 and Argo F-38 have exceptionally low values of CIA between 6 and 50 and all are therefore suspect.

4.3 Further evaluation of the role of cements

Plots were made of of Al_2O_3, P_2O_5, FeO_t, MgO and CaO vs. SiO_2. Most samples fall on a regular linear trend, but outlier samples with particularly high P_2O_5, FeO_t, MgO or CaO (Fig. 4) appear to correspond to samples with francolite, siderite, dolomite, ankerite or calcite cements. No chemical method was found to identify samples with abundant silica cement, nor to correct for the effect of such cement.

4.4 Data sets used in this study

Arising from this analysis of diagenetic changes in the sample, four data sets are used in this study:

1. The "raw" data set that includes all 103 analysed samples.
2. The "lightly screened" data set that has only the eight samples listed above with extreme CIA values removed.

3. The "normal" data set that includes all samples that fall on the general trend of samples when plotted on diagrams of Al_2O_3, P_2O_5, FeO_t, MgO and CaO vs. SiO_2. This totals 79 samples.
4. The "abnormal" data set that consists of the 16 samples not in the "normal" data set. The major elements in this data set have been recalculated on the assumption that P_2O_5, FeO_t, MgO and CaO values are similar to those of samples of similar SiO_2 content (Appendix 1).

5. Geochemical discrimination diagrams for provenance

5.1 Introduction

An evaluation of the use of standard geochemical discrimination diagrams for provenance was made using the "lightly screened" data set. First, the effectiveness of the method was evaluated using data from the Alma field. The technique was then extended to Glenelg and North Triumph fields and the Sambro I-29, Naskapi N-30, Peskowesk A-99, Dauntless D-35, Fox I-22 and Argo F-38 wells.

Among the geochemical discrimination diagrams used, some discriminate between different lithologies in the source area, whereas others identify the "tectonic setting" of the source area. Within the Appalachians of the Atlantic Provinces, the Avalon terrane would supply sediment with an active continental margin or island arc signature, because of the predominance of Neoproterozoic volcanic and plutonic rocks and immature sedimentary rocks that accumulated in a continental island arc setting. Within the Dunnage zone, island arc and oceanic crust igneous rocks are present, but both in the Humber and Gander zones, granitoid rocks predominate.

5.2 A case study: data from the Alma field

5.2.1 Evaluation of alteration and sorting

The Alma K-85 well has 28 geochemical analyses. These analyses include two mudstones and five shales from the Logan Canyon Formation as well as nine mudstones and twelve shales from the Missisauga Formation. The Alma F-67 well has 6 whole-rock chemical analyses, which include 4 shales and 2 sandstones from the Missisauga Formation. Determining the degree of weathering of the source rocks and the diagenesis of these samples is important since this is a geochemical study, and thus we will be using the chemistry of these sedimentary rocks as provenance and tectonic setting indicators. If the source rocks have been overly affected by weathering and the analysed rocks by diagenesis then the chemistry of the analysed shales and sandstone will not be a reliable account of provenance and tectonic setting and other methods will have to be used to determine their geological history. Distinguishing effects of

weathering of source rocks from effects of diagenesis is in general not possible simply from consideration of the geochemical analyses. However, we might expect diagenetic change to be more extensive in permeable sandstones that are variable cemented compared with mudrocks that show similar degrees of compaction and fluid expulsion.

The Logan Canyon Formation mudrocks (mudstones and shales) have CIA values that range from 71 to 74, while those for the Missisauga Formation mudrocks range from 71 to 80. This suggests that either the source rocks for the Missisauga mudrocks were slightly more altered than the Logan Canyon Formation ones or that the more deeply buried Missisauga mudrocks experienced a little more diagenetic loss of alkalis to formation waters. However, the CIA values for both sets of mudrocks suggest that the effects of weathering had not proceeded to the stage where alkali and alkaline earth elements are substantially removed from the clay minerals (Taylor and McLennan, 1985).

When the molecular proportions of Al_2O_3, Na_2O+CaO and K_2O are plotted on a ternary diagram (Fig. 5), all the analysed samples from these wells plot approximately halfway between the typical shale value field and the illite field. The Logan Canyon Formation samples plot closer to the typical shale, which is what we see from the CIA values as well, whereas the mudrocks from the Missisauga Formation plot closer to the illite field. This is a typical weathering trend of shales from plagioclase towards illite.

However since the samples do not actually reach the field of the illite it suggests low to moderate alteration of source rocks, thus indicating that the alteration of these rocks was essentially the conversion of plagioclase to clays. A plot of CIA value versus depth (Fig. 6) shows no systematic variation within the Missisauga Formation. One outlying sample (2912.04) with lower CIA has unusually high Na_2O (2.9 % compared with a normal value of ~ 1.0 %) and Nb, and slightly elevated Sr and LREE, with unusually low K_2O and Rb: it is discussed further in section 7.1 below.

With increasing alteration, the Th/U ratios of the sedimentary rocks are expected to increase due to the oxidation and loss of uranium (Taylor & McLennan 1985; Gu et al. 2000). Typical upper crust values for unaltered rocks are about 3.8. The analysed samples (Fig. 7) do not show a clear alteration trend in this figure, but they do have slightly elevated Th/U ratios compared with average upper crust. Whether this is an effect of alteration, or whether it is a consequence of source is uncertain. For example, Devonian - Carboniferous plutonic rocks of the Cobequid Highlands, which are an important source to the Chaswood Formation of central Nova Scotia, generally have Th/U in the range of 4 – 7. Nevertheless, Figure 7 is consistent with the CIA values (Fig. 5) in showing a lack of major alteration of detritus from the source area.

Sorting is another issue of concern, particularly in sandstones and mudstones with silt

laminae, as it preferentially concentrates minerals within beds and this may cause significant change in the geochemistry of the sedimentary rocks. This is prominent in trace and rare earth elements that are largely concentrated in such minerals as zircon, apatite, allanite and titanite, which are also minerals that withstand transport and weathering. If these heavy minerals are being preferentially accumulated in the sediments, then the chemistry of the rocks will not reflect the provenance and/or tectonic setting of source rocks. Figure 8 shows three plots that evaluate sorting. Tb/Yb versus Hf (Fig. 8b) shows a general trend that might result from titanite or zircon accumulation, however no such trend is apparent in either of the other two plots. All these plots together indicate that there has been no significant sorting of zircon, titanite, and allanite. The ternary plot Al_2O_3–TiO2–Hf of La Flèche and Camiré, 1996 (Fig. 9) also suggests that there is not an abnormally large amount of zircon or titanite in the samples, that would be represented by a trend towards the Hf apex of the diagram. The same figure also indicates that there is little mobility of the incompatible elements Al and Ti, since there is no trend towards either of these apices. Al and Ti are preferentially present in the clay particles within mudrocks. This plot is consistent with previous results.

In summary the CIA values are typical of shales and the ternary plot of these values along with their down well variation indicate that the source rocks and these rocks themselves have not been subjected to major weathering or diagenetic changes. Furthermore, there is little heavy mineral sorting of apatite, titanite, allanite or zircon, which could have a major effect on the trace and rare earth elements. These combined results indicate that the geochemistry of the mudrocks from the Alma field was largely unaffected by alteration and sorting during the sediment transport and thus the geochemistry of the analysed rocks may be used to obtain reliable provenance and tectonic setting results.

5.2.2 Evaluation of dominant lithology in source area

Provenance is the key factor in determining and reconstructing the paleogeography of a region. The provenance may be interpretable as from a specific source and it may thus constrain sediment transport pathways. In southeastern Canada, the terranes of the Appalachians broadly parallel the northern margin of the Scotian Basin, making recognition of specific sources more difficult.

The TiO_2 to Ni concentrations of sediments have been used by Floyd et al. (1989) to determine the source rock of a sedimentary rock suite. Using the fields of Floyd et al. (1989) it seems that the mudrocks from both wells have been derived from a basic magmatic source rock, indicated by high Ti and Ni contents (Fig. 10A). One sample (2912.04) that plotted abnormally on the CIA plot (Fig.6) also plots abnormally in this diagram. The one Alma F-67 sandstone

plots in the felsic source field (Fig. 10A).

Floyd and Leveridge (1987) used K_2O and Rb contents as an indicator of source rock for sandstones. The low Rb and K_2O of the one Alma F-67 sandstone (Fig. 10B) suggests derivation from a mafic source, contradicting Figure 10A. The mudrock samples plotted on the same diagram show a tight cluster for the Logan Canyon formation samples and a linear trend of increasing Rb within the Missisauga Formation samples.

Floyd and Leveridge (1987) have also used the trace element ratio of La/Th versus Hf in sandstones to determine the lithology of the source rocks and amount of incorporation of older sediments. Using such a plot (Fig. 11A) the one Alma F-67 sandstone may have a mixed felsic/mafic source. Mudrocks plotted on the same diagram show that the Missisauga Formation mudrocks have a higher Hf content.

Figure 11B plots Co/Th ratios versus La/Sc, which shows that both the Logan Canyon and Missisauga Formation mudrocks from both wells plot just on the mafic side of the Co/Th ratio of 1.27 used to separate felsic from intermediate sources. It suggests a mixed felsic and intermediate to mafic source ragion. There is very little scatter in any of the data except again sample 2912.04. The chemistry of the one Alma F-67 sandstone suggests a felsic source.

In conclusion, the inconsistencies in interpretations of sources from the discrimination diagrams suggests that they are not very robust, and that further evaluation of source may be needed. Most discrimination diagrams suggest that the studied rocks were derived from a felsic to intermediate source. Figure 10A contradicts the other plots, but the interpretation of a mafic source is based entirely on the unusually high TiO_2 content of the mudrocks. Ilmenite is an important minor component of many felsic igneous rocks, so that high amounts of detrital ilmenite with high TiO_2 could be derived from a felsic source.

5.2.3 Evaluation of "tectonic setting" of source area

One of the principal applications of sedimentary geochemistry of clastic rocks has been to understanding the tectonic setting of source areas in complex orogens. Several criteria have been proposed to distinguish sediments derived from passive margins, active continental margins and oceanic island arcs. The Scotian Basin forms part of a passive margin. Nevertheless, the identification of "tectonic setting" of the sources may be of value in localising a source. For example, crystalline rocks of the Avalon terrane formed in an active continental margin, so that this signature may be preserved in sediments derived from the Avalon terrane.

Roser and Korsch (1986), using the ratio of K_2O to Na_2O plotted versus SiO_2, have distinguished three tectonic settings: passive margin, active continental margin and oceanic island arc. All the analysed samples, except two noted previously as having unusual chemistry

(discussed below in section 7.1), tightly plot principally within the active continental margin field on this diagram (Fig. 12A). The one Alma F-67 sandstone plots within the passive margin field. In a similar plot of K_2O/Na_2O vs. SiO_2/Al_2O_3 (Fig. 12B), Roser and Korsch discriminated four tectonic settings: passive margin (PM), active continental margin (ACM), and two arc settings, one with basaltic or andesitic detritus (A1), one with felsic volcanic detritus (A2). All the normal Alma K-85 mudrocks plot in a cluster within the ACM and A2 fields. The one Alma F-67 sandstone again plots in the passive continental margin field.

Ti/Zr ratios plotted versus La/Sc ratios, after Bhatia and Cook (1986), have also been used to determine tectonic setting of sandstones, while also evaluating the degree of sorting of the sediment (Fig. 13). There are four fields in this diagram: oceanic island arc (IA), continental island arc (CIA), active continental margin (ACM) and passive margin (PM). The Alma F-67 sandstone plots in the active continental margin field.

Plots proposed by Totten et al. (2000) use variation in the trace elements Th, Sc and La (Fig. 14). On a Th vs. Sc plot, the Alma mudrocks cluster between the field of "continental signature" and the field of "mafic signature", suggesting an intermediate or mixed felsic-mafic source. The mudrocks have Th/Sc similar to the North American Shale Composite, but slightly higher La/Sc suggesting a source from intermediate rocks.

The Hf–Th–Co plot (Fig. 15) shows that the Alma mudstones have relative abundances of these trace elements similar to upper continental crust composition, with elevated Co suggesting some component from a mafic source.

Bhatia and Cook (1986) used ternary discriminant diagrams for sandstones involving La, Th, Sc and Zr (Fig. 16). On all these plots, the one sandstone plots between the "passive margin" and "continental island arc" fields.

In conclusion, tectonic discrimination diagrams suggest that the geochemical character of the sediments of the Alma field have many characteristics of sediment formed at an active continental margin. The applicability of the Roser and Korsch (1986) major element discrimination diagrams is questioned, because adjacent mudrocks and sandstones fall in different fields.

5.2.4 Direct comparison with possible Avalonian source rocks

In contrast to the widely used techniques of discrimination diagrams based on modern sediments of known provenance, in a study of the provenance of the Carboniferous Horton Group in central Nova Scotia, Murphy (2000) successfully made direct comparison with the bulk composition of potential source rocks in the Meguma and Avalon terranes. This approach was likely successful because first cycle immature sediments predominate in the Horton Group. We

use a similar approach to compare mudrocks of the Alma field with the Meguma and Avalon terrane source rocks used by Murphy (2000), namely the Meguma Supergroup metasedimentary rocks, the Meguma terrane granitoid plutons, the Neoproterozoic active continental margin rocks of the Georgeville Group of the Avalon terrane and the Lower Paleozoic Beechill Cove Formation volcanic rocks also of the Avalon terrane. We also make a comparison with the Horton Group from the St. Mary's basin.

Plots of Al_2O_3 and Fe_2O_3 versus SiO_2 show that the Alma mudrocks have a high Al_2O_3 content compared with Horton Group siltstone samples (Fig. 17A) and most of them follow a similar trend to the Georgeville Group volcaniclastic sequence, with a negative correlation between Fe_2O_{3t} and SiO_2 (Fig. 17B). Figures 17C and D suggest that the mudrocks might contain some detrital kaolinite (and/or gibbsite) although the main weathering product is illite. Such a pattern could also be the result of diagenesis. Overall, in the analysed samples from both formations there is little variation in the degree of weathering/diagenesis. The trend of Alma mudrocks indicates a more mafic initial composition trending towards the hornblende composition compared to St. Mary's basin samples. Both the molar proportions of Al_2O_3 vs. CaO + Na_2O vs K_2O and the Al_2O_3 vs. CaO+Na_2O+K_2O vs Fe_2O_{3t} + MgO consistently indicate that the Alma mudrocks show different alteration/diagenesis from the St. Mary's basin samples of Murphy (2000). The St. Mary's basin samples appear to have a higher illite content, consistent with the known differences in clay mineralogy between the Lower Cretaceous offshore and Paleozoic shales of Nova Scotia.

Incompatible elements are often used because they are least affected by alteration and often they are fractionated into specific minerals. In Figures 18 and 19, TiO_2, Zr, P_2O_5, Nb, V, and Rb are plotted. Some of these elements are also most affected by heavy mineral accumulation, that may take place in the silt size fraction of mudrocks. There is a slight positive trend in Zr (Fig. 18B), a slight negative trend in Nb (Fig. 18D), and the concentrations of Ti are higher than in any of the potential source rocks plotted (Fig. 18A). The P_2O_5 concentrations for a small number of the analysed mudrocks are scattered, but the majority of samples are clustered. Of the four HFSE plots, only Zr and P_2O_5 show overlap with the Meguma Supergroup fields. In both of these cases the mudrocks from Alma do not follow the general trend of these fields and therefore it is unlikely that they are related. The Alma mudrocks are enriched in TiO_2 and Nb compared to the Meguma Supergroup fields.

Figure 19A shows that the Logan Canyon Formation mudrocks (Alma K-85) and the Missisauga shales from Alma F-67 have a K/Rb ratio of ~221 close to that of average upper crustal rocks (K/Rb ~250, Taylor and McLennan, 1985), whereas the Missisauga Formation mudrocks of Alma K-85 have a much lower value at ~185. Neither of these trends follow the

general trend from either of the two Meguma Supergroup rock fields that they overlap and they are completely different from the fields of all other comparison groups. Some samples have a higher Rb/K_2O ratio than any of the Meguma Supergroup rocks. In Figure 19B the samples show high amounts of V and Ti plotting outside the fields of Meguma Supergroup and all other comparison groups.

Figure 20A shows that the mudstone samples fall in the active continental margin field of Roser and Korch (1986) and the sandstone sample is in the passive margin field. This is consistent with the previous discrimination diagrams. There is a relatively constant ratio of alkalis to SiO_2 (Fig. 20A). Figs. 20B and 20C show that the Alma K-85 well mudrocks have higher ratios of Al_2O_3/SiO_2 and $Al_2O_3/(CaO+Na_2O)$ relative to the Meguma Supergroup samples. The offshore samples plot well outside the tectonic setting discrimination fields and suggest, as with Murphy (2000), that for some basins, standard geochemical discrimination diagrams are problematic. The geochemical signature for these sedimentary rocks is the result of more complicated processes than simply represented by their source rocks.

Figure 21 (after Garcia et al., 1994) shows the fields for the St. Mary's basin Horton Group relative to the Alma mudrocks. These samples show very little variation and plot almost in the center with no trend toward any apex. This again confirms that the minerals such as titanomagnetite and zircon had little effect on these samples.

In conclusion, the mudrock samples from the Alma field almost never plot in similar fields when compared with Meguma Supergroup metasedimentary rocks or the St. Mary's basin Horton Group samples, suggesting that neither of these rock groups is an important source for the Alma mudrocks. The same plots suggest that sorting of heavy minerals zircon, apatite, titanomagnetite, titanite and allanite in the mudrocks did not affect their geochemistry. This is in agreement with the previous results.

5.3 Application of geochemical discrimination diagrams to other wells

5.3.1 Introduction

The geochemical discrimination diagrams used for the samples from the Alma field have also been applied to the Glenelg and North Triumph fields (Appendix 2), Sambro I-29, Naskapi N-30, Fox I-22 and Argo F-38 wells (Appendix 3) and the Peskowesk A-99 and Dauntless D-35 wells (Appendix 4). Differences between the various wells and between different stratigraphic units are summarized in Table 3.

5.3.2 Evaluation of alteration and sorting

No significant differences are revealed between shales from different wells plotted on a ternary plot of molecular proportions of Al_2O_3, Na_2O+CaO and K_2O (Fig.5; Fig. 1 in each of

Appendices 2, 3 and 4). There are differences in the Th/U ratios of sandstones from different wells (Fig. 7; Fig. 2 in each of Appendices 2, 3 and 4): Naskapi, Alma, Fox, Peskowesk and Dauntless have Th/U typically of 3–4, whereas at Glenelg and North Triumph Th/U is typically 4–5. There is less data for the shales, but those from Sambro and Peskowesk have higher Th/U than at Alma and Glenelg. Shales from Naskapi and Alma have Th < 15 ppm; from Glenelg and North Triumph 10–15 ppm; and at Fox, Peskowesk and Dauntless > 12. Figures 8 and 9, which are used to evaluate sorting, show systematic variability in some element ratios, but not in others (cf. Figs. 3 and 4 in each of Appendices 2, 3 and 4). In particular, the La/Sm ratio is 6–7 at Alma and Naskapi; 4–6 at Glenelg and North Triumph; 5–7 at Fox; and 6–8 at Peskowesk and Dauntless. The lack of clear evidence for sorting in these figures may suggest that these variations are related to source. The issue of variation of these elements with grain size and facies is discussed in section 6.5.

5.3.3 Evaluation of dominant lithology in source area

The plot of TiO_2 to Ni concentrations (Fig. 10A; Fig. 5A in each of Appendices 2, 3 and 4) shows a wider range of Ni concentrations in shales from Peskowesk than elsewhere, but otherwise no systematic variability. The plot of K_2O and Rb (Fig. 10B; Fig. 5B in each of Appendices 2, 3 and 4) clearly shows elevated K_2O to Rb ratio for sandstones from Peskowesk, Dauntless and Fox compared with the western Scotian Basin, but no significant differences in shales. Sandstones at Fox, Peskowesk and Dauntless have elevated K_2O to Rb ratio, consistent with the abundance of detrital K-feldspar and alkali rhyolite at Peskowesk (Pe-Piper et al. 2006a), and imply "acid/intermediate" source compositions. In contrast, sandstones from Naskapi, Glenelg and North Triumph have a lower K_2O to Rb ratio and fall in the "basic" source composition.

The elemental ratios in Figure 11 (Fig. 6 in each of Appendices 2, 3 and 4) show no systematic differences between wells, except that Hf tends to be elevated in Glenelg and North Triumph sandstones.

The observations confirm the conclusion from the Alma well that these various discrimination diagrams for dominant lithology are not robust when applied to an area in which source rock variations are likely to be quite subtle.

5.3.4 Evaluation of "tectonic setting" of source area

Major element plots such as K_2O to Na_2O plotted versus SiO_2 (Fig. 12A; Fig. 8A in each of Appendices 2, 3 and 4) and the ratios of SiO_2/Al_2O_3 and K_2O/Na_2O (Fig. 12B; Fig. 8B in each of Appendices 2, 3 and 4) show no systematic variation except that mudrocks plot in active continental margin fields and sandstones in passive margin fields.

Ti/Zr versus La/Sc (Fig. 13; Fig. 9 in each of Appendices 2, 3 and 4) generally shows sandstones plotting in the continental island arc or passive margin field. Shales from Peskowesk have a particularly high Ti/Zr ratio.

Variation in the trace elements Th, Sc and La (Fig. 14; Fig. 10 in each of Appendices 2, 3 and 4) do not show systematic differences between different wells, but do show strong differences between mudrocks and sandstones. The Hf–Th–Co ternary plot (Fig. 15; Fig. 11 in each of Appendices 2, 3 and 4) shows some variation in Hf between wells, particularly the low Hf in Peskowesk mudrocks and high Hf in Glenelg sandstones. Ternary discriminant diagrams involving La, Th, Sc and Zr (Fig. 16; Fig. 12 in each of Appendices 2, 3 and 4) do not show systematic differences between different wells.

In summary, the "tectonic setting" discrimination diagrams generally show different chemical compositions for sandstones and mudrocks and are poor discriminators of observable differences between different wells.

5.3.5 Direct comparison with possible Avalonian source rocks

Various geochemical plots making direct comparison of mudrocks with possible Avalonian source rocks (Figs. 13–17 in each of Appendices 2, 3 and 4) in general show patterns similar to those for Alma mudrocks described above (Figs. 17-21). Mudrocks from Peskowesk have particularly high Fe_2O_{3t} (Fig. 13B, Appendix 4) and TiO_2 (Fig. 17, Appendix 4).

Sandstones tend to plot in a similar field to Horton Group sandstones in Figures 13 and 16 in each of Appendices 2, 3 and 4, except that Glenelg sandstones have a low K_2O to Na_2O ratio (Fig. 16A, Appendix 2). They also plot in a similar field to Horton Group sandstones in Figure 14, except that Sambro, Naskapi, Glenelg and North Triumph tend to have high Zr and Ti. In the same wells, the high Ti means that sandstones fall outside the field for Horton Group sandstones on a V vs. Ti plot (Fig. 15B in each of Appendices 2, 3 and 4) and as noted previously the K to Rb ratio is particularly high in Peskowesk and Dauntless sandstones (Fig. 15A in Appendix 4). In Figure 17 in each of Appendices 2, 3 and 4, Scotian Basin sandstones resemble fine-grained Horton Group sandstones, but with the previously noted variability in Ti and Zr resulting in geographic variability.

6. Variability in elements and element ratios

6.1. Introduction

Given the variability observed in the standard discrimination diagrams, we explored the

use of single elements or element ratios as indicators of variability in lithogeochemistry in different parts of the Scotian basin.

6.2. Correlation matrix

Examination of a correlation matrix of the "normal" data set, broken down into sandstones (Table 4) and mudrocks (Table 5) provides further insight into the reliability of discrimination diagrams. In these tables, highlighted cells have a correlation coefficient greater than ±0.7.

In the mudrocks, Al_2O_3 correlates positively (>0.7) with Ga, Rb, Cs and V, and there is also good correlation between K_2O and Ga and Sc (0.71, 0.70). This might be the result of a common mineralogical origin through K-feldspar or illite, although the correlation with V and Sc is not accounted for by these minerals. Al_2O_3 does not have a strong correlation with TiO_2, which may negate the concept of LaFlèche and Camiré (1996) that high TiO_2 is due to adsorption on clays from a mafic source. Rather, as suggested by Pe-Piper et al. (2005a), Ti is likely supplied to mudrocks as the silt-sized breakdown products of altered ilmenite. Likewise, Ni correlates positively (>0.7) with Co, but has a poorer correlation with Cr (0.36) and Sc (0.42), also indicators of a mafic source. The lack of correlation between REE and Al_2O_3 suggests that REE are not significantly incorporated in clay minerals. There is good correlation between Gd, Dy and Y (0.73). Zr correlates well (0.88) with Hf, indicating the presence of detrital zircon in the mudrocks.

Many of the elemental correlations in sandstones can be related to minor component minerals with high concentrations of particular elements. The good correlation between V and Fe_2O_3 (0.81), TiO_2 (0.79) and Nb (0.70) is likely due to the presence of ilmenite (containing Ti, Fe, Mn and V) and/or rutile (containing Ti, Ta and Nb). Correlation of Hf and Zr (0.99) is the result of the presence of zircon.

There is good correlation between TiO_2, REE, Sc, Ta, Th, U, V and Y, and good correlation between Cr and Zr. All these elements are incorporated in detrital heavy minerals, yet there is no single mineral with high contents of, for example, Ti and REE or Cr and Zr. This suggests that the amount of sorting of heavy minerals in sandstones may play a key role in such elemental correlations. For example, both zircon and chromite are common heavy minerals in the Glenelg and North Triumph sandstones (Pe-Piper et al. 2004b). If concentrated together, either by hydraulic sorting, or reworking of older sandstones containing both minerals, the observed good correlation between Cr and Zr would be produced. Likewise, good correlation between Zr and Y (0.78), Zr and HREE, and Hf and Y is likely the result of co-occurrence of detrital zircon (Zr, Hf, HREE), xenotime (Y, HREE) and monazite (Th, Y, HREE). Scandium correlates with Y

(0.75) and P_2O_5 (0.6) suggesting that the minerals thortveitite and kolbeckite might be present.

The correlation between Eu and P_2O_5 (0.7) is better than the correlation of either the LREE (~ 0.5) or the HREE (~ 0.4). Fractionation of La/Sm and Eu/Gd shows no systematic variation with P_2O_5, whereas Sm/Eu shows a correlation with P_2O_5 (Fig. 22). When the western and eastern wells are considered separately, Sr also shows a correlation with P_2O_5 (Fig. 22). These observations suggest that the variation in Eu and Sr with P_2O_5 might be in some way related to diagenesis of plagioclase.

The good positive correlation between Ga and Al_2O_3 (0.78) and Rb (0.74), as well as between Sr and Ba (0.74), indicates a common mineralogical origin in K-feldspar or possibly illite (Rb, Sr and Ba substitute for K and Ga for Al in the mineral lattice).

6.3 Rare-Earth element patterns

Rare-earth element patterns for mudrocks (Fig. 23) show strong fractionation from La to Eu and then a flatter pattern for the MREE and particularly for the HREE. Sandstones show rather similar patterns, but the LREE are less strongly fractionated than in the mudrocks. The western wells show a much stronger negative Eu anomaly than the eastern wells.

Neither mudrocks nor sandstones show much similarity to Meguma Supergroup metasedimentary rocks and the Meguma granitoid plutons described by Murphy (2000). In particular, the Meguma metasedimentary rocks tend to have a positive Eu anomaly.

6.4 Variation in elements from west to east

Some systematic differences have been noted above between wells in the western part of the Scotian basin and those in the east. For example, there are subtle differences in the REE patterns including the magnitude of the Eu anomaly (Fig. 23).

Some of the elements identified in the earlier part of this report as being relatively stable and of value as provenance indicators have been plotted against longitude, in order to look for systematic geographic differences between wells. For example, Nb contents of most mudrocks are between 30 and 40 ppm (Fig. 24A). However, in the west, Sambro has only 13 ppm and some mudrocks from Alma have 20-30 ppm. One Missisauga Formation mudrock from Alma K-85 has exceptionally high Nb content. The Sr content of mudrocks (Fig. 24B) tend to be higher in the west than in the east. The Cr content of mudrocks is slightly higher at Alma and Glenelg than at Peskowesk (Fig. 25).

In sandstones, the Th/U ratio and La/Sm ratio (Fig. 25) show systematic geographic variation. Th/U ratio is highest in the Glenelg and North Triumph fields and generally lower both to the east and to the west. Likewise, La/Sm tends to be lowest in the Glenelg and North

Triumph fields and also in the Fox well, and higher both to the east and west. Some very values of Cr are found at Glenelg and North Triumph and these same wells have the highest abundances of Sc in sandstones (Fig. 25), suggesting that Sc is present in heavy minerals.

6.5 Variation in elements with grain size and facies

For sandstones, the variation of elements with mean grain size of framework grains has been investigated (Fig. 26). Some elements, notably Al_2O_3, Ni, Sc, and Rb appear to have no systematic variation with grain size. Elements concentrated in feldspars, notably Sr and K_2O, tend to be more abundant in coarser-grained sandstone. Elements likely to be concentrated in heavy minerals, such as Zr and TiO_2, are concentrated in the finer-grained sandstones. So too are Cr and V, suggesting that their variation is principally dependant on heavy minerals.

The relationship of sandstone geochemistry to depositional facies has also been investigated. However, with the small sample size no systematic variation with facies was detected that could not be accounted for by geographic variation in detrital supply. In particular, none of the indicators of sorting from the literature showed significant variation with facies.

6.6 Principal component analysis

Principal component analysis (PCA) is a technique that transforms a large number of variables (e.g. concentrations of elements of a rock) into a smaller number of independent latent variables that explain the multivariate data. For this particular case, the original data were manipulated separately for mudstones and sandstones. The number of elements used was reduced to those considered representative of a predominantly detrital signature, namely TiO_2, Y, Zr, Nb, V, Cr, Co, La, Gd, Yb, Hf, Sc, Ta and Th. Only three REE were used, so that the covariation of the REE did not "swamp" the analysis.

The first principal component for the sandstones explained 61% of the variance in these elements, the second component a further 14%. The first principal component (PC1) is considered as a resistant factor, since it shows very good positive correlation with all the studied elements, except for Co (Fig. 27). All the elements are characteristic of heavy, detrital minerals identified in sandstones, and in particular:

- Rutile (TiO_2, Ta, Nb)
- Phosphates such as monazite (LREE-phosphate) and xenotime (Y-phosphate). Thorium is a common trace element substitute in these minerals.
- Zircon (Zr, Hf).

A similar interpretation can be applied to the second principal component (PC2) as it shows the highest positive loadings for Zr, Hf (zircon) and Cr (chromite). PC2 scores for Ni, V, Sc and Co

are negative, indicating the absence of a detrital mineral phase incorporating these elements. Their presence in the sandstones is most probably related to weathering products, such as clay minerals.

All sandstone samples plot on the diagonal of the biplot of PC1 vs. PC2 (Fig. 27), and are thus explained approximately equally by both factors. In particular, sandstones from the Missisauga Formation at Glenelg E-58 and North Triumph B-52 have a greater affinity towards PC2. These sandstones have the highest Zr, Hf and Cr content relative to the rest of the sandstones, perhaps related either to source (from polycyclic sandstone) or to hydraulic sorting.

For the mudstones, the first principal component accounts for 41% of the total variability and the second for a further 21%. The first principal component appears to reflect the concentration of heavy detrital minerals in the silt fraction, showing very good positive correlation with elements characteristic of heavy, detrital minerals, and in particular:

- Rutile (TiO_2).
- Phosphates such as monazite (LREE-phosphate) and xenotime (Y-phosphate). Thorium is a common trace element substitute in these minerals.
- Zircon (Zr).

On the other hand, the second principal component shows very good positive correlation with Ta and Nb and good positive correlation with Zr and Hf (characteristic of a felsic source), but negative correlation with V, Ni, Co, Cr and Sc (characteristic of a mafic to intermediate source). Overall, variability in the mudstones is best represented by PC2 rather than PC1. The majority of the mudstones indicate a possible mafic to intermediate source (slightly negative to zero values on PC2), whereas a small number of samples is characteristic of an intermediate to felsic source (positive loading on PC2), and in particular, mudstones from the Missisauga Formation at Dauntless D-35 and Peskowesk A-99, which show the highest Zr and Hf load.

7. The role of volcanic ash

7.1. Geochemical evidence for volcanic ash

Two mudstone samples from the Alma have unusual geochemical characteristics that might be related to deposition of volcanic ash.

Sample 2912.04 has unusually high Na_2O (2.9 % compared with a normal value of ~ 1.0 %), Nb (90 ppm compared with a normal value of ~35 ppm) and Ta (7 ppm). In addition, Sr and LREE (Fig. 28) are slightly elevated and K_2O and Rb are unusually low. This mix of elements would be consistent with elevated amounts of albite (after plagioclase) and a source from a

volcano with within-plate geochemical characteristics and thus high Nb and LREE. More specifically, the extremely high Ta is higher than the 4-5 ppm found in the New England Seamounts, Georges Bank and Baltimore Canyon, which are the most alkaline offshore Cretaceous volcanic rocks, but are in the range of 5-17 ppm found in the Monteregian Hills. Hafnium of 8 ppm in sample 2912.04 is also in the range of 4-23 ppm found in the Monteregian Hills (Fig. 29). Unfortunately, no Nb analyses are available for the Monteregian Hills.

Sample 2847.1 has a unusually high abundance of MREE and also has high LREE (Fig. 24). It also has high P_2O_5. A very similar REE pattern occurs at 145.9 m in the Chaswood Formation in borehole RR-97-23 in a sample at an unconformity that has unusually high P_2O_5 (0.4%). The same sample has very low K/Sr and some other unusual elemental abundances. Whether the unusual geochemical characteristics are the result of diagenetic processes at the unconformity or also represent an ash horizon is not known. A rather similar REE pattern, but with lower LREE, is termed type C by Pe-Piper et al. (2006b), and is represented by lignite samples from borehole CH97-10B: again, it is not known whether this represents volcanic ash, or is the consequence of diagenetic scavenging of the LREE.

8. Discussion

8.1 General nature of the source

The Scotian margin in the Cretaceous was clearly a passive continental margin, albeit one with rejuvenated relief as a result of strike-slip faulting that resulted from the rifting between Iberia and the Grand Banks. Studies of the Chaswood Formation on land (e.g. Gobeil et al. 2006) show that conglomerates include clasts of readily weathered lithologies such as diorite, despite the "passive margin" setting. Some terranes of the Appalachian orogen contain predominantly rocks of island arc (Avalon) or oceanic crust (Humber) origin that might be expected to yield sediment with distinctive chemical signature.

Chemical variation that has been used in the literature to distinguish between sediments of different provenance in complex orogenic belts were applied to the Scotian Basin sediments in the hope that they would indicate that different parts of the basin received varying proportions of sediment from different source rocks or terranes, even if the details of these sources were difficult to resolve. These discrimination diagrams show that all the Scotian Basin sediments have the characteristics of "active continental margin" or "passive margin" provenance. This is interpreted as showing that all were sourced by rather similar terranes that included significant amounts of intermediate and possibly mafic igneous rocks (the "active continental margin"

signature) together with an important felsic source (the "passive margin" signature). Petrographic evidence suggests that the predominant sediment source for sand-sized mineral grains was within the Appalachian orogen, which includes abundant intermediate rocks in the former active continental margin of the Avalon Terrane and abundant intermediate and mafic rocks in the Dunnage and Humber terranes. The abundant Appalachian granitoid rocks would provide minerals more resistant to weathering, with a high proportion of quartz, resulting in a strong "passive margin" signature.

One barrier to the use of some discrimination diagrams is that they involve Ti. In the Scotian basin, the mean abundance of Ti in both sandstones and mudrocks is substantially higher than average values, for example in Post-Archean Australian Shale or compilations of US average rocks (as summarized by Lentz, 2005) (Fig. 30). This abundance of Ti is related to the abundance of detrital ilmenite (Pe-Piper et al. 2005a) derived from abundant granitoid plutons of Atlantic Canada. It results in many of the rocks plotting away from diagnostic fields recognised in the literature (e.g. Figs. 5A, 9 in Appendices 2, 3 and 4).

The question as to whether variability in particular elements reflects different sources or differences in weathering or sorting is difficult to assess. It seems probable that the style of weathering throughout the source area is similar. The CIA diagram (Fig. 6) and the subarkosic character of many of the Scotian Basin sandstones suggests that the degree of alteration is relatively low. Some geochemical indicators of weathering may be reversed, or mimicked by, chemical changes due to burial diagenesis (Fig. 6). Although in the literature variations in Th and U (Fig. 7) have been used as a proxy for weathering, in the Scotian Basin variation of these elements may rather reflect variability in source rocks, particularly given their high abundance in some granitoids in the region.

There is an important distinction between the chemical composition of a source rock and the chemical composition of the sediments derived therefrom. In cases where relief is high and transport distances short, changes in relative abundance of elements as a result of weathering of source rocks may be small, as appears to be the case for the Carboniferous Horton Group of central Nova Scotia (Murphy 2000). It is unclear whether it can similarly be assumed that there is little change from source to deposit in the case of the Cretaceous of the Scotian Basin.

Hydraulic sorting may be important in the case of reworking of older sediments. The Al_2O_3 - Hf - TiO_2 diagram has been used to assess such sorting in the literature and shows some variability in Hf content between wells (Fig. 9; Fig. 4 in Appendices 2, 3 and 4), which is much higher in Glenelg and North Triumph sandstones than in wells either to the west or the east (Fig. 32). It can be compared with the similar plot from Horton Group sandstones (Fig. 31) derived directly from Meguma and Avalon terrane basement rocks that shows Hf contents similar to all

the wells except Glenelg and North Triumph. The fact that mudrocks do not show a similar peak in Hf abundance in Glenelg and North Triumph (Fig. 32) suggests that its abundance in sandstone in those wells results more from sorting than from source, although these two wells also show high Th/U in sandstones (Fig. 26).

8.2 Geographic variation in provenance

There is clear evidence from variations in geochemistry that different wells received sediment of different composition. The correlation matrix (Tables 4 and 5) provides some guidance as to which elements can be used as reasonably indicative of source. Plots of elements against sandstone grain size indicate which are influenced by grain size. As noted above, there is no clear evidence for variation with sandstone depositional facies. The most striking variations in sandstones are:

- A decrease in Ti from west to east (Fig. 30)
- Th/U ratio highest in the Glenelg and North Triumph fields (Fig. 25), where Hf is also highest (Fig. 32), and generally lower both to the east and to the west.
- Strong covariance of Cr and Zr from the principal component analysis, with very high values of these elements at the Glenelg and North Triumph fields.
- La/Sm ratio tends to be lowest in the Glenelg and North Triumph fields and also in the Fox well, and is higher both to the east and west (Fig. 26).
- A high K/Rb ratio at Peskowesk, Dauntless and Fox compared with other wells (Fig. 10B, Figs. 5B in Appendices 2, 3, 4).

The number of wells from which there are good analyses of mudrocks is limited, with few samples from either the extreme east (Dauntless) or extreme west (Naskapi, Sambro). As a result, there are fewer trends visible in the mudrock data. The most prominent are:

- An increase in both Nb (Fig. 24) and Y (Fig. 33) from west to east
- A decrease in Sr from west to east (Fig. 24)
- Low Hf in most Peskowesk mudrocks (Fig. 33)
- High Ti/Zr in Logan Canyon Formation mudrocks and some Missisauga Formation mudrocks at Peskowesk and very low Ti/Zr in other Missisauga Formation mudrocks at Peskowesk
- Variations in Th content of mudrocks between the west (Naskapi and Alma), the centre (Glenelg and North Triumph) and the east (Fox, Peskowesk and Dauntless) (Fig. 7; Fig. 2. in Appendices 2, 3 and 4).

9. Conclusions

1. There are consistent differences in whole rock geochemistry of Lower Cretaceous sandstones and mudrocks between the western, central and eastern Scotian Basin. Data are insufficient to properly evaluate stratigraphic variability.

2. The overall geochemical signature is consistent with a source predominantly from the Appalachians, with only minor effects of weathering and hydraulic sorting.

3. Geochemical results are generally consistent with information derived from detrital petrology, with greater supply of K feldspar in the east and of plagioclase in the west and regionally high supply of detrital ilmenite. Supply to the Glenelg and North Triumph fields may include a substantial source of polycyclic sandstone yielding resistant heavy minerals zircon and chromite, compared with predominantly crystalline sources in wells to the west and east.

4. There are regional variations in abundance of Ti and K, elements that may have an important influence on diagenesis.

5. The geochemical signature of volcanic ash has been recognised in rare samples.

References

Bhatia, M. R., 1983. Plate tectonics and geochemical composition of sandstones. Journal of Geology, 91, 611-627.

Bhatia, M. R., and Crook, K. A. W., 1986. Trace element characteristics of graywackes and tectonic setting discrimination of sedimentary basins. Contributions to Mineralogy and Petrology, 92, 181-193.

Condie, K. C., 1993. Chemical composition and evolution of the upper continental crust: Contrasting results from surface samples and shales. Chemical Geology, 104, 1-37.

Chuhan, F.A., Bjørlykke, K., and Lowrey, C.J., 2000. The role of provenance in illitization of deeply buried reservoir sandstones from Haltenbanken and north Viking Graben, offshore Norway. Marine and Petroleum Geology, v. 17, p. 673-689.

Chuhan, F.A., Bjørlykke, K., and Lowrey, C.J., 2001. Closed system burial diagenesis in reservoir sandstones. Journal of Sedimentary Research, v. 71, p. 15-26.

Cummings, D.I., Hart, B.S. and Arnott, R.W.C., 2006a. Sedimentology and stratigraphy of a thick, areally extensive fluvial-marine transition, Missisauga Formation, offshore Nova Scotia, and its correlation with shelf margin and slope strata. Bulletin of Canadian Petroleum Geology, v. 54, p. 152-174.

Drummond, K. J., 1992, Geology of Venture, a geopressured gas field, offshore Nova Scotia, *in* M. T. Halbouty, ed., Giant oil and gas fields of the decade 1978-1988: AAPG Memoir 54, p. 55-71.

Floyd, P. A., and Leveridge, B. E., 1987. Tectonic environment of the Devonian Gramscatho basin, south Cornwall: framework mode and geochemical evidence from turbiditic sandstones. Journal of the Geological Society, London, 144, 531-542.

Floyd, P. A., Winchester, J. A., and Park, R. G., 1989. Geochemistry and tectonic setting of Lewisian clastic metasediments from the Early Proterozoic Loch Maree Group of Gairloch, NW Scotland. Precambrian Research, 45, 203-214.

Garcia, D., Fonteilles, M., and Moutte, J., 1994. Sedimentary fractionations between Al, Ti, and Zr and the genesis of strongly peraluminous granites. Journal of Geology, 94, 411-422.

Gobeil, J.-P., Pe-Piper, G., and Piper, D.J.W. 2006. The Early Cretaceous Chaswood Formation in the West Indian Road pit, central Nova Scotia. Canadian Journal of Earth Sciences, 43, 391-403.

Gould, K., Pe-Piper, G. and Piper, D.J.W., 2007. Origin of chlorite rims in reservoir sandstones of the Lower Missisauga Formation, offshore Nova Scotia. Atlantic Geoscience Society Meeting, Moncton N.B., February 2007, p. 20.

Gromet, P.L. and Silver, L.T. 1983. Rare earth element distributions among minerals in a

granodiorite and their petrogenetic implications. Geochimica et Cosmochimica Acta, 47, 925-939.

Gu, X. X., Liu, J. M., Zheng, M. H., Tang J. X., and Qi, L., 2002. Provenance and tectonic setting of the Proterozoic turbidites in Hunan, South China: Geochemical evidence. Journal of Sedimentary Research, 72, 393-407.

Hundert, T., Piper, D.J.W. and Pe-Piper, G., 2006. Exploration model for kaolin beneath unconformities in the Lower Cretaceous fluvial Chaswood Formation, Nova Scotia. Exploration and Mining Geology, v. 15, p. 9-26.

Jansa, L.F. and Wade, J.A., 1975. Geology of the continental margin off Nova Scotia and Newfoundland. Geological Survey of Canada Paper 74-30, p. 51-105.

La Flèche, M. R., and Camiré, G., 1996. Geochemistry and provenance of metasedimentary rocks from the Archean Golden Pond sequence (Casa Berardi mining district, Abitibi subprovince). Canadian Journal of Earth Science, 33, 676-690.

Lentz, D. 2003. Geochemistry of sediments and sedimentary rocks. Geological Association of Canada, Geotext 4.

MacLean, B.C. and Wade, J.A. 1993. Seismic markers and stratigraphic picks in Scotian Basin wells. Atlantic Geoscience Centre, Geological Survey of Canada.

MacRae, R.A. and Jauer, C. 2001. Sequence stratigraphy and palynology, Upper Missisauga Formation, Glenelg area, offshore Nova Scotia. Poster presented at the Atlantic Geoscience Society annual colloquium.

Murphy, B. J., 2000. Tectonic influence on sedimentation along the southern flank of the late Paleozoic Magdalen basin in the Canadian Appalachians: Geochemical and isotopic constraints on the Horton Group in the St. Marys basin, Nova Scotia. GSA Bulletin, 112, 997-1011.

Nesbitt, H. W., and Young G. M., 1982. Early Proterozoic climates and plate motions inferred from major element chemistry of lutites. Nature 299, 715-717.

Nesbitt, H. W., and Young G. M., 1996. Petrogenesis of sediments in the absence of chemical weathering: Effects of abrasion and sorting on bulk composition and mineralogy. Sedimentology, 43, 341-358.

Nesbitt, H. W., Young, G. M., McLennan, S.M., and Keays, R.R., 1996. Effects of chemical weathering and sorting on the petrogenesis of siliciclastic sediments, with implications for provenance studies. Journal of Geology, 104, 525-542.

Pe-Piper, G. and Mackay, R.M. 2006. Provenance of Lower Cretaceous sandstones onshore and offshore Nova Scotia from electron microprobe geochronology and chemical variation of detrital monazite. Bulletin of Canadian Petroleum Geology, v. 54, p. 366-379.

Pe-Piper, G. and Piper, D.J.W. 2004. The effects of strike-slip motion along the Cobequid-Chedabucto-SW Grand Banks fault system on the Cretaceous - Tertiary evolution of Atlantic Canada. Canadian Journal of Earth Sciences, 41, 799-808.

Pe-Piper, G. and Piper, D.J.W., 2007. Sedimentary petrology of the Lower Cretaceous in the Naskapi N-30 and Sambro I-29 wells, LaHave Platform, Scotian basin, offshore eastern Canada. Geological Survey of Canada Open File

Pe-Piper, G., Dolansky, L., and Piper, D.J.W. 2004a. Petrography of the mid-Cretaceous Chaswood Formation in borehole RR-97-23, Elmsvale Basin, Nova Scotia: sedimentary environment, detrital mineralogy and diagenesis. Geological Survey of Canada Open File 4837, 231 p.

Pe-Piper, G., Piper, D.J.W., and Dolansky, L.M., 2005a. Alteration of ilmenite in the Cretaceous sands of Nova Scotia, southeastern Canada. Clays and Clay Minerals, v. 53, p. 490-510.

Pe-Piper, G., Piper, D.J.W., Gould, K.M. and Shannon, J. 2006a. Depositional environment and provenance analysis of the Lower Cretaceous sedimentary rocks at the Peskowesk A-99 well, Scotian Basin. Geological Survey of Canada, Open File 5383, 171 p.

Pe-Piper, G., Piper, D.J.W., Hundert, T. and Stea, R.R. 2005b. Outliers of Lower Cretaceous Chaswood Formation in northern Nova Scotia: results of scientific drilling and studies of sedimentology and sedimentary petrography. Geological Survey of Canada Open File 4845, 305 p.

Pe-Piper, G., Okwese, A. and Piper, D.J.W., 2006b. Volcanic ash and lignite of the Lower Cretaceous Chaswood Formation, central Nova Scotia. Geological Survey of Canada Open File 4973.

Pe-Piper, G., Piper, D.J.W., Vaughan, A.D., Shannon, J. and Ingram S., 2004b. Sedimentary petrology of Lower Cretaceous rocks of the southwestern Sable sub-basin (North Triumph B-52, Alma K-85 and Glenelg N-49 wells), Scotian Basin. Geological Survey of Canada, Open File 4836.

Pe-Piper, G., Stea, R.R., Ingram, S., and Piper, D.J.W. 2004c. Heavy minerals and sedimentary petrology of the Cretaceous sands from the Shubenacadie outlier, Nova Scotia. Nova Scotia Department of Natural Resources, Open File Report ME 2004-5, 78 p.

Piper, D.J.W., Pe-Piper, G. and Ingram, S.I., 2004. Early Cretaceous sediment failure in the southwestern Sable sub-basin, offshore Nova Scotia. American Association of Petroleum Geologists Bulletin, 88, 991-1006.

Piper, D.J.W., Pe-Piper, G., Hundert, T. and Venugopal, D.K., 2007. The Lower Cretaceous Chaswood Formation in southern New Brunswick: provenance and tectonics. Canadian Journal of Earth Sciences (*May 2007 issue*)

Reimer, C., 2002, Missisauga Formation at the Venture field: proximal delta and shallow marine reservoirs. Core Conference guide book, Petroleum Society of CIM, Halifax, N.S. p. 65-76.

Roser, B. P., and Korsch, R. J., 1986. Determination of tectonic setting of sandstone-mudstone suites using SiO2 and K2O/Na2O ratio. Journal of Geology, 94, 635-650.

Shannon, J., 2002, Lower Cretaceous lithofacies and petrology of Peskowesk A-99 and Dauntless D-35 wells, Scotian Basin. Unpublished B.Sc. (honours) thesis, Saint Mary's University, Halifax, N.S., 121 p

Stea, R. and Pullan, S. 2001. Hidden Cretaceous basins in Nova Scotia. Canadian Journal of Earth Sciences, v. 38, p. 1335-1354.

Sun, S.-s. and McDonough, W.F., 1989. Chemical and isotopic systematics of oceanic basalts: implications for mantle composition and processes. In: Saunders, A.D. and Norry, M.J., eds., Magmatism in the Ocean Basins, Geological Society Special Publication 42, p. 313-345.

Taylor, S. R., and MacLennan, S. M., 1985. The continental crust: Its composition and evolution. An examination of the geological record preserved in sedimentary rocks. Blackwell, Oxford.

Totten, M. W., Hanan, M. A., and Weaver, B. L., 2000. Beyond whole-rock geochemistry of shales: The importance of assessing mineralogic controls for revealing tectonic discriminants of multiple sediment sources for the Ouachita Mountain flysch deposits. GSA Bulletin, 112, 1012-1022.

Wade, J.A. and MacLean, B.C. 1990. Aspects of the geology of the Scotian Basin from recent seismic and well data. Geology of Canada, v. 2, p. 190-238.

Weir-Murphy, S.L., 2004. Cretaceous rocks of the Orpheus graben, offshore Nova Scotia. M.Sc. thesis, Saint Mary's University.

Williams, G.L., Ascoli, P., Barss, M.S., Bujak, J.P., Davies, E.H., Fensome, R.A., and Williamson, M.A., 1990. Biostratigraphy and related studies. Geology of Canada, v. 2, p. 87-137.

Williams, H. and Grant, A.C. 1998. Tectonic assemblages, Atlantic region, Canada. [1:3m map]. Geological Survey of Canada Open File 3657, 1 sheet.

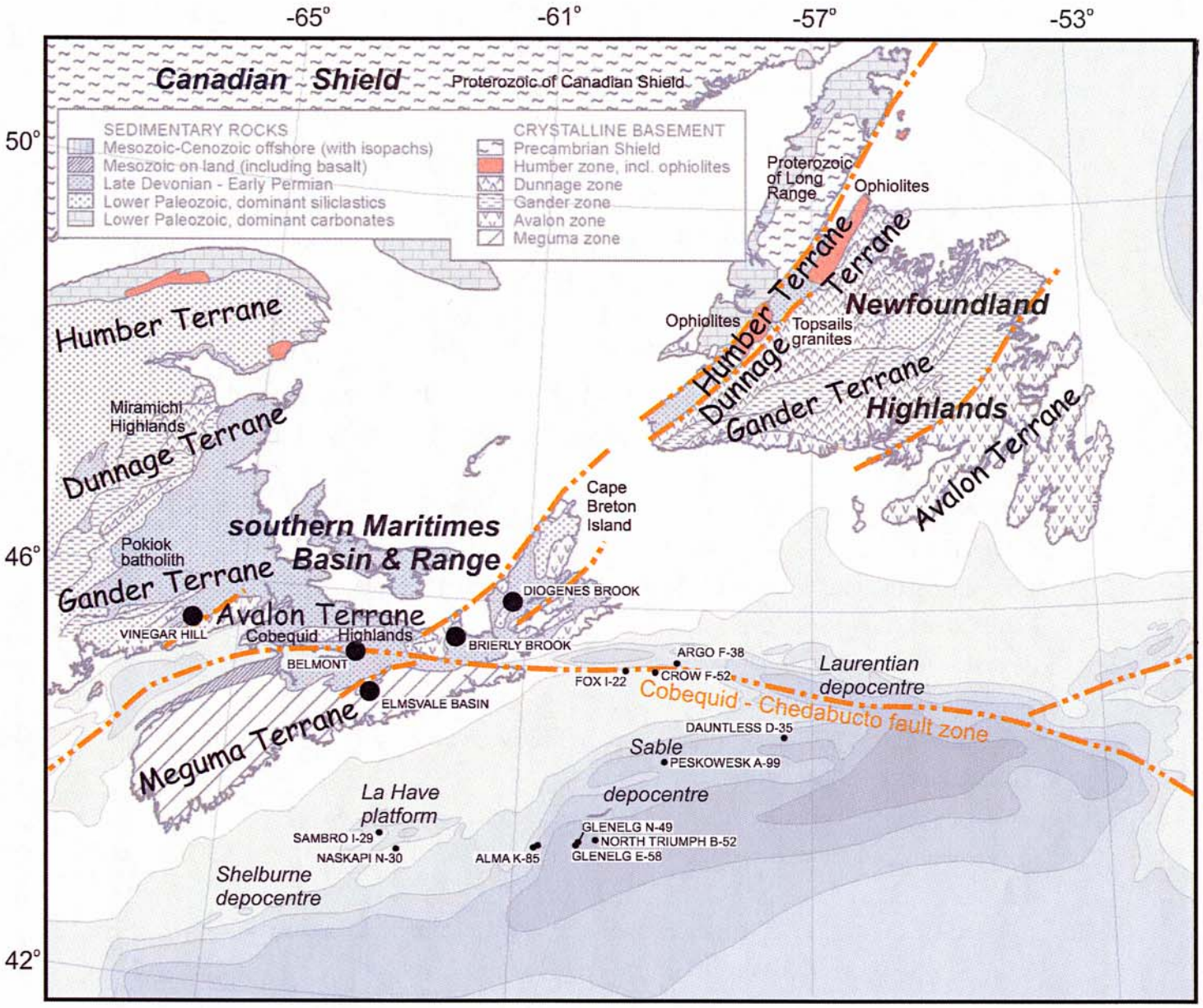

Fig. 1. Location map showing wells from which samples were studied. Also shows principal areas of Chaswood Formation on land (solid circles), 2 km isopachs of offshore basins, principal rock types on land, and key paleogeographic elements of the early Cretaceous. Base map from Williams and Grant (1998).

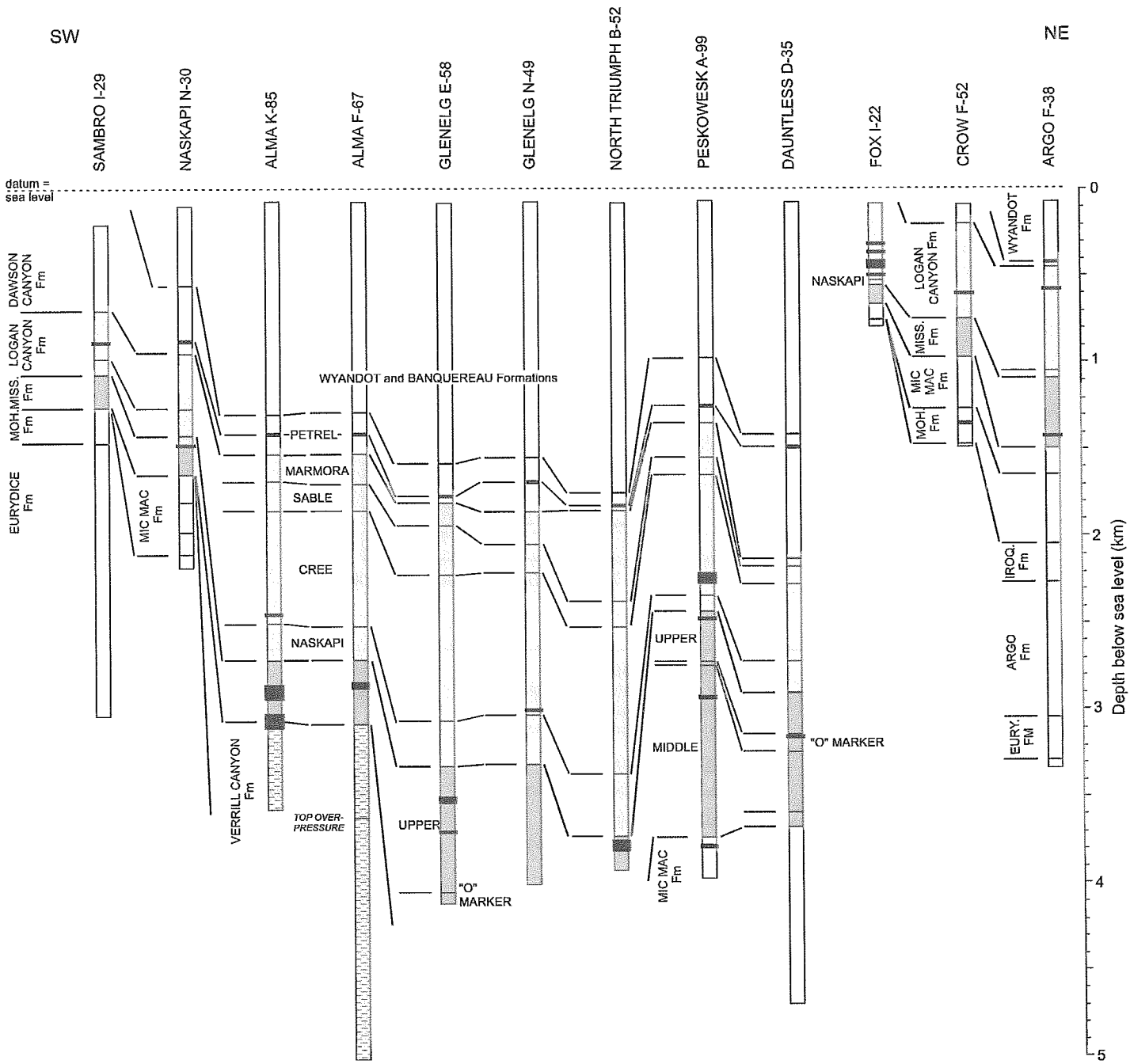

Fig. 2. Stratigraphic sections of the studied wells showing location of samples (black bars). Data from MacLean and Wade (1993) and the BASIN database.

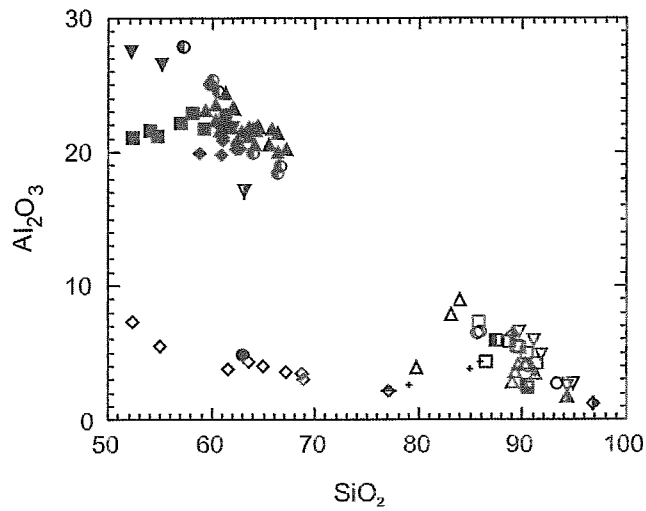

Sambro I-29
▼ - Logan Canyon Formation shale

Naskapi N-30
▽ - Missisauga Formation sandstone

Alma K-85
◆ - Logan Canyon Formation shale
▲ - Missisauga Formation shale

Alma F-67
▼ - Mississauga Formation shale
▲ - Missisauga Formation sandstone

Glenelg N-49
◆ - Logan Canyon Formation shale
● - Missisauga Formation shale
◆ - Missisauga Formation sandstone

Glenelg E-58
△ - Missisauga Formation sandstone

N. Triumph B-52
+ - Missisauga Formation sandstone

Fox I-22
◇ - Logan Canyon Formation sandstone

Argo F-38
◆ - Missisauga Formation sandstone

Peskowesk A-99
■ - Logan Canyon Formation shale
□ - Logan Canyon Formation sandstone
◐ - Missisauga Formation shale
◧ - Missisauga Formation sandstone
▬ - Micmac Formation sandstone

Dauntless D-35
◓ - Missisauga Formation shale
○ - Missisauga Formation sandstone

Figure 3: Al_2O_3 vs SiO_2 plot for all analysed samples, showing outlying samples with low Al_2O_3 and SiO_2 that have high proportions of carbonate cement.

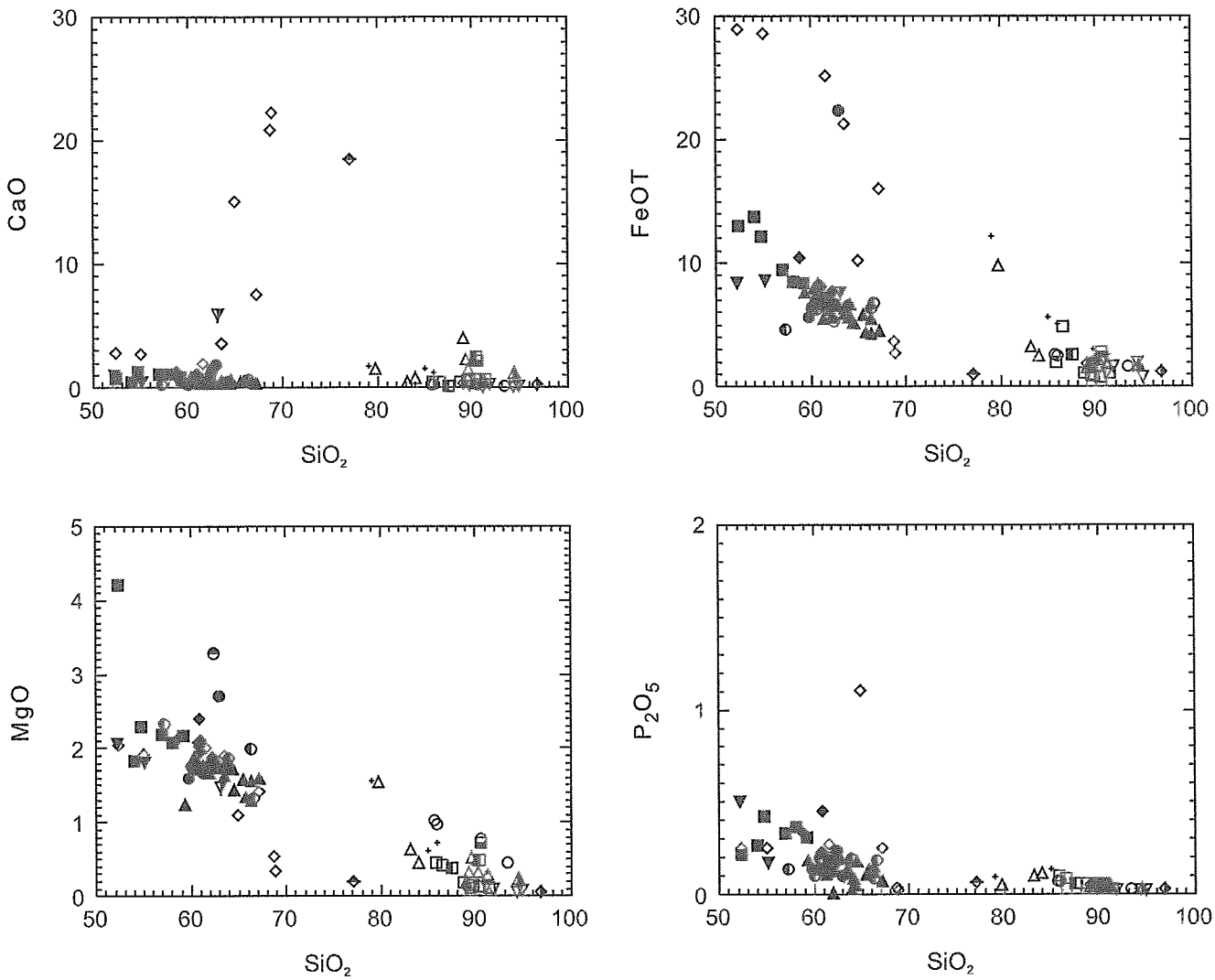

Figure 4: CaO vs SiO_2, FeO_T vs SiO_2, MgO vs SiO_2 and P_2O_5 vs SiO_2 plots. Symbols as in Fig. 3.

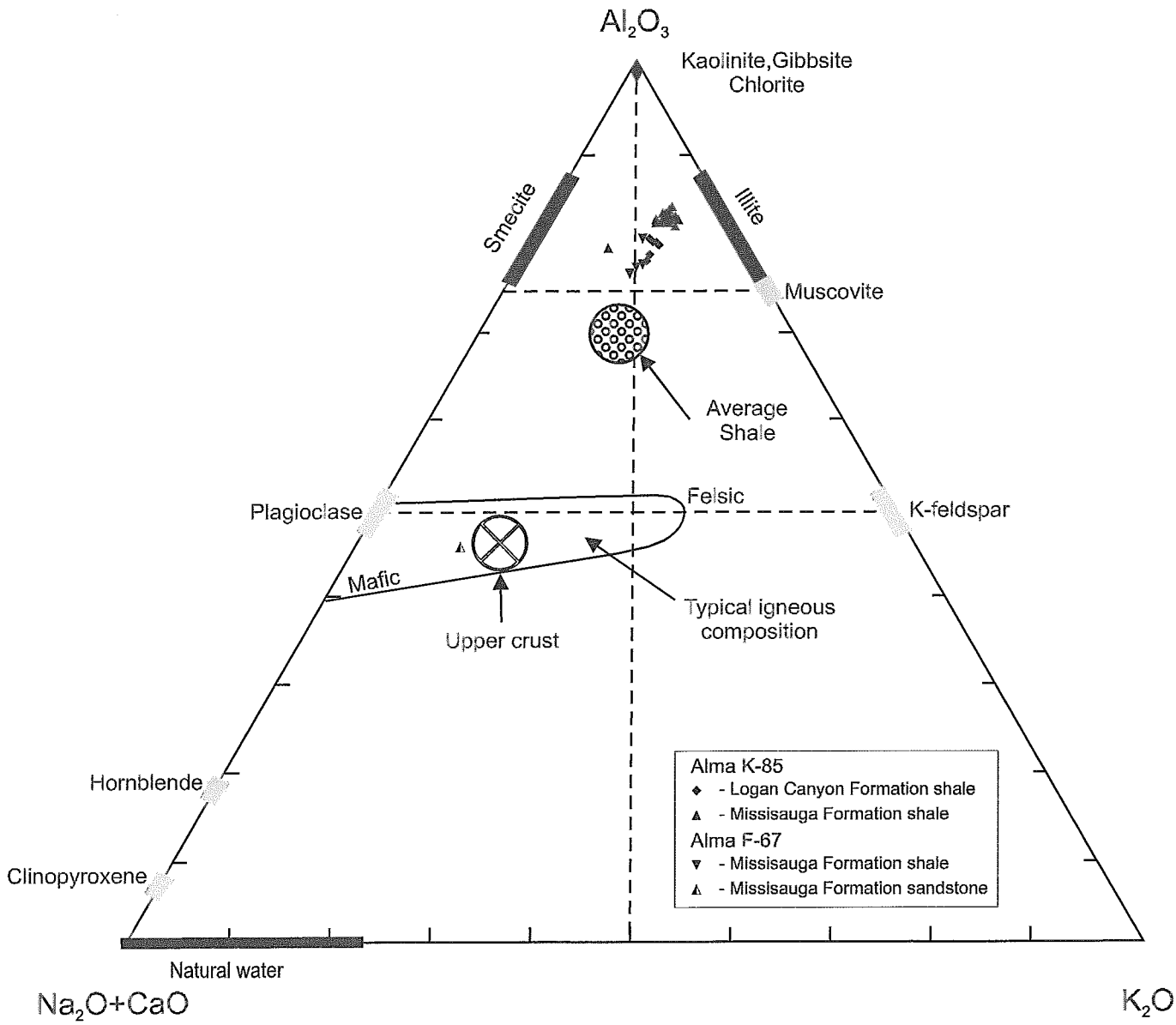

Figure 5: Ternary plot of molecular proportions of Al_2O_3 - Na_2O+CaO - K_2O. Fields from Gu et al. (2002). Idealized clinopyroxene and hornblende compositions from Taylor and MacLennan (1985).

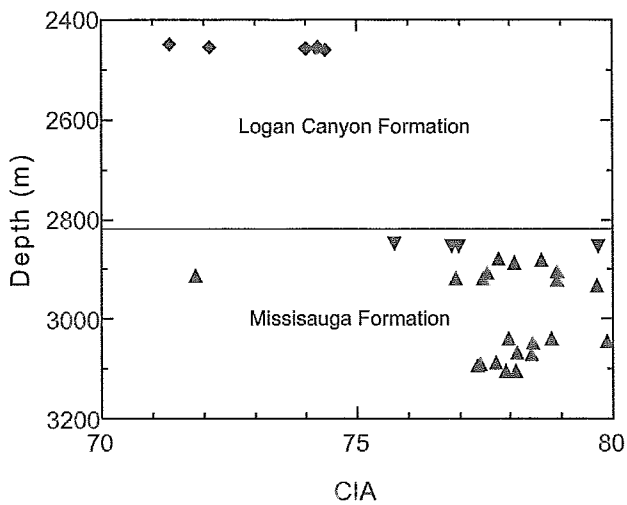

Figure 6: Binary plot of CIA vs depth for the Alma K-85 well

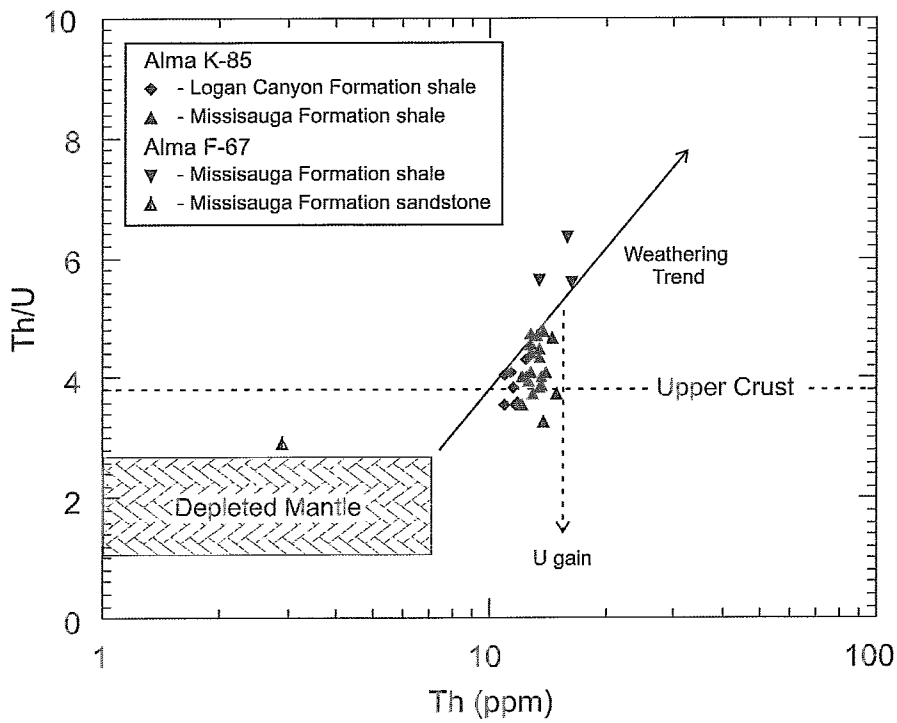

Figure 7: Th/U vs. Th plot. Fields and trends from Gu et al. (2002).

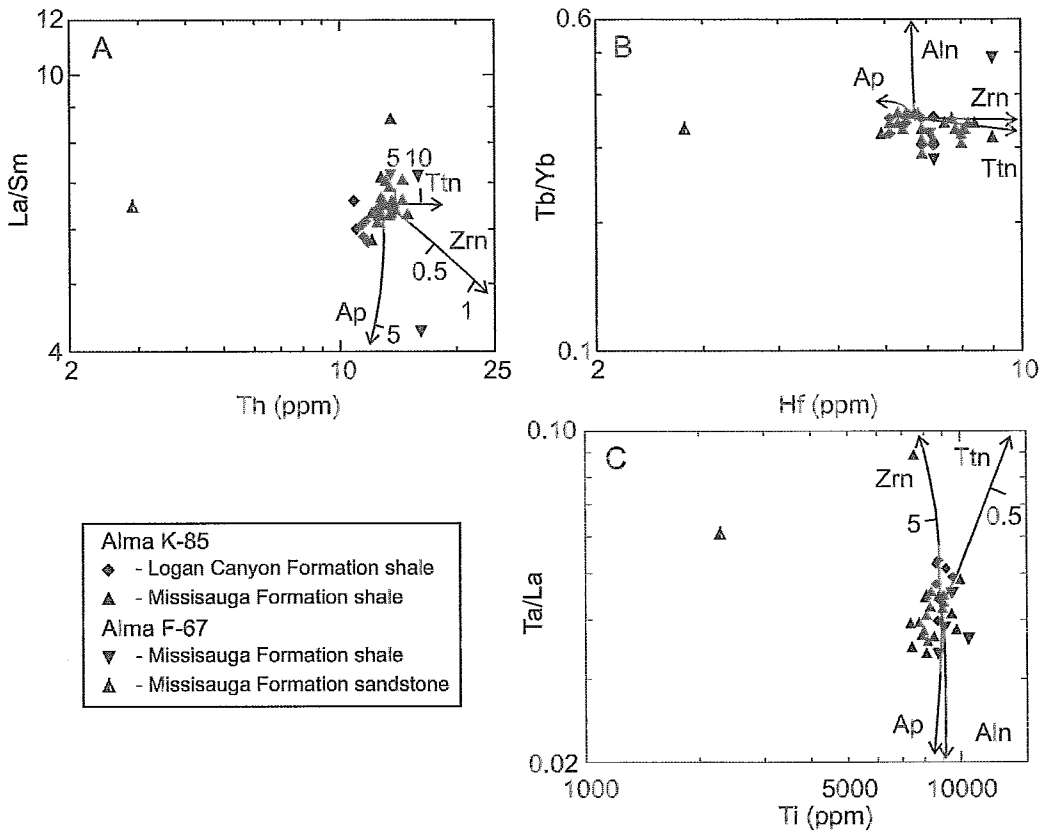

Figure 8: A: La/Sm vs. Th plot. B: Tb/Yb vs. Hf plot. C. Ta/La vs. Ti plot. Heavy mineral accumulation trends modified from LaFlèche and Camiré (1996).

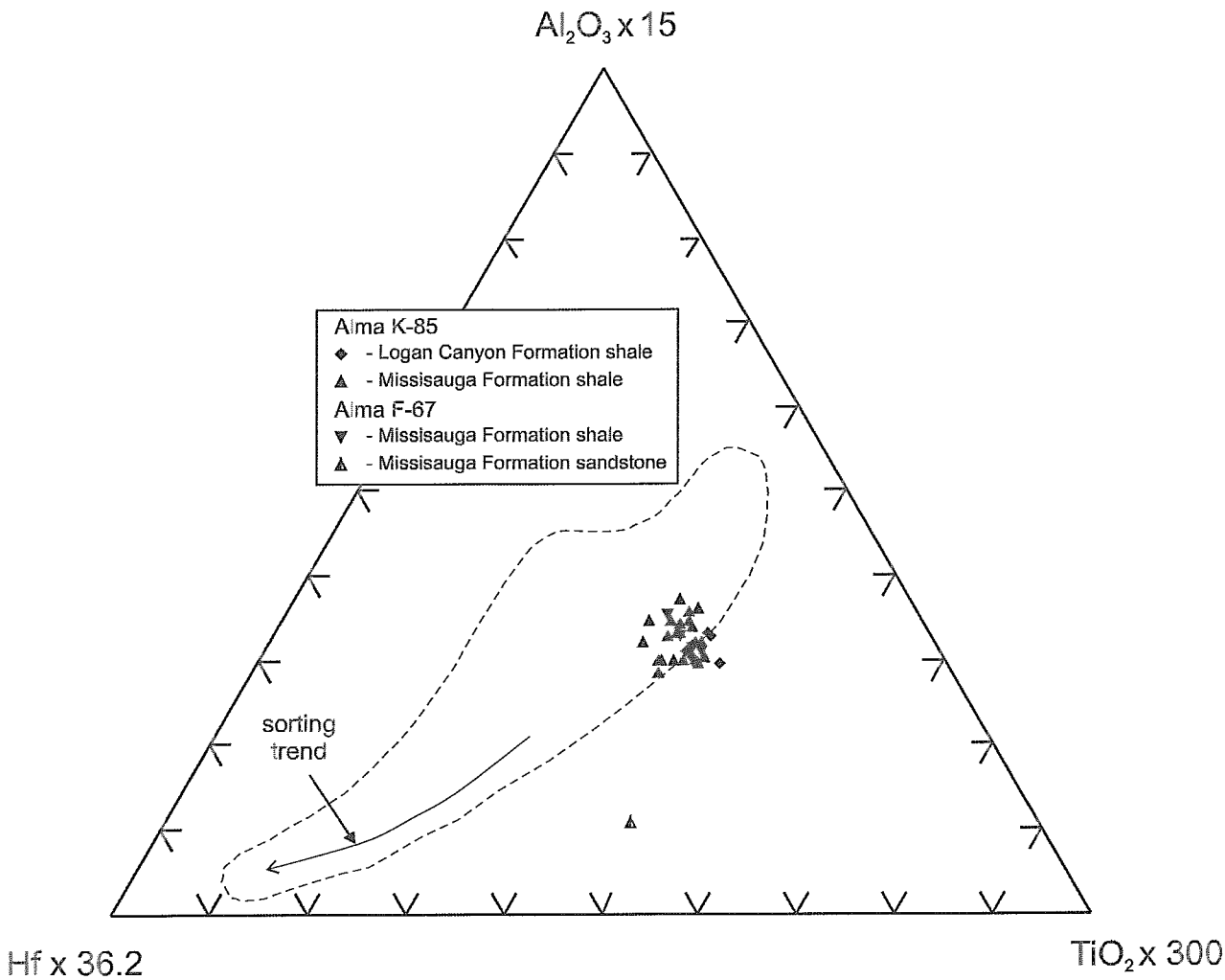

Figure 9: Al_2O_3*15 - Hf*36.2 - TiO_2*300 plot. Field after LaFlèche and Camiré (1996), and Garcia et al. (1994).

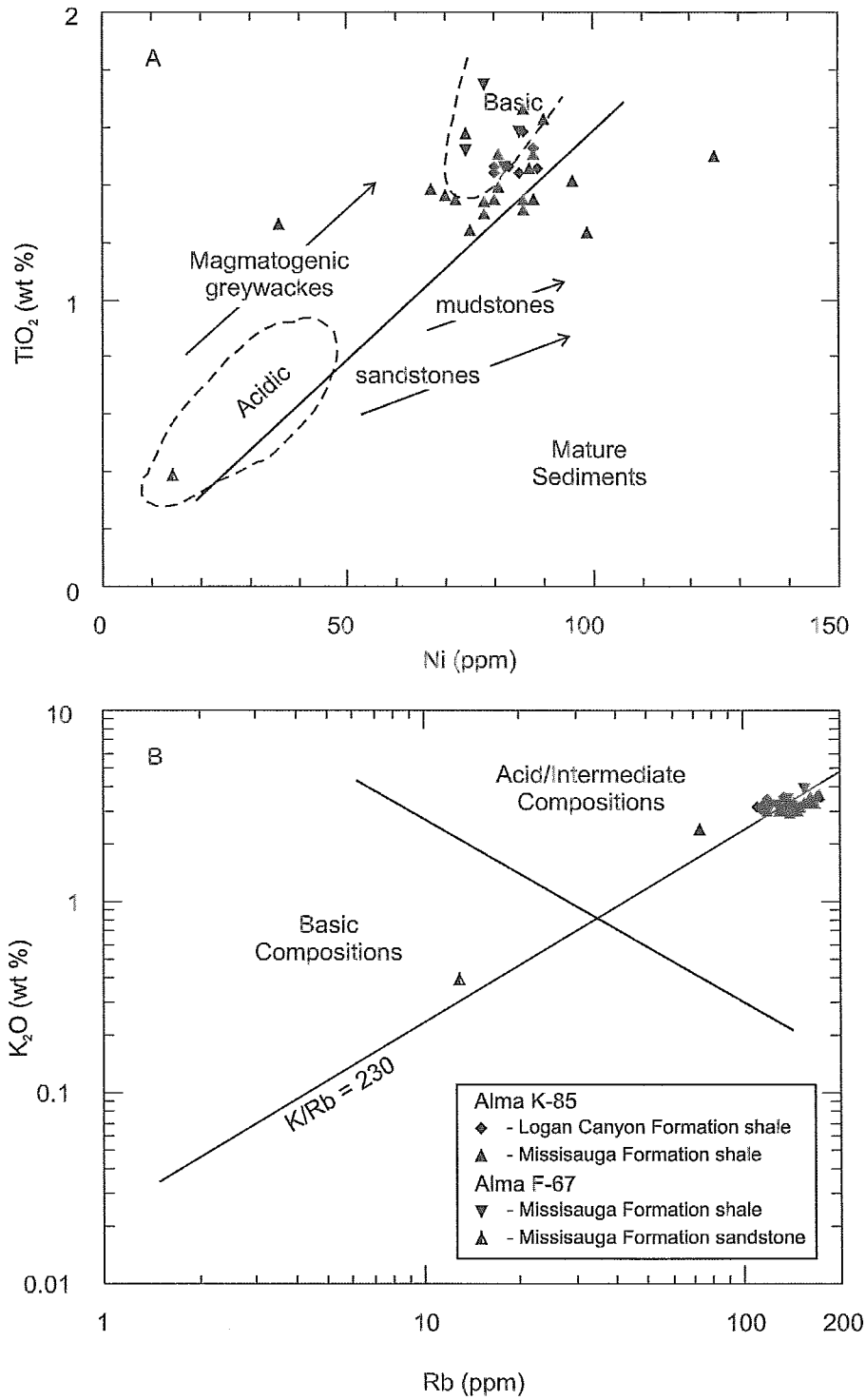

Figure 10A: TiO_2 vs. Ni plot. Fields and trends after Gu et al., 2002 and Floyd et al. (1989). B: K_2O vs. Rb plot. Fields after Floyd and Leveridge (1987). Samples the same for both plots.

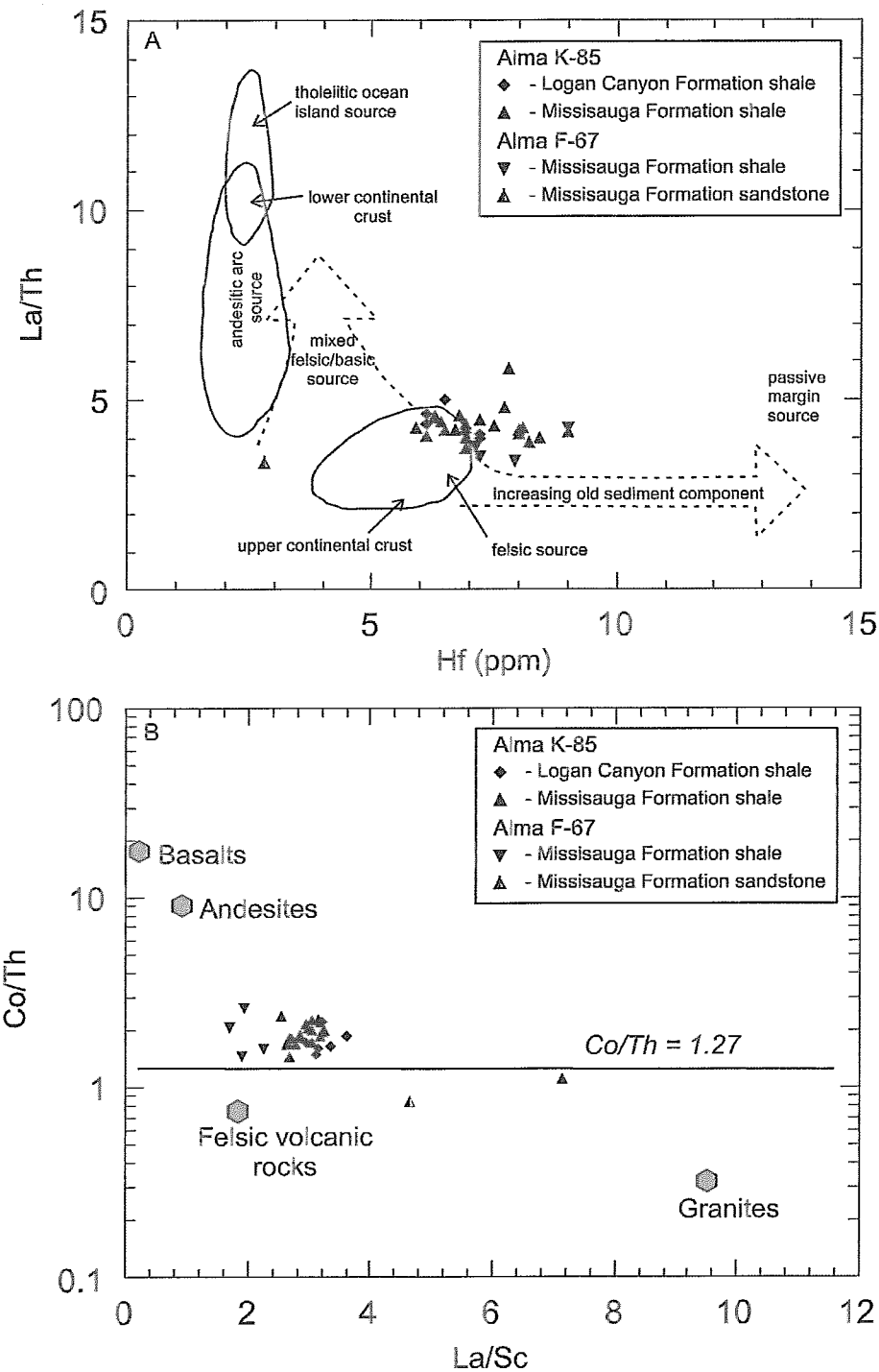

Figure 11A: La/Th ratio vs. Hf plot. Fields after Floyd and Leveridge (1987), and Gu et al. (2002). B: Co/Th ratio vs. La/Sc ratio plot. Average compositions of igneous rocks from Condie (1993), and Gu et al. (2002).

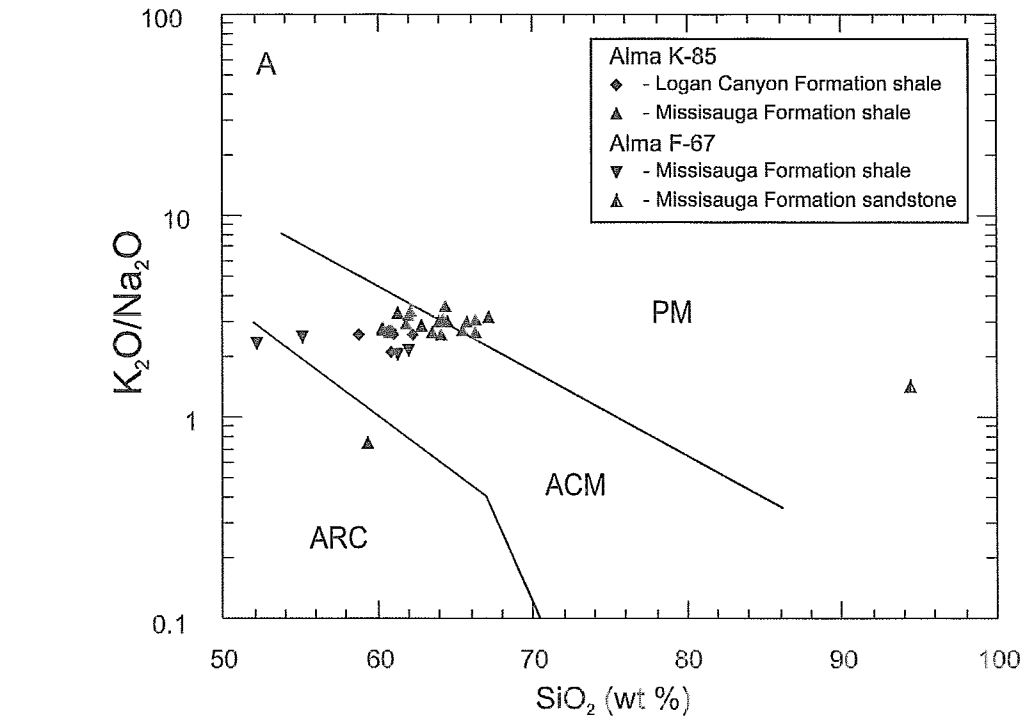

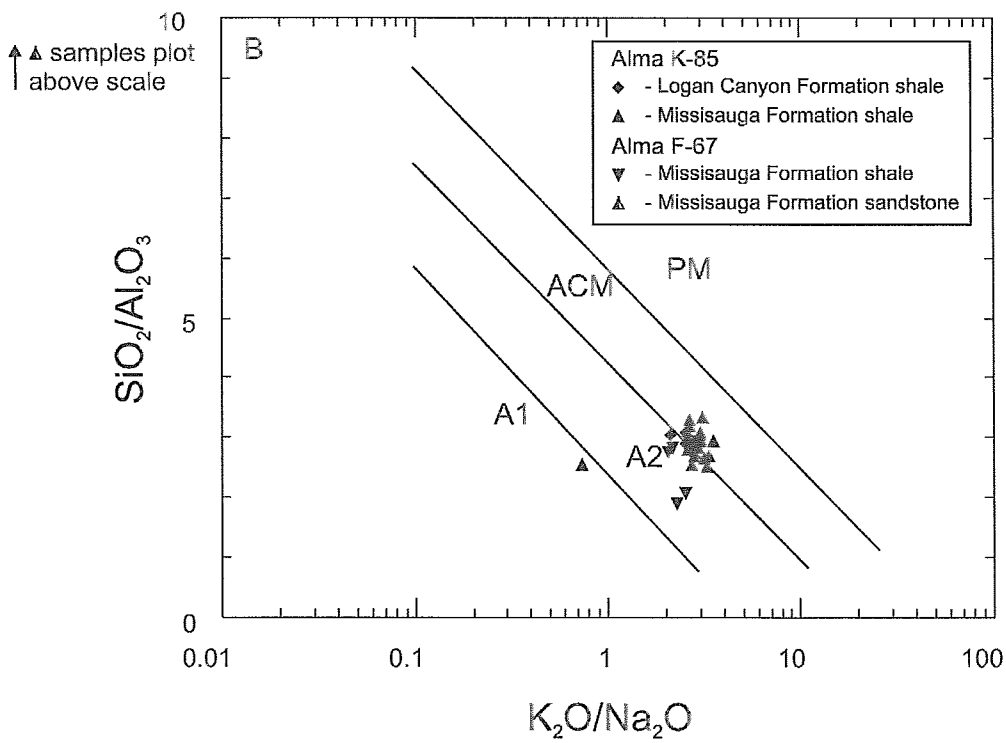

Figure 12A: K_2O/Na_2O ratio versus SiO_2 plot. Fields after Roser and Korsch (1986): passive margin = PM, active continental margin = ACM and oceanic island arc =ARC. B: SiO_2/Al_2O_3 ratio versus K_2O/Na_2O ratio plot. Fields and boundary lines after Roser and Korsch (1986) : passive margin = PM, active continental margin = ACM, arc setting, basaltic and andesitic detritus = A1 and evolved arc setting (felsic plutonic detritus) = A2.

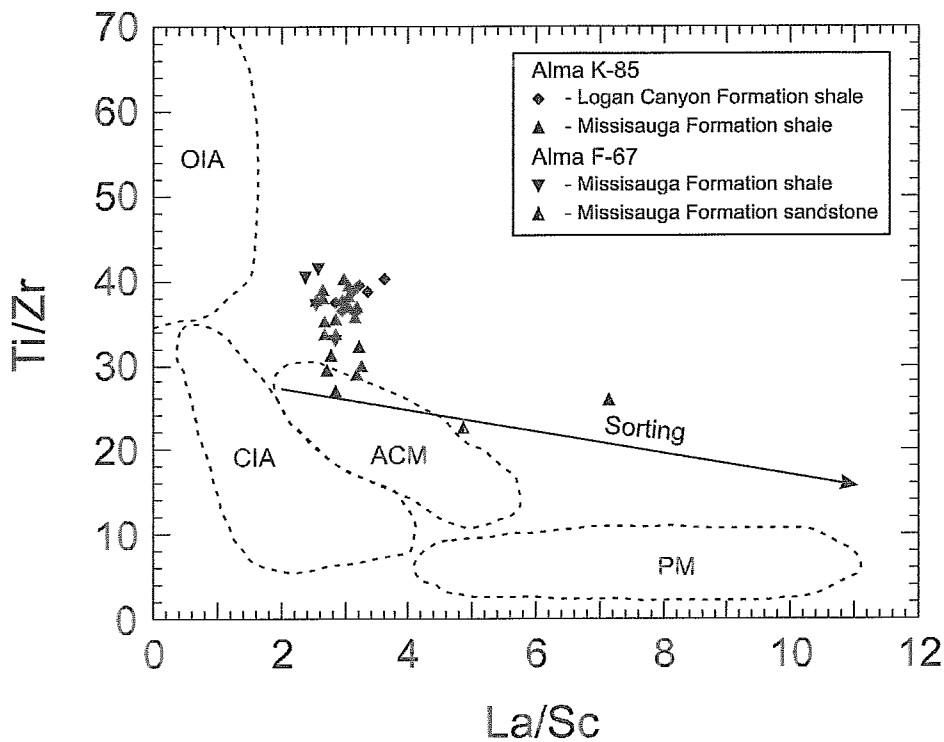

Figure 13: Ti/Zr ratio versus La/Sc ratio plot. Fields after Bhatia and Crook (1986): oceanic island arc = OIA, continental island arc = CIA, active continental margin = ACM and passive margin = PM. The sorting trend after Gu et al., 2002.

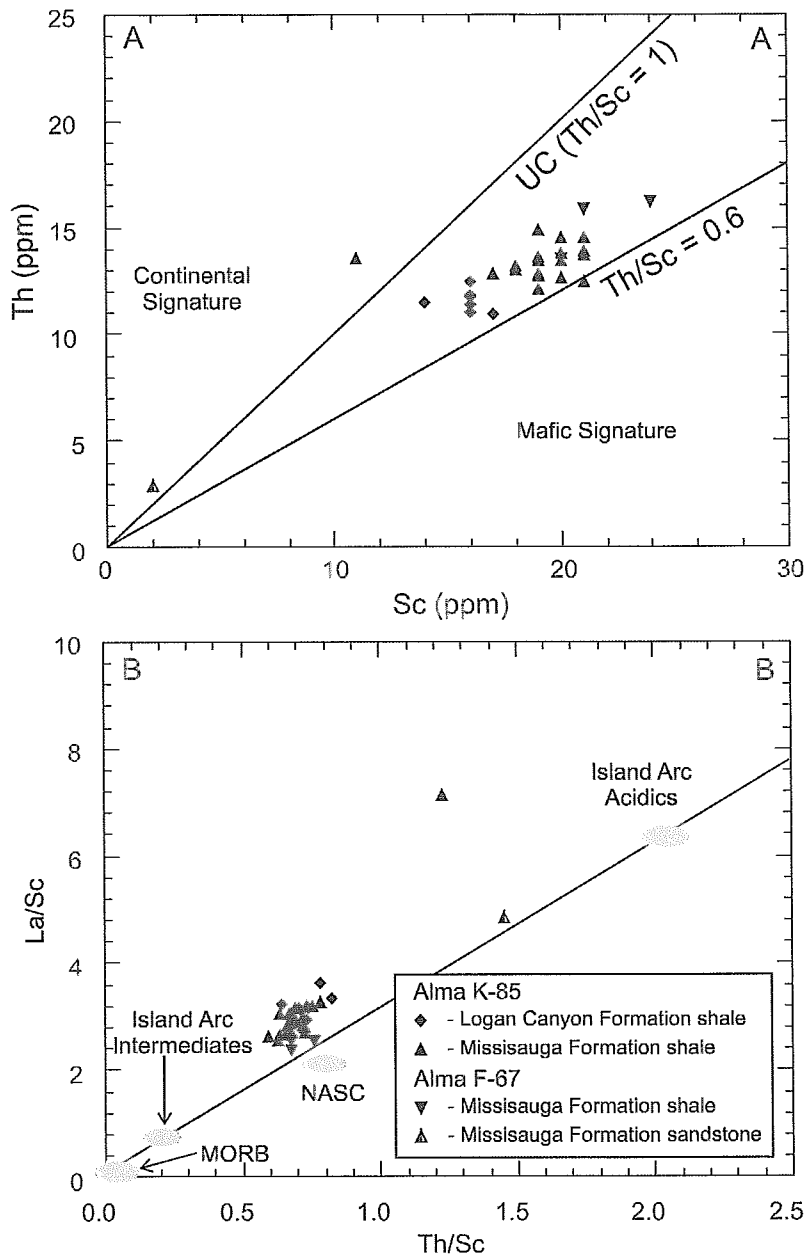

Figure 14A: Th vs. Sc plot. Fields and trends from Totten et al. (2000). B: La/Sc vs. Th/Sc ratio plot. Fields from Totten et al. (2000). Values of different igneous rock types and the North American shale composite (NASC) are included for reference (Taylor and McLennan,1985; Sun and McDonough, 1989; Gromet and Silver, 1983). Same symbols are used in both plots.

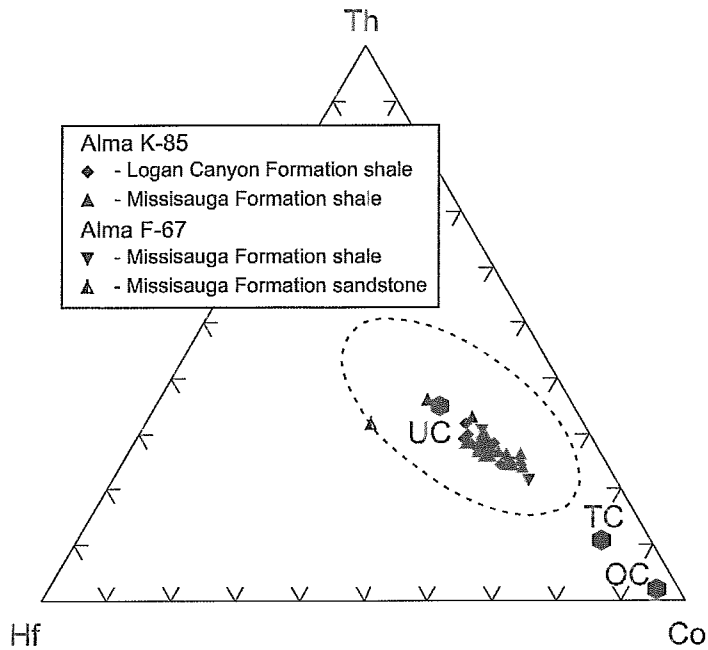

Figure 15: Th - Hf - Co plot. Fields after Taylor and McLennan, 1985. UC = Upper continental crust; TC = bulk continental crust; OC = average oceanic crust.

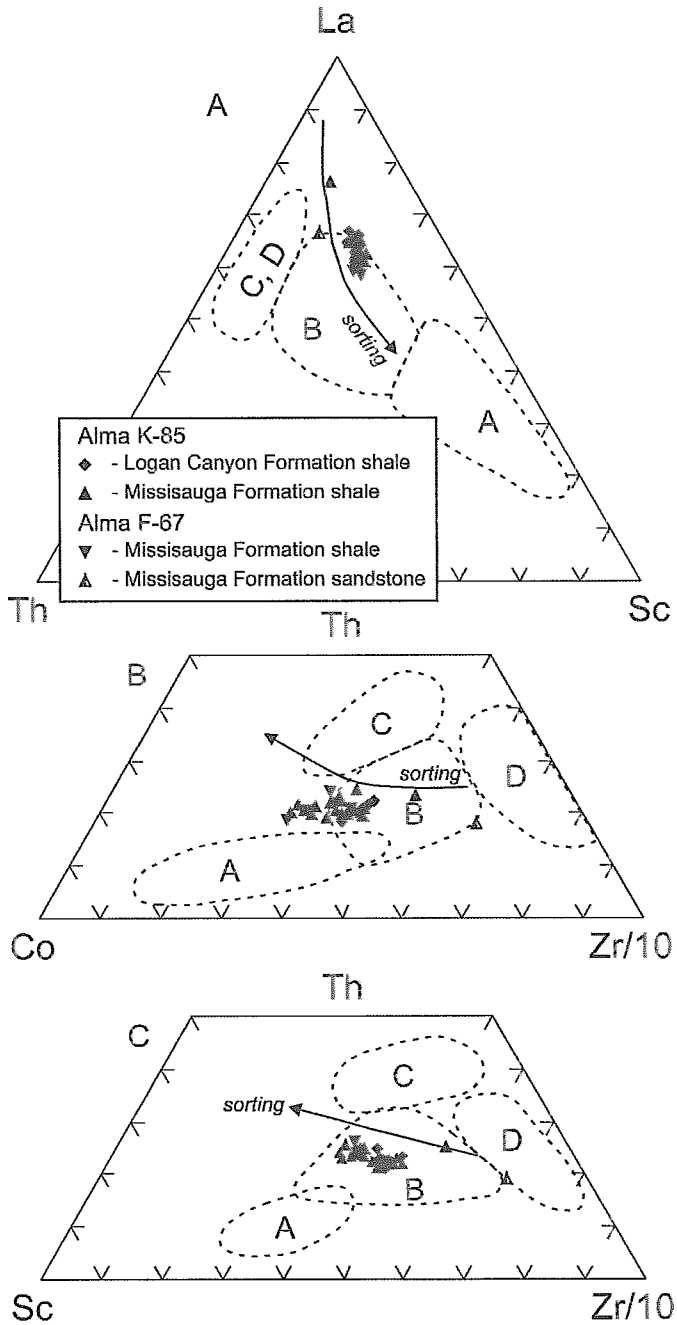

Figure 16 A: La - Th - Sc plot. B: Th - Co - Zr/10 plot. C: Th - Sc - Zr/10 plot. All fields from Bhatia and Crook (1986): A = oceanic island arc; B = continental island arc; C = active continental margin; D = passive margin. Sorting curves from Gu et al. (2002). Same symbols are used in all diagrams.

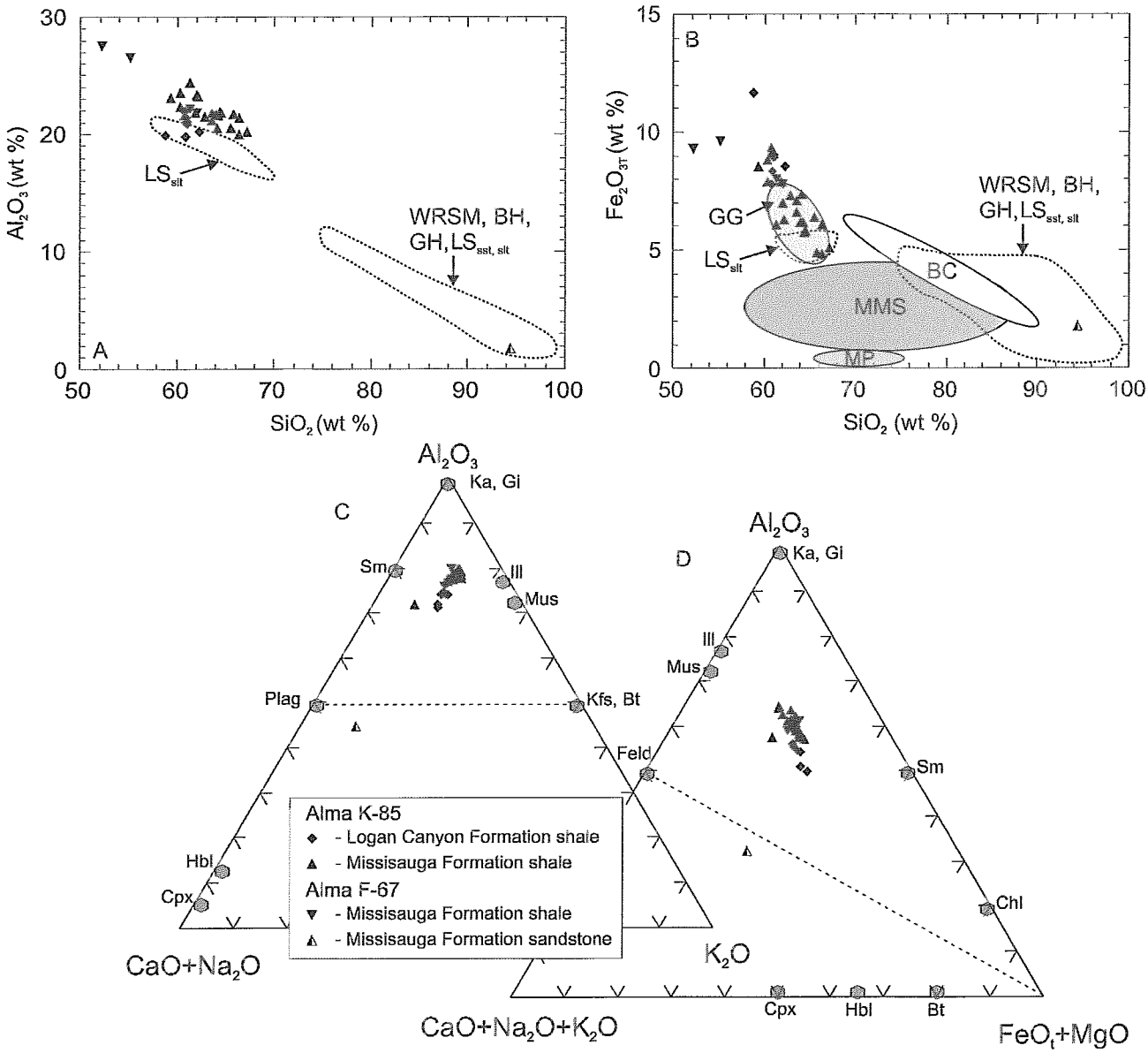

Figure 17: A: Al_2O_3 vs. SiO_2 wt % plot. LS_{sst} = Little Stewiacke sandstone, WRSM = West River St. Marys, BH = Barren Hills, GH = Graham Hill, LS_{slt} = Little Stewiacke siltstone (same for B.) B: Fe_2O_{3t} vs. SiO_2 wt % plot. Fields from Murphy (2000): GG = Neoproterozoic Georgeville Group, BC = Lower Silurian Beechill Cove Formation, MMS = Meguma Group metasedimentary rocks and MP = Meguma granitoid plutons. C: Al_2O_3 - $CaO+Na_2O$ - K_2O ternary plot and D: Al_2O_3 - $CaO+Na_2O+K_2O$ - FeO_t+MgO molar proportions (after Murphy, 2000; Nesbitt and Young, 1996; Nesbitt et al., 1996). mineral field abbreviations: Cpx = clinopyroxene, Hbl = hornblende, Bt = biotite, Chl = chlorite, Sm = smectite, Ka = kaolinite, Gi = gibbsite, Ill = illite, Mus = muscovite, Feld = feldspars, Kfs = K-feldspar, Plag = plagioclase. Same symbols used in all plots.

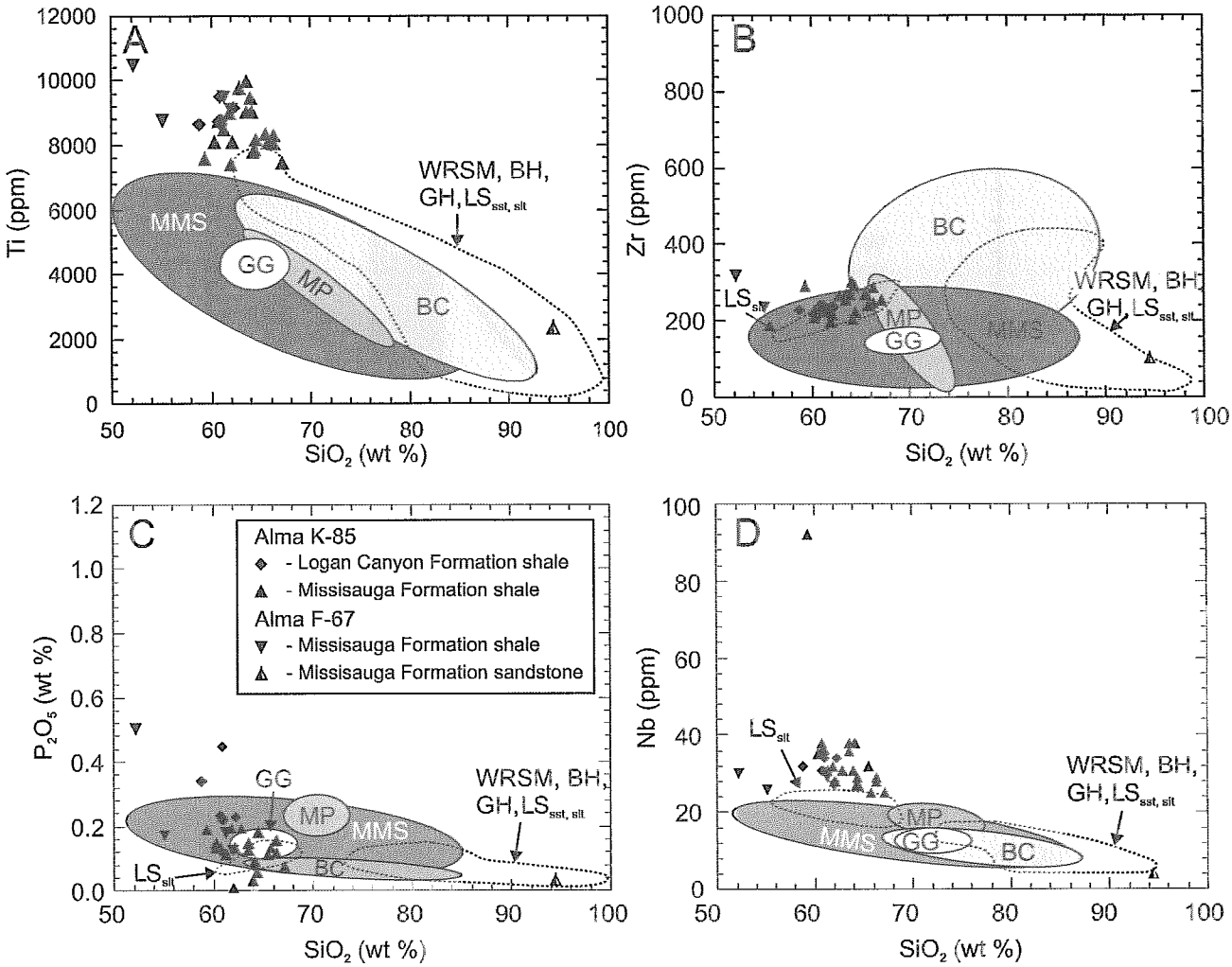

Figure 18: Selected Harker diagrams of major and trace elements. Fields are modified from Murphy (2000). A: Ti vs. SiO_2. B: Zr vs. SiO_2. LS_{sst} = Little Stewiacke sandstone, WRSM = West River St. Marys, BH = Barren Hills, GH = Graham Hill, Ls_{slt} = Little Stewiacke siltstone (same for all plots). C: P_2O_5 vs SiO_2. D: Nb vs SiO_2. MMS = Meguma Group metasedimentary rocks, MP = Meguma granitoid plutons, BC = Beechill Cove Formation and GG = Georgeville Group. Legend is the same for all plots.

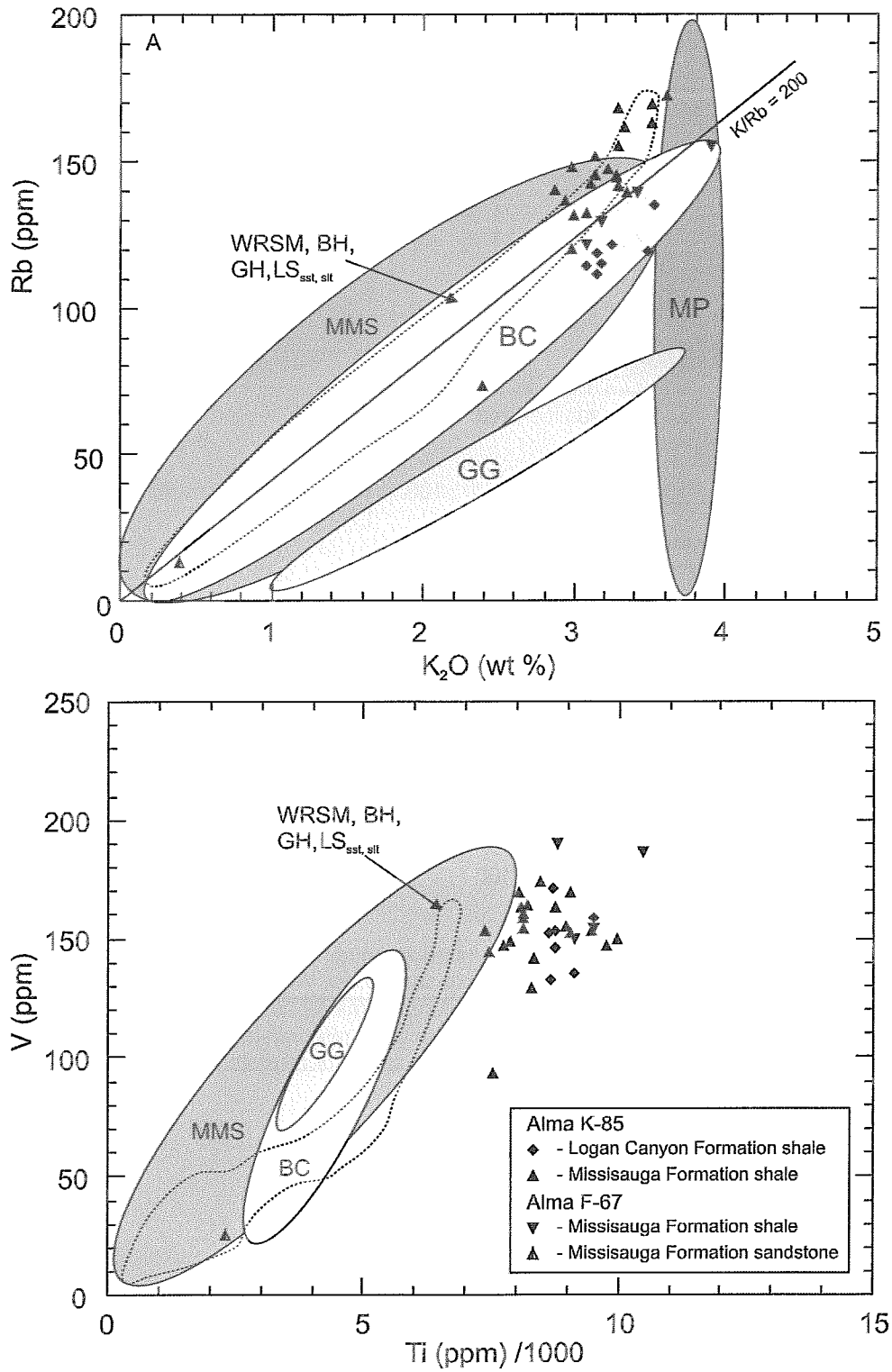

Figure 19: A: Rb vs. K_2O wt % plot. B: V vs. Ti/1000 ppm plot. Fields after Murphy (2000) MMS = Meguma Group metasedimentary rocks; MP = Meguma granitoid plutons; BC = Beechill Cove Formation; GG = Georgeville Group; LS_{sst} = Little Stewiacke sandstone; LS_{slt}, = Little Stewiacke siltstone; BH = Barren Hills; GH = Graham Hill; WRSM = West River St. Marys. Same legend for both plots.

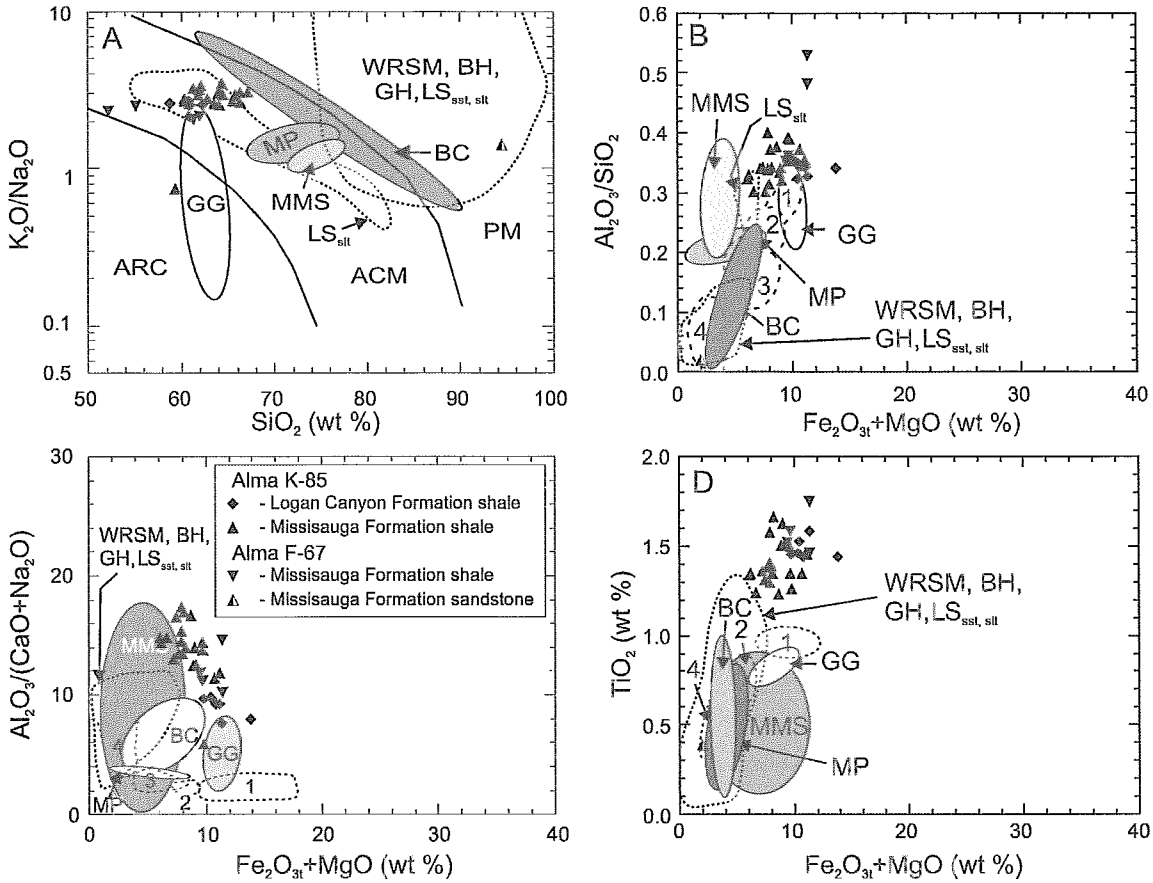

Figure 20: A: K_2O/Na_2O vs SiO_2 (wt %) plot. B: Al_2O_3/SiO_2 vs Fe_2O_{3t}+MgO (wt %) plot. C: $Al_2O_3/(CaO+Na_2O)$ vs Fe_2O_{3t}+MgO (wt %) plot. D: TiO_2 vs Fe_2O_{3t}+MgO (wt %) plot. Solid-line fields after Murphy (2000), doted-line fields have been drawn with data from Murphy (2000). MMS = Meguma Group metasedimentary rocks; MP = Meguma granitoid plutons; GG = Georgeville Group; and, BC = Beechill Cove Formation. In A discrimination fields modified from Roser and Korch, 1986: ARC = volcanic arc; ACM = active continental margin, and, PM = passive margin. In B, C and D tectonic setting fields after Bhatia, 1983: 1 = oceanic island arc, 2 = continental island arc, 3 = active continental margin, 4 = passive margin; LS_{sst} = Little Stewiacke sandstone, LS_{slt} = Little Stewiacke siltstone, BH = Barren Hills, GH = Graham Hill, WRSM = West River St. Marys. Legend is the same for all plots.

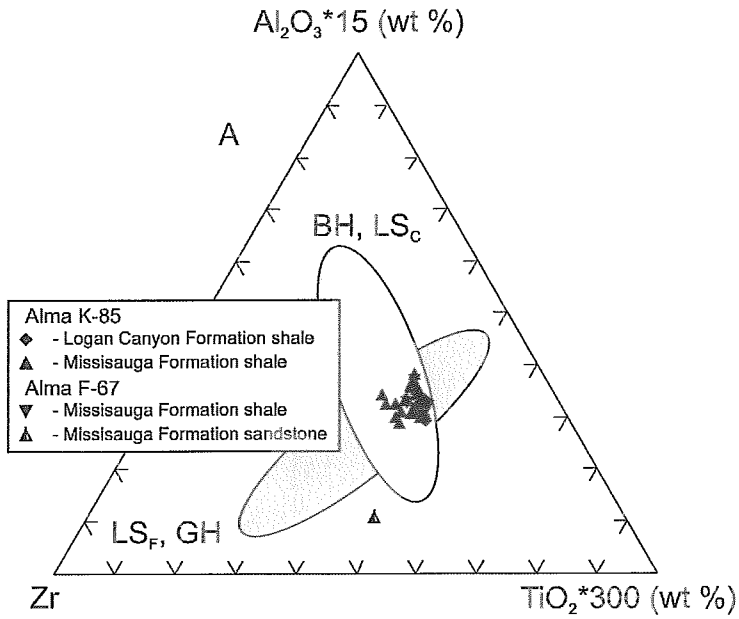

Figure 21: A: Al_2O_3*15 (wt %)- Zr (ppm)-TiO_2*300 (wt %) plot after Garcia et al. (1994) and La Flèche and Camiré (1995) comparing the fine-grained Little Stewiacke (LS_F) and Graham Hill (GH) rocks (ellipse pointing towards the Zr apex) as well as the coarse-grained Little Stewiacke (LS_C) and Barren Hills (BH) rocks (ellipse pointing towards the Al_2O_3 apex) with the Alma K-85 shales (modified from Murphy 2000).

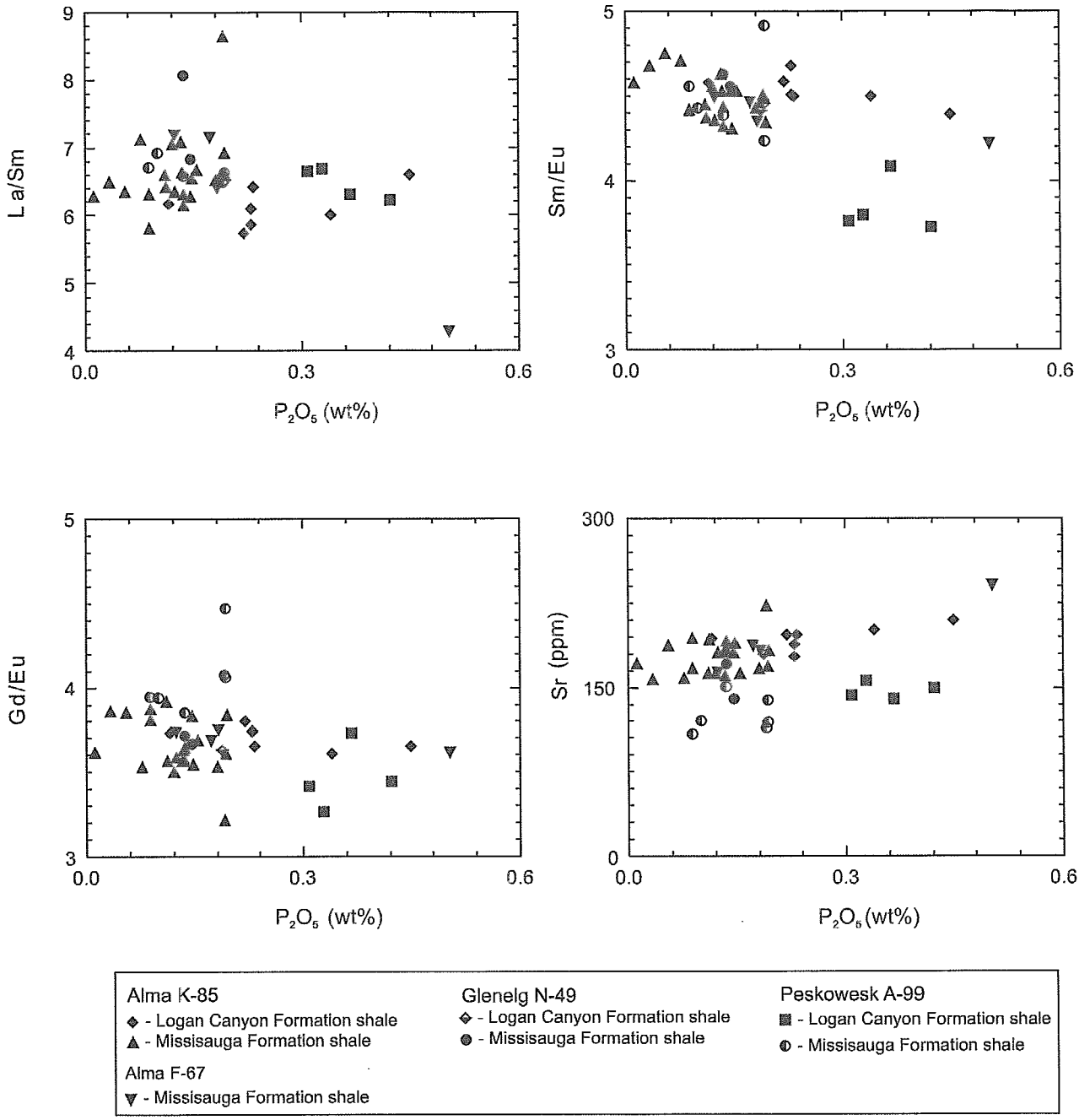

Figure 22: La/Sm vs P_2O_5, Sm/Eu vs P_2O_5, Gd/Eu vs P_2O_5 and Sr vs P_2O_5 plots for normal mudrocks-shales.

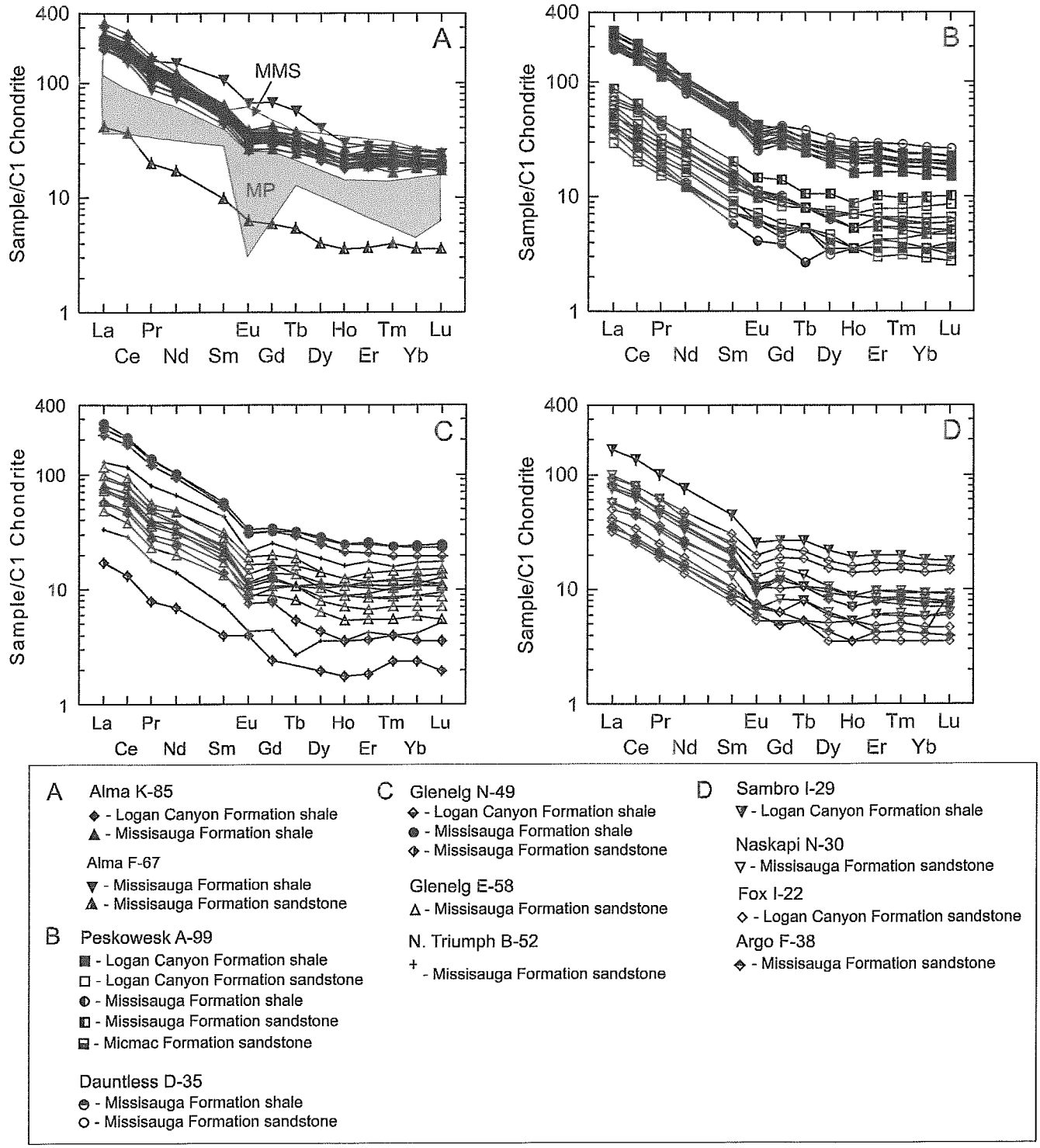

Figure 23: Rare Earth Element Plots: MMS = Meguma Group meta-sedimentary rocks, MG = Meguma granitoid plutons. Fields are from Murphy (2000). A: Alma K-85 and Alma F-67; B: Peskowesk A-99 and Dauntless D-35; C: Glenelg N-49, Glenelg E-58 and N. Triumph B-52; D: Sambro I-29, Naskapi N-30, Fox I-22 and Crow F-52.

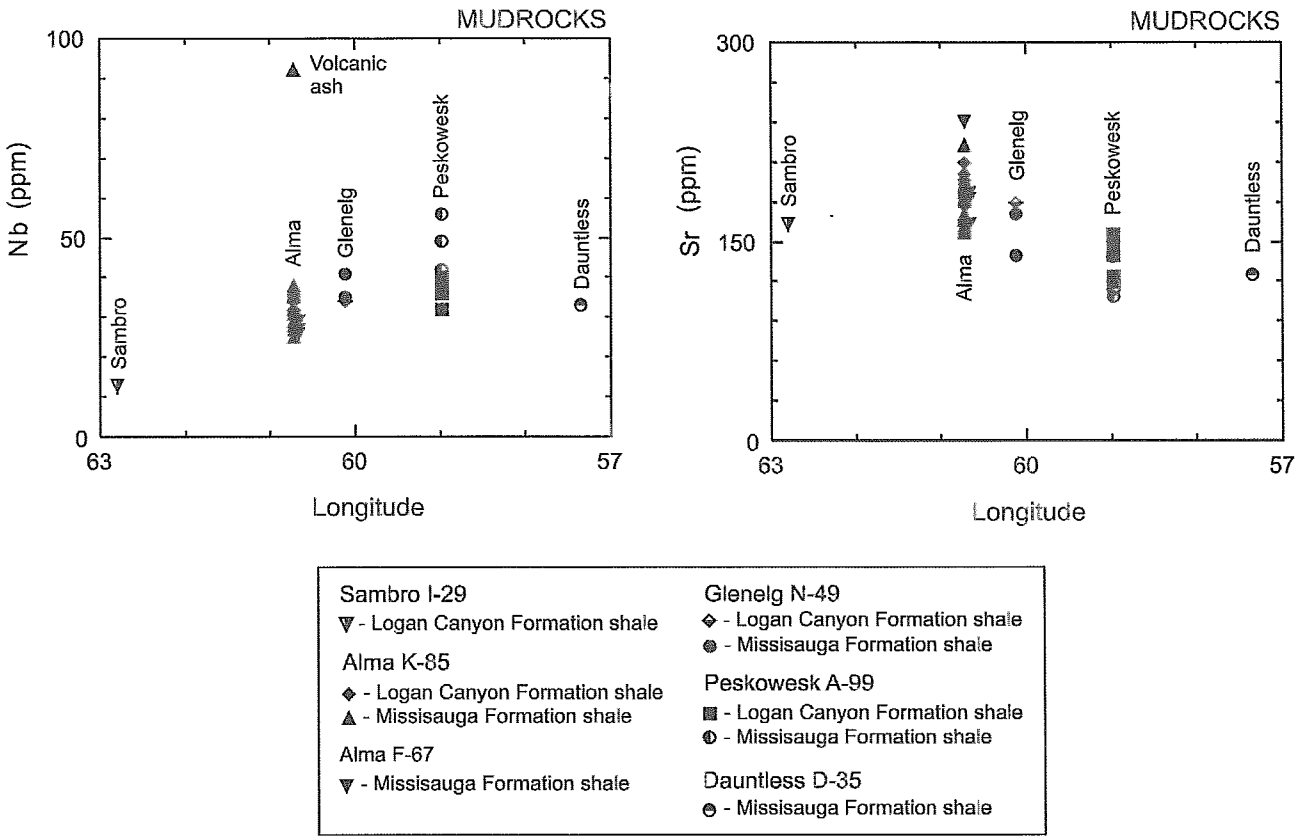

Figure 24: Nb and Sr vs longitude plot for mudrocks and corrected abnormal mudrocks

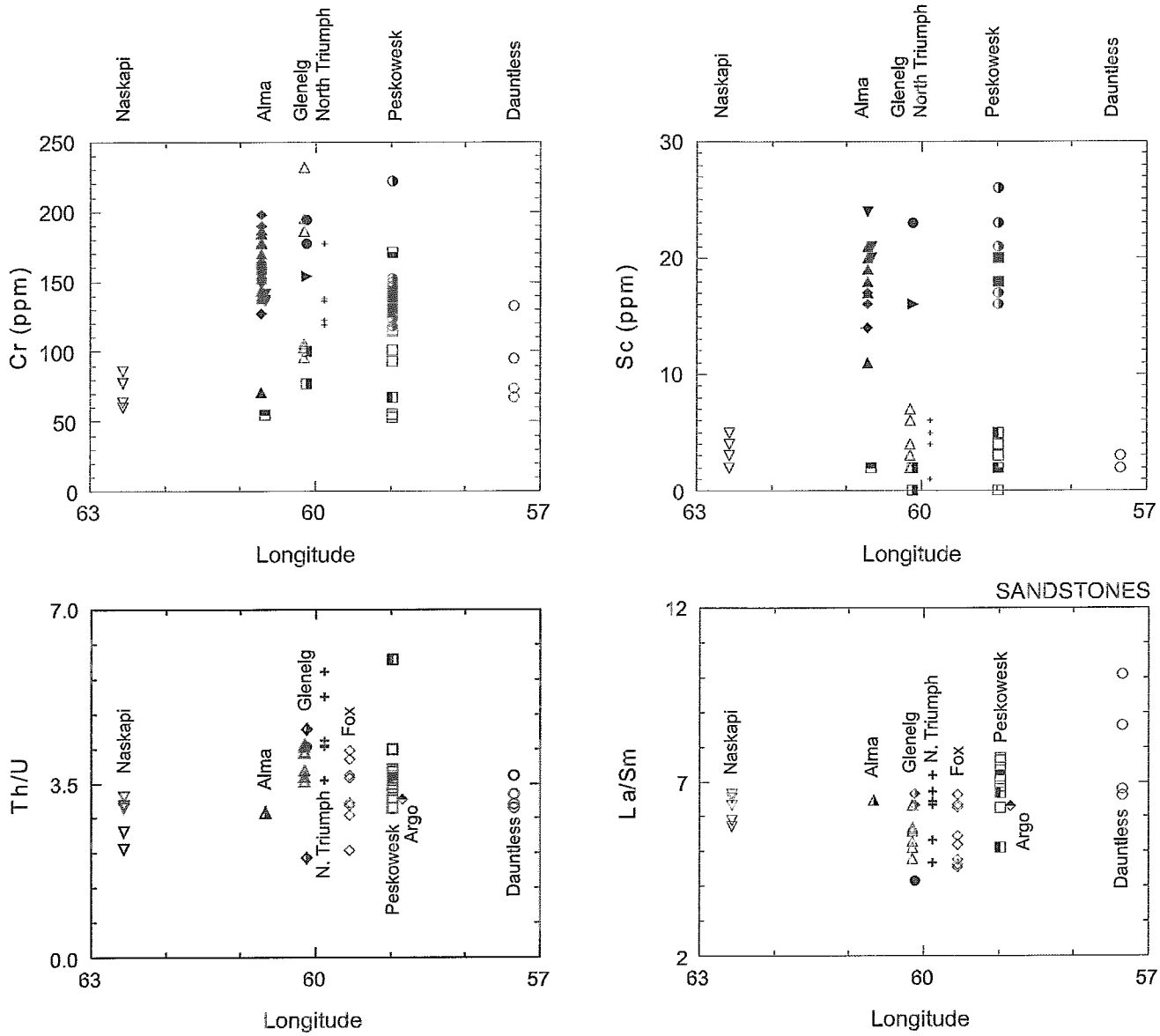

Naskapi N-30
▽ - Missisauga Formation sandstone

Alma F-67
▲ - Missisauga Formation sandstone

Glenelg N-49
● - Missisauga Formation shale*
◆ - Missisauga Formation sandstone

Glenelg E-58
△ - Missisauga Formation sandstone

N. Triumph B-52
+ - Missisauga Formation sandstone

Fox I-22
◇ - Logan Canyon Formation sandstone

Argo F-38
◆ - Missisauga Formation sandstone

Peskowesk A-99
□ - Logan Canyon Formation sandstone
◧ - Missisauga Formation sandstone
▣ - Micmac Formation sandstone

Dauntless D-35
○ - Missisauga Formation sandstone

* Although the sample is a shale, after the correction is considered as a sandstone

Figure 25: Cr vs. longitude and Sc vs. longitude for all normal samples; Th/U vs longitude and La/Sm vs longitude plots for sandstones and corrected abnormal sandstones.

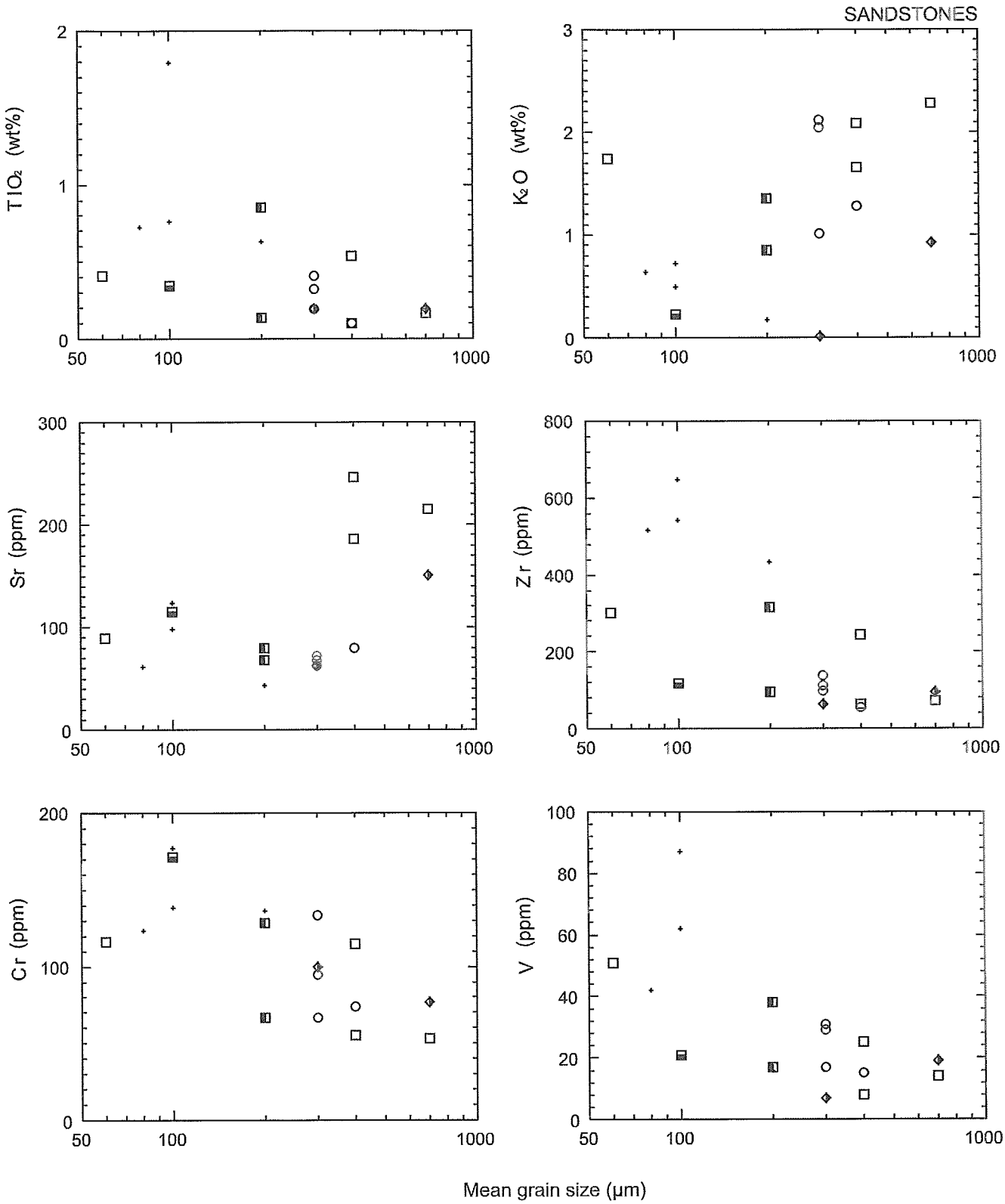

Figure 26: TiO_2, K_2O, Sr, Zr, Cr and V vs mean grain size of framework grains (µm) for all normal sandstones.

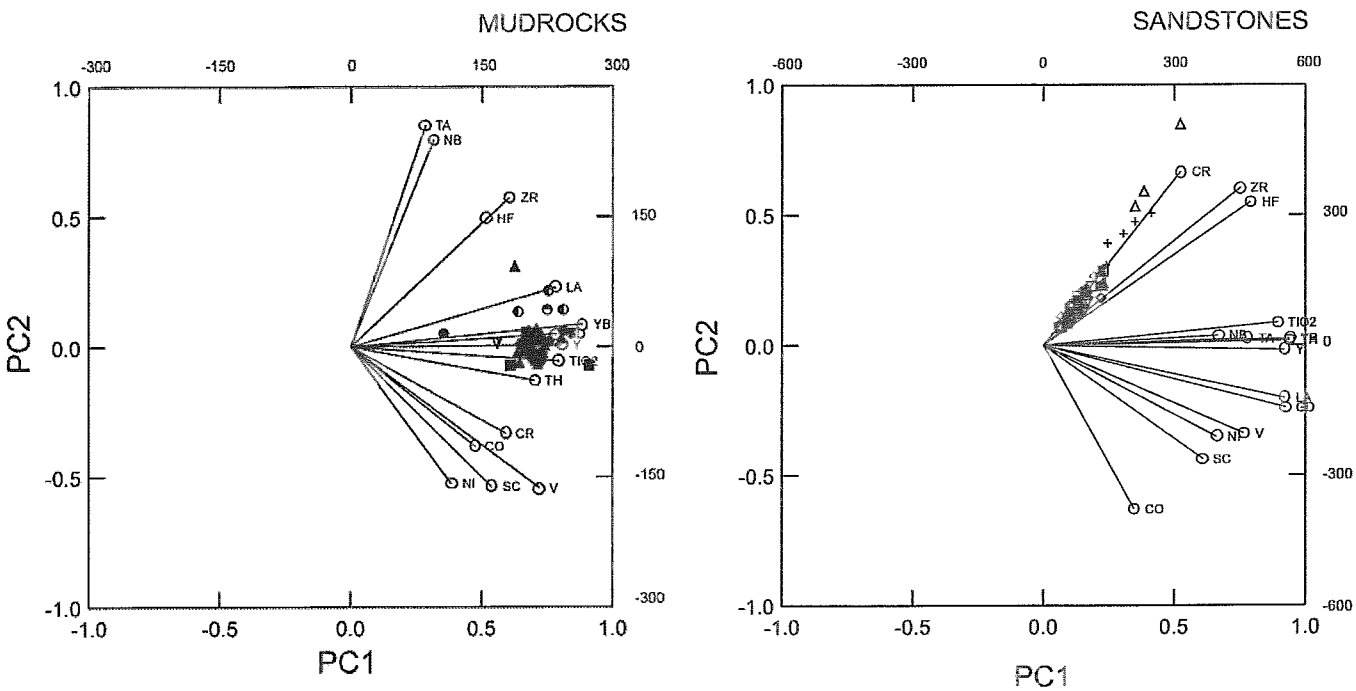

Sambro I-29
▼ - Logan Canyon Formation shale

Alma K-85
◆ - Logan Canyon Formation shale
▲ - Missisauga Formation shale

Alma F-67
▼ - Missisauga Formation shale

Glenelg N-49
◆ - Logan Canyon Formation shale
● - Missisauga Formation shale

Peskowesk A-99
■ - Logan Canyon Formation shale
◐ - Missisauga Formation shale

Dauntless D-35
◓ - Missisauga Formation shale

Naskapi N-30
▽ - Missisauga Formation sandstone

Alma F-67
△ - Missisauga Formation sandstone

Glenelg N-49
● - Missisauga Formation shale*
◇ - Missisauga Formation sandstone

Glenelg E-58
△ - Missisauga Formation sandstone

N. Triumph B-52
+ - Missisauga Formation sandstone

Fox I-22
◇ - Logan Canyon Formation sandstone

Argo F-38
◆ - Missisauga Formation sandstone

Peskowesk A-99
□ - Logan Canyon Formation sandstone
▣ - Missisauga Formation sandstone
▬ - Micmac Formation sandstone

Dauntless D-35
○ - Missisauga Formation sandstone

Figure 27: Principal component analysis of normal mudrock and sandstone samples.

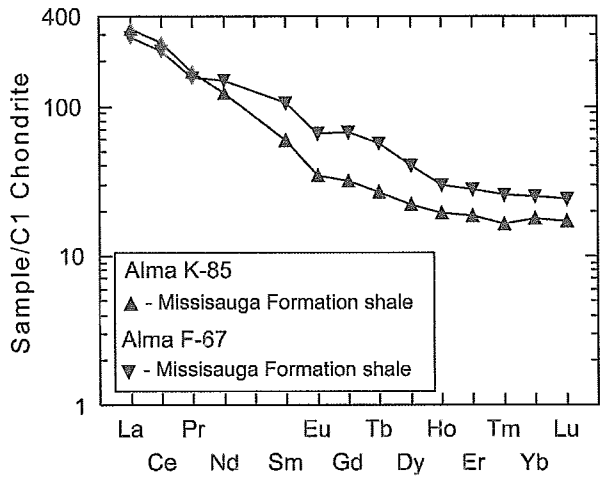

Figure 28: REE plot of samples 2912.04 and 2847.10 from Alma

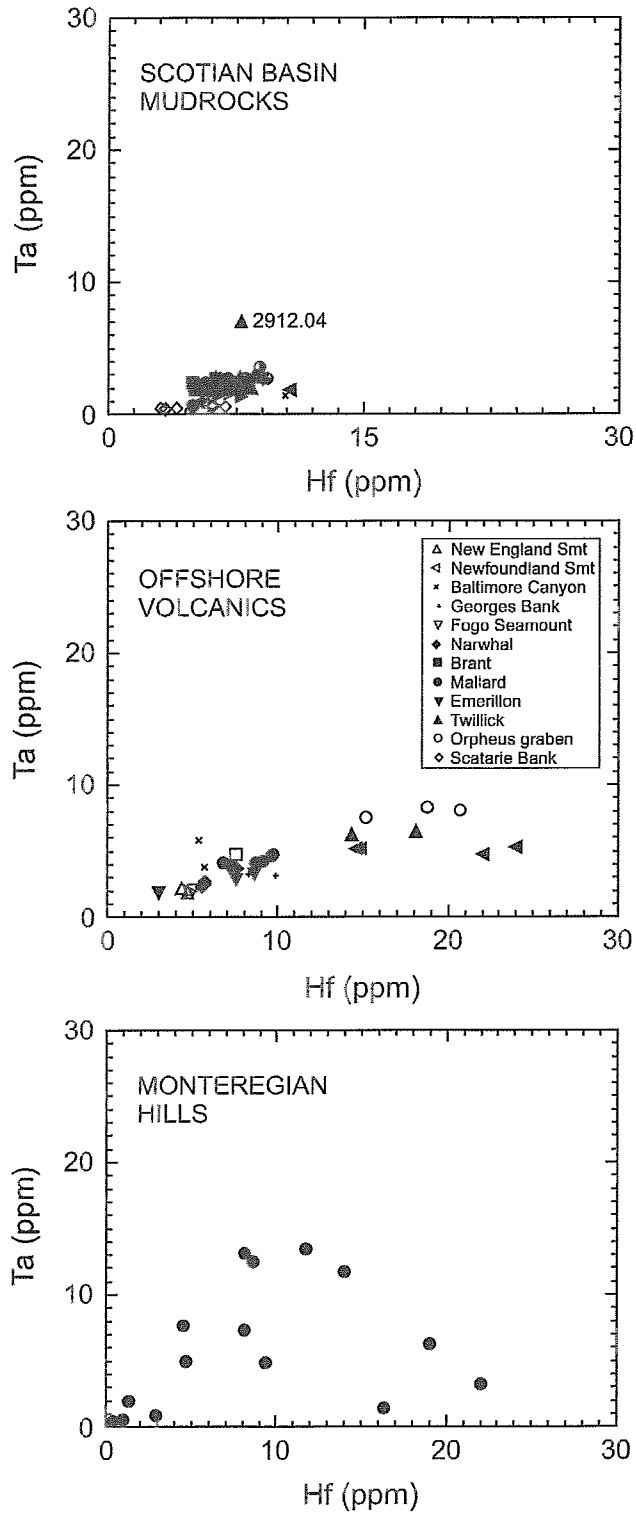

Figure 29. Comparison of Ta and Hf contents of Scotian Basin mudrocks compared with offshore Cretaceous volcanic rocks and the Cretaceous igneous rocks of the Monteregian Hills. Data sources for the igneous rocks summarized in Pe-Piper et al. (2006b).

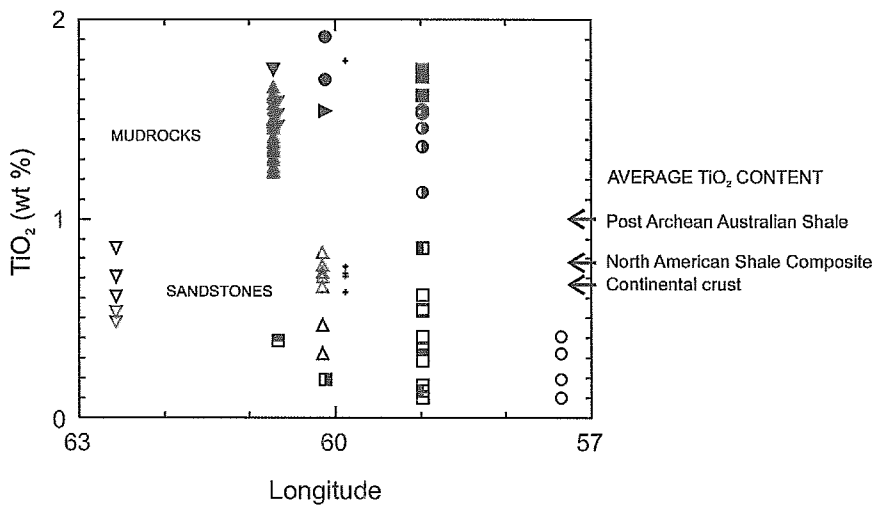

Figure 30: TiO_2 vs. longitude plot for all normal analyses. Average TiO_2 values from Lentz (2003).

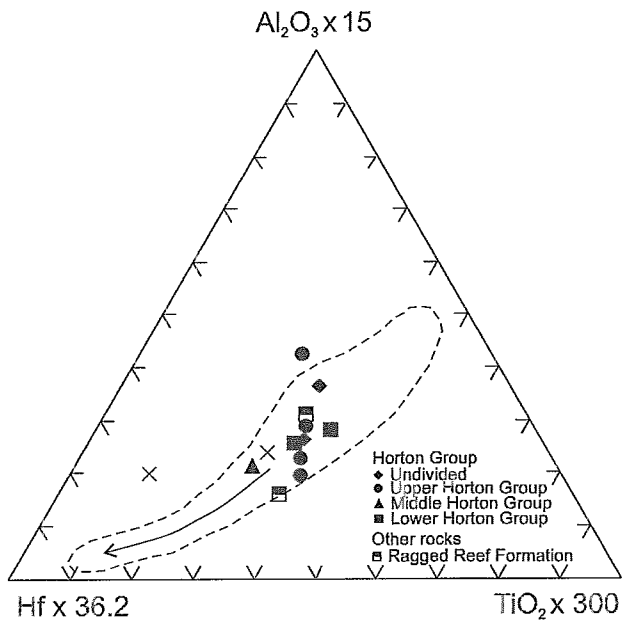

Figure 31: (Al_2O_3 x 15) - (Hf x 36.2) - (TiO_2 x 300) plot for first cycle Carboniferous sandstones of northern Nova Scotia. Fields after Garcia et al., 1994 and LaFlèche and Camiré, 1996.

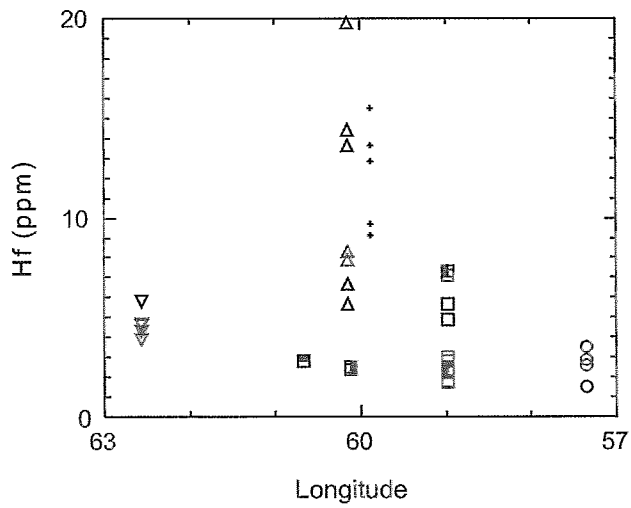

Figure 32: Hf vs. longitude plot for all normal sandstone analyses.

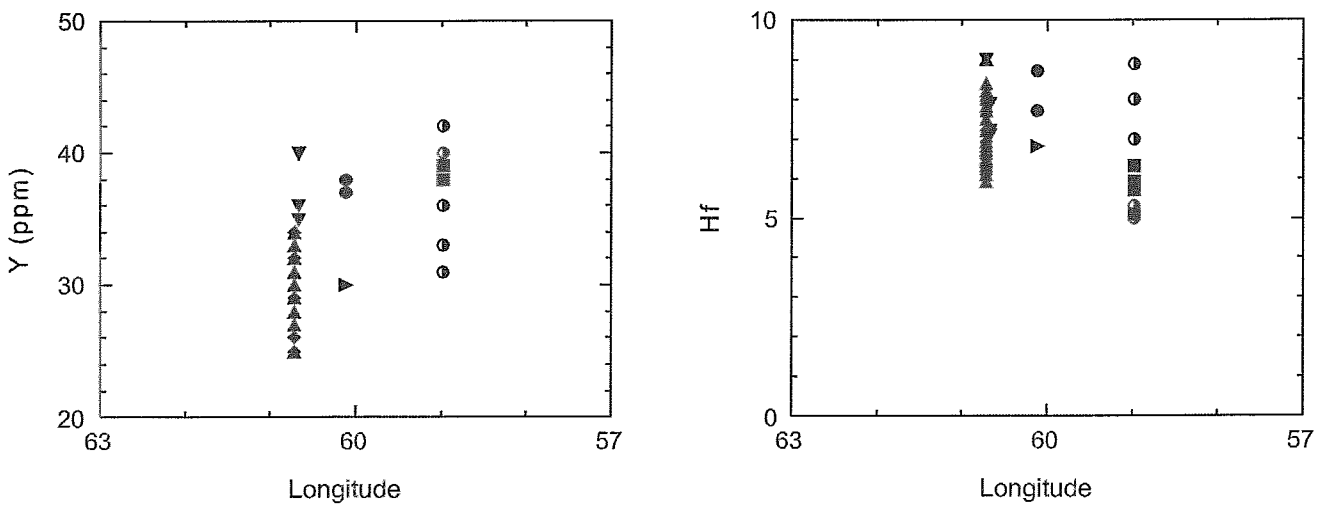

Figure 33: Hf and Y vs. longitude plot for all normal mudstone analyses.

Table 1: Location and other information on analytical samples

File #	Sample Type[1]	Well	Depth (m)	Depth (ft)	Formation (member)	Facies[2]	Lithology[3]	MGS[4] (µm)	Type of cement[5]
14-224	X	Alma (K-85)	2449.40	8036.09	Logan Canyon (Cree)	8	mds		
16-57	X	Alma (K-85)	2453.85	8050.69	Logan Canyon (Cree)	6	sh		
16-58	X	Alma (K-85)	2455.00	8054.46	Logan Canyon (Cree)	6	sh		
16-59	X	Alma (K-85)	2456.40	8059.06	Logan Canyon (Cree)	6	sh		
14-225	X	Alma (K-85)	2456.50	8059.38	Logan Canyon (Cree)	6	mds		
16-60	X	Alma (K-85)	2458.15	8064.80	Logan Canyon (Cree)	6	sh		
16-61	X	Alma (K-85)	2460.75	8073.33	Logan Canyon (Cree)	6	sh		
14-226	X	Alma (K-85)	2878.90	9445.21	Missisauga (Upper member)	1,2	mds		
14-227	X	Alma (K-85)	2880.22	9449.54	Missisauga (Upper member)	1,2	mds		
14-228	X	Alma (K-85)	2888.26	9475.92	Missisauga (Upper member)	1,2	mds		
14-229	X	Alma (K-85)	2904.15	9528.05	Missisauga (Upper member)	1,2	mds		
14-230	X	Alma (K-85)	2906.78	9536.68	Missisauga (Upper member)	1,2	mds		
14-231	X	Alma (K-85)	2912.04	9553.94	Missisauga (Upper member)	1,2	mds		
16-62	X	Alma (K-85)	2919.00	9576.77	Missisauga (Upper member)	1	sh		
16-63	X	Alma (K-85)	2919.45	9578.25	Missisauga (Upper member)	1	sh		
14-232	X	Alma (K-85)	2920.30	9581.04	Missisauga (Upper member)	1	mds		
16-64	X	Alma (K-85)	2931.87	9619.00	Missisauga (Upper member)	1	sh		
16-65	X	Alma (K-85)	3038.00	9967.19	Missisauga (Upper member)	3	sh		
14-233	X	Alma (K-85)	3039.88	9973.36	Missisauga (Upper member)	1	mds		
16-66	X	Alma (K-85)	3044.60	9988.85	Missisauga (Upper member)	2	sh		
16-67	X	Alma (K-85)	3047.90	9999.67	Missisauga (Upper member)	1	sh		
16-68	X	Alma (K-85)	3068.15	10066.11	Missisauga (Upper member)	1	sh		
16-69	X	Alma (K-85)	3071.80	10078.08	Missisauga (Upper member)	2	sh		
16-70	X	Alma (K-85)	3089.05	10134.68	Missisauga (Upper member)	1	sh		
16-71	X	Alma (K-85)	3090.45	10139.27	Missisauga (Upper member)	1	sh		
16-72	X	Alma (K-85)	3093.80	10150.26	Missisauga (Upper member)	1	sh		
14-234	X	Alma (K-85)	3104.10	10184.06	Missisauga (Upper member)	2	mds		
16-73	X	Alma (K-85)	3104.70	10186.02	Missisauga (Upper member)	1	sh		
14-579	X	Alma (F-67)	2847.10	9340.88	Missisauga (Upper member)	4	sh		
14-580	X	Alma (F-67)	2851.77	9356.20	Missisauga (Upper member)	4	sh		
14-581	X	Alma (F-67)	2852.85	9359.74	Missisauga (Upper member)	1	sh		
14-582	X	Alma (F-67)	2853.30	9361.22	Missisauga (Upper member)	1	sh		
14-583	X	Alma (F-67)	2879.65	9447.67	Missisauga (Upper member)	2	ss	600	sil, lm, cal
14-584	X	Alma (F-67)	2884.30	9462.93	Missisauga (Upper member)	2	ss	130	sil, cal, chl,
14-235	X	Glenelg (N-49)	3007.53	9867.22	Logan Canyon (Cree)	1,2	mds		
14-567	X	Glenelg (N-49)	3576.78	11734.84	Missisauga (Upper member)	1,2	sh		
14-568	X	Glenelg (N-49)	3596.89	11800.82	Missisauga (Upper member)	4	ss	300	sil, py
14-236	X	Glenelg (N-49)	3622.08	11883.46	Missisauga (Upper member)	4	mds		
14-569	X	Glenelg (N-49)	3628.43A	11904.30	Missisauga (Upper member)	4	ss	540	sil, kln, cal
14-237	X	Glenelg (N-49)	3628.43B	11904.30	Missisauga (Upper member)	4	mds		
14-570	X	Glenelg (N-49)	3628.92	11905.91	Missisauga (Upper member)	4	ss	700	dol, sil, py
14-572	X	Glenelg (E-58)	3526.28	11569.16	Missisauga (Upper member)	1	ss	1500	cal, sd, dol, sil
14-573	X	Glenelg (E-58)	3528.08A	11575.07	Missisauga (Upper member)	1	ss	140	sil, cal, kln
14-571	X	Glenelg (E-58)	3528.08B	11575.07	Missisauga (Upper member)	1	ss	140	sil, cal, kln
14-574	X	Glenelg (E-58)	3530.06	11581.56	Missisauga (Upper member)	1	ss	1500	cal, sd, sil
14-575	X	Glenelg (E-58)	3530.3A	11582.35	Missisauga (Upper member)	1	ss	1500	cal, sd, sil
14-577	X	Glenelg (E-58)	3535.3B	11598.75	Missisauga (Upper member)	1	ss	1500	cal, sd, sil
14-576	X	Glenelg (E-58)	3535.35	11598.92	Missisauga (Upper member)	1	ss	150	sd, cal, sil
14-578	X	Glenelg (E-58)	3710.80	12174.54	Missisauga (Upper member)	4	ss	120	cal, sd, qz
14-239	X	N.Triumph(B-52)	3771.30	12373.03	Missisauga (Upper member)	5	ss	100	sil, sd, cal, chl, py
14-240	X	N.Triumph(B-52)	3776.62	12390.49	Missisauga (Upper member)	4	ss	80	sd, sil, cal, clays
14-238	X	N.Triumph(B-52)	3784.17	12415.26	Missisauga (Upper member)	8	css	100	cal, glt, py
14-241	X	N.Triumph(B-52)	3791.95	12440.78	Missisauga (Upper member)	4	ss	180	cal, kln, chl
14-242	X	N.Triumph(B-52)	3798.95	12463.75	Missisauga (Upper member)	8	ss	100	sil, sd, cal, py
14-243	X	N.Triumph(B-52)	3803.50	12478.67	Missisauga (Upper member)	4	ss	80	sil, sd, cal, py, chl
14-244	X	N.Triumph(B-52)	3809.98	12499.93	Missisauga (Upper member)	4	ss	200	sil, sd, py
14-461	X	Sambro (I-29)	883.88	2899.87	Logan Canyon	5	mds		
14-422	X	Naskapi (N-30)	1469.00	4819.55	Missisauga (Upper member)		ss	300	kln, ill, lm, sil
14-423	X	Naskapi (N-30)	1469.89	4822.47	Missisauga (Upper member)		ss	700	py, kln, ill, lm
14-424	X	Naskapi (N-30)	1471.75	4828.58	Missisauga (Upper member)		ss	240	py, ill
14-425	X	Naskapi (N-30)	1472.25	4830.22	Missisauga (Upper member)		ss	100	py
14-426	X	Naskapi (N-30)	1473.81	4835.33	Missisauga (Upper member)		ss	1100	kln, ill, py, sil
14-428	X	Dauntless (D-35)	3162.76	10376.51	Missisauga (Upper member)	4	ss	300	sil, kln, chl, py
14-432	X	Dauntless (D-35)	3163.21	10377.99	Missisauga (Upper member)	4	sh		
14-429	X	Dauntless (D-35)	3164.43	10381.99	Missisauga (Upper member)	4	ss	300	sil, kln, chl, py
14-430	X	Dauntless (D-35)	3165.04	10383.99	Missisauga (Upper member)	4	ss	300	sil, chl, kln, py
14-431	X	Dauntless (D-35)	3165.65	10385.99	Missisauga (Upper member)	4	ss	400	chl, sil, kln, py

Table 1 continued

File #	Sample Type[1]	Well	Depth (m)	Depth (ft)	Formation (member)	Facies[2]	Lithology[3]	MGS[4] (µm)	Type of cement[5]
14-535	X	Peskowesk (A-99)	2209.25	7248.20	Logan Canyon (Cree Member)	5	sh		
14-524	X	Peskowesk (A-99)	2210.37	7251.87	Logan Canyon (Cree Member)	4	ss	250	chl, sil, ill, py
14-536	X	Peskowesk (A-99)	2213.57	7262.37	Logan Canyon (Cree Member)	6	sh		
14-537	X	Peskowesk (A-99)	2215.78	7269.62	Logan Canyon (Cree Member)	5	sh		
14-538	X	Peskowesk (A-99)	2219.03	7280.28	Logan Canyon (Cree Member)	5	sh		
14-539	X	Peskowesk (A-99)	2221.69	7289.01	Logan Canyon (Cree Member)	3	sh		
14-540	X	Peskowesk (A-99)	2228.42	7311.09	Logan Canyon (Cree Member)	4	sh		
14-526	X	Peskowesk (A-99)	2233.62A	7328.15	Logan Canyon (Cree Member)	4	ss	700	chl, sil, ill, sd
14-525	X	Peskowesk (A-99)	2233.62B	7328.15	Logan Canyon (Cree Member)	4	ss	700	chl, sil, ill, sd
14-527	X	Peskowesk (A-99)	2233.62	7328.15	Logan Canyon (Cree Member)	4	ss	700	chl, sil, ill, sd
14-528	X	Peskowesk (A-99)	2238.65	7344.65	Logan Canyon (Cree Member)	4	ss	400	sil, chl, ill
14-529	X	Peskowesk (A-99)	2267.67	7439.86	Logan Canyon (Cree Member)	4	ss	400	sil, chl, kln, sd
14-530	X	Peskowesk (A-99)	2276.11	7467.55	Logan Canyon (Cree Member)	3	ss	60	sd
14-541	X	Peskowesk (A-99)	2479.35	8134.35	Missisauga (Upper member)	6	sh		
14-531	X	Peskowesk (A-99)	2482.14	8143.50	Missisauga (Upper member)	2	ss	200	sil, chl, ill, kln, py
14-542	X	Peskowesk (A-99)	2488.85	8165.52	Missisauga (Upper member)	6	sh		
14-543	X	Peskowesk (A-99)	2492.62	8177.89	Missisauga (Upper member)	3	sh		
14-544	X	Peskowesk (A-99)	2927.36	9604.20	Missisauga (Upper member)	6	sh		
14-532	X	Peskowesk (A-99)	2933.62	9624.74	Missisauga (Upper member)	2	ss	200	cal, chl, py
14-533	X	Peskowesk (A-99)	2940.48	9647.24	Missisauga (Upper member)	2	sh		
14-545	X	Peskowesk (A-99)	2940.90	9648.62	Missisauga (Upper member)	6	sh		
14-546	X	Peskowesk (A-99)	2947.43	9670.05	Missisauga (Upper member)	6	sh		
14-534	X	Peskowesk (A-99)	3796.33	12455.15	Micmac Formation	2	ss	100	sil, cal, py
14-547	X	Peskowesk (A-99)	3806.51	12488.55	Micmac Formation	1	cslt		
14-548	X	Peskowesk (A-99)	3812.64	12508.66	Micmac Formation	1	cmds		
14-451	C	Fox (I-22)	316.98 (2)	1039.96	Logan Canyon (Marmora)	5	sss		sd, cal
14-450	C	Fox (I-22)	316.99 (1)	1039.99	Logan Canyon (Marmora)	5	sss		sd, cal
14-452	C	Fox (I-22)	362.69 (3)	1189.93	Logan Canyon (Sable)	5	sss		sd, cal, ill
14-453	C	Fox (I-22)	408.41 (4)	1339.93	Logan Canyon (Cree)	6	css		
14-454	C	Fox (I-22)	417.56 (5)	1369.95	Logan Canyon (Cree)	5	sss		
14-455	C	Fox (I-22)	417.561 (6	1369.95	Logan Canyon (Cree)	7	css		
14-456	C	Fox (I-22)	454.13 (7)	1489.93	Logan Canyon (Cree)	5	csss		
14-457	C	Fox (I-22)	499.85 (8)	1639.93	Logan Canyon (Cree)	1	scss		
14-458	C	Crow (F-52)	600.46	1970.01	Logan Canyon (Sable)	2	sss		sd, chl
14-459	C	Argo (F-38)	579.12	1900.00	Logan Canyon (Marmora)	3	sss		sd, ill, kln, phs, py
14-460	C	Argo (F-38)	1426.48	4680.05	Missisauga (Middle member)	4	css		cal, chl, sd

Footnotes

[1]Type of sample
C: cuttings
X: core

[2]Facies
1: bioturbated mudstone
2: bioturbated fine sandstone
3: bioturbated shelly, sandy mudstone
4: fine to coarse sandstone, interbedded mudstone
5: fine sandstone, mudstone
6: laminated mudstone and siltstone
7: coal
8: gray-green sandy, highly bioturbated mudstone
9: oolithic limestone

[3]Lithology
ss: sandstone
mds: mudstone
sh: shale
fss: fine grained sandstone
cslt: calcite cemented siltstone
sss: siderite cements sandstone
csss: calcite siderite cemented sandstone
scss: siderite calcite cemented sandstone
cmds: calcite cemented mudstone
css: calcite cemented sandstone

[4]MGS Mean grain size of framework grains (µm)

[5]Type of cement
sil: silica
dol: dolomite
cal: calcite
py: pyrite
glt: glauconite
chl: chlorite
ill: illite
kln: kaolinite
sd: siderite
phs: phosphates
lm: limonite

Table 2: Representative whole rock analyses from offshore Cretaceous sediments

Well	Alma K-85								
Formation	Logan Canyon							Missisauga	
Depth (m)	2449.40	2453.85	2455.00	2456.40	2456.50	2458.15	2460.75	2878.90	2880.22
Lithology[1]	mds	shale	shale	shale	mds	shale	shale	mds	mds
MGS[4] (μm)									
File	14-224	16-57	16-58	16-59	14-225	16-60	16-61	14-226	14-227
Major Elements (wt%)									
SiO_2	52.8	50.2	54.3	52.9	52.2	52.9	53.1	57.3	60.3
TiO_2	1.38	1.23	1.33	1.27	1.25	1.25	1.27	1.21	1.22
Al_2O_3	17.22	17.00	17.59	18.63	18.82	18.25	18.20	19.42	19.46
Fe_2O_{3t}	7.85	9.94	7.47	7.25	6.69	7.74	7.88	5.17	4.39
MnO	0.04	0.05	0.04	0.03	0.03	0.03	0.04	0.06	0.04
MgO	2.08	1.84	1.65	1.77	1.78	1.70	1.84	1.27	1.18
CaO	0.94	1.08	0.72	0.80	0.83	0.90	0.91	0.55	0.38
Na_2O	1.32	1.04	1.09	1.11	1.11	1.07	1.05	0.94	0.93
K_2O	2.81	2.68	2.77	3.02	3.02	2.72	2.67	2.78	2.84
P_2O_5	0.39	0.29	0.20	0.20	0.20	0.19	0.10	0.16	0.11
L.O.I	12.59	13.71	12.49	12.18	12.64	12.79	12.93	9.89	9.54
Total	99.45	99.03	99.69	99.15	98.53	99.52	100.00	98.77	100.33
CIA[3]	71.3	72.1	74.3	74.0	74.0	74.2	74.4	77.8	78.6
Trace Elements (ppm)									
Ba	423	425	442	426	407	459	517	330	341
Rb	121	111	115	119	135	118	114	145	151
Sr	210	201	177	188	197	197	194	167	162
Y	32	25	25	29	34	29	26	32	31
Zr	242	231	237	226	217	239	240	222	249
Nb	36	32	34	31	31	34	35	27	28
Pb	28	21	18	19	23	25	20	26	28
Ga	26	25	25	27	29	27	27	28	28
Zn	107	90	103	97	97	108	113	93	86
Cu	21	23	23	21	20	26	22	24	25
Ni	86	85	88	80	89	80	83	70	78
V	159	133	135	153	171	152	146	164	169
Cr	198	156	156	127	190	164	152	170	185
La	54.8	45.7	46.9	50.0	57.8	50.5	46.9	58.1	57.8
Ce	112.0	94.6	97.7	102.0	120.0	108.0	100.0	122.0	120.0
Pr	11.8	10.6	11.1	11.4	12.5	11.8	10.8	12.5	11.8
Nd	44.7	40.2	42.2	43.1	47.8	44.8	40.3	47.9	44.8
Sm	8.3	7.6	8.0	8.2	9.0	8.8	7.6	8.9	8.2
Eu	1.89	1.69	1.71	1.82	2.00	1.92	1.66	2.01	1.80
Gd	6.9	6.1	6.4	6.8	7.3	7.3	6.2	7.1	6.3
Tb	1.1	1.0	1.1	1.1	1.2	1.2	1.0	1.2	1.1
Dy	6.3	5.3	5.5	6.1	6.6	6.2	5.6	6.7	6.1
Ho	1.2	1.0	1.0	1.1	1.3	1.2	1.1	1.3	1.2
Er	3.5	3.3	3.4	3.5	3.6	3.6	3.3	3.6	3.5
Tm	0.47	0.51	0.51	0.53	0.47	0.55	0.53	0.49	0.49
Yb	3.2	3.3	3.1	3.4	3.4	3.4	3.3	3.3	3.3
Lu	0.48	0.48	0.46	0.48	0.49	0.48	0.48	0.49	0.49
Co	24	20	19	17	23	19	20	22	26
Cs	6.0	5.6	5.6	6.8	6.7	5.7	5.8	8.1	8.3
Hf	6.5	6.9	7.2	6.1	6.1	6.9	7.2	6.3	6.9
Sb	b.d.[2]	1.0	0.9	1.4	1.4	1.9	0.8	b.d.	0.5
Sc	17.0	16.0	14.0	16.0	16.0	16.0	16.0	19.0	18.0
Ta	2.7	2.4	2.4	2.2	2.3	2.4	2.5	2.1	2.2
Th	10.9	11.0	11.5	11.4	12.5	11.8	11.7	12.8	13.2
U	2.7	3.1	3.0	2.8	2.9	3.3	3.3	2.8	2.8

[1] mds = mudstone, ss = sandstone, fss = fine grained sandstone, css = calcite cemented sandstone, sss = siderite cemented sandstone ($Al_2O_3/SiO_2 \leq 0.2$), csss = calcite siderite cemented sandstone, cmds = calcite cemented mudstone ($Al_2O_3/SiO_2 > 0.2$), cslt = calcite cemented sandstone (Al2O3/SiO2 ≤ 0.2), scss = siderite calcite cemented sandstone

[2] b.d. = below detection limit, [3] CIA = Chemical Index of Alteration (Nesbitt and Young, 1982)

[4] MGS = mean grain size, [5] n.c. = not calculated

Table 2 Continued

Well	Alma K-85									
Formation					Missisauga					
Depth (m)	2888.26	2904.15	2906.78	2912.04	2919.00	2919.45	2920.30	2931.87	3038.00	3039.88
Lithology[1]	mds	mds	mds	mds	shale	shale	mds	shale	shale	mds
MGS[4] (μm)										
File	14-228	14-229	14-230	14-231	16-62	16-63	14-232	16-64	16-65	14-233
Major Elements (wt%)										
SiO_2	59.0	56.5	62.1	52.9	53.8	53.1	53.4	55.8	56.6	55.5
TiO_2	1.21	1.23	1.15	1.12	1.29	1.19	1.19	1.11	1.48	1.43
Al_2O_3	19.43	21.05	18.69	20.64	19.12	19.70	20.83	21.06	19.39	18.96
Fe_2O_{3t}	4.38	5.71	4.71	7.63	8.29	7.79	7.00	6.28	5.87	6.46
MnO	0.04	0.03	0.02	0.06	0.07	0.06	0.03	0.02	0.05	0.04
MgO	1.20	1.70	1.48	1.11	1.60	1.66	1.53	1.51	1.46	1.53
CaO	0.37	0.27	0.28	0.58	0.61	0.74	0.37	0.32	0.39	0.35
Na_2O	0.98	0.97	0.98	2.88	1.00	0.98	1.07	0.94	1.00	1.01
K_2O	2.93	3.27	3.04	2.13	2.60	2.73	2.90	2.99	2.65	2.83
P_2O_5	0.12	0.12	0.07	0.17	0.12	0.12	0.13	0.01	0.11	0.17
L.O.I	8.95	9.60	7.78	9.98	11.39	10.85	10.53	9.48	10.99	10.51
Total	98.61	100.43	100.28	99.19	99.89	98.92	98.93	99.56	99.94	98.76
CIA[3]	78.08	78.9	77.6	71.8	77.5	76.9	78.9	79.7	78.8	78.0
Trace Elements (ppm)										
Ba	367	366	340	343	376	356	343	396	361	369
Rb	145	172	168	73	136	142	155	161	120	147
Sr	160	182	158	223	191	184	189	171	181	169
Y	33	32	29	27	30	29	33	25	29	34
Zr	241	215	254	292	229	209	227	196	254	265
Nb	25	28	25	92	38	35	35	28	38	31
Pb	24	29	25	19	16	12	33	30	25	29
Ga	25	31	27	22	27	28	30	29	27	28
Zn	86	83	82	109	102	90	109	100	120	87
Cu	33	32	25	9	27	24	22	26	31	27
Ni	86	80	75	36	87	72	88	99	86	90
V	154	160	144	93	163	159	163	153	150	147
Cr	163	177	163	71	152	143	162	138	144	178
La	53.7	61.6	51.3	78.6	58.1	55.4	62.9	50.9	57.7	60.2
Ce	114.0	127.0	107.0	161.0	122.0	115.0	134.0	110.0	119.0	124.0
Pr	11.7	12.8	10.8	16.0	13.2	12.5	13.7	11.5	13.2	12.7
Nd	44.3	48.8	40.6	57.5	49.7	47.1	53.4	43.5	49.9	47.4
Sm	8.1	8.7	7.2	9.1	9.2	9.0	9.6	8.1	9.1	8.7
Eu	1.79	1.88	1.53	2.02	2.13	2.03	2.23	1.77	2.09	1.94
Gd	6.5	6.7	5.4	6.5	7.6	7.4	7.9	6.4	7.5	7.0
Tb	1.1	1.1	0.9	1.0	1.3	1.2	1.2	1.1	1.3	1.1
Dy	6.4	6.4	5.6	5.6	6.7	6.5	6.8	5.6	6.7	6.7
Ho	1.2	1.2	1.1	1.1	1.3	1.3	1.3	1.1	1.3	1.3
Er	3.6	3.6	3.2	3.1	3.9	3.9	3.7	3.4	4.0	3.7
Tm	0.53	0.51	0.48	0.42	0.58	0.58	0.51	0.52	0.60	0.53
Yb	3.5	3.4	3.1	3.0	3.6	3.6	3.5	3.2	3.7	3.5
Lu	0.52	0.50	0.46	0.43	0.53	0.50	0.52	0.47	0.53	0.51
Co	21	31	23	15	29	21	31	30	24	30
Cs	7.4	9.1	8.6	5.4	7.5	7.9	8.7	9.0	6.1	7.6
Hf	6.9	5.9	6.9	7.8	6.8	6.4	6.3	6.1	7.7	7.2
Sb	b.d.	0.5	b.d.	b.d.	1.1	0.8	b.d.	0.8	1.5	b.d.
Sc	20.0	21.0	19.0	11.0	19.0	21.0	20.0	20.0	19.0	19.0
Ta	2.2	2.1	1.8	7.0	2.6	2.5	2.8	2.0	2.8	2.3
Th	14.5	14.5	12.8	13.5	12.7	12.5	13.8	12.6	12.1	13.4
U	3.1	3.1	2.7	3.0	3.1	3.1	2.9	3.2	3.4	3.1

[1] mds = mudstone, ss = sandstone, fss = fine grained sandstone, css = calcite cemented sandstone, sss = siderite cemented sandstone ($Al_2O_3/SiO_2 \leq 0.2$), csss = calcite siderite cemented sandstone, cmds = calcite cemented mudstone ($Al_2O_3/SiO_2 > 0.2$), cslt = calcite cemented sandstone (Al2O3/SiO2 ≤ 0.2), scss = siderite calcite cemented sandstone

[2] b.d. = below detection limit, [3] CIA = Chemical Index of Alteration (Nesbitt and Young, 1982)

[4] MGS = mean grain size, [5] n.c. = not calculated

Table 2 Continued

Well	Alma K-85								
Formation					Missisauga				
Depth (m)	3044.60	3047.90	3068.15	3071.80	3089.05	3090.45	3093.80	3104.10	3104.70
Lithology[1]	shale	shale	shale	shale	shale	shale	shale	mds	shale
MGS[4] (μm)									
File	16-66	16-67	16-68	16-69	16-70	16-71	16-72	14-234	16-73
Major Elements (wt%)									
SiO_2	54.6	58.4	57.5	57.6	54.3	57.4	56.9	60.1	59.2
TiO_2	1.26	1.19	1.16	1.42	1.31	1.35	1.35	1.25	1.26
Al_2O_3	21.79	19.90	19.38	19.58	19.09	18.37	18.97	18.17	18.55
Fe_2O_{3t}	5.43	5.24	5.54	5.59	6.91	6.60	6.39	5.53	5.80
MnO	0.03	0.05	0.05	0.04	0.06	0.06	0.06	0.04	0.04
MgO	1.59	1.56	1.54	1.55	1.58	1.62	1.59	1.42	1.43
CaO	0.29	0.30	0.36	0.27	0.41	0.42	0.47	0.37	0.37
Na_2O	0.96	0.90	0.97	1.00	0.98	1.04	1.05	0.98	1.01
K_2O	3.12	3.18	2.93	3.01	2.88	2.67	2.75	2.60	2.70
P_2O_5	0.10	0.05	0.08	0.03	0.17	0.08	0.13	0.14	0.10
L.O.I	10.34	9.34	9.77	9.70	11.23	10.22	10.48	8.95	9.08
Total	99.50	100.08	99.32	99.77	98.87	99.83	100.16	99.59	99.57
CIA[3]	80.0	78.4	78.1	78.4	77.7	77.4	77.3	78.1	77.9
Trace Elements (ppm)									
Ba	426	414	366	370	357	397	349	333	385
Rb	169	163	144	139	141	148	132	140	131
Sr	193	187	167	157	183	194	181	162	162
Y	29	28	28	30	29	34	31	32	28
Zr	239	293	205	270	224	303	269	287	269
Nb	31	29	27	31	32	38	36	29	32
Pb	29	20	17	16	27	23	26	28	23
Ga	32	29	27	30	28	31	28	26	27
Zn	91	96	105	76	112	96	94	88	93
Cu	31	31	29	30	32	30	31	26	31
Ni	96	86	78	74	125	88	81	67	81
V	174	149	147	153	155	169	152	129	142
Cr	160	152	140	163	166	187	164	170	156
La	59.7	53.9	50.5	55.9	56.8	61.9	57.2	54.1	50.2
Ce	124.0	108.0	106.0	115.0	114.0	127.0	117.0	111.0	102.0
Pr	13.5	12.1	11.8	12.3	12.4	13.7	12.8	11.5	11.0
Nd	50.3	45.1	45.4	46.2	46.6	52.2	48.2	44.0	41.7
Sm	9.3	8.5	8.7	8.6	8.6	9.8	9.1	8.1	7.6
Eu	2.13	1.79	1.97	1.84	1.98	2.22	2.01	1.79	1.71
Gd	7.6	6.9	7.5	7.1	7.6	8.6	7.7	6.6	6.7
Tb	1.3	1.2	1.3	1.2	1.3	1.4	1.3	1.1	1.2
Dy	6.8	6.2	6.6	6.8	6.6	7.8	6.9	6.3	6.2
Ho	1.3	1.2	1.3	1.3	1.3	1.5	1.3	1.2	1.2
Er	4.2	3.7	4.0	4.2	3.9	4.7	4.2	3.6	3.8
Tm	0.62	0.57	0.59	0.64	0.59	0.71	0.64	0.51	0.59
Yb	3.8	3.5	3.6	3.9	3.6	4.4	3.9	3.4	3.5
Lu	0.56	0.52	0.52	0.58	0.52	0.63	0.56	0.50	0.52
Co	26	25	21	25	28	30	25	24	22
Cs	9.2	8.3	7.6	7.7	7.7	7.9	7.2	6.8	6.9
Hf	7.5	8.4	6.5	8.0	6.7	9.0	8.1	8.0	8.2
Sb	1.2	0.6	0.7	0.8	1.1	1.2	0.6	b.d.	0.8
Sc	21.0	19.0	19.0	21.0	19.0	19.0	20.0	17.0	18.0
Ta	2.2	2.0	2.0	2.3	2.4	2.8	2.5	2.3	2.3
Th	13.9	13.6	12.1	13.7	13.6	14.9	13.4	12.8	13.0
U	3.4	3.4	3.0	4.2	3.5	4.0	3.5	2.9	3.5

[1] mds = mudstone, ss = sandstone, fss = fine grained sandstone, css = calcite cemented sandstone, sss = siderite cemented sandstone ($Al_2O_3/SiO_2 \leq 0.2$), csss = calcite siderite cemented sandstone, cmds = calcite cemented mudstone ($Al_2O_3/SiO_2 > 0.2$), cslt = calcite cemented sandstone (Al2O3/SiO2 ≤ 0.2), scss = siderite calcite cemented sandstone

[2] b.d. = below detection limit, [3] CIA = Chemical Index of Alteration (Nesbitt and Young, 1982)

[4] MGS = mean grain size, [5] n.c. = not calculated

Table 2 continued

Well	Alma F-67					
Formation	Missisauga					
Depth (m)	2847.10	2851.77	2852.85	2853.30	2879.65	2884.30
Lithology[1]	shale	shale	shale	shale	ss	ss
MGS[4] (μm)					600	130
File	14-579	14-580	14-581	14-582	14-583	14-584
Major Elements (wt%)						
SiO_2	45.6	48.2	55.0	53.7	92.9	72.3
TiO_2	1.53	1.28	1.35	1.39	0.38	0.59
Al_2O_3	24.10	23.17	19.35	19.40	1.74	1.88
Fe_2O_{3t}	8.15	8.39	6.94	7.04	1.74	1.79
MnO	0.08	0.03	0.04	0.04	0.01	0.10
MgO	1.80	1.58	1.51	1.46	0.20	0.29
CaO	0.88	0.39	0.31	0.43	0.74	11.51
Na_2O	1.48	1.19	1.32	1.31	0.27	0.44
K_2O	3.41	2.98	2.82	2.69	0.38	0.45
P_2O_5	0.44	0.15	0.11	0.16	0.03	0.70
L.O.I	11.56	12.17	10.48	11.04	1.65	9.54
Total	99.05	99.52	99.24	98.63	100.00	99.61
CIA[3]	75.7	79.7	77.0	76.8	44.5	7.8
Trace Elements (ppm)						
Ba	390	426	368	397	1070	790
Rb	155	139	129	121	13	15
Sr	241	187	163	183	62	490
Y	63	35	36	40	7	35
Zr	318	236	226	230	102	283
Nb	30	26	27	29	4	6
Pb	20	28	25	37	5	7
Ga	31	30	25	24	1	3
Zn	89	80	92	108	47	46
Cu	37	33	32	36	11	11
Ni	78	82	74	85	14	16
V	186	190	150	154	25	29
Cr	148	142	137	136	55	54
La	68.6	53.7	47.5	51.2	9.7	30.5
Ce	144	105	91	99	22	94
Pr	14.9	9.3	8.3	9.3	1.9	9.6
Nd	69.0	38.0	33.9	37.4	7.9	48.5
Sm	16.0	7.5	6.6	8.0	1.5	12.4
Eu	3.79	1.68	1.47	1.84	0.36	3.12
Gd	13.7	6.2	5.5	6.9	1.2	10.7
Tb	2.1	1.0	0.9	1.1	0.2	1.5
Dy	10.3	5.4	5.5	6.2	1.0	6.4
Ho	1.7	1.0	1.0	1.1	0.2	0.9
Er	4.6	3.0	3.1	3.3	0.6	2.4
Tm	0.66	0.47	0.49	0.52	0.10	0.30
Yb	4.3	3.1	3.2	3.4	0.6	1.8
Lu	0.61	0.46	0.46	0.47	0.09	0.24
Co	29	26	30	36	3	b.d.[2]
Cs	8.7	8.4	7.4	7.0	b.d.	b.d.
Hf	9.0	7.9	7.2	7.1	2.8	4.5
Sb	0.5	0.5	0.6	b.d.	b.d.	b.d.
Sc	24	21	20	20	2	6
Ta	2.6	1.9	1.9	2.4	0.6	0.9
Th	16.2	15.9	13.5	13.5	2.9	3.7
U	2.9	2.5	2.4	2.4	1.0	2.3

[1] mds = mudstone, ss = sandstone, fss = fine grained sandstone, css = calcite cemented sandstone, sss = siderite cemented sandstone ($Al_2O_3/SiO_2 \leq 0.2$), csss = calcite siderite cemented sandstone, cmds = calcite cemented mudstone ($Al_2O_3/SiO_2 > 0.2$), cslt = calcite cemented sandstone (Al2O3/SiO2 ≤ 0.2), scss = siderite calcite cemented sandstone

[2] b.d. = below detection limit, [3] CIA = Chemical Index of Alteration (Nesbitt and Young, 1982)

[4] MGS = mean grain size, [5] n.c. = not calculated

Table 2 continued

Well	Glenelg N-49						
Formation	Logan Canyon	Missisauga					
Depth (m)	3007.53	3576.78	3596.89	3622.08	3628.43A	3628.43B	3628.92
Lithology[1]	mds	shale	ss	mds	ss	mds	ss
MGS[4] (μm)			300		540		700
File	14-235	14-567	14-568	14-236	14-569	14-237	14-570
Major Elements (wt%)							
SiO_2	53.7	53.9	95.9	55.0	93.2	53.2	86.1
TiO_2	1.33	0.42	0.19	1.52	0.05	1.70	0.19
Al_2O_3	17.32	4.11	1.16	20.44	3.56	22.29	6.19
Fe_2O_{3t}	6.32	21.23	1.26	6.57	0.80	5.59	1.96
MnO	0.02	0.36	0.01	0.07	0.01	0.06	0.02
MgO	1.54	2.31	0.05	1.49	0.03	1.42	0.12
CaO	1.24	1.56	0.24	0.43	0.20	0.35	0.32
Na_2O	1.18	0.81	0.16	0.76	0.09	0.66	0.98
K_2O	3.00	0.72	0.01	3.23	b.d.	3.64	0.90
P_2O_5	0.16	0.09	0.03	0.13	0.02	0.12	0.05
L.O.I	12.84	14.79	1.14	10.35	2.01	10.38	3.54
Total	98.63	100.28	100.11	99.96	99.98	99.40	100.41
CIA[3]	70.0	45.4	62.0	78.7	87.0	79.8	66.2
Trace Elements (ppm)							
Ba	397	164	1490	407	1280	430	232
Rb	119	23	2	166	b.d.	178	26
Sr	180	113	62	140	65	171	151
Y	30	9	4	37	2	38	7
Zr	267	149	65	275	35	315	94
Nb	34	12	6	35	4	41	7
Pb	22	14	92	22	523	25	104
Ga	24	4	0	30	0	34	4
Zn	121	79	31	72	25	73	290
Cu	17	14	37	24	23	18	20
Ni	70	23	16	85	11	86	20
V	136	76	7	154	8	155	19
Cr	154	65	100	177	58	194	77
La	51.8	14.9	4.0	59.5	4.4	65.4	13.3
Ce	110.0	33.3	8.1	122.0	9.1	128.0	27.9
Pr	11.30	3.35	0.75	12.60	0.81	13.00	2.62
Nd	43.4	15.7	3.2	47.7	3.3	47.5	11.0
Sm	7.9	3.6	0.6	8.7	0.6	8.1	2.1
Eu	1.79	0.84	0.23	1.91	0.20	1.75	0.44
Gd	6.5	3.0	0.5	7.0	0.5	6.5	1.6
Tb	1.1	0.5	b.d.[2]	1.2	b.d.	1.2	0.2
Dy	6.2	2.5	0.5	7.2	0.3	7.0	1.1
Ho	1.2	0.4	0.1	1.4	b.d.	1.4	0.2
Er	3.4	1.2	0.3	4.1	0.2	4.2	0.6
Tm	0.49	0.18	0.06	0.60	b.d.	0.60	0.10
Yb	3.3	1.2	0.4	3.9	0.2	4.1	0.6
Lu	0.49	0.17	0.05	0.58	b.d.	0.62	0.09
Co	19	9	7	29	3	24	17
Cs	5.4	0.7	b.d.	8.9	b.d.	9.0	b.d.
Hf	6.8	4.9	2.4	7.7	1.5	8.7	2.5
Sc	16	18	b.d.	23	b.d.	23	2
Ta	2.6	0.7	0.3	2.5	b.d.	2.9	0.5
Th	11.4	3.4	1.0	13.9	1.2	15.3	2.3
U	3.4	0.8	0.5	3.6	0.3	4.0	0.5

[1] mds = mudstone, ss = sandstone, fss = fine grained sandstone, css = calcite cemented sandstone, sss = siderite cemented sandstone ($Al_2O_3/SiO_2 \leq 0.2$), csss = calcite siderite cemented sandstone, cmds = calcite cemented mudstone ($Al_2O_3/SiO_2 > 0.2$), cslt = calcite cemented sandstone (Al2O3/SiO2 ≤ 0.2), scss = siderite calcite cemented sandstone

[2] b.d. = below detection limit, [3] CIA = Chemical Index of Alteration (Nesbitt and Young, 1982)

[4] MGS = mean grain size, [5] n.c. = not calculated

Table 2 continued

Well	Glenelg E-58							
Formation	Missisauga							
Depth (m)	3526.28	3528.08A	3528.08B	3530.06	3530.3A	3535.3B	3535.35	3710.80
Lithology[1]	ss	ss	ss	ss	ss	ss	ss	ss
MGS[4] (μm)	1500	140	140	1500	1500	1500	150	120
File	14-572	14-573	14-571	14-574	14-575	14-577	14-576	14-578
Major Elements (wt%)								
SiO_2	73.8	88.7	88.8	86.8	85.4	79.9	86.5	78.9
TiO_2	0.39	0.71	0.46	0.64	0.74	0.80	0.31	0.67
Al_2O_3	3.58	3.41	4.12	3.43	2.70	7.61	3.94	8.44
Fe_2O_{3t}	10.02	2.01	2.33	2.04	1.64	3.42	2.15	2.63
MnO	0.20	0.02	0.01	0.03	0.04	0.04	0.04	0.04
MgO	1.43	0.29	0.32	0.31	0.19	0.60	0.50	0.42
CaO	1.40	0.52	0.32	2.24	3.88	0.39	1.51	0.68
Na_2O	1.20	1.18	1.37	1.22	0.99	2.19	1.39	1.15
K_2O	0.46	0.37	0.64	0.49	0.44	1.07	0.27	0.90
P_2O_5	0.05	0.04	0.05	0.03	0.04	0.10	0.04	0.11
L.O.I	7.71	1.92	1.83	3.15	3.92	4.06	3.34	5.22
Total	100.21	99.12	100.27	100.35	100.01	100.20	100.00	99.17
CIA[3]	41.6	50.9	53.9	34.2	22.8	58.2	42.5	67.3
Trace Elements (ppm)								
Ba	404	581	177	319	190	236	875	220
Rb	14	16	20	19	15	37	11	33
Sr	88	81	65	92	103	131	82	168
Y	12	22	14	20	26	25	12	17
Zr	241	660	220	589	969	289	221	302
Nb	7	10	8	11	11	15	8	14
Pb	10	11	10	9	4	10	11	12
Ga	3	3	3	3	3	7	2	7
Zn	52	61	63	94	43	73	33	104
Cu	18	19	18	15	19	23	16	23
Ni	15	21	29	21	20	35	18	36
V	23	26	23	27	16	48	18	43
Cr	103	195	96	186	232	103	103	106
La	12.5	17.9	13.8	17.0	18.9	23.0	11.2	27.2
Ce	25.3	36.7	29.6	35.4	41.2	48.7	22.9	56.7
Pr	2.39	3.49	2.83	3.33	3.76	4.76	2.18	5.25
Nd	10.4	15.2	12.2	14.3	17.1	21.9	9.3	22.4
Sm	2.2	3.2	2.6	3.0	3.7	4.8	2.0	4.3
Eu	0.52	0.66	0.57	0.65	0.78	1.09	0.52	0.94
Gd	1.8	2.8	2.2	2.6	3.3	4.1	1.8	3.4
Tb	0.3	0.5	0.4	0.4	0.6	0.7	0.3	0.5
Dy	1.7	2.9	2.0	2.6	3.6	3.6	1.6	2.6
Ho	0.3	0.6	0.4	0.5	0.7	0.7	0.3	0.5
Er	0.9	1.9	1.1	1.5	2.3	1.9	0.9	1.4
Tm	0.15	0.31	0.18	0.26	0.37	0.30	0.14	0.22
Yb	1.0	2.2	1.2	1.8	2.5	2.0	1.0	1.5
Lu	0.16	0.34	0.18	0.27	0.38	0.28	0.14	0.22
Co	5	4	7	4	3	10	5	12
Cs	b.d.	b.d.	b.d.[2]	b.d.	b.d.	1.1	b.d.	0.9
Hf	5.8	14.4	5.7	13.6	19.8	7.9	6.7	8.3
Sb	b.d.	b.d.	b.d.	b.d.	b.d.	b.d.	b.d.	b.d.
Sc	6	3	4	3	4	7	2	6
Ta	0.5	0.9	0.7	0.9	1.0	1.2	0.7	1.1
Th	3.0	5.3	3.7	4.9	6.2	6.0	2.9	5.1
U	0.8	1.5	0.9	1.3	1.7	1.4	0.7	1.2

[1] mds = mudstone, ss = sandstone, fss = fine grained sandstone, css = calcite cemented sandstone, sss = siderite cemented sandstone ($Al_2O_3/SiO_2 \leq 0.2$), csss = calcite siderite cemented sandstone, cmds = calcite cemented mudstone ($Al_2O_3/SiO_2 > 0.2$), cslt = calcite cemented sandstone (Al2O3/SiO2 ≤ 0.2), scss = siderite calcite cemented sandstone

[2] b.d. = below detection limit, [3] CIA = Chemical Index of Alteration (Nesbitt and Young, 1982)

[4] MGS = mean grain size, [5] n.c. = not calculated

Table 2 continued

Well	N. Triumph B-52						
Formation				Missisauga			
Depth (m)	3771.30	3776.62	3784.17	3791.95	3798.95	3803.50	3809.98
Lithology[1]	ss	ss	css	ss	ss	ss	ss
MGS[4] (μm)	100	80	100	180	100	80	200
File	14-239	14-240	14-238	14-241	14-242	14-243	14-244
Major Elements (wt%)							
SiO_2	82.3	72.7	56.3	88.0	82.4	89.7	91.3
TiO_2	1.74	0.45	0.23	0.69	0.73	0.72	0.61
Al_2O_3	3.62	2.41	2.53	3.68	4.16	3.27	2.80
Fe_2O_{3t}	6.08	12.47	2.10	3.30	5.38	2.82	1.38
MnO	0.07	0.22	0.13	0.02	0.08	0.01	0.02
MgO	0.60	1.44	0.31	0.42	0.69	0.32	0.12
CaO	1.43	1.58	20.95	0.92	1.14	0.34	0.42
Na_2O	0.43	0.35	0.38	0.53	0.67	0.47	0.38
K_2O	0.48	0.31	0.53	0.55	0.69	0.62	0.17
P_2O_5	0.13	0.09	0.03	0.03	0.04	0.04	0.03
L.O.I	3.40	8.25	16.65	1.81	3.26	1.23	1.46
Total	100.27	100.24	100.10	99.90	99.21	99.51	98.65
CIA[3]	48.6	38.9	6.0	54.0	51.5	61.2	64.0
Trace Elements (ppm)							
Ba	259	281	89	323	256	145	410
Rb	18	13	17	19	25	21	5
Sr	98	85	719	89	124	61	43
Y	26	9	7	12	16	15	5
Zr	649	191	131	359	543	517	432
Nb	23	7	4	12	16	12	7
Pb	7	5	5	5	6	5	13
Ga	6	4	3	5	6	6	2
Zn	96	54	11	65	91	70	25
Cu	17	6	3	10	16	11	10
Ni	26	9	9	18	25	15	12
V	87	68	23	47	62	42	16
Cr	138	71	59	119	177	123	136
La	30.6	13.3	10.3	17.4	21.6	18.7	7.9
Ce	70.7	31.0	24.1	37.8	47.4	42.5	17.5
Pr	7.59	2.99	2.34	3.84	4.62	4.39	1.70
Nd	31.0	11.6	9.2	14.8	18.0	17.3	6.6
Sm	6.5	2.1	1.7	2.7	3.2	3.5	1.1
Eu	1.23	0.43	0.43	0.49	0.61	0.65	0.25
Gd	5.2	1.6	1.4	2.1	2.5	2.6	0.9
Tb	0.8	0.3	0.2	0.4	0.4	0.4	0.1
Dy	4.7	1.8	1.3	2.2	2.8	2.6	0.9
Ho	0.9	0.4	0.3	0.5	0.6	0.6	0.2
Er	2.9	1.1	0.7	1.4	1.8	1.7	0.7
Tm	0.4	0.2	0.1	0.2	0.3	0.3	0.1
Yb	2.9	1.1	0.7	1.5	1.9	1.8	0.7
Lu	0.44	0.18	0.12	0.24	0.32	0.29	0.13
Co	5	3	b.d.[2]	4	7	3	5
Cs	0.5	b.d.	b.d.	b.d.	0.7	b.d.	b.d.
Hf	15.5	5.1	3.3	9.1	13.6	12.8	9.7
Sb	b.d.	b.d.	b.d.	b.d.	b.d.	b.d.	b.d.
Sc	6	6	2	4	5	4	1
Ta	2.1	0.7	0.4	1.1	1.2	1.1	0.7
Th	10.5	4.6	2.8	4.8	6.4	5.5	2.5
U	2.0	0.8	0.5	1.1	1.5	1.3	0.7

[1] mds = mudstone, ss = sandstone, fss = fine grained sandstone, css = calcite cemented sandstone, sss = siderite cemented sandstone ($Al_2O_3/SiO_2 \leq 0.2$), csss = calcite siderite cemented sandstone, cmds = calcite cemented mudstone ($Al_2O_3/SiO_2 > 0.2$), cslt = calcite cemented sandstone ($Al2O3/SiO2 \leq 0.2$), scss = siderite calcite cemented sandstone

[2] b.d. = below detection limit, [3] CIA = Chemical Index of Alteration (Nesbitt and Young, 1982)

[4] MGS = mean grain size, [5] n.c. = not calculated

Table 2 continued

Well	Sambro I-29
Formation	Logan Canyon
Depth (m)	883.88
Lithology[1]	mds
MGS[4] (μm)	
File	14-461
Major Elements (wt%)	
SiO_2	55.9
TiO_2	0.83
Al_2O_3	15.16
Fe_2O_{3t}	7.54
MnO	0.05
MgO	1.31
CaO	5.21
Na_2O	0.55
K_2O	1.86
P_2O_5	0.09
L.O.I	0.00
Total	88.52
CIA[3]	55.0
Trace Elements (ppm)	
Ba	266
Rb	105
Sr	163
Y	30
Zr	204
Nb	13
Pb	27
Ga	22
Zn	72
Cu	17
Ni	53
V	121
Cr	124
La	39.4
Ce	83.2
Pr	9.68
Nd	35.8
Sm	6.9
Eu	1.49
Gd	5.5
Tb	1
Dy	5.6
Ho	1.1
Er	3.3
Tm	0.5
Yb	3.1
Lu	0.45
Co	14
Cs	6.1
Hf	5.6
Sb	b.d.[2]
Sc	16
Ta	1.2
Th	10.6
U	2.3

[1] mds = mudstone, ss = sandstone, fss = fine grained sandstone, css = calcite cemented sandstone, sss = siderite cemented sandstone ($Al_2O_3/SiO_2 \leq 0.2$), csss = calcite siderite cemented sandstone, cmds = calcite cemented mudstone ($Al_2O_3/SiO_2 > 0.2$), cslt = calcite cemented sandstone (Al2O3/SiO2 ≤ 0.2), scss = siderite calcite cemented sandstone

[2] b.d. = below detection limit, [3] CIA = Chemical Index of Alteration (Nesbitt and Young, 1982)

[4] MGS = mean grain size, [5] n.c. = not calculated

Table 2 continued

Well	Naskapi N-30				
Formation			Missisauga		
Depth (m)	1469.00	1469.89	1471.75	1472.25	1473.81
Lithology[1]	ss	ss	ss	ss	ss
MGS[4] (μm)	300	700	240	100	1100
File	14-422	14-423	14-424	14-425	14-426
Major Elements (wt%)					
SiO_2	93.6	85.6	92.2	87.3	88.6
TiO_2	0.84	0.51	0.47	0.59	0.69
Al_2O_3	2.67	6.25	2.44	5.71	4.64
Fe_2O_{3t}	0.82	1.78	2.11	1.12	1.75
MnO	0.01	0.01	b.d.	0.01	0.01
MgO	0.08	0.14	0.06	0.12	0.09
CaO	0.13	0.16	0.07	0.06	0.24
Na_2O	0.26	0.28	0.21	0.35	0.19
K_2O	0.21	0.65	0.20	0.58	0.39
P_2O_5	0.02	0.03	0.02	0.03	0.02
L.O.I	1.43	4.22	2.32	3.42	2.98
Total	100.06	99.67	100.09	99.31	99.56
CIA[3]	75.0	81.1	77.9	81.3	79.8
Trace Elements (ppm)					
Ba	1960	5500	895	1600	1850
Rb	10	31	12	29	21
Sr	55	103	38	60	55
Y	12	14	10	16	15
Zr	154	169	186	228	183
Nb	10	9	6	8	8
Pb	15	37	14	14	22
Ga	4	9	4	9	7
Zn	38	103	40	45	31
Cu	18	29	15	15	15
Ni	7	30	17	16	34
V	24	38	23	39	29
Cr	86	77	60	64	78
La	8.3	20.3	13.3	23.5	17.7
Ce	b.d.[2]	42.0	28.2	48.9	37.4
Pr	4.67	4.67	3.11	5.84	4.29
Nd	6.8	16.4	11.1	19.4	15.4
Sm	3.2	3.1	2.0	3.7	3.0
Eu	0.55	0.54	0.39	0.73	0.56
Gd	2.5	2.7	1.7	3.2	2.7
Tb	0.4	0.4	0.3	0.5	0.4
Dy	2.1	2.4	1.6	2.7	2.4
Ho	0.4	0.5	0.3	0.5	0.5
Er	1.3	1.4	1.0	1.6	1.4
Tm	0.19	0.21	0.16	0.25	0.22
Yb	1.2	1.3	1.0	1.6	1.4
Lu	0.18	0.19	0.16	0.23	0.20
Co	2	19	6	8	20
Cs	b.d.	2.4	1.1	2.7	1.4
Hf	3.9	4.3	4.6	5.8	4.7
Sb	b.d.	b.d.	b.d.	b.d.	b.d.
Sc	3	5	2	5	4
Ta	1.2	1.0	0.7	0.9	1.0
Th	3.5	5.5	3.6	5.5	4.8
U	1.6	1.7	1.2	1.8	1.9

[1] mds = mudstone, ss = sandstone, fss = fine grained sandstone, css = calcite cemented sandstone, sss = siderite cemented sandstone ($Al_2O_3/SiO_2 \leq 0.2$), csss = calcite siderite cemented sandstone, cmds = calcite cemented mudstone ($Al_2O_3/SiO_2 > 0.2$), cslt = calcite cemented sandstone (Al2O3/SiO2 ≤ 0.2), scss = siderite calcite cemented sandstone

[2] b.d. = below detection limit, [3] CIA = Chemical Index of Alteration (Nesbitt and Young, 1982)

[4] MGS = mean grain size, [5] n.c. = not calculated

Table 2 continued

Well	Dauntless D-35				
Formation			Missisauga		
Depth (m)	3162.76	3163.21	3164.43	3165.04	3165.65
Lithology[1]	ss	shale	ss	ss	ss
MGS[4] (μm)	300		300	300	400
File	14-428	14-432	14-429	14-430	14-431
Major Elements (wt%)					
SiO_2	92.6	56.9	84.1	83.5	89.2
TiO_2	0.19	1.46	0.32	0.40	0.10
Al_2O_3	2.66	18.72	6.42	6.28	3.97
Fe_2O_{3t}	1.82	5.40	2.72	2.86	2.33
MnO	0.01	0.02	b.d.	b.d.	0.01
MgO	0.44	3.00	0.95	1.00	0.77
CaO	0.18	0.98	0.21	0.19	0.22
Na_2O	0.34	1.07	1.04	1.28	0.62
K_2O	1.01	3.45	2.07	1.99	1.26
P_2O_5	0.03	0.22	0.07	0.07	0.04
L.O.I	1.09	8.38	1.80	1.99	1.43
Total	100.39	99.61	99.73	99.60	99.97
CIA[3]	57.4	72.0	59.7	57.7	58.8
Trace Elements (ppm)					
Ba	1850	362	414	388	2520
Rb	25	142	44	40	31
Sr	63	125	68	72	80
Y	5	46	8	10	5
Zr	97	335	111	139	55
Nb	6	33	12	16	5
Pb	14	19	8	9	20
Ga	4	31	7	7	5
Zn	55	86	51	49	33
Cu	18	36	16	15	11
Ni	9	42	10	10	7
V	17	150	29	31	15
Cr	133	150	67	95	74
La	9.1	48.5	16.3	17.2	9.5
Ce	6.5	101.0	34.7	36.2	18.3
Pr	1.71	12.30	3.91	4.07	1.89
Nd	5.6	45.4	13.4	14.0	6.2
Sm	0.9	9.3	2.4	2.6	1.1
Eu	0.24	2.24	0.64	0.66	0.34
Gd	0.8	8.5	1.9	2.1	0.9
Tb	0.1	1.4	0.3	0.3	0.2
Dy	0.9	8.2	1.6	1.8	0.8
Ho	0.2	1.7	0.3	0.4	0.2
Er	0.6	4.8	0.9	1.1	0.6
Tm	0.09	0.73	0.14	0.16	0.09
Yb	0.6	4.5	0.9	1.0	0.6
Lu	0.09	0.66	0.13	0.15	0.08
Co	3	16	4	4	2
Cs	b.d.[2]	6.0	0.5	b.d.	b.d.
Hf	2.6	9.3	2.9	3.5	1.5
Sb	1.7	b.d.	b.d.	b.d.	b.d.
Sc	2	21	3	3	2
Ta	0.5	2.7	1.2	1.4	0.6
Th	2.3	13.4	3.3	3.4	2.1
U	0.7	3.8	0.9	1.1	0.7

[1] mds = mudstone, ss = sandstone, fss = fine grained sandstone, css = calcite cemented sandstone, sss = siderite cemented sandstone ($Al_2O_3/SiO_2 \leq 0.2$), csss = calcite siderite cemented sandstone, cmds = calcite cemented mudstone ($Al_2O_3/SiO_2 > 0.2$), cslt = calcite cemented sandstone ($Al2O3/SiO2 \leq 0.2$), scss = siderite calcite cemented sandstone

[2] b.d. = below detection limit, [3] CIA = Chemical Index of Alteration (Nesbitt and Young, 1982)

[4] MGS = mean grain size, [5] n.c. = not calculated

Table 2 continued

Well	Peskowesk A-99							
Formation				Logan Canyon				
Depth	2209.25	2210.37	2213.57	2215.78	2219.03	2221.69	2228.42	2233.62
Lithology[1]	shale	ss	shale	shale	shale	shale	shale	ss
MGS[4] (μm)		250						700
File	14-535	14-524	14-536	14-537	14-538	14-539	14-540	14-527
Major Elements (wt%)								
SiO_2	44.5	82.1	45.3	47.0	49.8	49.0	44.0	86.8
TiO_2	1.38	0.59	1.45	1.41	1.46	1.37	1.59	0.16
Al_2O_3	17.80	7.04	17.55	18.28	18.33	19.30	17.67	5.35
Fe_2O_{3t}	12.64	2.03	11.18	8.65	7.84	8.00	12.13	1.11
MnO	0.09	0.02	0.14	0.06	0.08	0.09	0.24	0.01
MgO	1.50	0.43	1.90	1.80	1.82	1.76	3.53	0.10
CaO	0.39	0.46	1.05	0.94	0.74	0.89	0.66	0.54
Na_2O	0.93	0.98	1.01	1.10	1.07	0.98	1.10	0.79
K_2O	2.98	1.95	2.90	2.88	2.76	2.75	2.90	2.21
P_2O_5	0.22	0.10	0.35	0.27	0.26	0.31	0.18	0.04
L.O.I	17.74	3.55	16.75	16.53	14.97	14.38	14.89	2.41
Total	100.13	99.29	99.60	98.87	99.17	98.82	98.84	99.55
CIA[3]	76.5	60.7	72.4	73.4	75.1	75.7	74.2	53.4
Trace Elements (ppm)								
Ba	407	3890	413	406	411	368	372	6120
Rb	109	46	108	109	115	114	129	49
Sr	119	164	150	156	143	140	124	215
Y	27	11	39	38	38	38	43	6
Zr	172	122	251	217	223	215	294	72
Nb	32	13	40	38	36	37	40	10
Pb	28	11	14	14	30	12	18	22
Ga	27	8	27	24	26	25	45	6
Zn	86	62	108	95	97	97	125	50
Cu	38	23	23	33	29	31	32	12
Ni	130	24	78	98	76	79	100	12
V	122	37	140	153	142	167	227	14
Cr	131	101	131	143	139	143	242	53
La	55.2	14.7	49.1	62.2	50.5	51.7	65.8	8.4
Ce	109.0	26.2	93.9	122.0	94.2	108.0	130.0	13.9
Pr	11.90	3.02	10.40	13.00	10.40	13.20	15.50	1.60
Nd	43.8	11.8	41.6	50.9	40.8	43.5	48.8	5.9
Sm	7.8	2.2	7.9	9.3	7.6	8.2	8.5	1.1
Eu	1.84	0.64	2.12	2.45	2.02	2.01	2.16	0.36
Gd	5.7	2.0	7.3	8.0	6.9	7.5	7.5	1.0
Tb	0.9	0.3	1.1	1.2	1.1	1.1	1.1	0.2
Dy	4.9	1.8	6.4	6.9	6.2	6.4	6.6	0.9
Ho	0.9	0.4	1.2	1.3	1.2	1.3	1.4	0.2
Er	2.7	1.1	3.6	3.8	3.7	3.7	4.3	0.6
Tm	0.42	0.15	0.50	0.54	0.53	0.51	0.60	0.09
Yb	2.6	1.0	3.3	3.5	3.5	3.4	4.0	0.6
Lu	0.38	0.15	0.49	0.51	0.51	0.47	0.57	0.08
Co	32	9	16	27	21	21	19	2
Cs	6.0	0.8	5.2	5.2	6.0	5.8	7.2	b.d.
Hf	4.9	3.0	6.3	5.7	5.9	5.1	6.8	1.8
Sb	0.9	b.d.[2]	b.d.	0.7	0.6	0.9	b.d.	b.d.
Sc	16	5	20	18	20	20	26	b.d.
Ta	2.4	0.9	2.7	2.2	1.9	1.9	1.9	0.6
Th	10.0	2.9	11.4	11.7	11.6	15.8	18.5	2.1
U	2.8	0.9	2.5	2.5	2.5	3.5	4.7	0.5

[1] mds = mudstone, ss = sandstone, fss = fine grained sandstone, css = calcite cemented sandstone, sss = siderite cemented sandstone ($Al_2O_3/SiO_2 \leq 0.2$), csss = calcite siderite cemented sandstone, cmds = calcite cemented mudstone ($Al_2O_3/SiO_2 > 0.2$), cslt = calcite cemented sandstone ($Al2O3/SiO2 \leq 0.2$), scss = siderite calcite cemented sandstone

[2] b.d. = below detection limit, [3] CIA = Chemical Index of Alteration (Nesbitt and Young, 1982)

[4] MGS = mean grain size, [5] n.c. = not calculated

Table 2 Continued

Well	Peskowesk A-99								
Formation	Logan Canyon					Missisauga			
Depth	2233.62A	2233.62B	2238.65	2267.67	2276.11	2479.35	2482.14	2488.85	2492.62
Lithology[1]	ss	ss	ss	ss	ss	shale	ss	shale	shale
MGS[4] (μm)	700	700	400	400	60		200		
File	14-526	14-525	14-528	14-529	14-530	14-541	14-531	14-542	14-543
Major Elements (wt%)									
SiO_2	87.1	87.0	86.0	87.5	81.8	53.4	84.9	53.6	59.4
TiO_2	0.53	0.28	0.52	0.10	0.39	1.21	0.83	1.35	1.30
Al_2O_3	5.21	4.76	5.66	4.06	4.07	22.55	5.75	21.74	16.86
Fe_2O_{3t}	0.99	0.86	1.18	1.17	5.15	6.28	2.83	6.12	6.78
MnO	0.01	0.01	0.02	0.02	0.07	0.04	0.01	0.05	0.03
MgO	0.14	0.12	0.17	0.10	0.39	1.57	0.37	1.52	1.18
CaO	0.49	0.62	0.45	0.68	0.44	0.19	0.13	0.40	0.32
Na_2O	0.74	0.84	0.87	0.50	0.61	0.82	0.87	0.88	0.89
K_2O	1.80	1.78	2.02	1.59	1.65	2.76	1.32	2.70	2.26
P_2O_5	0.06	0.05	0.06	0.03	0.08	0.09	0.06	0.17	0.17
L.O.I	2.73	3.03	2.67	3.22	4.50	10.97	3.16	11.45	10.01
Total	99.80	99.39	99.61	98.99	99.15	99.87	100.19	100.00	99.24
CIA[3]	56.2	51.8	56.1	51.8	53.2	82.8	65.0	81.0	79.0
Trace Elements (ppm)									
Ba	5700	6700	5020	7810	1190	361	353	359	357
Rb	39	39	43	35	44	146	39	144	104
Sr	194	230	186	246	89	121	68	139	114
Y	11	7	10	5	12	33	18	36	38
Zr	223	113	245	64	300	217	316	237	359
Nb	19	11	19	6	15	32	18	37	49
Pb	21	23	23	21	9	25	5	19	11
Ga	6	6	7	4	6	27	8	30	23
Zn	51	54	72	51	36	86	39	81	84
Cu	13	12	14	15	13	37	14	34	33
Ni	11	16	28	13	21	82	20	69	60
V	29	18	25	8	51	170	38	170	139
Cr	93	56	115	55	116	147	128	152	222
La	12.4	10.0	13.5	6.9	14.9	50.5	20.8	47.0	45.5
Ce	21.3	17.2	23.3	12.5	33.0	102.0	39.5	97.7	93.3
Pr	2.47	1.98	2.71	1.44	3.01	12.30	4.30	11.90	11.20
Nd	9.5	7.7	10.4	5.7	11.4	39.6	16.6	38.9	36.8
Sm	1.8	1.3	1.9	1.1	2.1	7.3	3.1	7.2	7.0
Eu	0.57	0.42	0.56	0.38	0.58	1.65	0.85	1.70	1.57
Gd	1.7	1.2	1.7	1.0	1.9	6.5	2.9	6.9	6.4
Tb	0.3	0.2	0.3	0.2	0.3	0.9	0.4	1.0	1.0
Dy	1.7	1.2	1.7	0.9	1.9	5.3	2.7	5.5	5.8
Ho	0.4	0.2	0.3	0.2	0.4	1.1	0.5	1.2	1.2
Er	1.1	0.7	1.1	0.5	1.3	3.3	1.7	3.3	3.7
Tm	0.17	0.11	0.17	0.08	0.20	0.47	0.25	0.45	0.52
Yb	1.1	0.8	1.1	0.5	1.4	3.0	1.7	3.1	3.5
Lu	0.17	0.12	0.17	0.07	0.22	0.42	0.26	0.43	0.50
Co	2	6	7	2	8	29	7	23	15
Cs	b.d.	b.d.	b.d.	b.d.	0.7	7.7	1.0	8.3	5.3
Hf	4.9	2.8	5.7	1.7	7.1	5.0	7.3	5.3	8.0
Sb	b.d.	b.d.	b.d.	b.d.	b.d.	b.d.	0.9	0.6	0.7
Sc	3	2	4	b.d.	5	23	5	21	16
Ta	1.0	0.7	1.0	0.3	0.7	1.8	1.0	2.1	2.7
Th	2.7	2.1	2.7	1.5	3.8	21.4	4.7	19.5	15.3
U	0.8	0.6	0.9	0.4	1.0	4.5	1.3	3.9	4.1

[1] mds = mudstone, ss = sandstone, fss = fine grained sandstone, css = calcite cemented sandstone, sss = siderite cemented sandstone ($Al_2O_3/SiO_2 \leq 0.2$), csss = calcite siderite cemented sandstone, cmds = calcite cemented mudstone ($Al_2O_3/SiO_2 > 0.2$), cslt = calcite cemented sandstone (Al2O3/SiO2 ≤ 0.2), scss = siderite calcite cemented sandstone

[2] b.d. = below detection limit, [3] CIA = Chemical Index of Alteration (Nesbitt and Young, 1982)

[4] MGS = mean grain size, [5] n.c. = not calculated

Table 2 Continued

Well	Peskowesk A-99							
Formation			Missisauga				Mic Mac	
Depth	2927.36	2933.62	2940.48	2940.90	2947.43	3796.33	3806.51	3812.64
Lithology[1]	shale	ss	shale	shale	shale	ss	cslt	cmds
MGS[4] (μm)		200				100		
File	14-544	14-532	14-533	14-545	14-546	14-534	14-547	14-548
Major Elements (wt%)								
SiO_2	60.2	86.9	50.3	51.1	56.3	87.2	23.9	34.2
TiO_2	1.03	0.13	0.11	1.37	1.36	0.33	0.49	0.63
Al_2O_3	16.65	2.55	2.59	24.81	17.56	2.26	9.80	9.15
Fe_2O_{3t}	6.42	2.30	1.54	4.64	6.38	2.97	2.64	2.65
MnO	0.02	0.04	0.13	0.03	0.13	0.06	0.06	0.05
MgO	1.81	0.47	0.30	2.07	1.64	0.69	2.37	2.37
CaO	0.63	2.44	24.23	0.18	0.39	2.11	29.38	23.75
Na_2O	0.89	0.50	0.34	0.75	1.03	0.47	0.44	0.48
K_2O	3.01	0.82	0.92	4.12	3.12	0.22	1.96	1.65
P_2O_5	0.08	0.03	0.04	0.12	0.17	0.06	0.24	0.10
L.O.I	8.65	3.60	19.76	10.64	11.30	3.86	28.12	24.02
Total	99.34	99.77	100.24	99.80	99.35	100.26	99.39	99.02
CIA[3]	74.0	29.3	5.3	80.5	75.2	31.8	n.c[5]	n.c[5]
Trace Elements (ppm)								
Ba	306	1040	187	440	345	1360	151	145
Rb	136	22	23	185	124	5	94	78
Sr	109	80	311	151	119	115	689	552
Y	31	9	11	40	42	7	20	18
Zr	283	95	56	229	359	117	107	196
Nb	42	8	8	37	56	11	19	19
Pb	23	17	b.d.	b.d.	27	b.d.	7	6
Ga	22	3	3	34	26	3	13	13
Zn	83	30	b.d.	93	123	40	14	20
Cu	30	13	8	49	28	14	53	12
Ni	63	11	7	73	65	16	28	24
V	112	17	16	181	123	21	85	82
Cr	118	67	134	150	124	171	66	86
La	44.9	11.8	12.3	60.5	58.4	10.3	24.2	24.1
Ce	93.8	23.5	23.8	121.0	122.0	20.3	48.5	47.1
Pr	11.20	2.72	2.74	15.00	14.70	2.18	6.28	5.89
Nd	36.8	11.2	11.4	49.2	48.0	8.1	21.2	19.2
Sm	6.7	2.3	2.1	9.2	8.8	1.4	4.3	3.5
Eu	1.47	0.58	0.58	2.10	1.79	0.35	1.01	0.82
Gd	5.8	2.0	2.1	8.1	8.0	1.1	4.1	3.2
Tb	0.9	0.3	0.3	1.2	1.2	0.2	0.6	0.5
Dy	5.3	1.7	1.7	6.9	7.1	1.1	3.3	3.0
Ho	1.1	0.3	0.3	1.4	1.5	0.2	0.7	0.7
Er	3.2	0.9	0.9	4.3	4.5	0.7	2.0	2.0
Tm	0.46	0.13	0.12	0.61	0.60	0.10	0.27	0.28
Yb	3.0	0.8	0.8	4.0	4.0	0.6	1.7	1.9
Lu	0.42	0.13	0.11	0.56	0.56	0.10	0.25	0.28
Co	18	2	b.d.	21	27	2	1	3
Cs	6.1	b.d.	b.d.	9.6	5.4	b.d.	4.8	4.1
Hf	7.0	2.2	1.4	5.7	8.9	2.8	2.8	5.1
Sb	b.d.	b.d.	b.d.	b.d.	0.5	b.d.	n.d.	n.d.
Sc	17	2	2	26	18	2	10	8
Ta	2.7	0.4	0.4	2.4	3.6	0.7	0.8	1.1
Th	14.2	3.0	2.4	19.3	14.2	2.2	7.1	7.3
U	2.7	0.5	0.4	4.4	3.9	0.6	1.4	1.6

[1] mds = mudstone, ss = sandstone, fss = fine grained sandstone, css = calcite cemented sandstone, sss = siderite cemented sandstone ($Al_2O_3/SiO_2 \leq 0.2$), csss = calcite siderite cemented sandstone, cmds = calcite cemented mudstone ($Al_2O_3/SiO_2 > 0.2$), cslt = calcite cemented sandstone (Al2O3/SiO2 ≤ 0.2), scss = siderite calcite cemented sandstone

[2] b.d. = below detection limit, [3] CIA = Chemical Index of Alteration (Nesbitt and Young, 1982)

[4] MGS = mean grain size, [5] n.c. = not calculated

Table 2 continued

Well	Fox I-22							
Formation	Logan Canyon							
Depth (m)	317-326 (2)	317-326 (1)	363-372 (3)	408-418 (4)	418-427(5)	418-427(6)	454-463 (7)	500-509 (8)
Lithology[1]	sss	sss	sss	css	ss	css	csss	scss
MGS[4] (μm)								
File	14-451	14-450	14-452	14-453	14-454	14-455	14-456	14-457
Major Elements (wt%)								
SiO_2	45.7	43.1	52.5	58.0	54.5	58.0	55.1	58.0
TiO_2	0.52	0.54	0.31	0.22	0.40	0.19	0.21	0.29
Al_2O_3	4.60	6.01	3.18	2.91	3.71	2.55	3.35	3.09
Fe_2O_{3t}	26.45	26.51	23.83	3.42	20.26	2.58	9.66	15.38
MnO	0.45	0.54	0.39	0.18	0.37	0.18	0.23	0.33
MgO	1.60	1.69	1.71	0.45	1.63	0.29	0.93	1.23
CaO	2.23	2.36	1.70	17.60	3.10	18.71	12.80	6.51
Na_2O	0.26	0.24	0.16	0.19	0.19	0.19	0.22	0.18
K_2O	1.09	1.21	1.24	1.46	1.47	1.45	1.51	1.18
P_2O_5	0.21	0.21	0.23	0.03	0.10	0.02	0.94	0.22
L.O.I	15.96	16.42	14.74	15.69	13.80	15.66	14.66	13.65
Total	99.06	98.86	99.95	100.18	99.52	99.77	99.63	100.04
CIA[3]	44.8	50.1	40.4	7.9	33.0	6.6	11.7	18.7
Trace Elements (ppm)								
Ba	346	353	380	350	402	363	421	308
Rb	38	45	34	41	41	39	41	33
Sr	116	119	79	290	96	305	283	149
Y	23	26	15	7	12	5	10	9
Zr	268	241	164	130	260	141	135	191
Nb	8	10	6	4	8	4	6	6
Pb	16	18	6	9	9	7	12	14
Ga	7	10	5	4	5	3	4	5
Zn	35	76	17	19	26	17	15	23
Cu	33	29	15	8	17	8	12	12
Ni	18	29	6	7	13	7	7	10
V	66	83	43	16	32	9	12	23
Cr	118	106	63	94	148	100	71	130
La	18.6	21.8	11.8	10.0	13.6	7.6	9.3	8.3
Ce	40.5	48.4	26.7	20.7	29.4	15.3	16.3	17.1
Pr	4.88	5.82	3.19	2.40	3.42	1.79	1.93	2.05
Nd	18.5	22.1	12.0	8.8	12.6	6.4	7.3	7.8
Sm	3.9	4.7	2.6	1.6	2.5	1.2	1.4	1.6
Eu	0.95	1.15	0.64	0.40	0.62	0.31	0.43	0.44
Gd	3.9	4.7	2.5	1.3	2.1	b.d.	1.3	1.3
Tb	0.7	0.8	0.4	0.2	0.4	0.2	0.2	0.3
Dy	3.9	4.5	2.6	1.3	2.1	0.9	1.3	1.5
Ho	0.8	0.9	0.5	0.3	0.4	0.2	0.3	0.3
Er	2.4	2.8	1.6	0.7	1.3	0.6	0.8	1.0
Tm	0.38	0.43	0.24	0.11	0.21	0.09	0.13	0.15
Yb	2.4	2.8	1.6	0.7	1.3	0.6	0.8	1.0
Lu	0.37	0.41	0.24	0.24	0.20	0.09	0.12	0.15
Co	7	9	4	b.d.	4	b.d.	1	5
Cs	1.7	2.3	0.9	0.6	0.7	b.d.	b.d.	0.5
Hf	6.9	6.1	4.0	3.1	6.1	3.3	3.3	4.9
Sb	b.d.	b.d.[2]	b.d.	b.d.	b.d.	b.d.	b.d.	b.d.
Sc	14	15	9	2	6	1	3	4
Ta	0.6	0.7	0.5	0.4	0.6	0.3	0.5	0.4
Th	4.3	5.0	2.9	2.5	3.3	2.0	1.3	2.0
U	1.4	1.6	0.8	0.6	0.9	0.5	0.6	0.7

[1] mds = mudstone, ss = sandstone, fss = fine grained sandstone, css = calcite cemented sandstone, sss = siderite cemented sandstone ($Al_2O_3/SiO_2 \leq 0.2$), csss = calcite siderite cemented sandstone, cmds = calcite cemented mudstone ($Al_2O_3/SiO_2 > 0.2$), cslt = calcite cemented sandstone (Al2O3/SiO2 ≤ 0.2), scss = siderite calcite cemented sandstone

[2] b.d. = below detection limit, [3] CIA = Chemical Index of Alteration (Nesbitt and Young, 1982)

[4] MGS = mean grain size, [5] n.c. = not calculated

Table 2 continued

Well	Crow F-52	Argo F-38	
Formation	Logan Canyon	Logan Canyon	Missisauga
Depth (m)	600	579-588	1426-1433
Lithology[1]	sss	sss	css
MGS[4] (μm)			
File	14-458	14-459	14-460
Major Elements (wt%)			
SiO_2	38.5	45.0	66.7
TiO_2	0.54	0.45	0.33
Al_2O_3	4.01	2.88	1.92
Fe_2O_{3t}	32.05	30.60	0.96
MnO	0.57	0.43	0.12
MgO	1.48	1.20	0.17
CaO	2.22	1.08	16.01
Na_2O	0.40	0.20	0.13
K_2O	0.99	0.77	0.17
P_2O_5	0.38	0.19	0.06
L.O.I	0.00*	0.00*	12.86
Total	81.09	82.76	99.47
CIA[3]	n.c[5]	n.c[5]	6.1
Trace Elements (ppm)			
Ba	379	708	141
Rb	32	28	4
Sr	136	71	182
Y	31	25	7
Zr	333	319	143
Nb	10	7	5
Pb	11	11	13
Ga	7	4	3
Zn	40	24	8
Cu	24	22	3
Ni	16	14	3
V	70	54	23
Cr	106	83	58
La	27.1	18.6	8.2
Ce	59.0	42.2	17.3
Pr	6.98	5.15	2.01
Nd	26.8	20.1	7.3
Sm	5.4	4.2	1.3
Eu	1.30	1.01	0.35
Gd	4.9	3.8	1.0
Tb	0.9	0.7	0.2
Dy	5.1	4.1	1.1
Ho	1.0	0.9	0.2
Er	3.0	2.7	0.7
Tm	0.47	0.42	0.11
Yb	2.8	2.6	0.7
Lu	0.43	0.39	0.10
Co	10	7	b.d.[2]
Cs	1.0	1.1	b.d.
Hf	7.7	7.7	3.2
Sb	n.d.	n.d.	b.d.
Sc	13	12	3
Ta	0.7	0.5	0.5
Th	4.1	4.4	1.6
U	1.5	1.5	0.5

[1] mds = mudstone, ss = sandstone, fss = fine grained sandstone, css = calcite cemented sandstone, sss = siderite cemented sandstone ($Al_2O_3/SiO_2 \leq 0.2$), csss = calcite siderite cemented sandstone, cmds = calcite cemented mudstone ($Al_2O_3/SiO_2 > 0.2$), cslt = calcite cemented sandstone (Al2O3/SiO2 ≤ 0.2), scss = siderite calcite cemented sandstone

[2] b.d. = below detection limit, [3] CIA = Chemical Index of Alteration (Nesbitt and Young, 1982)

[4] MGS = mean grain size, [5] n.c. = not calculated, * unsufficient sample to determing LOI

Table 3. Suggested tectonic environment and lithology of the source rocks for the analysed samples based on various discriminant diagrams from the literature

	Alma K-85		Alma F-67	
Plots	**LC[2] sh (7)[3]**	**MS[2] sh (21)**	**MS[2] sst (2)**	**MS[2] sh (4)**
*TiO_2 vs Ni	Basic	Basic	Acidic	Basic
K_2O vs Rb	n/a	n/a	Basic	n/a
La/Th vs Hf	n/a	n/a	Outside-mixed	n/a
*Co/Th vs La/Sc	Andesites	Andesites	Felsic	Andesites
*REE	? (-) Eu anomaly	? (-) Eu anomaly	Very slight (-) Eu anomaly	Small (-) Eu anomaly
K_2O/Na_2O vs SiO_2	ACM	ACM, ARC (1)	PM	ACM
SiO_2/Al_2O_3 vs K_2O/Na_2O	ACM	ACM, ARC (1) (basalt, and andesitic detritus)	PM	ARC (with felsic plutonic detritus) (2) and boundary (2)
Ti/Zr vs La/Sc	n/a	n/a	Outside ACM	n/a
*Th vs Sc	Continental -> mafic signature	Continental -> mafic signature	Continental signature	Continental -> mafic signature
*La/Sc vs Th/Sc	IA intermediate	IA intermediate, IA acidic (1)	IA acidics -> IA intermediate	IA intermediate
*Th-Hf-Co	UCC	UCC	UCC	UCC
La-Th-Sc	n/a	n/a	CIA (boundary)	n/a
Th-Co-Zr/10	n/a	n/a	CIA (boundary)	n/a
Th-Sc-Zr/10	n/a	n/a	CIA (boundary)	n/a

	Glenelg N-49		Glenelg E-58	North Triumph B-52
Plots	**MS[2] sst (3)[3]**	**MS[2] sh (4)**	**MS[2] sst (8)**	**MS[2] sst (6)**
*TiO_2 vs Ni	Outside of Acidic (mature)	Basic	Acidic	Acidic and Outside
K_2O vs Rb	Basic -> acid/intermediate	n/a	Acid/Intermediate -> Basic	Basic
La/Th vs Hf	Andesitic	n/a	UCC -> old sediments	UCC -> old sed.
*Co/Th vs La/Sc	Andesites	Andesites	Felsic -> Andesites	Felsic (5), Andesites (1)
*REE	No or (+) Eu anomaly	Small (-) Eu anomaly	Small (-) Eu anomaly	(-) Eu anomaly
K_2O/Na_2O vs SiO_2	PM or outside fields	ACM (3), ARC (1)	PM -> ACM	PM (5), ACM (1)
SiO_2/Al_2O_3 vs K_2O/Na_2O	PM	ACM (3), PM (1)	PM	PM
Ti/Zr vs La/Sc	Close to PM or outside fields	n/a	ACM (2), CIA (2), PM (4)	ACM (2), CIA (1), PM (3)
*Th vs Sc	Continental signature	Mafic signature (and mixed)	Continental->mafic signature	UC signature
*La/Sc vs Th/Sc	IA acidics (1) /mafic (1)	IA intermediates (1), close to IA intermediates (3)	IA acidics->IA intermediate	IA acidics->IA intermediate
*Th-Hf-Co	Outside fields towards TC	UCC[1]	Outside UCC	Outside UCC
La-Th-Sc	Outside fields towards La	n/a	CIA and outside	ACM + PM (2), CIA (4)
Th-Co-Zr/10	OIA	n/a	Outside of CIA and PM	PM and outside
Th-Sc-Zr/10	Outside of CIA and PM	n/a	Outside of CIA and PM	PM and outside

	Sambro I-29	Naskapi N-30	Fox I-22	Argo F-38
Plots	**LC[2] sst(1)[3]**	**MS[2] sst(5)**	**LC[2] sst (8)**	**LC[2] sst (1)**
*TiO_2 vs Ni	Basic -> Acidic	Acidic and outside (1)	Acidic and outside	outside acidic
K_2O vs Rb	Acid/intermediate	Basic -> acid/intermediate	Acid/intermediate	Basic
La/Th vs Hf	UCC[1]	UCC, mixed (1)	UCC, mixed (3)	Mixed
*Co/Th vs La/Sc	Boundary felsic/andesitic	Andesites (4), felsic (1)	Andesites	
*REE	Small (-) Eu anomaly	(-) Eu anomaly	(-) Eu anomaly	No Eu anomaly
K_2O/Na_2O vs SiO_2	Boundary PM - ACM	PM	PM (2 samples in ACM)	PM
SiO_2/Al_2O_3 vs K_2O/Na_2O	ACM	PM	PM	PM
Ti/Zr vs La/Sc	Outside CIA and ACM	ACM and outside	CIA (6), ACM (1), PM (1)	CIA
*Th vs Sc	Mafic signature -> continental signature	Continental Signature	Continental (2) -> mafic signature (6)	Mafic signature
*La/Sc vs Th/Sc	Close to IA intermediate	Between IA acidics and IA intermediate	IA intermediate (2 samples towards acidics)	IA Intermediate
*Th-Hf-Co	UCC	UCC and outside (1)	outside UCC	Outside UCC
La-Th-Sc	CIA	Outside of CIA, ACM, PM	CIA and outside	Outside of CIA
Th-Co-Zr/10	CIA	OIA, PM and outside of CIA	PM (1) and outside of CIA and PM	Outside ?
Th-Sc-Zr/10	CIA	PM, CIA and outside of these fields	Outside of CIA and PM	Outside ?

Plots	Peskowesk A-99			
	LC[2] sst (7)[3]	LC[2] sh (6)	MS[2] sst (2)	MS[2] sh (6)
*TiO_2 vs Ni	Acidic & outside of this field	Basic	Outside acidic	Basic and outside
K_2O vs Rb	Acid/Intermediate	n/a	Acid/Intermediate and basic	n/a
La/Th vs Hf	Mixed felsic/basic	n/a	Outside of UCC & outside of mixed	n/a
*Co/Th vs La/Sc	Felsic volcanic -> intermediate volcanic	Felsic volcanic -> intermediate volcanic	Felsic (closer to granite) -> intermediate	Felsic volcanic -> intermediate volcanic
*REE	No Eu	Small (-) Eu	No Eu	
K_2O/Na_2O vs SiO_2	PM	ACM	PM	ACM and PM
SiO_2/Al_2O_3 vs K_2O/Na_2O	PM	ACM	PM	ACM
Ti/Zr vs La/Sc	(CIA, ACM)	n/a	PM & ACM	n/a
*Th vs Sc	Continental Signature	Mafic->CC	Continental Signature	Continental Signature
*La/Sc vs Th/Sc	IA acidics - IA intermediate	Close to intermediates	IA acidics -> IA Intermediates	Close to intermediate and NASC
*Th-Hf-Co	UCC and outside	UCC & mixed	UCC and outside	UCC
La-Th-Sc	CIA and outside	n/a	Outside CIA	n/a
Th-Co-Zr/10	CIA and outside	n/a	Outside CIA and PM	n/a
Th-Sc-Zr/10	CIA and outside (PM)	n/a	Boundary of CIA & PM and outside	n/a

Plots	Dauntless D-35	
	MS[2] sst	MS[2] sh
*TiO_2 vs Ni	Acidic, outside acidic and outside basic	Outside acidic
K_2O vs Rb	Acid/Intermediate	n/a
La/Th vs Hf	Mixed and outside UCC[1] (old sediment component)	n/a
*Co/Th vs La/Sc	Felsic	Intermediate
*REE	Small (-) Eu	No Eu anomalies
K_2O/Na_2O vs SiO_2	ACM (one sample), PM	PM
SiO_2/Al_2O_3 vs K_2O/Na_2O	ACM	ACM
Ti/Zr vs La/Sc	ACM & outside	n/a
*Th vs Sc	Continental signature	
*La/Sc vs Th/Sc	IA acidic, IA intermediate	IA acidic -> IA intermediate
*Th-Hf-Co	UCC	
La-Th-Sc	CIA & outside	n/a
Th-Co-Zr/10	CIA & outside	n/a
Th-Sc-Zr/10	CIA & outside	n/a

* indicates plot that compares with source-rock composition rather than indicating source

n/a = not applicable

[1]UCC = upper continental crust; PM = passive margin; ACM = active continental margin; ARC and OIA = oceanic island arc; CIA = continental island arc; IA = Island arc; CC = continental crust

[2]LC = Logan Canyon Formation; MS = Missassauga Formation; sst = sandstone; sh = shale

Table 4: Correlation coefficient for normal sandstones

	Na2O	MgO	Al2O3	SiO2	P2O5	K2O	CaO	TiO2	MnO	Fe2O3	Ba	Rb	Sr	Y	Zr	Nb	Pb	Ga	Zn	Cu	Ni	V	Cr	Co	La	Ce	Pr	Nd	Sm	Eu	Gd	Tb	Dy	Ho	Er	Tm	Yb	Lu	Cs	Hf	Sb	Sc	Ta	Th	U	CIA	Depth
Na2O	1.00																																															
MgO	0.40	1.00																																														
Al2O3	0.56	0.23	1.00																																														
SiO2	-0.66	-0.61	-0.75	1.00																																												
P2O5	0.49	0.47	0.58	-0.80	1.00																																											
K2O	0.31	0.24	0.59	-0.50	0.39	1.00																																										
CaO	0.13	0.12	-0.32	-0.14	0.01	-0.26	1.00																																									
TiO2	0.06	0.07	0.10	-0.35	0.46	-0.28	0.13	1.00																																								
MnO	0.17	0.32	-0.03	-0.49	0.47	-0.15	0.55	0.38	1.00																																							
Fe2O3	0.14	0.61	0.07	-0.60	0.56	-0.04	0.15	0.50	0.74	1.00																																						
Ba	-0.19	-0.40	0.17	0.14	-0.12	0.54	-0.20	-0.36	-0.27	-0.49	1.00																																					
Rb	0.36	0.21	0.75	-0.62	0.44	0.94	-0.31	-0.14	-0.10	0.05	0.47	1.00																																				
Sr	0.26	-0.17	0.44	-0.34	0.30	0.62	0.07	-0.19	0.13	-0.18	0.74	0.57	1.00																																			
Y	0.42	0.11	0.22	-0.49	0.38	-0.24	0.36	0.79	0.41	0.42	-0.41	-0.04	-0.13	1.00																																		
Zr	0.20	0.02	-0.14	-0.24	0.14	-0.33	0.54	0.67	0.43	0.36	-0.43	-0.26	-0.16	0.78	1.00																																	
Nb	0.32	0.34	0.42	-0.70	0.70	0.39	0.08	0.64	0.43	0.53	-0.04	0.43	0.27	0.51	0.38	1.00																																	
Pb	-0.15	-0.39	0.02	0.28	-0.17	-0.06	-0.25	-0.35	-0.21	-0.30	0.15	-0.09	0.15	-0.36	-0.35	-0.30	1.00																																
Ga	0.14	0.19	0.78	-0.61	0.42	0.55	-0.37	0.28	-0.06	0.19	0.24	0.74	0.25	0.27	-0.06	0.53	-0.20	1.00																															
Zn	0.21	-0.07	0.37	-0.28	0.21	0.02	-0.06	0.06	0.12	0.13	-0.11	0.10	0.26	0.10	0.04	0.08	0.57	0.11	1.00																														
Cu	0.10	-0.12	0.16	-0.01	0.16	-0.20	-0.10	0.03	0.02	-0.07	-0.02	-0.12	-0.02	0.15	-0.06	-0.07	0.55	-0.03	0.22	1.00																													
Ni	0.37	-0.06	0.48	-0.48	0.43	-0.12	0.03	0.45	0.38	0.32	-0.14	0.10	0.13	0.59	0.29	0.33	0.00	0.34	0.30	0.39	1.00																											
V	0.09	0.36	0.31	-0.62	0.61	-0.01	-0.04	0.79	0.53	0.81	-0.32	0.17	-0.08	0.61	0.42	0.70	-0.34	0.51	0.18	-0.02	0.47	1.00																									
Cr	0.21	0.19	-0.24	-0.18	0.11	-0.34	0.58	0.43	0.50	0.34	-0.44	-0.34	-0.17	0.56	0.82	0.32	-0.28	-0.22	0.01	0.06	0.20	0.22	1.00																								
Co	0.04	-0.22	0.50	-0.21	0.12	-0.09	-0.30	0.12	0.02	0.05	-0.02	0.13	0.00	0.18	-0.10	-0.01	0.44	0.42	0.49	0.45	0.71	0.21	-0.18	1.00																							
La	0.25	0.26	0.46	-0.62	0.51	-0.11	0.07	0.81	0.35	0.53	-0.40	0.13	-0.13	0.83	0.53	0.60	-0.33	0.58	0.24	0.11	0.56	0.82	0.29	0.33	1.00																						
Ce	0.20	0.27	0.37	-0.57	0.48	-0.20	0.10	0.82	0.39	0.59	-0.48	0.03	-0.21	0.82	0.57	0.55	-0.32	0.49	0.24	0.10	0.53	0.83	0.30	0.30	0.99	1.00																				
Pr	0.11	0.25	0.38	-0.52	0.44	-0.14	0.02	0.82	0.29	0.52	-0.38	0.08	-0.21	0.76	0.46	0.56	-0.32	0.58	0.18	0.07	0.46	0.82	0.19	0.30	0.97	0.98	1.00																			
Nd	0.24	0.24	0.37	-0.58	0.52	-0.18	0.13	0.86	0.39	0.55	-0.43	0.04	-0.15	0.85	0.56	0.59	-0.31	0.48	0.23	0.11	0.55	0.82	0.29	0.28	0.98	0.99	0.97	1.00																		
Sm	0.29	0.22	0.34	-0.56	0.52	-0.21	0.18	0.86	0.40	0.53	-0.43	0.01	-0.15	0.89	0.60	0.56	-0.30	0.41	0.22	0.14	0.56	0.78	0.31	0.25	0.95	0.96	0.94	0.99	1.00																
Eu	0.49	0.32	0.50	-0.73	0.70	0.06	0.18	0.77	0.41	0.52	-0.34	0.24	0.02	0.86	0.52	0.70	-0.33	0.49	0.15	0.12	0.55	0.73	0.27	0.18	0.89	0.87	0.84	0.91	0.93	1.00														
Gd	0.32	0.18	0.36	-0.57	0.51	-0.18	0.20	0.85	0.39	0.49	-0.39	0.05	-0.13	0.92	0.61	0.57	-0.32	0.44	0.18	0.15	0.59	0.75	0.32	0.27	0.95	0.94	0.92	0.97	0.99	0.95	1.00													
Tb	0.38	0.18	0.32	-0.57	0.47	-0.15	0.26	0.81	0.39	0.47	-0.34	0.06	-0.07	0.94	0.64	0.54	-0.41	0.40	0.12	0.06	0.56	0.70	0.34	0.17	0.90	0.90	0.87	0.93	0.96	0.92	0.97	1.00											
Dy	0.30	0.17	0.25	-0.54	0.44	-0.20	0.30	0.87	0.44	0.52	-0.39	0.01	-0.14	0.97	0.74	0.60	-0.38	0.38	0.11	0.10	0.56	0.75	0.48	0.19	0.91	0.91	0.88	0.94	0.96	0.90	0.97	0.97	1.00										
Ho	0.28	0.19	0.24	-0.53	0.42	-0.18	0.25	0.86	0.41	0.55	-0.38	0.02	-0.14	0.94	0.75	0.60	-0.40	0.40	0.10	0.08	0.54	0.77	0.49	0.17	0.89	0.90	0.86	0.92	0.93	0.87	0.94	0.94	0.98	1.00									
Er	0.22	0.16	0.17	-0.49	0.40	-0.20	0.30	0.89	0.44	0.54	-0.39	-0.01	-0.16	0.94	0.80	0.62	-0.41	0.36	0.07	0.04	0.49	0.76	0.54	0.12	0.88	0.88	0.85	0.90	0.92	0.85	0.93	0.93	0.99	0.98	1.00								
Tm	0.27	0.11	0.16	-0.46	0.35	-0.23	0.32	0.84	0.42	0.49	-0.40	-0.03	-0.17	0.97	0.83	0.57	-0.39	0.32	0.08	0.06	0.52	0.70	0.58	0.14	0.86	0.86	0.82	0.88	0.90	0.84	0.92	0.93	0.98	0.97	0.99	1.00							
Yb	0.27	0.13	0.13	-0.47	0.37	-0.23	0.33	0.85	0.44	0.52	-0.41	-0.04	-0.16	0.96	0.85	0.58	-0.39	0.29	0.08	0.04	0.50	0.71	0.60	0.10	0.84	0.85	0.80	0.87	0.89	0.83	0.90	0.91	0.97	0.97	0.99	0.99	1.00						
Lu	0.23	0.13	0.09	-0.45	0.34	-0.24	0.34	0.85	0.47	0.55	-0.43	-0.07	-0.17	0.93	0.88	0.59	-0.41	0.26	0.08	0.00	0.47	0.72	0.64	0.07	0.82	0.83	0.78	0.85	0.86	0.79	0.87	0.88	0.95	0.96	0.98	0.98	0.99	1.00					
Cs	-0.12	-0.10	0.45	-0.20	0.09	-0.07	-0.30	0.26	-0.02	0.11	0.02	0.21	-0.16	0.32	-0.04	0.06	-0.04	0.66	0.02	0.28	0.46	0.40	-0.21	0.63	0.53	0.49	0.56	0.46	0.41	0.35	0.45	0.38	0.38	0.35	0.33	0.33	0.27	0.24	1.00				
Hf	0.22	0.05	-0.11	-0.27	0.17	-0.36	0.50	0.70	0.46	0.42	-0.47	-0.27	-0.18	0.80	0.99	0.41	-0.35	-0.04	0.06	-0.04	0.34	0.49	0.80	-0.07	0.58	0.62	0.51	0.61	0.64	0.55	0.64	0.67	0.77	0.78	0.82	0.85	0.87	0.90	-0.01	1.00			
Sb	-0.12	0.06	-0.09	0.12	-0.09	0.06	-0.17	-0.08	-0.19	-0.03	-0.06	0.07	-0.18	-0.11	-0.10	-0.04	-0.08	0.04	-0.07	0.01	-0.18	-0.08	0.13	-0.09	-0.09	-0.13	-0.12	-0.15	-0.16	-0.13	-0.14	-0.20	-0.11	-0.12	-0.09	-0.11	-0.10	-0.10	-0.02	-0.11	1.00		
Sc	0.35	0.28	0.54	-0.68	0.60	0.02	-0.01	0.69	0.38	0.55	-0.33	0.27	-0.09	0.75	0.42	0.62	-0.36	0.64	0.16	0.14	0.69	0.81	0.27	0.41	0.88	0.84	0.82	0.84	0.81	0.83	0.83	0.80	0.81	0.81	0.78	0.76	0.74	0.72	0.55	0.47	-0.03	1.00	
Ta	0.20	0.40	0.33	-0.57	0.55	0.03	0.03	0.85	0.28	0.53	-0.29	0.13	-0.11	0.66	0.49	0.76	-0.40	0.50	0.08	-0.03	0.33	0.80	0.29	0.08	0.83	0.83	0.86	0.84	0.82	0.77	0.79	0.76	0.79	0.80	0.79	0.74	0.74	0.73	0.23	0.53	-0.14	0.70	1.00
Th	0.13	0.20	0.16	-0.47	0.39	-0.28	0.24	0.88	0.45	0.62	-0.43	-0.07	-0.22	0.88	0.72	0.53	-0.37	0.36	0.15	0.05	0.52	0.83	0.43	0.20	0.90	0.93	0.90	0.93	0.94	0.82	0.93	0.91	0.95	0.95	0.95	0.93	0.93	0.93	0.41	0.76	-0.10	0.76	0.80	1.00
U	-0.04	0.00	0.13	-0.22	0.12	-0.35	0.06	0.79	0.18	0.32	-0.34	-0.12	-0.37	0.80	0.59	0.35	-0.33	0.41	-0.01	0.12	0.47	0.64	0.33	0.33	0.83	0.84	0.86	0.83	0.81	0.65	0.83	0.80	0.84	0.84	0.85	0.86	0.82	0.80	0.58	0.61	-0.09	0.71	0.73	0.86
CIA	-0.28	-0.29	0.37	0.15	-0.09	0.01	-0.84	0.08	-0.49	-0.19	0.12	0.16	-0.17	-0.13	-0.35	-0.10	0.28	0.50	0.12	0.24	0.16	0.13	-0.50	0.56	0.20	0.18	0.27	0.14	0.07	-0.03	0.06	-0.03	-0.05	-0.02	-0.06	-0.08	-0.11	-0.13	0.62	-0.32	0.06	0.19	0.11	0.01
Depth	0.37	0.47	-0.16	-0.23	0.26	-0.26	0.39	0.12	0.38	0.42	-0.58	-0.34	-0.12	0.17	0.41	0.10	-0.01	-0.44	0.23	0.03	0.05	0.13	0.55	-0.25	0.05	0.11	-0.04	0.10	0.14	0.14	0.08	0.08	0.13	0.15	0.13	0.14	0.20	0.23	-0.52	0.45	0.01	0.01	0.11	0.17

	CIA	Depth
CIA	1.00	
Depth	-0.54	1.00

Table 5: Correlation coefficient for normal shales

	Na2O	MgO	Al2O3	SiO2	P2O5	K2O	CaO	TiO2	MnO	Fe2O3	Ba	Rb	Sr	Y	Zr	Nb	Pb	Ga	Zn	Cu	Ni	V	Cr	Co	La	Ce	Pr	Nd	Sm	Eu	Gd	Tb	Dy	Ho	Er	Tm	Yb	Lu	Cs	Hf	Sb	Sc	Ta	Th	U	CIA	Depth
Na2O	1.00																																														
MgO	0.16	1.00																																														
Al2O3	0.22	0.20	1.00																																													
SiO2	-0.30	-0.58	-0.66	1.00																																											
P2O5	0.33	0.40	0.07	-0.55	1.00																																										
K2O	0.01	0.45	0.73	-0.56	0.17	1.00																																									
CaO	-0.21	-0.20	-0.70	0.29	0.07	-0.61	1.00																																									
TiO2	0.39	0.52	0.40	-0.57	0.49	0.53	-0.36	1.00																																								
MnO	0.06	0.55	0.01	-0.50	0.37	0.06	0.00	0.41	1.00																																							
Fe2O3	0.10	0.48	0.05	-0.70	0.54	0.06	-0.02	0.29	0.65	1.00																																						
Ba	0.14	0.05	-0.31	0.10	0.20	-0.18	0.36	0.19	-0.06	-0.03	1.00																																					
Rb	-0.05	0.18	0.71	-0.21	-0.25	0.73	-0.65	0.29	-0.15	-0.33	-0.27	1.00																																				
Sr	0.43	-0.13	-0.23	0.07	0.17	-0.29	0.52	0.09	-0.14	-0.18	0.49	-0.19	1.00																																			
Y	0.08	0.38	0.39	-0.45	0.47	0.43	-0.15	0.49	0.35	0.13	-0.20	0.24	-0.14	1.00																																		
Zr	0.05	-0.04	-0.42	0.35	0.02	-0.21	0.27	0.11	0.08	-0.22	0.15	-0.22	0.22	0.32	1.00																																	
Nb	0.75	0.19	0.27	-0.28	0.20	0.13	-0.37	0.42	0.22	0.13	-0.06	0.03	0.08	0.11	0.20	1.00																																
Pb	-0.21	-0.20	0.08	0.05	-0.17	0.00	-0.15	-0.22	-0.12	0.03	-0.38	0.10	-0.23	-0.07	-0.21	-0.28	1.00																															
Ga	0.08	0.58	0.72	-0.57	-0.03	0.71	-0.63	0.53	0.32	0.14	-0.28	0.74	-0.28	0.38	-0.18	0.19	0.05	1.00																														
Zn	0.24	0.32	0.00	-0.22	0.20	0.11	-0.10	0.18	0.32	0.30	0.02	-0.20	0.04	-0.02	-0.02	0.28	0.11	0.11	1.00																													
Cu	-0.28	0.27	0.51	-0.33	-0.01	0.55	-0.46	0.17	0.05	0.08	-0.27	0.43	-0.50	0.41	-0.18	-0.16	0.07	0.42	0.01	1.00																												
Ni	0.03	0.24	0.50	-0.48	0.09	0.53	-0.54	0.45	0.19	0.33	-0.11	0.49	-0.16	-0.03	-0.48	0.00	0.23	0.56	0.18	0.36	1.00																											
V	0.10	0.52	0.72	-0.56	0.10	0.61	-0.58	0.53	0.22	0.11	-0.21	0.69	-0.16	0.43	-0.27	0.09	0.00	0.86	0.10	0.45	0.56	1.00																										
Cr	-0.14	0.33	0.09	-0.04	0.04	0.24	-0.22	0.44	0.15	-0.04	0.03	0.39	-0.02	0.21	0.16	-0.06	-0.01	0.54	0.00	0.12	0.35	0.59	1.00																									
Co	0.12	0.02	0.62	-0.33	-0.08	0.49	-0.63	0.38	-0.02	0.03	-0.28	0.64	-0.16	0.23	-0.29	0.07	0.44	0.50	0.04	0.44	0.69	0.55	0.23	1.00																								
La	0.56	0.22	0.68	-0.49	0.11	0.52	-0.60	0.54	0.22	0.05	-0.29	0.55	0.03	0.35	-0.04	0.63	0.01	0.67	0.16	0.11	0.44	0.58	0.26	0.58	1.00																							
Ce	0.53	0.16	0.64	-0.41	0.06	0.47	-0.57	0.44	0.16	-0.01	-0.32	0.53	0.05	0.31	-0.01	0.59	0.03	0.63	0.17	0.06	0.39	0.54	0.25	0.55	0.98	1.00																						
Pr	0.34	0.30	0.57	-0.42	0.08	0.48	-0.49	0.41	0.29	0.04	-0.37	0.46	-0.10	0.38	0.08	0.58	-0.14	0.65	0.23	0.20	0.31	0.51	0.24	0.37	0.98	0.89	1.00																				
Nd	0.45	0.21	0.61	-0.45	0.21	0.49	-0.47	0.46	0.17	0.03	-0.29	0.49	0.10	0.44	0.04	0.47	-0.05	0.59	0.18	0.12	0.37	0.52	0.19	0.48	0.98	0.93	0.89	1.00																			
Sm	0.36	0.21	0.57	-0.46	0.32	0.46	-0.36	0.43	0.13	0.04	-0.22	0.44	0.15	0.60	0.08	0.27	-0.05	0.51	0.12	0.21	0.30	0.52	0.16	0.45	0.98	0.76	0.73	0.93	1.00																	
Eu	0.37	0.34	0.54	-0.57	0.48	0.45	-0.30	0.52	0.26	0.19	-0.17	0.34	0.15	0.67	0.05	0.27	-0.12	0.48	0.16	0.25	0.30	0.53	0.14	0.39	0.68	0.69	0.67	0.87	0.96	1.00																
Gd	0.23	0.30	0.51	-0.45	0.39	0.44	-0.30	0.45	0.22	0.06	-0.21	0.37	0.07	0.73	0.16	0.21	-0.12	0.47	0.16	0.32	0.22	0.52	0.16	0.36	0.58	0.61	0.67	0.82	0.95	0.95	1.00														
Tb	0.15	0.20	0.46	-0.33	0.26	0.43	-0.28	0.38	0.11	-0.05	-0.23	0.42	0.12	0.60	0.16	0.11	-0.03	0.46	0.13	0.26	0.25	0.48	0.20	0.37	0.56	0.59	0.60	0.81	0.93	0.89	0.94	1.00												
Dy	0.13	0.28	0.44	-0.31	0.26	0.49	-0.29	0.47	0.17	-0.09	-0.27	0.47	0.04	0.73	0.25	0.15	-0.05	0.52	0.07	0.26	0.17	0.50	0.28	0.37	0.60	0.63	0.65	0.80	0.89	0.87	0.92	0.94	1.00											
Ho	0.01	0.34	0.36	-0.23	0.15	0.47	-0.24	0.43	0.22	-0.14	-0.30	0.45	-0.07	0.69	0.34	0.19	-0.09	0.54	0.12	0.28	0.07	0.48	0.35	0.26	0.54	0.57	0.69	0.70	0.73	0.72	0.81	0.82	0.92	1.00										
Er	-0.03	0.36	0.37	-0.20	0.03	0.49	-0.33	0.43	0.25	-0.13	-0.31	0.49	-0.12	0.56	0.30	0.20	-0.12	0.61	0.12	0.33	0.17	0.50	0.37	0.28	0.53	0.54	0.69	0.67	0.68	0.65	0.76	0.80	0.88	0.93	1.00									
Tm	-0.14	0.30	0.29	-0.12	-0.10	0.42	-0.28	0.33	0.13	-0.13	-0.26	0.43	-0.12	0.44	0.28	0.02	-0.05	0.53	0.09	0.39	0.18	0.41	0.29	0.27	0.36	0.38	0.50	0.53	0.59	0.54	0.66	0.76	0.79	0.82	0.93	1.00								
Yb	-0.01	0.35	0.40	-0.22	0.01	0.51	-0.35	0.45	0.20	-0.13	-0.29	0.50	-0.12	0.60	0.32	0.17	-0.07	0.62	0.08	0.34	0.16	0.51	0.37	0.31	0.52	0.53	0.63	0.65	0.67	0.63	0.74	0.78	0.88	0.91	0.97	0.94	1.00							
Lu	-0.07	0.31	0.35	-0.16	-0.01	0.50	-0.33	0.42	0.17	-0.15	-0.28	0.50	-0.11	0.54	0.35	0.11	-0.01	0.60	0.05	0.28	0.16	0.47	0.41	0.29	0.50	0.51	0.57	0.62	0.63	0.58	0.67	0.76	0.85	0.88	0.95	0.93	0.98	1.00						
Cs	-0.06	0.04	0.79	-0.27	-0.32	0.60	-0.63	0.12	-0.12	-0.25	-0.39	0.91	-0.23	0.19	-0.36	-0.04	0.22	0.73	-0.22	0.43	0.47	0.68	0.26	0.65	0.55	0.54	0.43	0.47	0.42	0.32	0.33	0.38	0.39	0.34	0.38	0.35	0.42	0.41	1.00					
Hf	0.11	-0.12	-0.30	0.35	-0.11	-0.15	0.15	0.10	-0.07	-0.29	0.12	-0.08	0.32	0.21	0.88	0.11	-0.06	-0.11	-0.04	-0.17	-0.33	-0.20	0.11	-0.11	0.05	0.09	0.05	0.15	0.21	0.13	0.23	0.33	0.35	0.35	0.37	0.45	0.43	0.48	-0.19	1.00				
Sb	0.22	0.06	0.18	-0.14	0.04	0.10	-0.26	0.23	-0.08	0.09	0.12	0.11	0.19	-0.23	-0.25	0.17	-0.15	0.17	0.15	0.05	0.45	0.26	0.07	0.20	0.17	0.17	0.16	0.24	0.24	0.21	0.21	0.27	0.10	0.01	0.15	0.20	0.13	0.06	0.08	-0.07	1.00			
Sc	-0.14	0.44	0.74	-0.51	-0.03	0.70	-0.54	0.45	0.28	0.03	-0.34	0.77	-0.35	0.57	-0.17	-0.01	0.03	0.81	-0.08	0.64	0.42	0.80	0.36	0.54	0.48	0.42	0.47	0.43	0.45	0.47	0.50	0.46	0.55	0.57	0.60	0.55	0.62	0.59	0.76	-0.14	-0.06	1.00		
Ta	0.79	0.04	0.23	-0.20	0.16	0.09	-0.30	0.30	0.06	0.04	-0.05	0.00	0.20	0.05	0.21	0.93	-0.15	0.09	0.27	-0.26	-0.07	-0.04	-0.16	0.08	0.63	0.63	0.54	0.52	0.34	0.29	0.22	0.18	0.20	0.19	0.16	0.03	0.15	0.12	-0.03	0.22	0.09	-0.13	1.00		
Th	0.09	0.27	0.71	-0.37	-0.10	0.47	-0.56	0.32	0.15	-0.10	-0.34	0.61	-0.34	0.48	-0.02	0.30	-0.11	0.66	-0.09	0.54	0.23	0.69	0.29	0.41	0.49	0.47	0.56	0.38	0.33	0.31	0.39	0.26	0.33	0.41	0.41	0.28	0.41	0.32	0.62	-0.12	-0.04	0.74	0.14	1.00	
U	-0.09	0.30	0.27	-0.07	-0.22	0.25	-0.35	0.22	0.18	-0.11	0.02	0.32	-0.31	0.11	0.10	0.25	-0.30	0.48	0.04	0.31	0.11	0.33	0.33	0.02	0.21	0.21	0.42	0.16	0.07	0.03	0.15	0.10	0.16	0.30	0.42	0.35	0.39	0.33	0.28	-0.01	0.11	0.41	0.10	0.58	1.00	
CIA	0.03	0.11	0.76	-0.29	-0.16	0.59	-0.96	0.27	-0.02	-0.01	-0.46	0.70	-0.58	0.17	-0.33	0.23	0.22	0.65	0.01	0.54	0.55	0.62	0.22	0.66	0.55	0.53	0.47	0.44	0.36	0.29	0.31	0.31	0.30	0.27	0.36	0.32	0.38	0.35	0.73	-0.21	0.23	0.63	0.16	0.62	0.36	1.00	
Depth	0.26	-0.01	0.16	0.12	-0.17	0.28	-0.22	0.35	-0.18	-0.41	0.15	0.42	0.39	0.03	0.31	0.32	-0.08	0.17	0.01	-0.02	0.05	0.16	0.22	0.28	0.36	0.35	0.20	0.27	0.21	0.15	0.15	0.25	0.28	0.29	0.28	0.27	0.30	0.33	0.26	0.44	0.06	0.20	0.38	0.15	0.16	0.14	1.00

APPENDIX 1: Abnormal samples with high cement content

File	Well	Formation	depth	Lithology	Remarks
14-450	Fox I-22	LC	316.99	sss	High Fe_2O_3 content
14-451	Fox I-22	LC	316.98	sss	High Fe_2O_3 content
14-452	Fox I-22	LC	362.69	sss	High Fe_2O_3 content
14-453	Fox I-22	LC	408.41	css	High CaO content
14-454	Fox I-22	LC	417.56	sss	High Fe_2O_3 content
14-455	Fox I-22	LC	417.561	css	High CaO content
14-456	Fox I-22	LC	454.13	csss	High CaO, Fe_2O_3 and P_2O_5 content
14-457	Fox I-22	LC	499.85	scss	High Fe_2O_3 and CaO content
14-460	Argo F-38	M	1426.48	css	High CaO content
14-567	Glen N-49	M	3576.78	sh	High Fe_2O_3 content
14-535	Pesk A-99	LC	2209.25	sh	High Fe_2O_3 content
14-461	Sam I-29	LC	883.88	mds	High CaO and Fe_2O_3 content
14-572	Glen E-58	M	3526.28	ss	High Fe_2O_3 content
14-240	N-Tri B-52	M	3776.62	ss	High Fe_2O_3 content
14-540	Pesk A-99	LC	2228.42	sh	High Fe_2O_3 and MgO content
14-432	Daut D-35	M	3163.21	sh	High Fe_2O_3 and MgO content

Appendix 2.

Geochemical discrimination diagrams from the Glenelg and North Triumph fields.

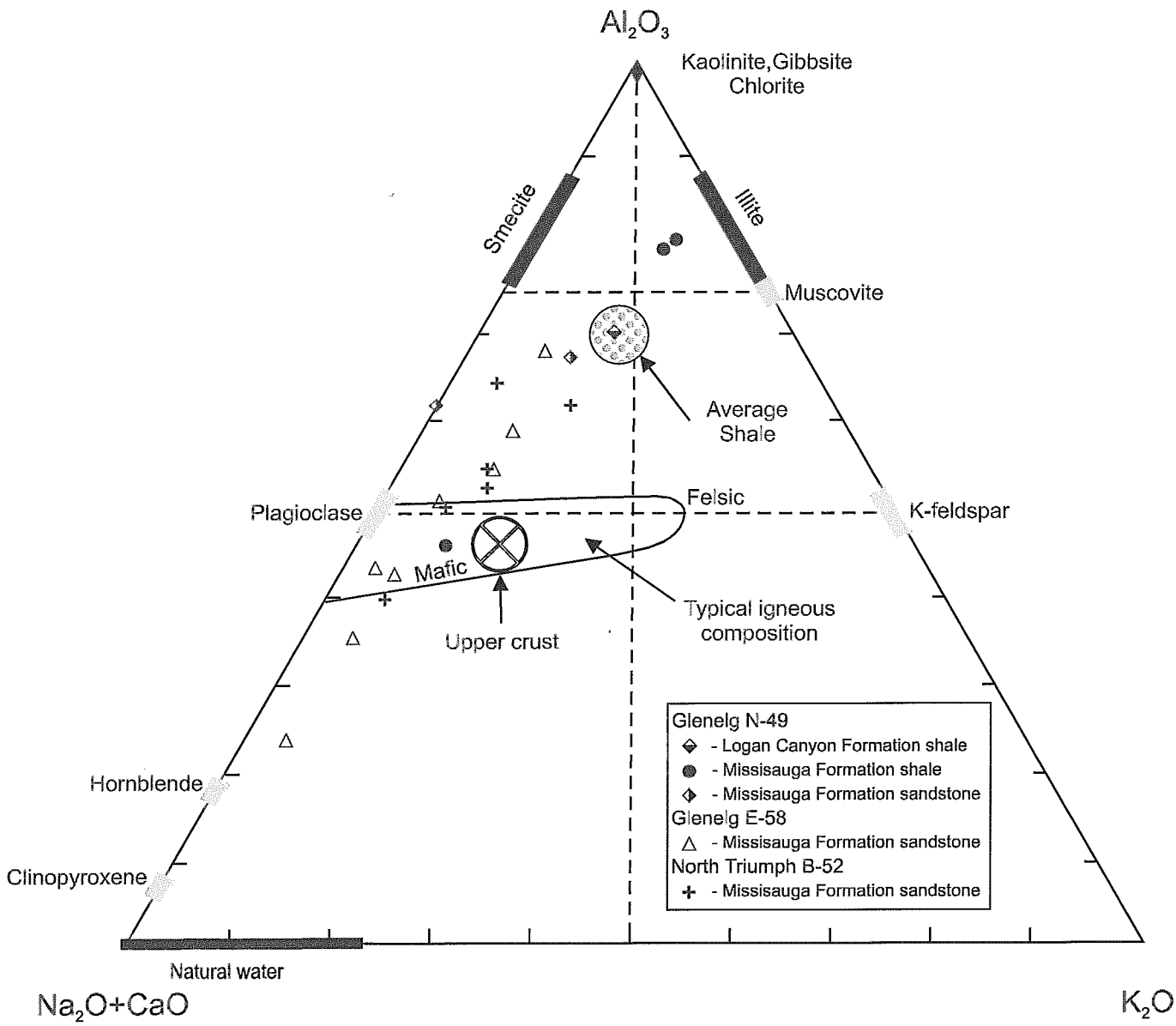

Figure 1: Ternary plot of molecular proportions of Al_2O_3 - Na_2O+CaO - K_2O. Fields from Gu et al. (2002). Idealized clinopyroxene and hornblende compositions from Taylor and MacLennan (1985).

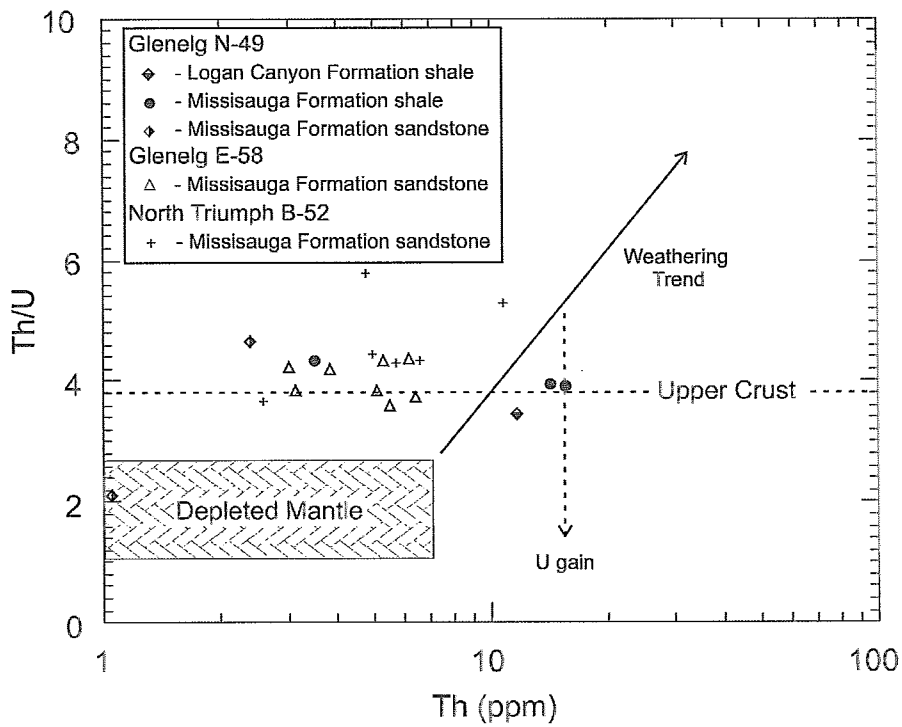

Figure 2: Th/U vs. Th plot. Fields and trends from Gu et al. (2002).

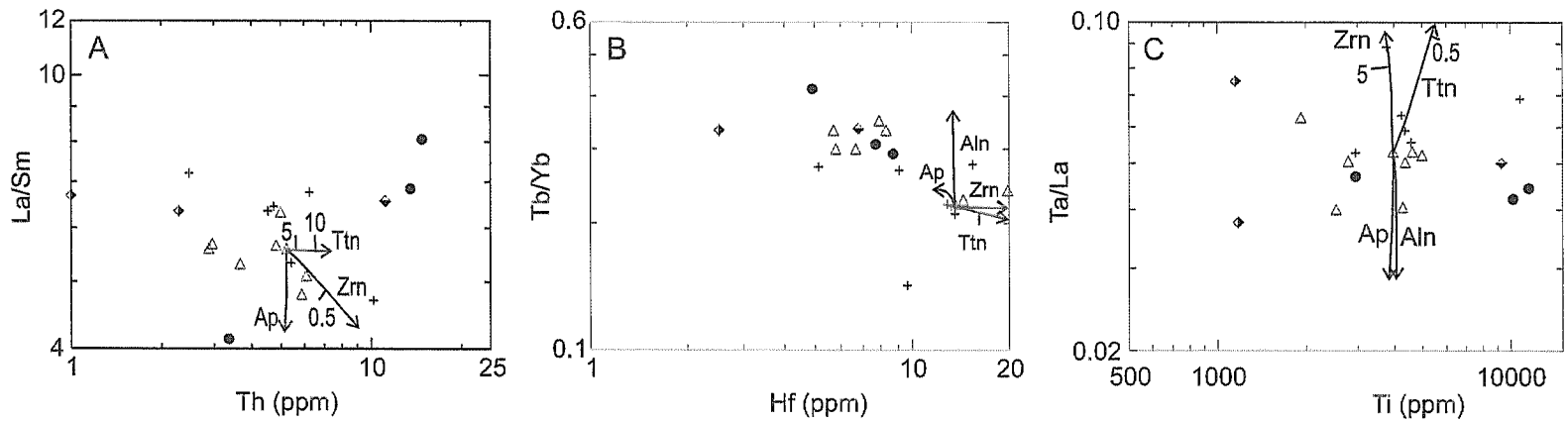

Glenelg N-49
- Logan Canyon Formation shale
- Missisauga Formation shale
- Missisauga Formation sandstone

Glenelg E-58
- Missisauga Formation sandstone

North Triumph B-52
- Missisauga Formation sandstone

Figure 3: A: La/Sm vs. Th plot. B: Tb/Yb vs. Hf plot. C. Ta/La vs. Ti plot. Heavy mineral accumulation trends modified from Flèche and Camiré (1996).

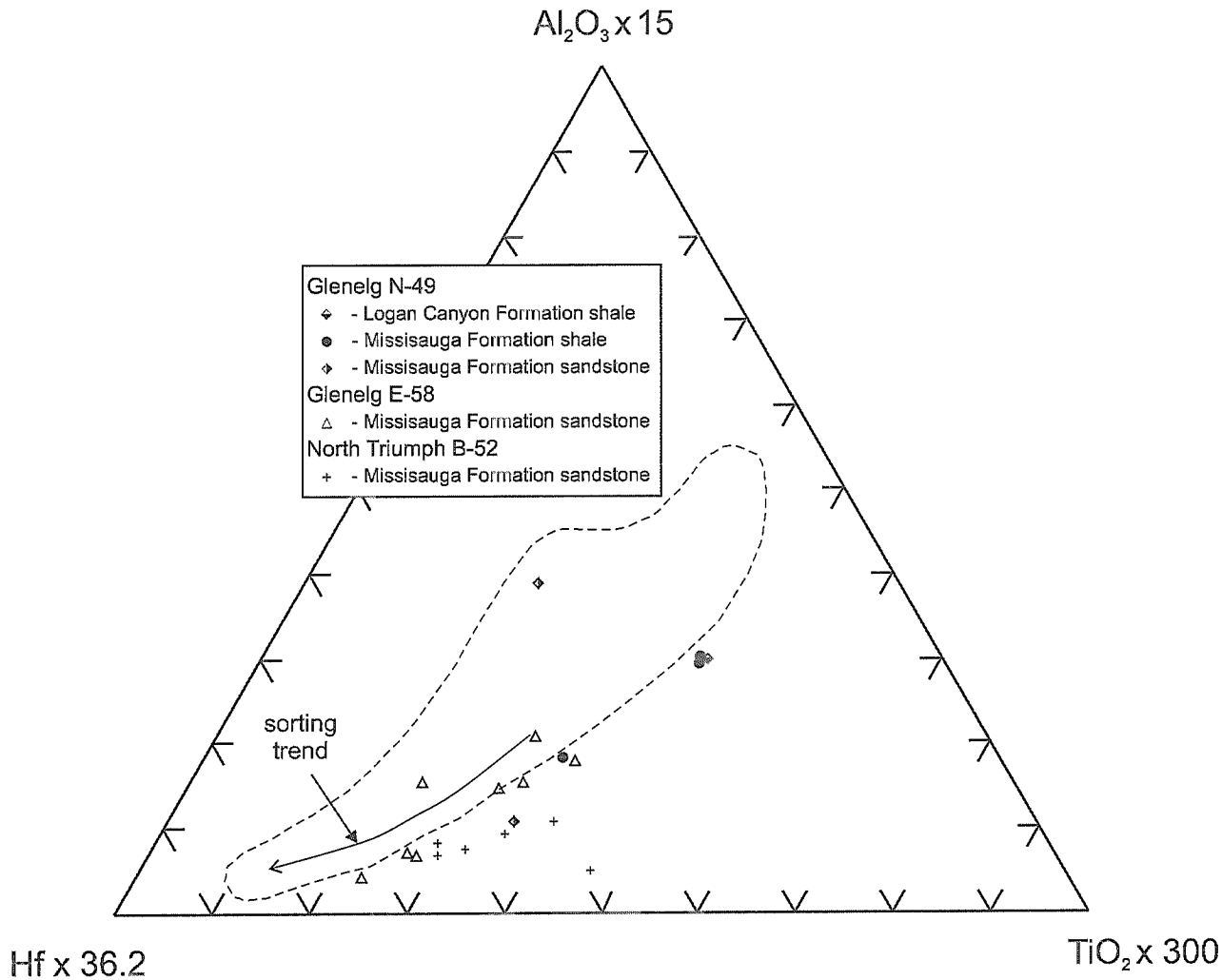

Figure 4: Al_2O_3*15 - Hf*36.2 - TiO_2*300 plot. Field after La Fleche and Camire (1996), and Garcia et al. (1994).

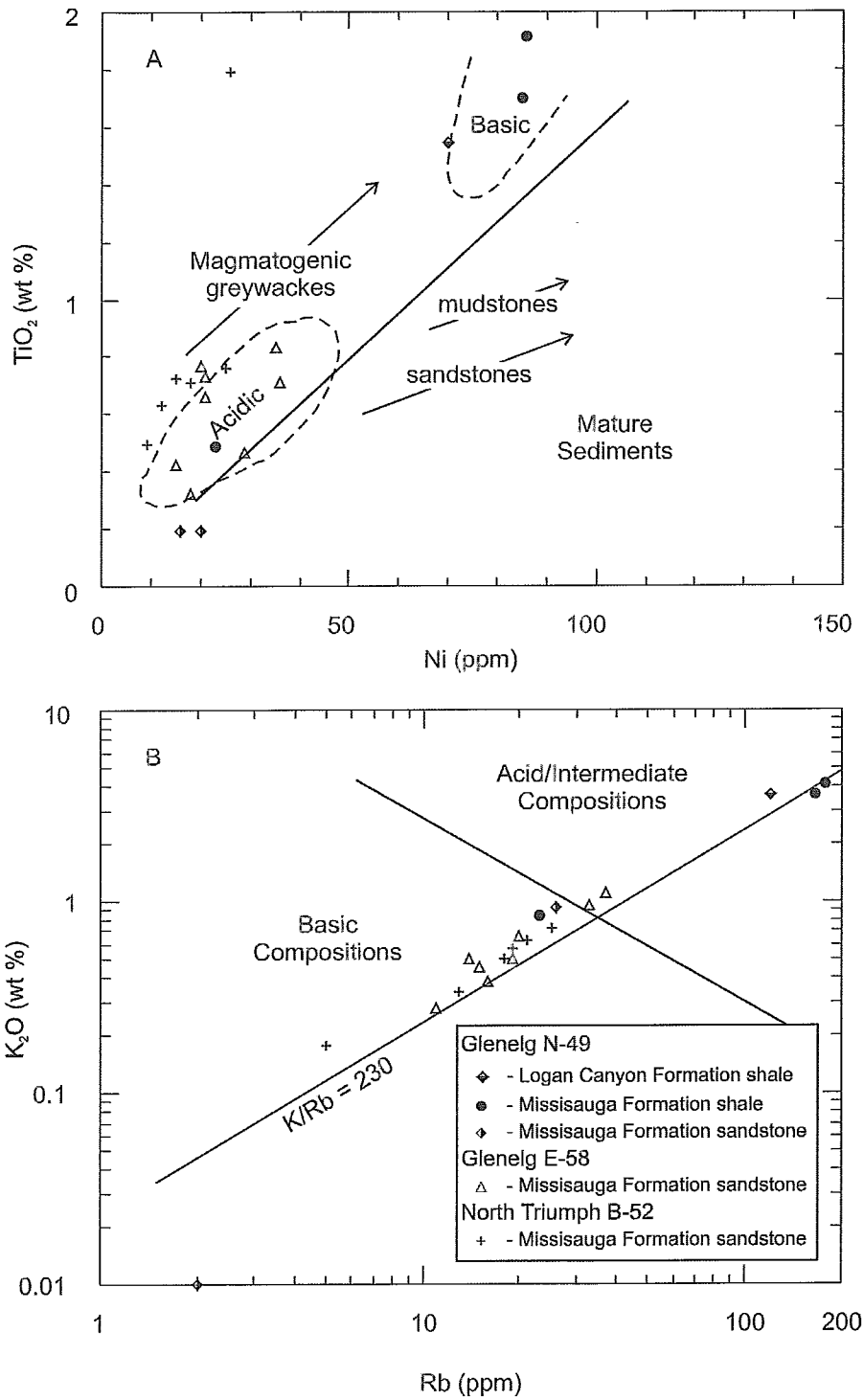

Figure 5 A: TiO_2 vs. Ni plot. Fields and trends after Gu et al. (2002) and Floyd et al. (1989). B: K_2O vs. Rb plot. Fields after Floyd and Leveridge (1987). Same symbols used in both plots.

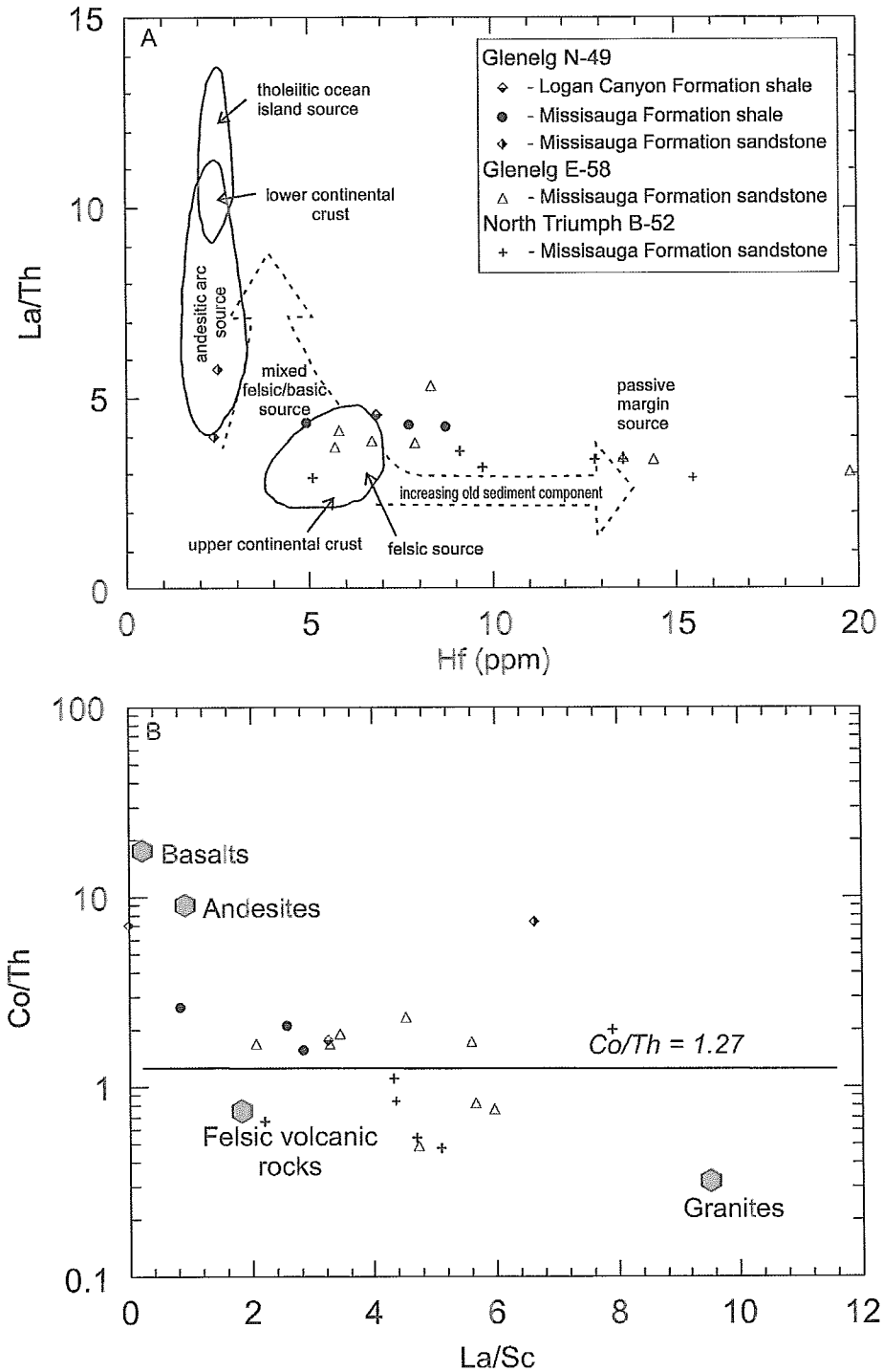

Figure 6 A: La/Th ratio vs. Hf plot. Fields after Floyd and Leveridge (1987) and Gu et al. (2002). B: Co/Th ratio vs. La/Sc ratio plot. Average compositions of igneous rocks from Condie (1993), and Gu et al. (2002). Same symbols used in both plots.

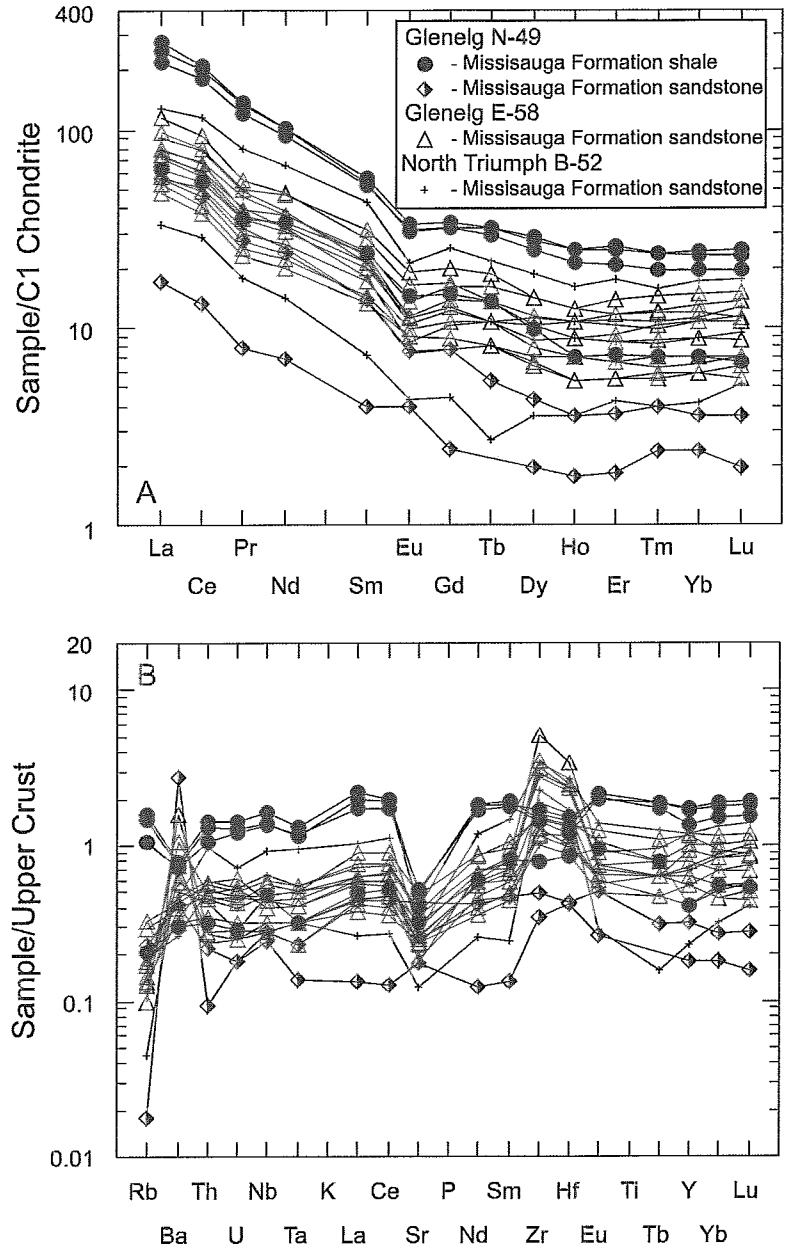

Figure 7A: Rare earth element plot normalized to C1 Chondrite values. B: Multi-element plots normalized to upper crustal values of Taylor and McLennan (1985). Same symbols are used in both plots.

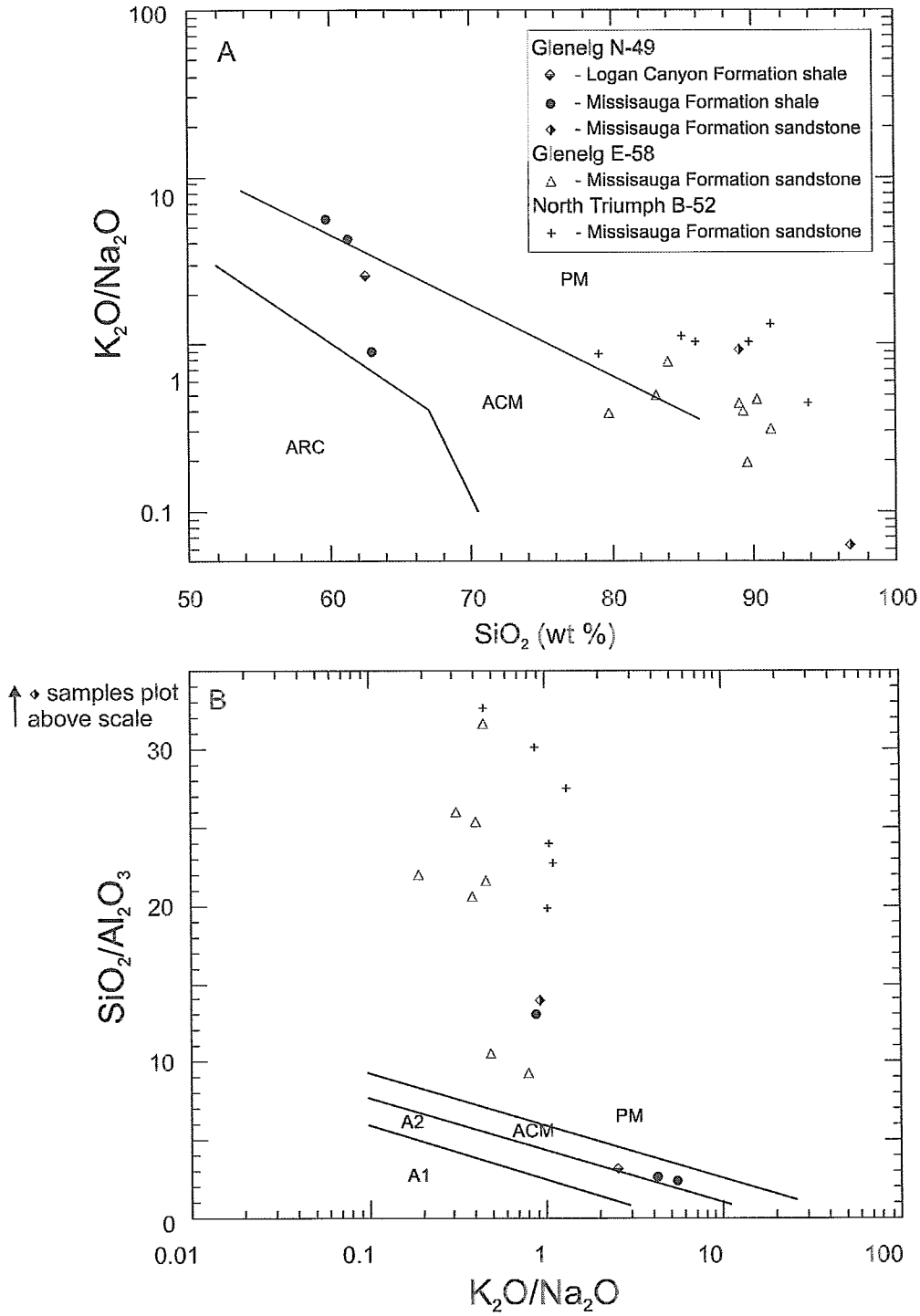

Figure 8 A: K_2O/Na_2O ratio versus SiO_2 plot. Fields after Roser and Korsch (1986): passive margin = PM, active continental margin = ACM and oceanic island arc =ARC. B: SiO_2/Al_2O_3 ratio versus K_2O/Na_2O ratio plot. Fields and boundary lines after Roser and Korsc. (1986) : passive margin = PM, active continental margin = ACM, arc setting, basaltic and andesitic detritus = A1 and evolved arc setting (felsic plutonic detritus) = A2. Same symbols used in both plots.

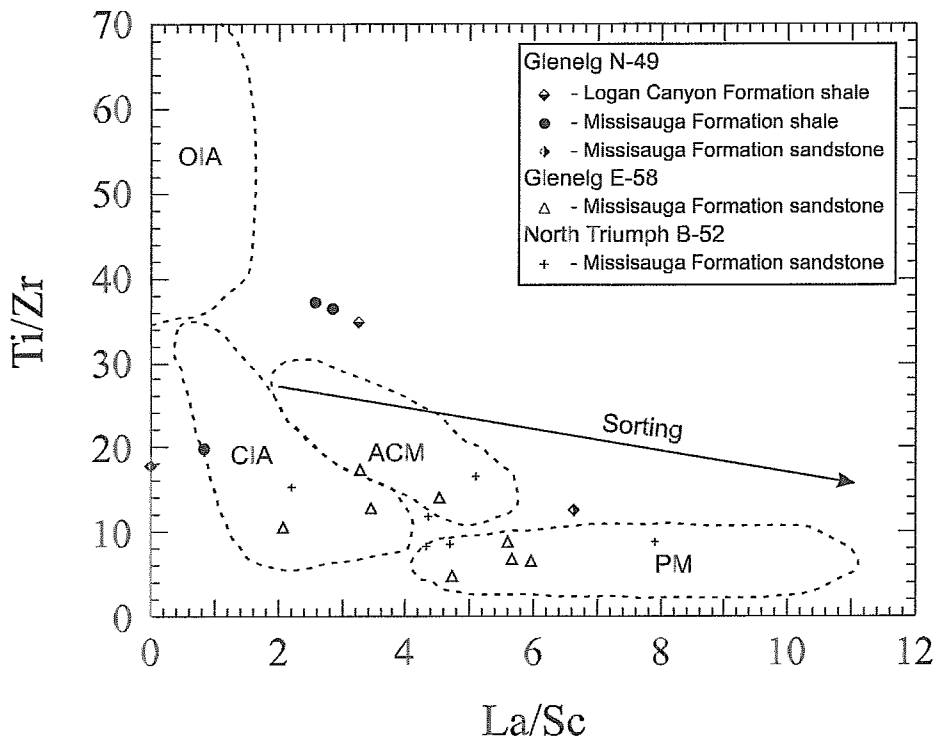

Figure 9: Ti/Zr ratio versus La/Sc ratio plot. Fields after Bhatia and Crook (1986): oceanic island arc = OIA, continental island arc = CIA, active continental margin = ACM and passive margin = PM. The sorting trend after Gu et al., 2002.

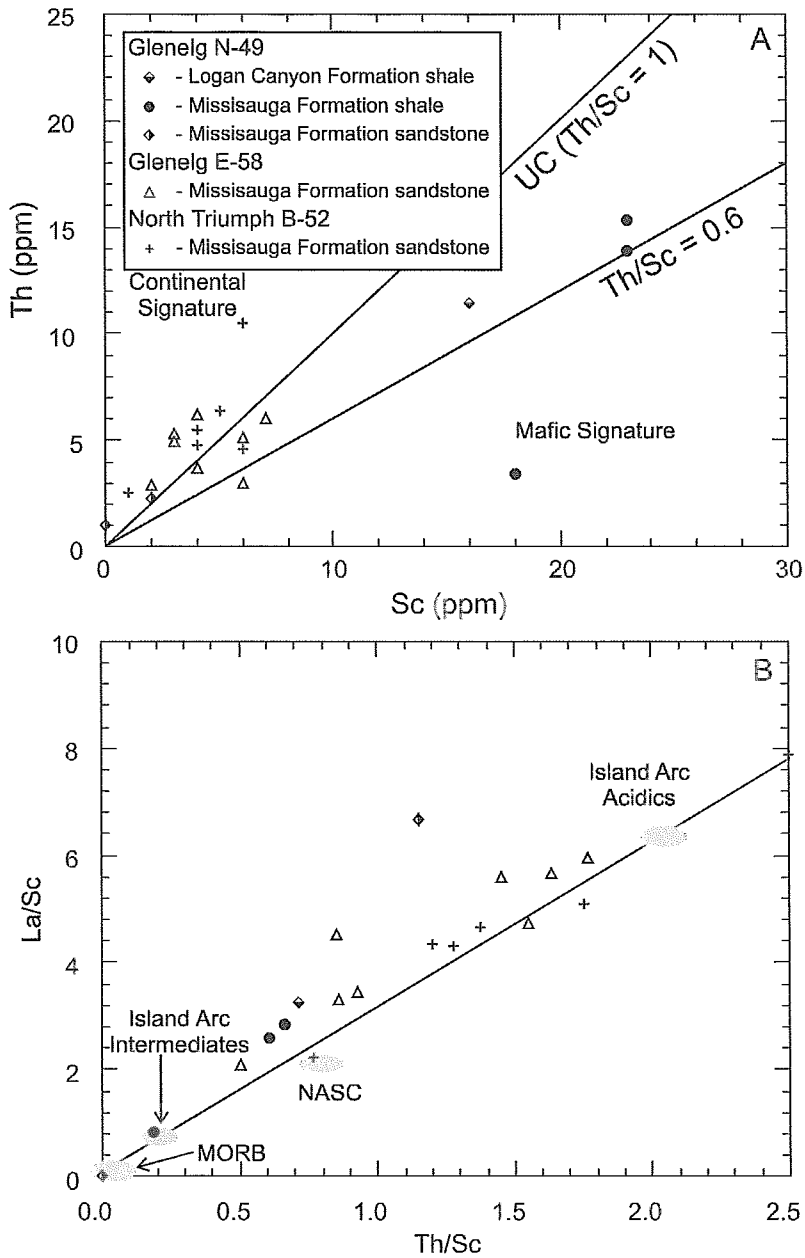

Figure 10A: Th vs. Sc plot. Fields and trends from Totten et al. (2000). B: La/Sc vs. Th/Sc ratio plot. Fields from Totten et al. (2000). Values of different igneous rock types and the North American shale composite (NASC) are included for reference (Taylor and McLennan,1985; Sun and McDonough, 1989; Gromet and Silver, 1983). Same symbols are used in both plots.

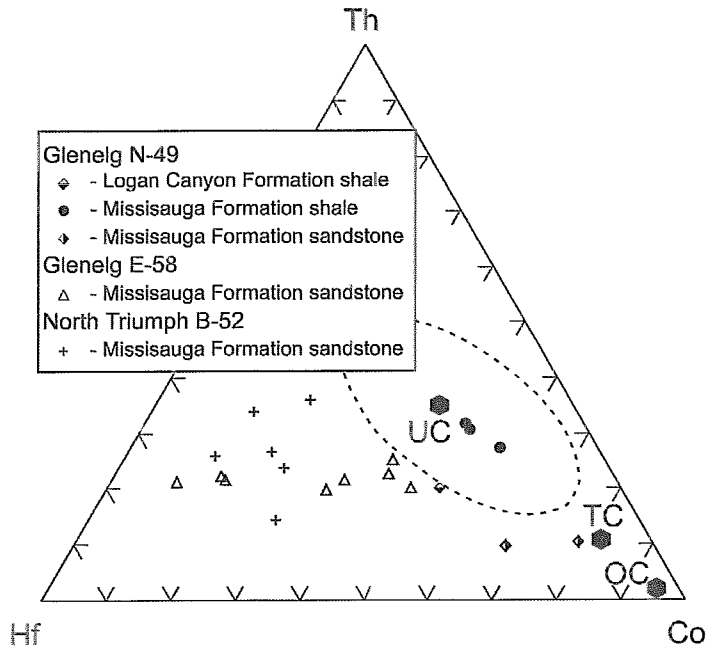

Figure 11: Th - Hf - Co plot. Fields after Taylor and McLennan, 1985. UC = Upper continental crust; TC = bulk continental crust; OC = average oceanic crust.

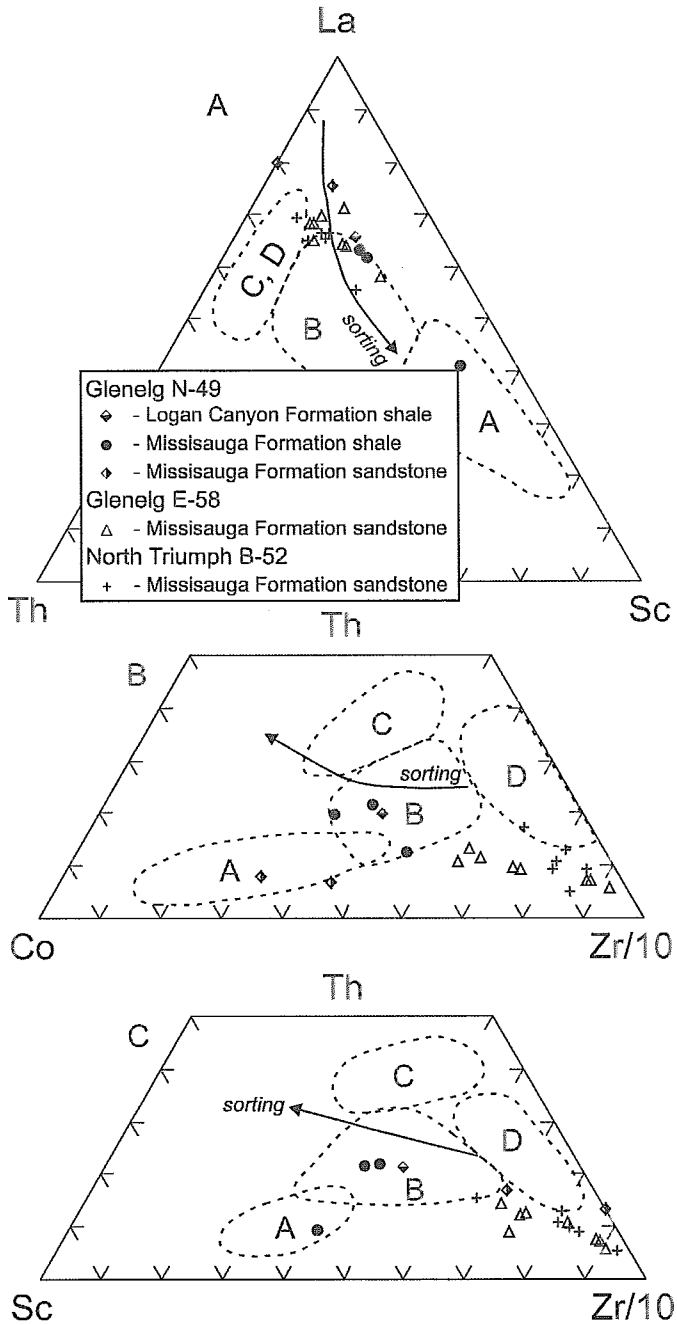

Figure 12 A: La - Th - Sc plot. B: Th - Co - Zr/10 plot. C: Th - Sc - Zr/10 plot. All fields from Bhatia and Crook (1986): A = oceanic island arc; B = continental island arc; C = active continental margin; D = passive margin. Sorting curves from Gu et al., 2002. Same symbols are used in all diagrams.

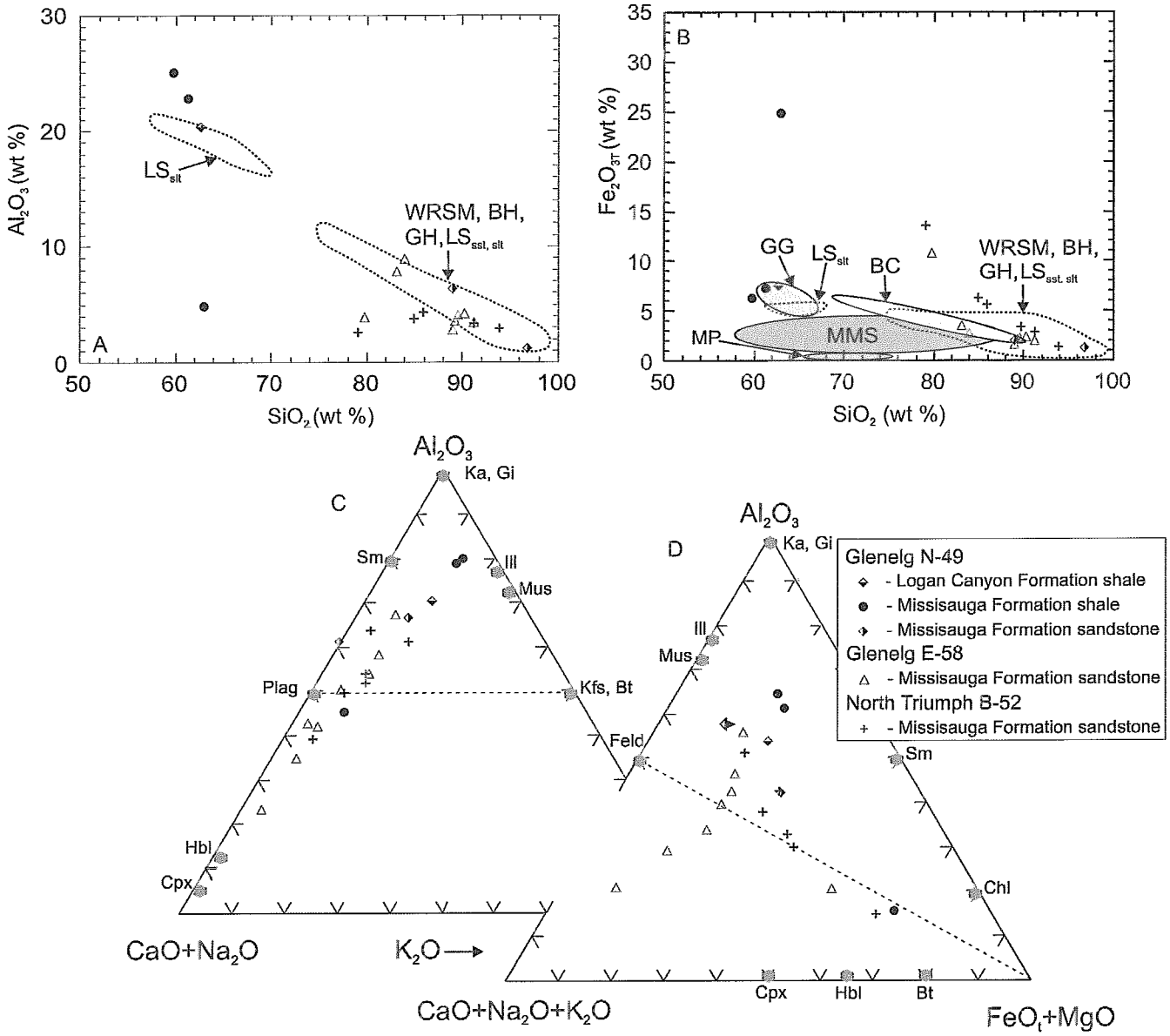

Figure 13: A: Al_2O_3 vs. SiO_2 wt % plot. LS_{sst} = Little Stewiacke sandstone, WRSM = West River St. Marys, BH = Barren Hills, GH = Graham Hill, LS_{slt} = Little Stewiacke siltstone (same for B.) B: Fe_2O_{3t} vs. SiO_2 wt % plot. Fields from Murphy (2000): GG = Neoproterozoic Georgeville Group, BC = Lower Silurian Beechill Cove Formation, MMS = Meguma Group metasedimentary rocks and MP = Meguma granitoid plutons. C: Al_2O_3 - $CaO+Na_2O$ - K_2O ternary plot and D: Al_2O_3 - $CaO+Na_2O+K_2O$ - FeO_t+MgO molar proportions (after Murphy, 2000; Nesbitt and Young, 1996; Nesbitt et al., 1995). ● mineral field abbreviations: Cpx = clinopyroxene, Hbl = hornblende, Bt = biotite, Chl = chlorite, Sm = smectite, Ka = kaolinite, Gi = gibbsite, Ill = illite, Mus = muscovite, Feld = feldspars, Kfs = K-feldspar, Plag = plagioclase. Same symbols used in all plots.

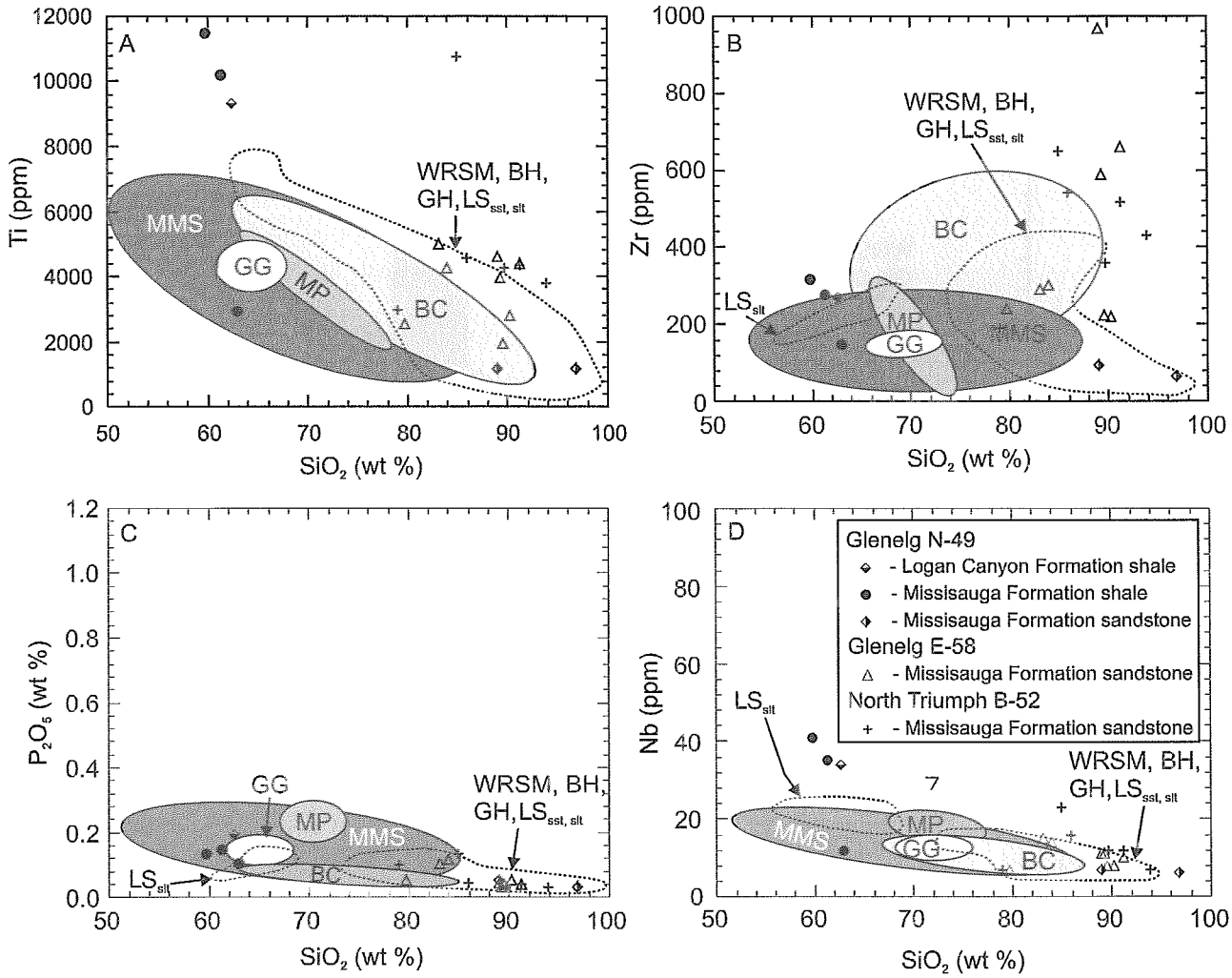

Figure 14: Selected Harker diagrams of major and trace elements. Fields are modified from Murphy (2000). A: Ti vs. SiO_2. B: Zr vs. SiO_2. LS_{sst} = Little Stewiacke sandstone, WRSM = West River St. Marys, BH = Barren Hills, GH = Graham Hill, LS_{slt} = Little Stewiacke siltstone (same for all plots). C: P_2O_5 vs SiO_2. D: Nb vs SiO_2. MMS = Meguma Group metasedimentary rocks, MP = Meguma granitoid plutons, BC = Beechill Cove Formation and GG = Georgeville Group. Legend is the same for all plots.

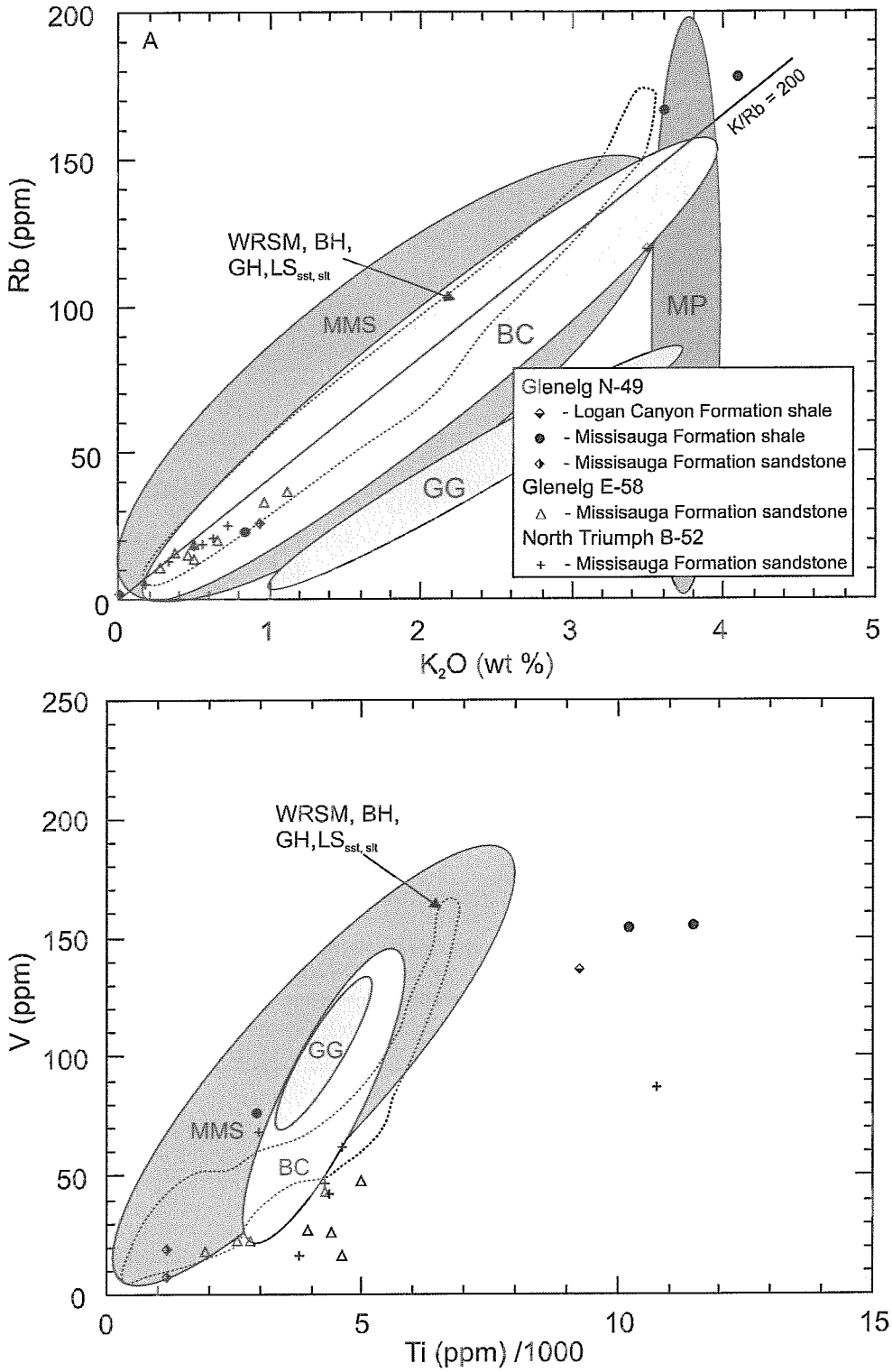

Figure 15: A: Rb vs. K_2O wt % plot. B: V vs. Ti/1000 ppm plot. Fields after Murphy (2000) MMS = Meguma Group metasedimentary rocks; MP = Meguma granitoid plutons; BC = Beechill Cove Formation; GG = Georgeville Group; LS_{sst} = Little Stewiacke sandstone; LS_{slt} = Little Stewiacke siltstone; BH = Barren Hills; GH = Graham Hill; WRSM = West River St. Marys. Same legend for both plots.

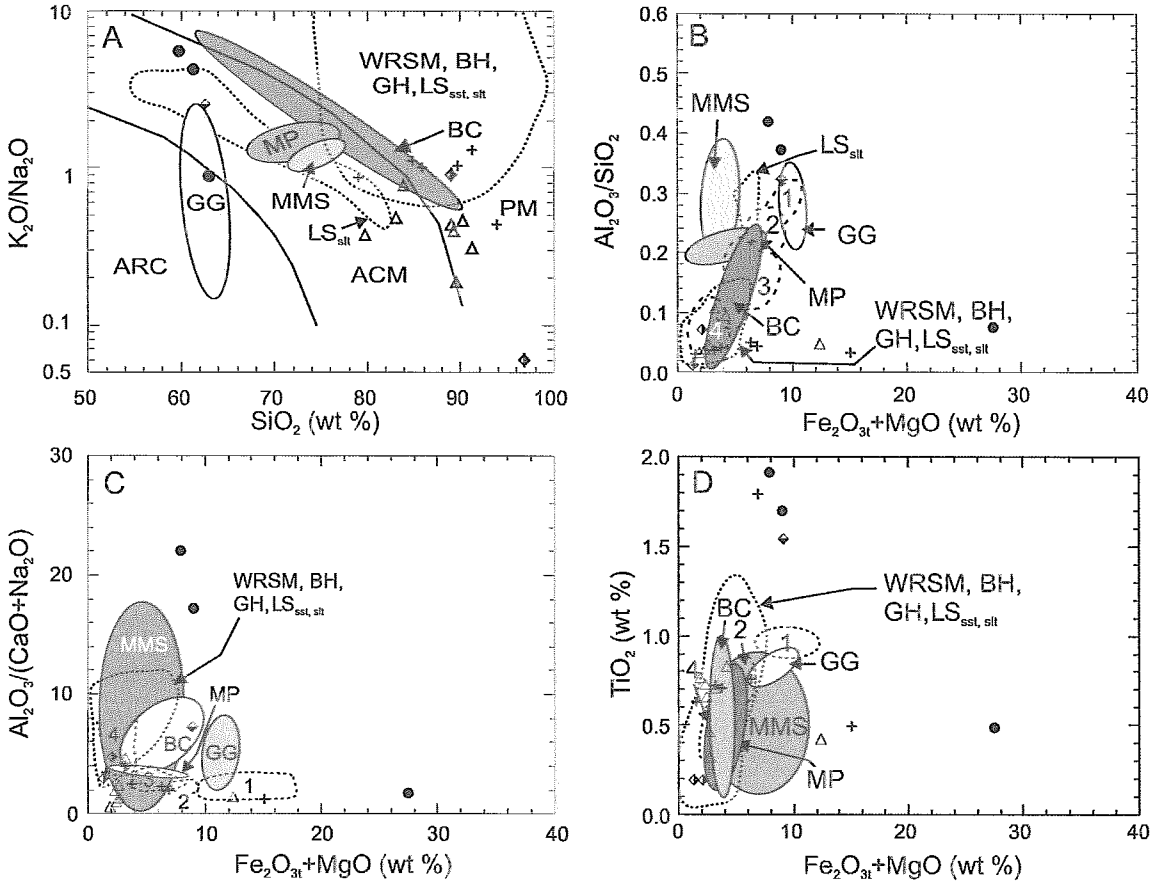

Glenelg N-49
- ◆ - Logan Canyon Formation shale
- ● - Missisauga Formation shale
- ◆ - Missisauga Formation sandstone

Glenelg E-58
- △ - Missisauga Formation sandstone

North Triumph B-52
- + - Missisauga Formation sandstone

Figure 16: A: K_2O/Na_2O vs SiO_2 (wt %) plot. B: Al_2O_3/SiO_2 vs Fe_2O_{3t}+MgO (wt %) plot. C: $Al_2O_3/(CaO+Na_2O)$ vs Fe_2O_{3t}+MgO (wt %) plot. D: TiO_2 vs Fe_2O_{3t}+MgO (wt %) plot. Solid-line fields after Murphy (2000), doted-line fields have been drawn with data from Murphy (2000). MMS = Meguma Group metasedimentary rocks; MP = Meguma granitoid plutons;GG = Georgeville Group; and, BC = Beechill Cove Formation. In A discrimination fields modified from Roser and Korch, 1986: ARC = volcanic arc; ACM = active continental margin, and, PM = passive margin. In B, C and D tectonic setting fields after Bhatia, 1983: 1 = oceanic island arc, 2 = continental island arc, 3 = active continental margin, 4 = passive margin; LS_{sst} = Little Stewiacke sandstone, LS_{slt} = Little Stewiacke siltstone, BH = Barren Hills, GH = Graham Hill, WRSM = West River St. Marys. Legend is the same for all plots.

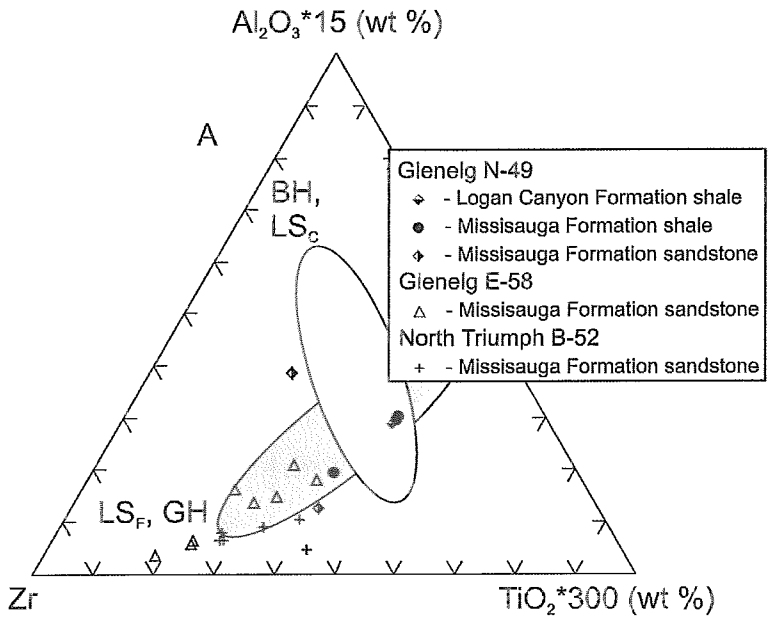

Figure 17: A: Al_2O_3*15 (wt %) - Zr (ppm) - TiO_2*300 (wt %) plot after Garcia et al. (1994) and La Flèche and Camiré (1995) comparing the fine-grained Little Stewiacke (LS_F) and Graham Hill (GH) rocks (ellipse pointing towards the Zr apex) as well as the coarse-grained Little Stewiacke (LS_C) and Barren Hills (BH) rocks (ellipse pointing towards the Al_2O_3 apex) with the Glenelg (N-49, E-58) and North Triumph (B-52) shales and sandstones (modified from Murphy 2000).

Appendix 3.

Geochemical discrimination diagrams from the Sambro I-29, Naskapi N-30, Fox I-22 and Argo F-38 wells.

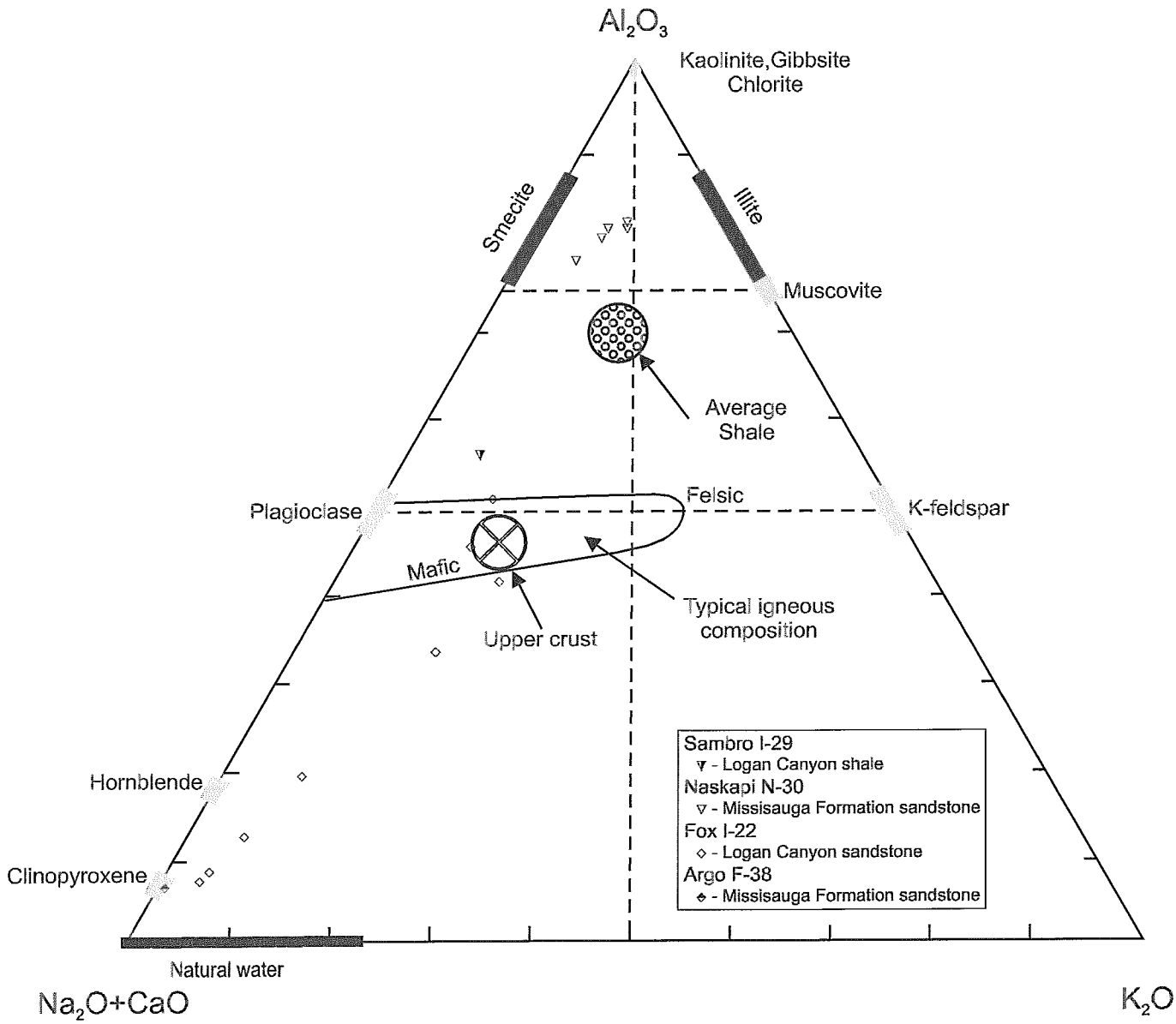

Figure 1: Ternary plot of molecular proportions of Al_2O_3 - Na_2O+CaO - K_2O. Fields from Gu et al. (2002). Idealized clinopyroxene and hornblende compositions from Taylor and MacLennan (1985).

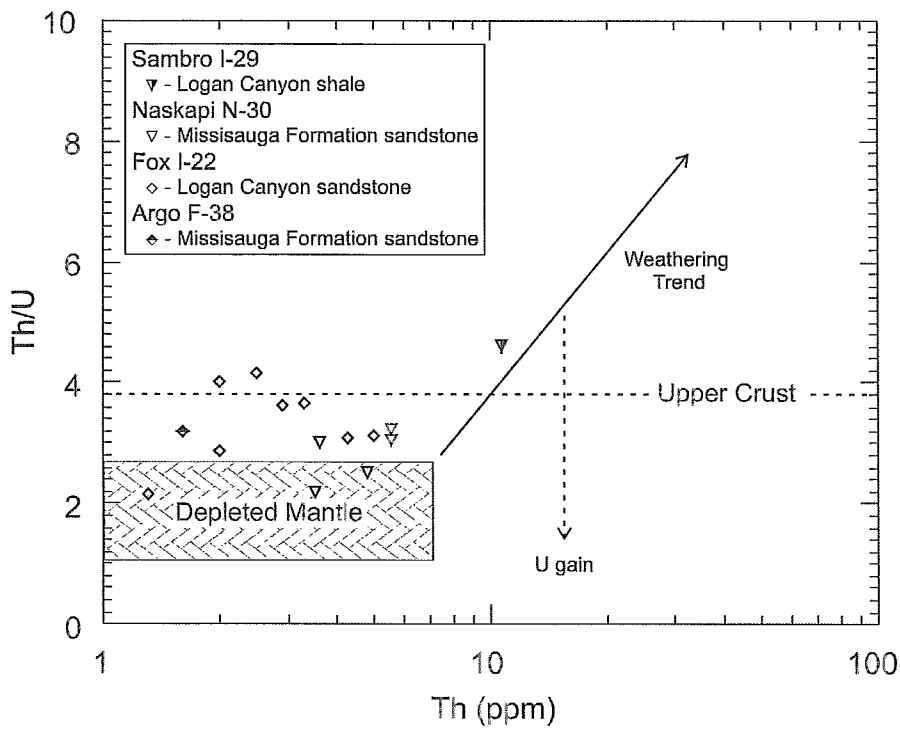

Figure 2: Th/U vs. Th plot. Fields and trends from Gu et al. (2002).

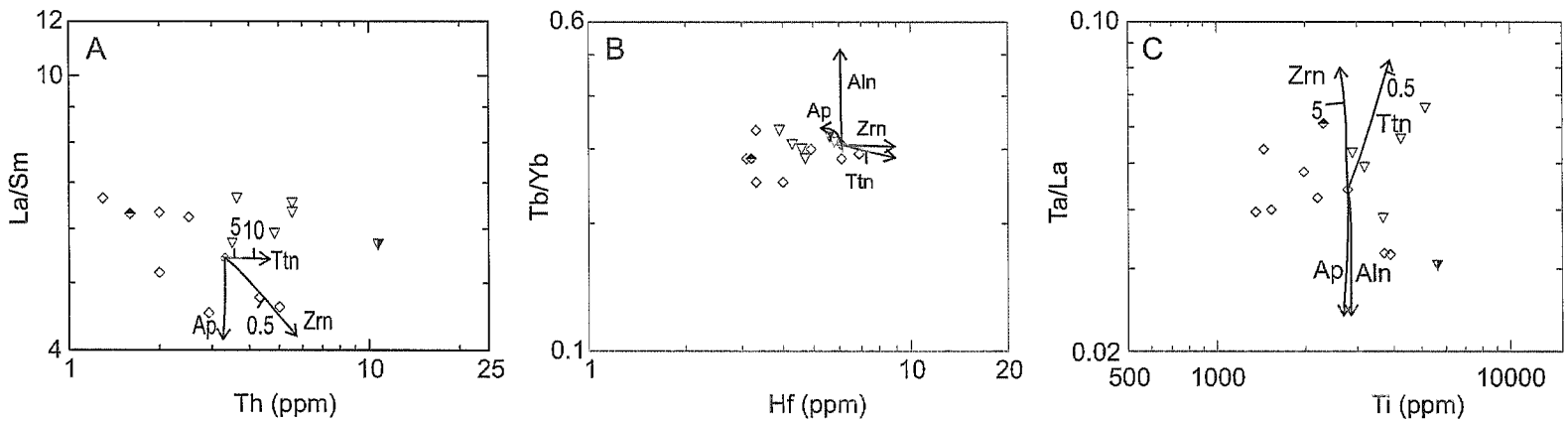

Figure 3: A: La/Sm vs. Th plot. B: Tb/Yb vs. Hf plot. C. Ta/La vs. Ti plot. Heavy mineral accumulation trends modified from Flèche and Camiré (1996).

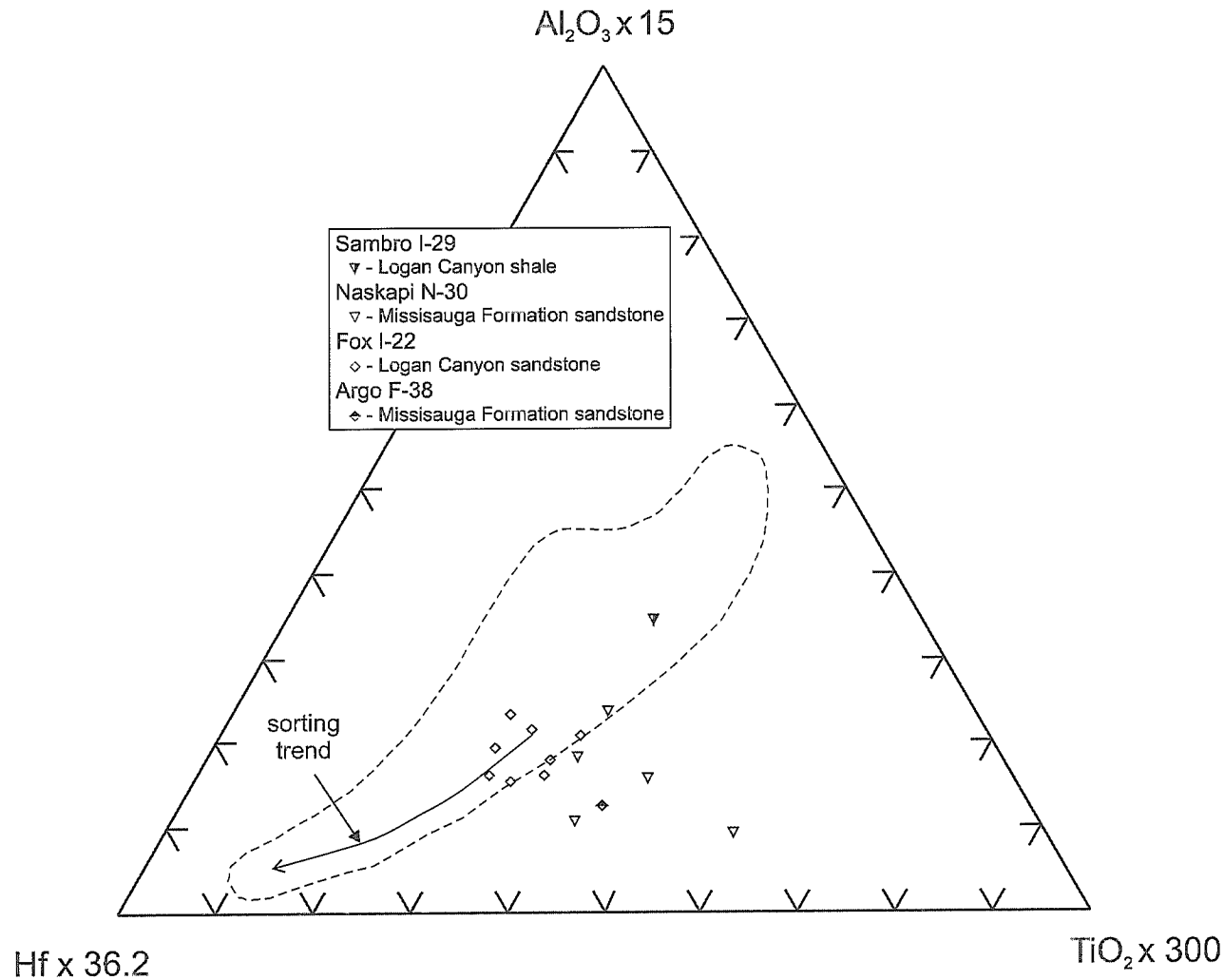

Figure 4: Al_2O_3*15 - Hf*36.2 - TiO_2*300 plot. Field after La Fleche and Camire (1996), and Garcia et al. (1994).

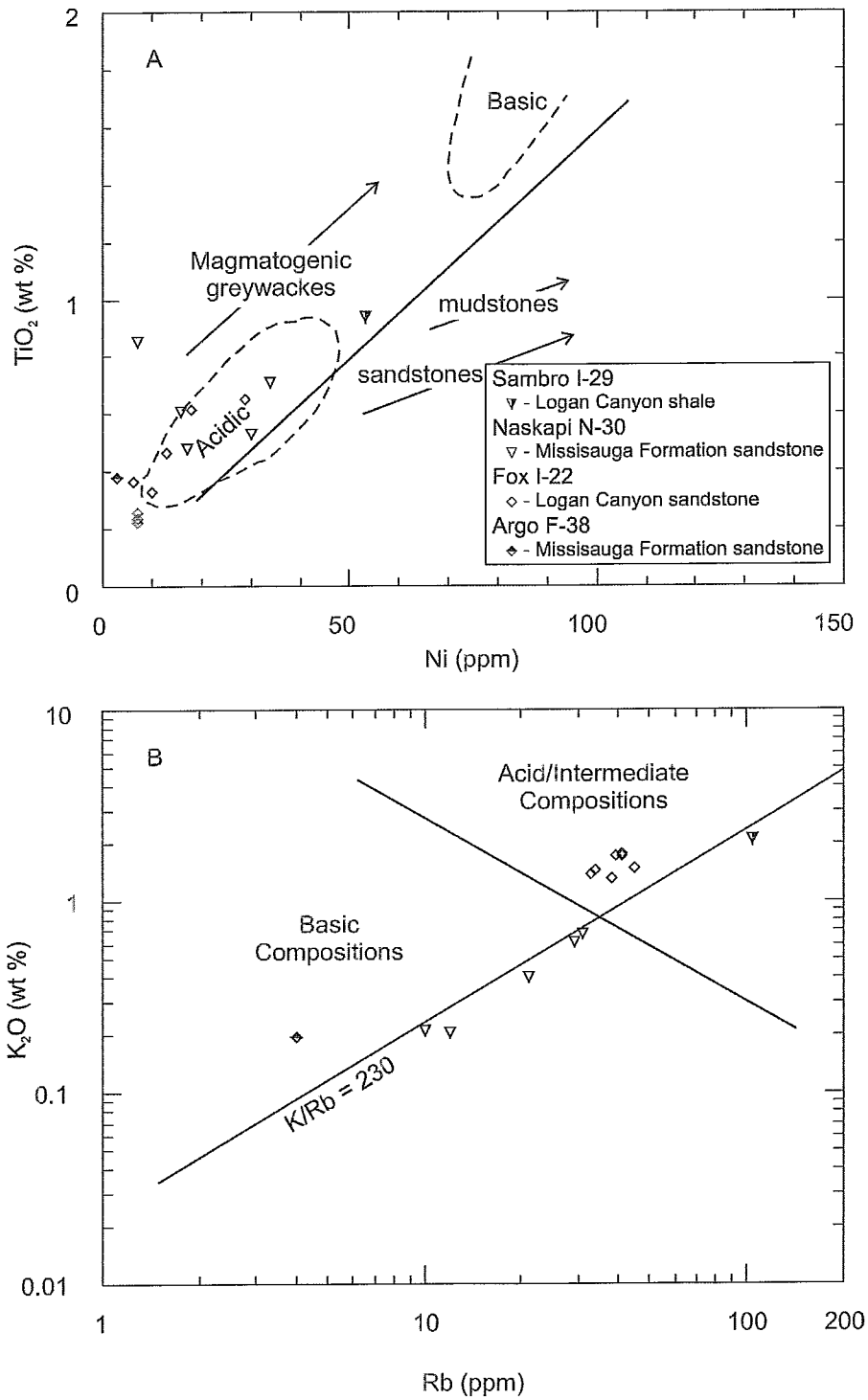

Figure 5A: TiO_2 vs. Ni plot. Fields and trends after Gu et al., 2002 and Floyd et al. (1989). B: K_2O vs. Rb plot. Fields after Floyd and Leveridge (1987). Samples the same for both plots.

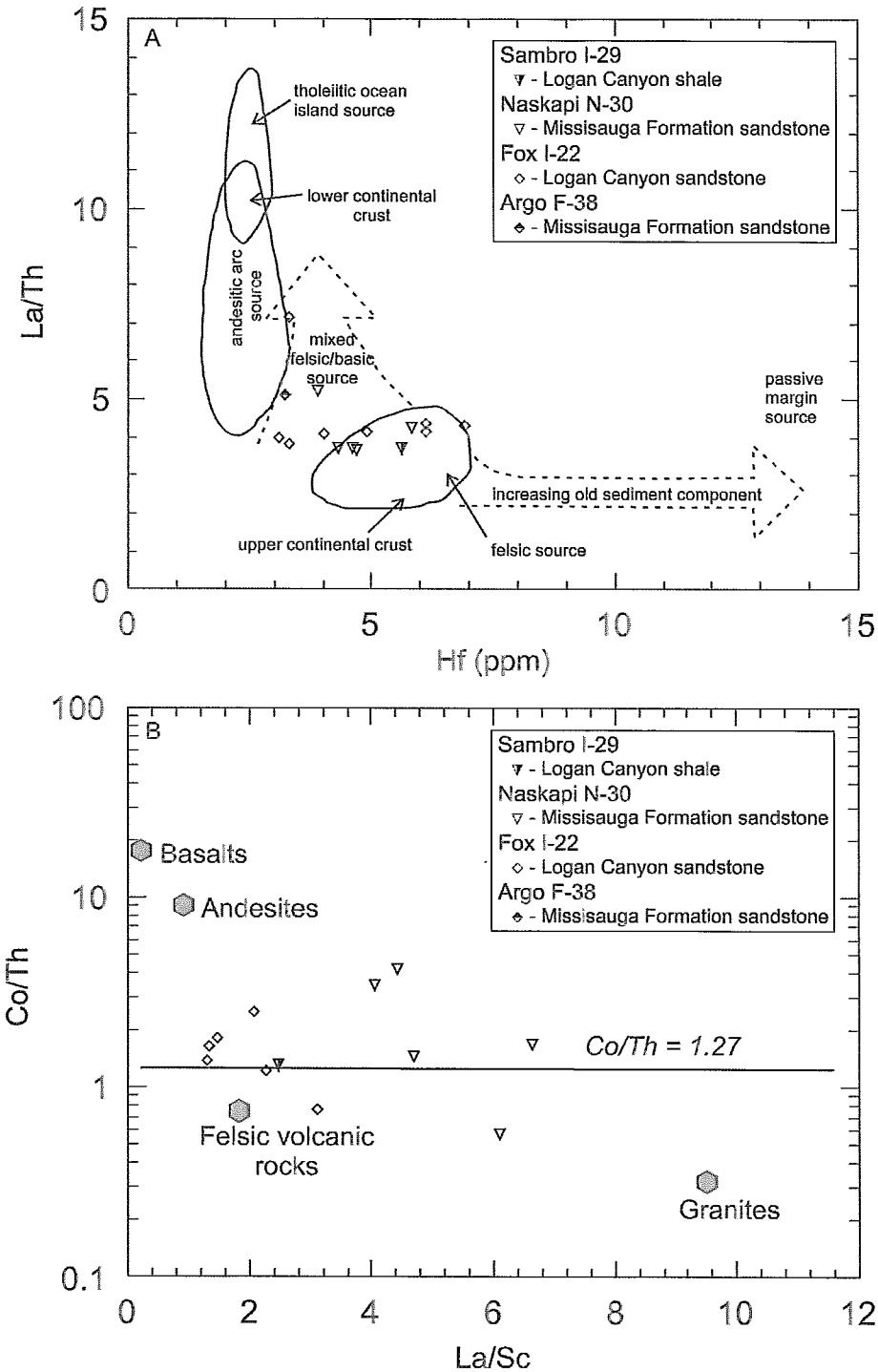

Figure 6 A: La/Th ratio vs. Hf plot. Fields after Floyd and Leveridge (1987) and Gu et al. (2002). B: Co/Th ratio vs. La/Sc ratio plot. Average compositions of igneous rocks from Condie (1993), and Gu et al. (2002).

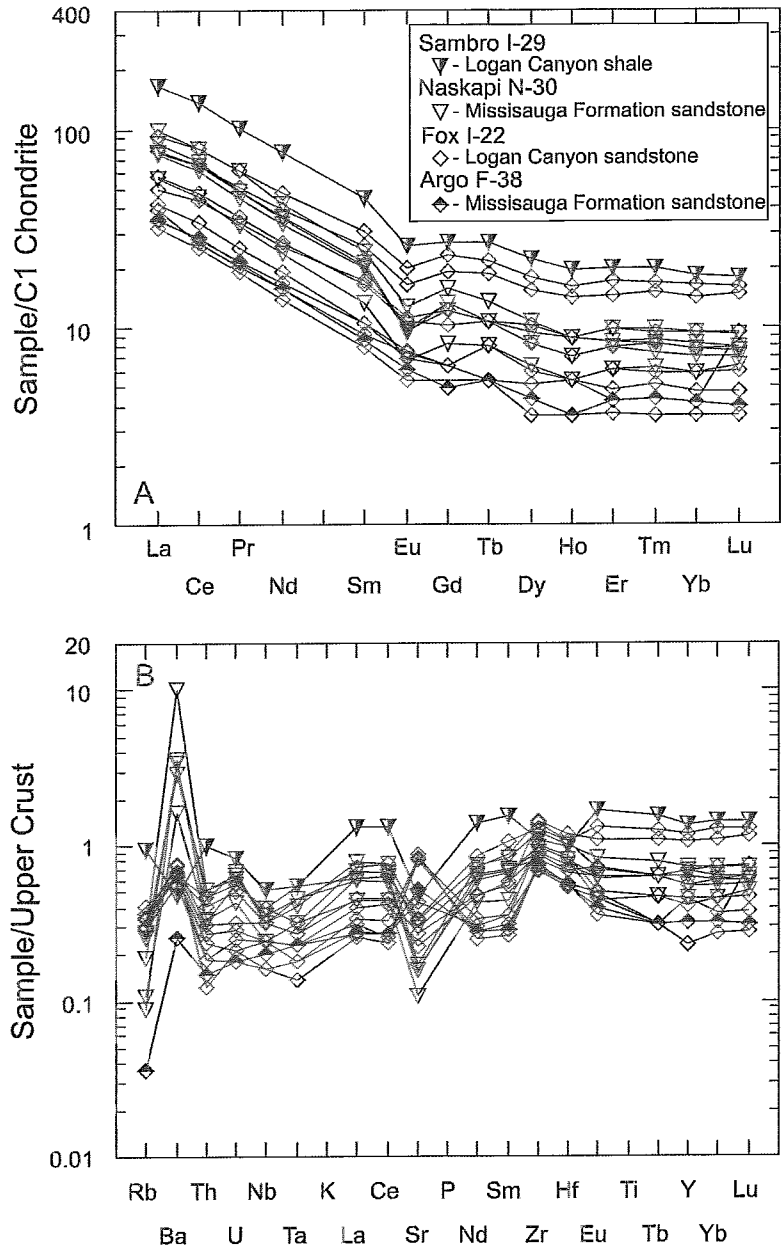

Figure 7A: Rare earth element plot normalized to C1 Chondrite values. B: Multi-element plots normalized to upper crustal values of Taylor and McLennan (1985). Same symbols are used in both plots.

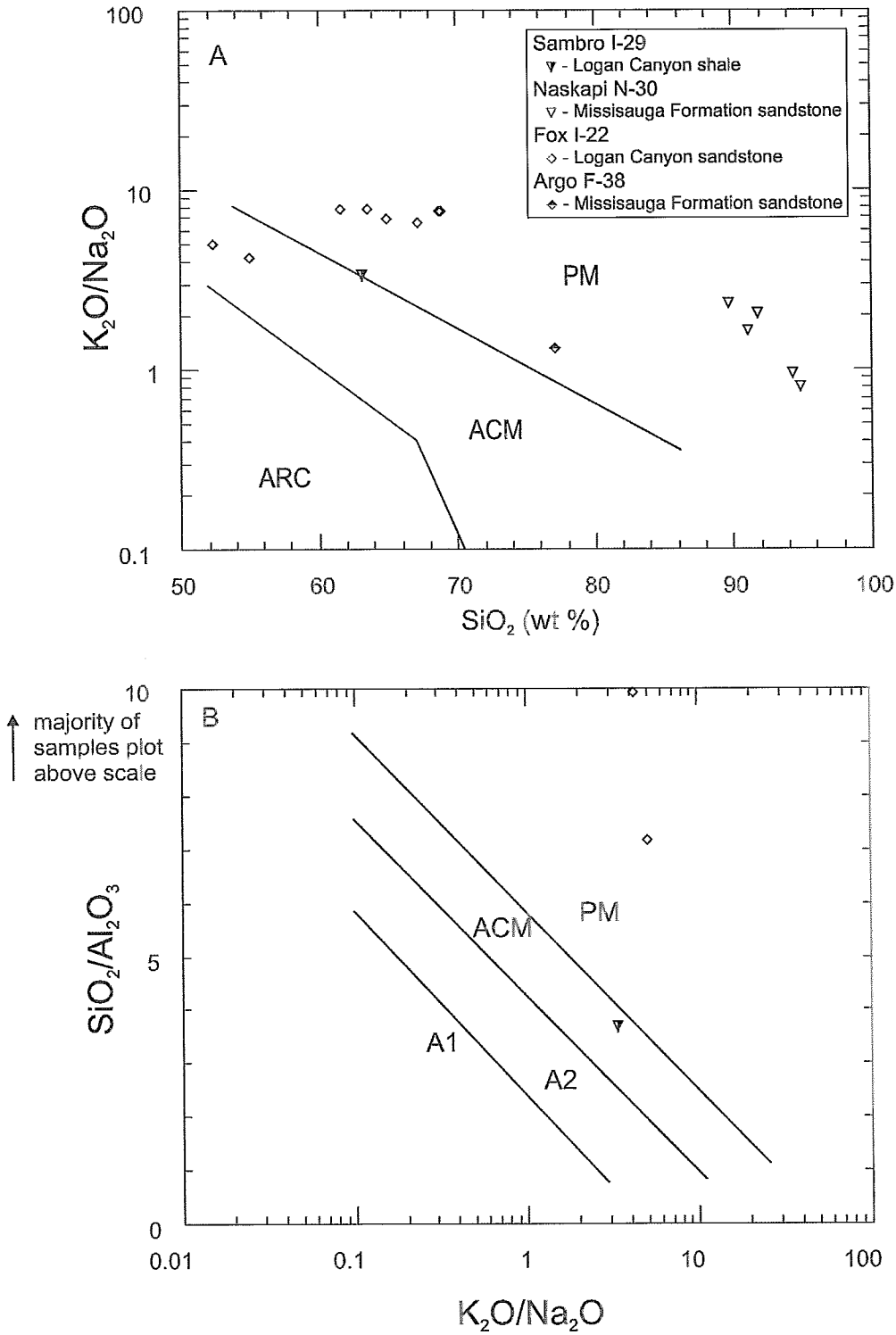

Figure 8 A: K_2O/Na_2O ratio versus SiO_2 plot. Fields after Roser and Korsch (1986): passive margin = PM, active continental margin = ACM and oceanic island arc =ARC. B: SiO_2/Al_2O_3 ratio versus K_2O/Na_2O ratio plot. Fields after Maynard et al. (1982) : passive margin = PM, active continental margin = ACM, arc setting, basaltic and andesitic detritus = A1 and evolved arc setting (felsic plutonic detritus) = A2.

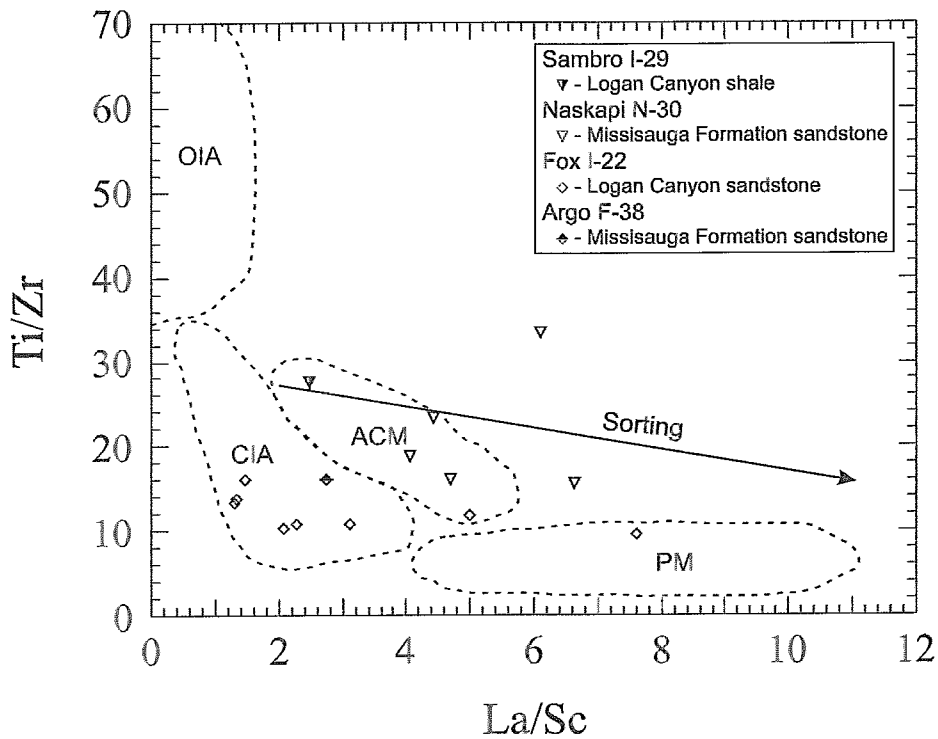

Figure 9: Ti/Zr ratio versus La/Sc ratio plot. Fields after Bhatia and Crook (1986): oceanic island arc = OIA, continental island arc = CIA, active continental margin = ACM and passive margin = PM. The sorting trend after Gu et al., 2002.

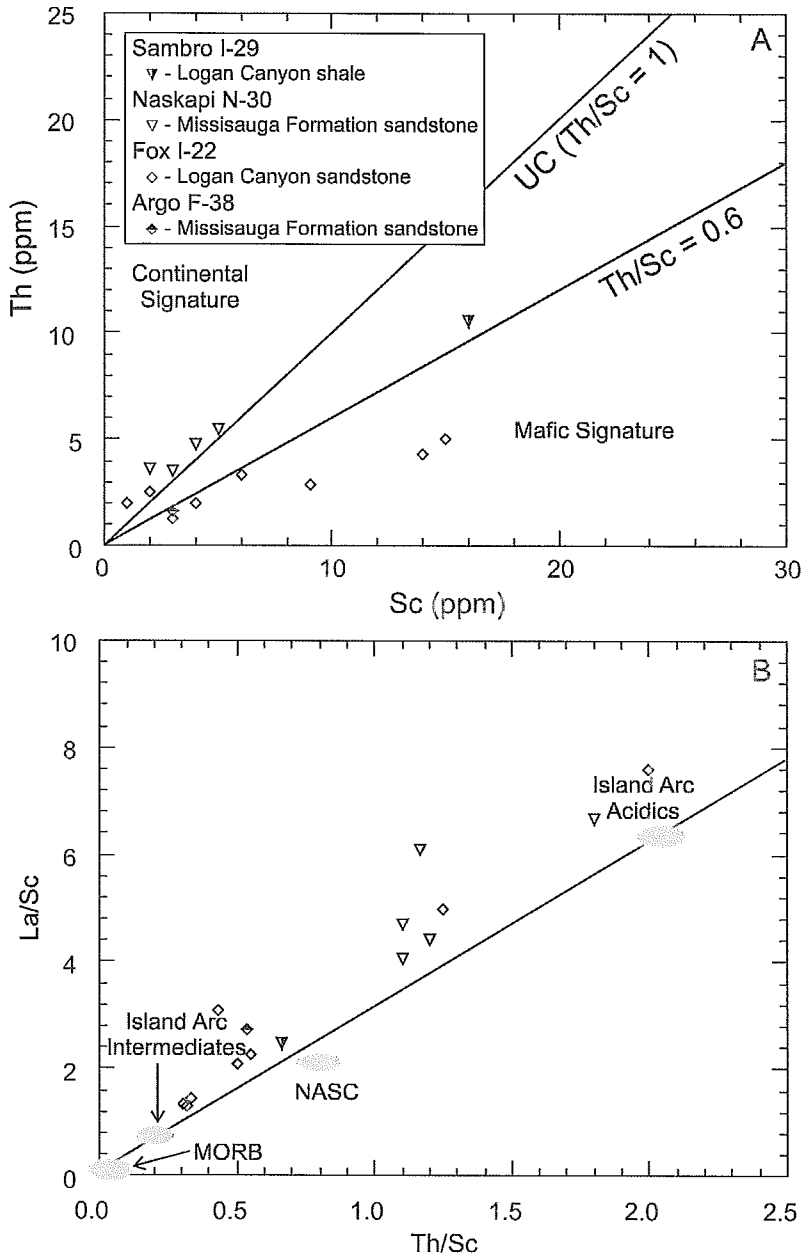

Figure 10 A: Th vs. Sc plot. Fields and trends from Totten et al. (2000). B: La/Sc vs. Th/Sc ratio plot. Fields from Totten et al. (2000). Values of different igneous rock types and the North American shale composite (NASC) are included for reference (Taylor and McLennan,1985; Sun and McDonough, 1989; Gromet and Silver, 1983). Same symbols are used in both plots.

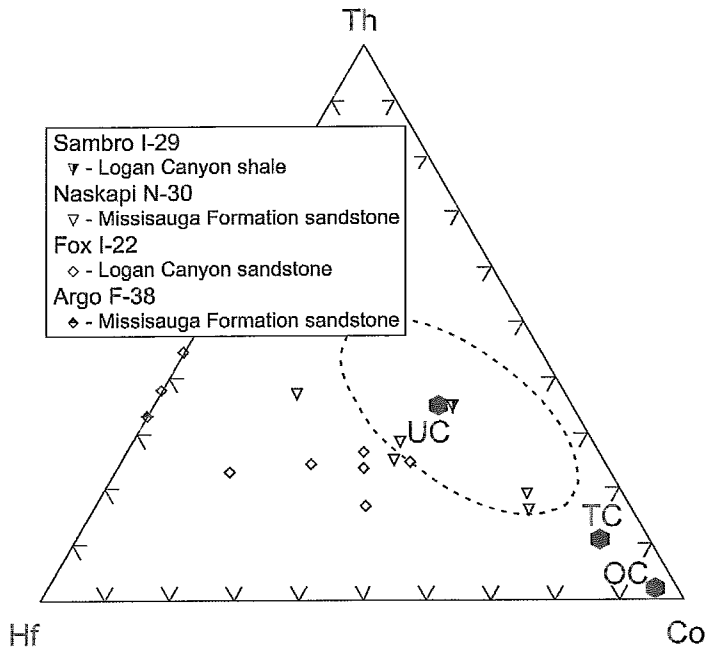

Figure 11: Th - Hf - Co plot. Fields after Taylor and McLennan, 1985. UC = Upper continental crust; TC = bulk continental crust; OC = average oceanic crust.

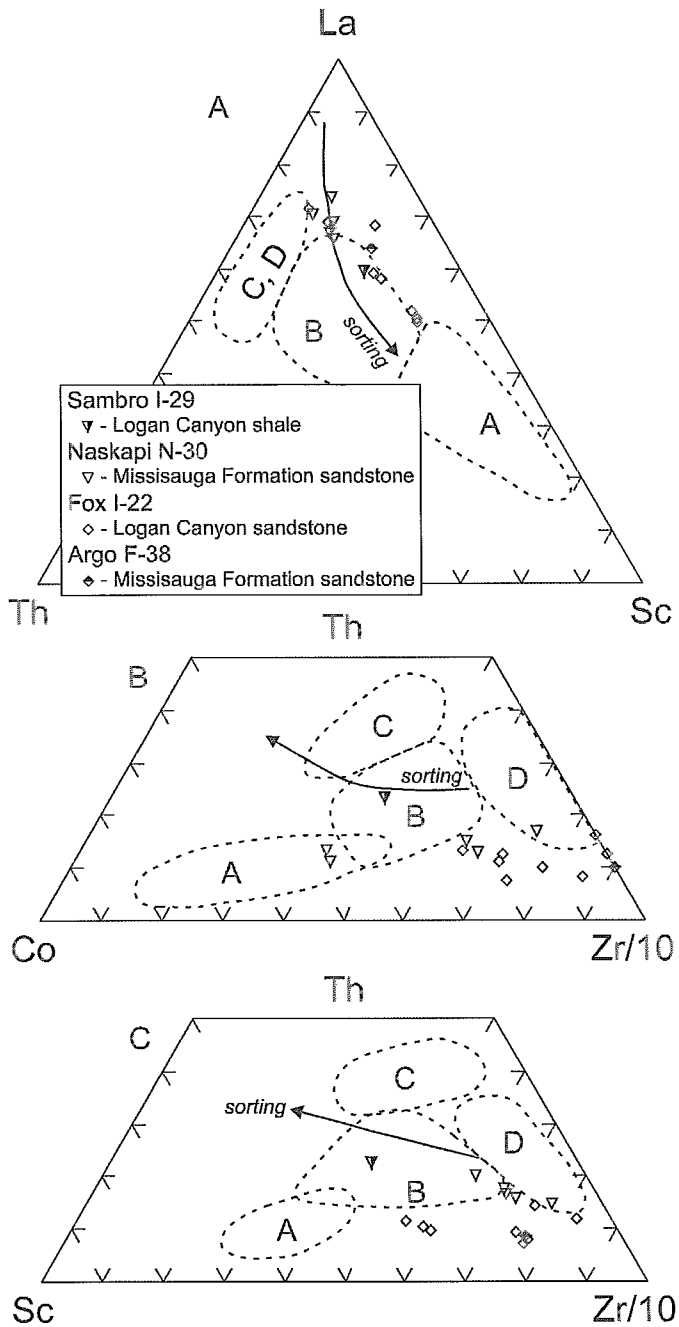

Figure 12 A: La - Th - Sc plot. B: Th - Co - Zr/10 plot. C: Th - Sc - Zr/10 plot. All fields from Bhatia and Crook (1986): A = oceanic island arc; B = continental island arc; C = active continental margin; D = passive margin. Sorting curves from Gu et al. (2002). Same symbols are used in all diagrams.

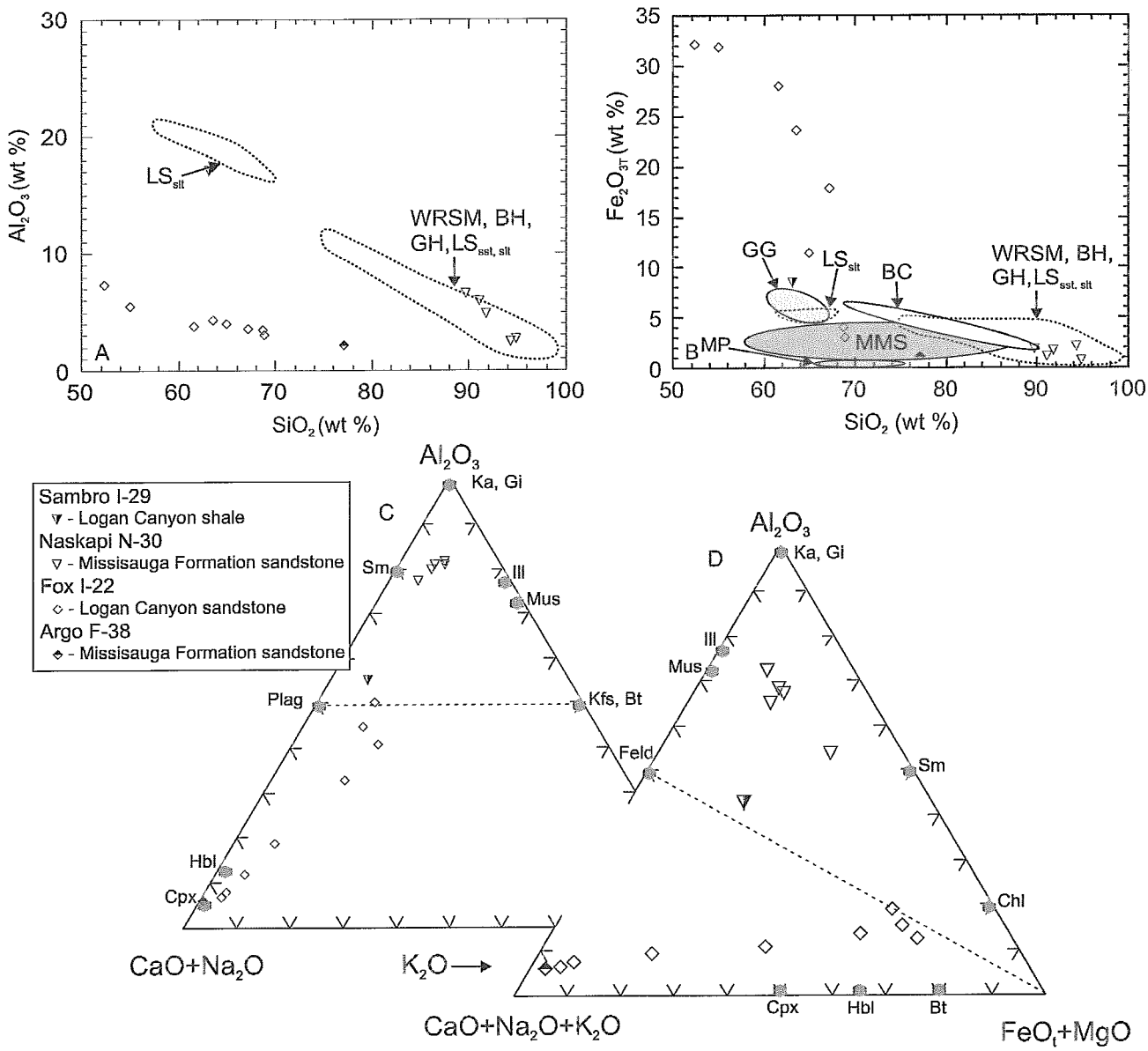

Figure 13: A: Al_2O_3 vs. SiO_2 wt % plot. LS_{sst} = Little Stewiacke sandstone, WRSM = West River St. Marys, BH = Barren Hills, GH = Graham Hill, LS_{slt} = Little Stewiacke siltstone (same for B.) B: Fe_2O_{3t} vs. SiO_2 wt % plot. Fields from Murphy (2000): GG = Neoproterozoic Georgeville Group, BC = Lower Silurian Beechill Cove Formation, MMS = Meguma Group metasedimentary rocks and MP = Meguma granitoid plutons. C: Al_2O_3 - $CaO+Na_2O$ - K_2O ternary plot and D: Al_2O_3 - $CaO+Na_2O+K_2O$ - FeO_t+MgO molar proportions (after Murphy, 2000; Nesbitt and Young, 1996; Nesbitt et al., 1995). ● mineral field abbreviations: Cpx = clinopyroxene, Hbl = hornblende, Bt = biotite, Chl = chlorite, Sm = smectite, Ka = kaolinite, Gi = gibbsite, Ill = illite, Mus = muscovite, Feld = feldspars, Kfs = K-feldspar, Plag = plagioclase. Same symbols used in all plots.

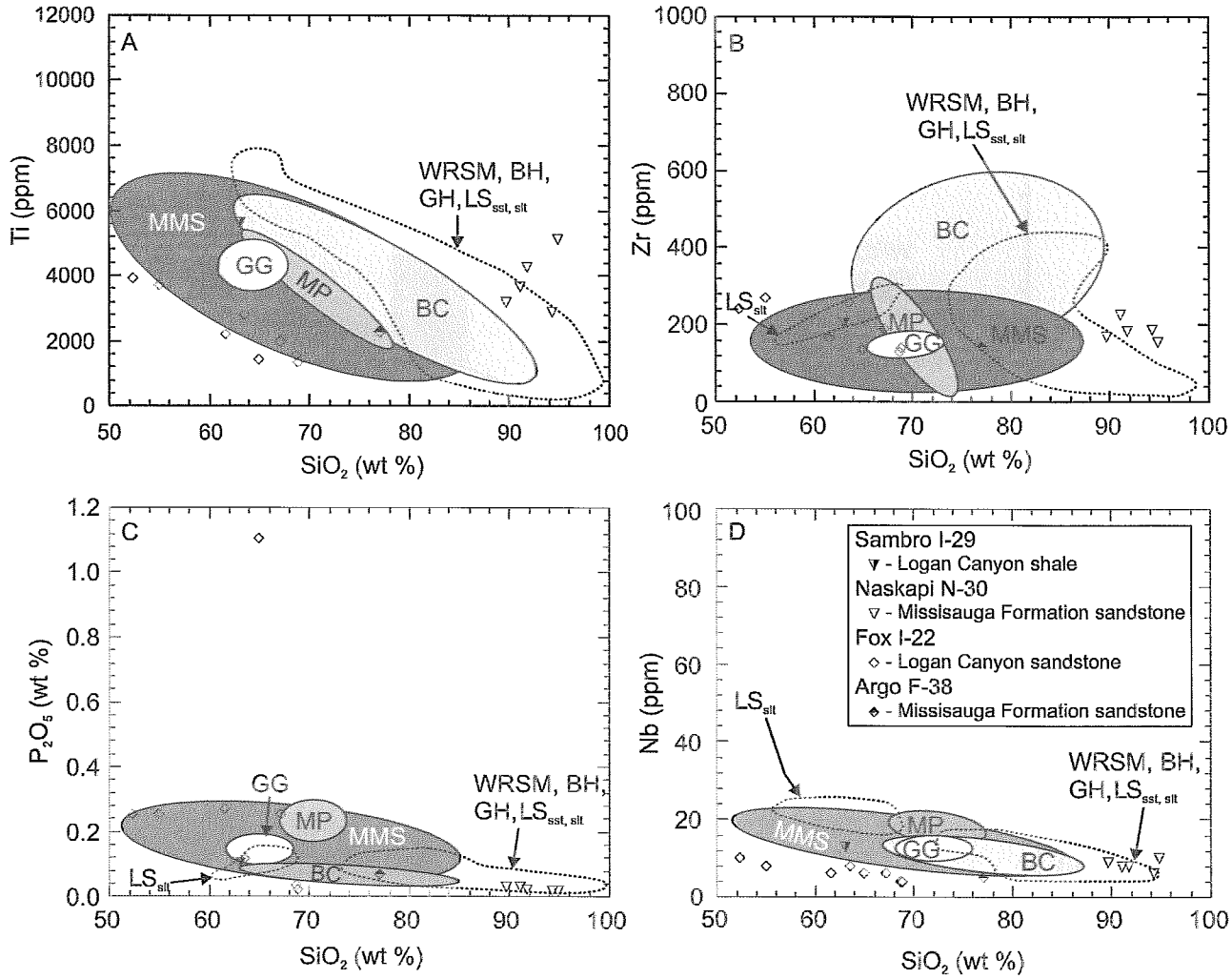

Figure 14: Selected Harker diagrams of major and trace elements. Fields are modified from Murphy (2000). A: Ti vs. SiO_2. B: Zr vs. SiO_2. LS_{sst} = Little Stewiacke sandstone, WRSM = West River St. Marys, BH = Barren Hills, GH = Graham Hill, LS_{slt} = Little Stewiacke siltstone (same for all plots). C: P_2O_5 vs SiO_2. D: Nb vs SiO_2. MMS = Meguma Group metasedimentary rocks, MP = Meguma granitoid plutons, BC = Beechill Cove Formation and GG = Georgeville Group. Legend is the same for all plots.

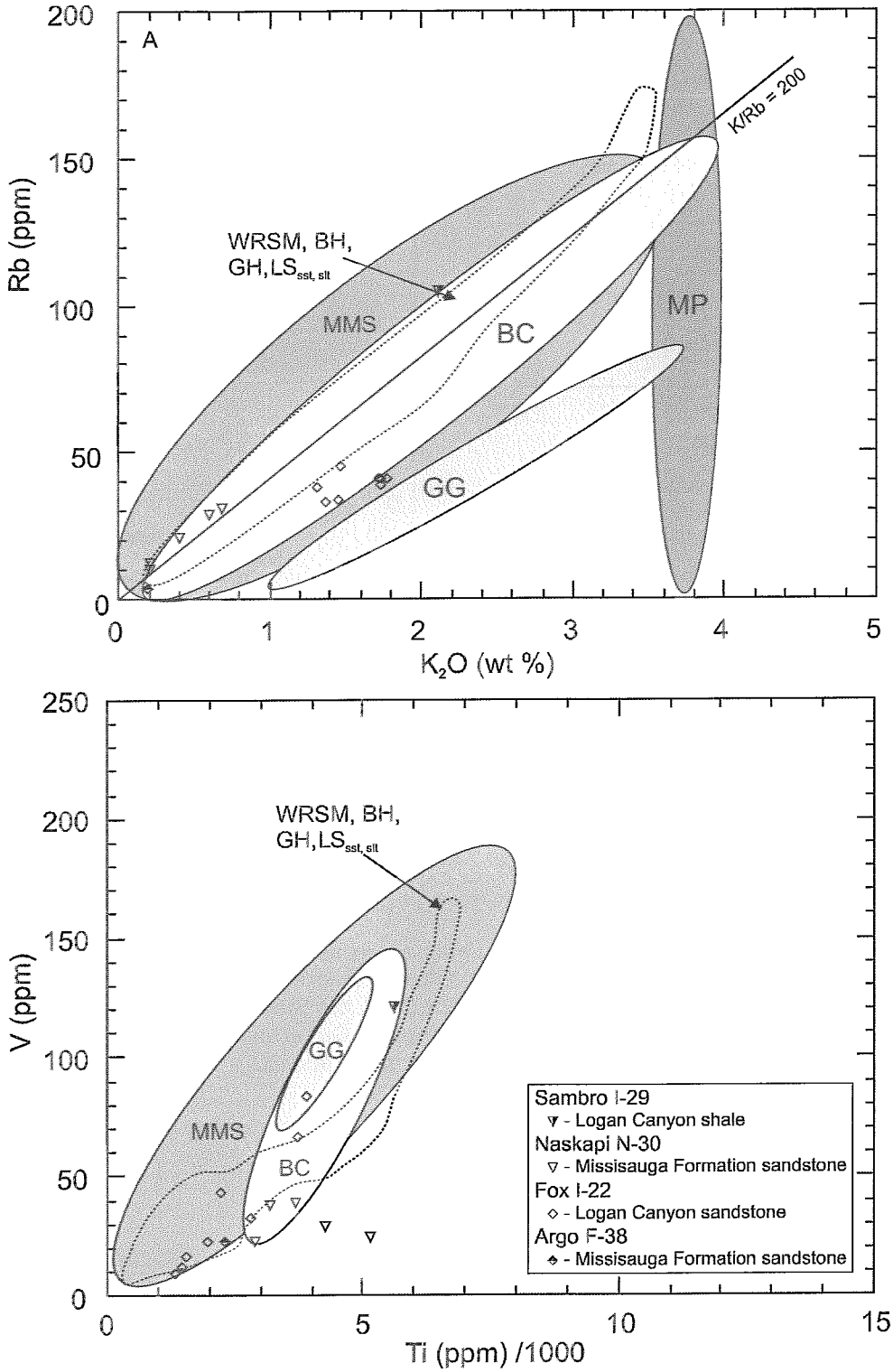

Figure 15: A: Rb vs. K_2O wt % plot. B: V vs. Ti/1000 ppm plot. Fields after Murphy (2000) MMS = Meguma Group metasedimentary rocks; MP = Meguma granitoid plutons; BC = Beechill Cove Formation; GG = Georgeville Group; LS_{sst} = Little Stewiacke sandstone; LS_{slt}, = Little Stewiacke siltstone; BH = Barren Hills; GH = Graham Hill; WRSM = West River St. Marys. Same legend for both plots.

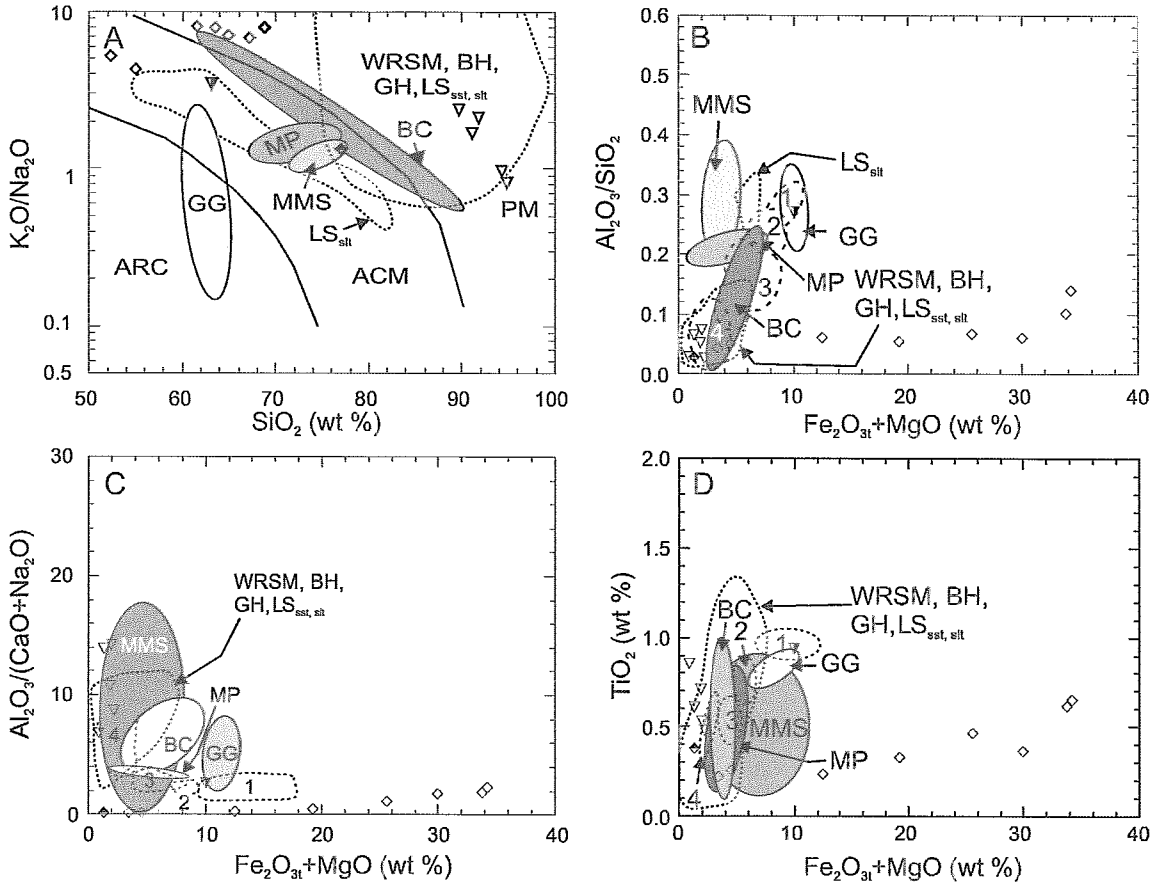

Sambro I-29
▽ - Logan Canyon shale
Naskapi N-30
▽ - Missisauga Formation sandstone
Fox I-22
◇ - Logan Canyon sandstone
Argo F-38
◆ - Missisauga Formation sandstone

Figure 16: A: K_2O/Na_2O vs SiO_2 (wt %) plot. B: Al_2O_3/SiO_2 vs Fe_2O_{3t}+MgO (wt %) plot. C: $Al_2O_3/(CaO+Na_2O)$ vs Fe_2O_{3t}+MgO (wt %) plot. D: TiO_2 vs Fe_2O_{3t}+MgO (wt %) plot. Solid-line fields after Murphy (2000), doted-line fields have been drawn with data from Murphy (2000). MMS = Meguma Group metasedimentary rocks; MP = Meguma granitoid plutons;GG = Georgeville Group; and, BC = Beechill Cove Formation. In A discrimination fields modified from Roser and Korch, 1986: ARC = volcanic arc; ACM = active continental margin, and, PM = passive margin. In B, C and D tectonic setting fields after Bhatia, 1983: 1 = oceanic island arc, 2 = continental island arc, 3 = active continental margin, 4 = passive margin; LS_{sst} = Little Stewiacke sandstone, LS_{slt} = Little Stewiacke siltstone, BH = Barren Hills, GH = Graham Hill, WRSM = West River St. Marys. Legend is the same for all plots.

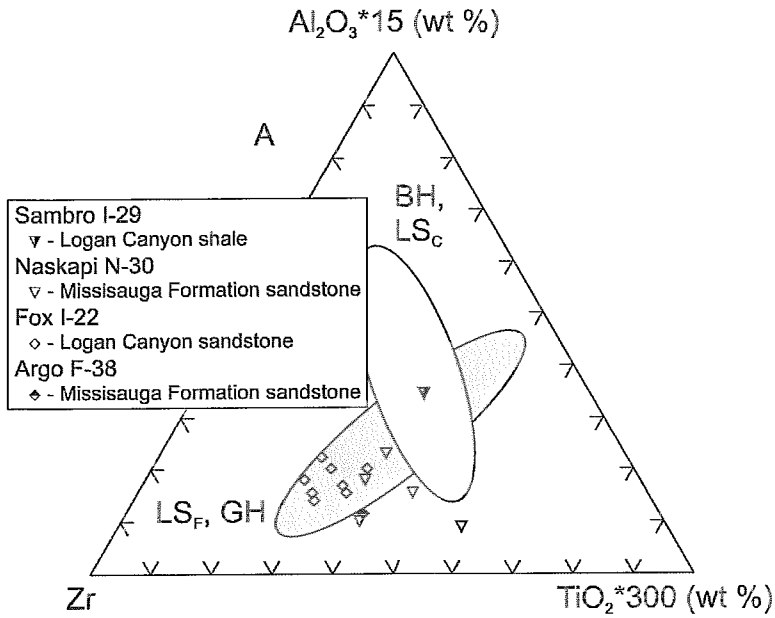

Figure 17: A: Al_2O_3*15 (wt %) - Zr (ppm) - TiO_2*300 (wt %) plot after Garcia et al. (1994) and La Flèche and Camiré (1995) comparing the fine-grained Little Stewiacke (LS_F) and Graham Hill (GH) rocks (ellipse pointing towards the Zr apex) as well as the coarse-grained Little Stewiacke (LS_C) and Barren Hills (BH) rocks (ellipse pointing towards the Al_2O_3 apex) with the Sambro (I-29), Naskapi (N-30), Fox (I-22) and Argo (F-38) sandstones (modified from Murphy 2000).

Appendix 4.

Geochemical discrimination diagrams from the Peskowesk A-99 and Dauntless D-35 wells.

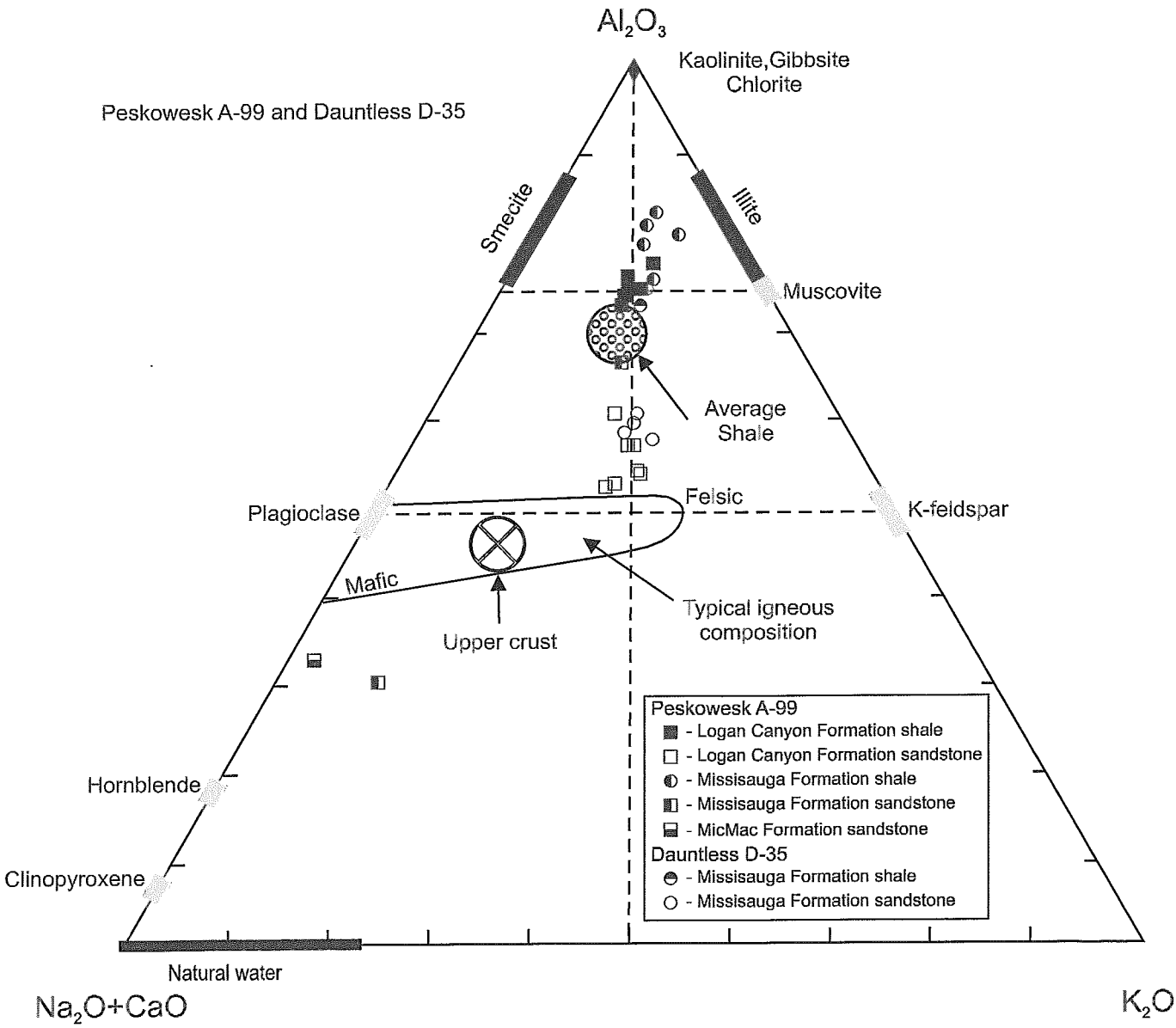

Figure 1: Ternary plot of molecular proportions of Al_2O_3 - Na_2O+CaO - K_2O. Fields from Gu et al. (2002). Idealized clinopyroxene and hornblende compositions from Taylor and MacLennan (1985).

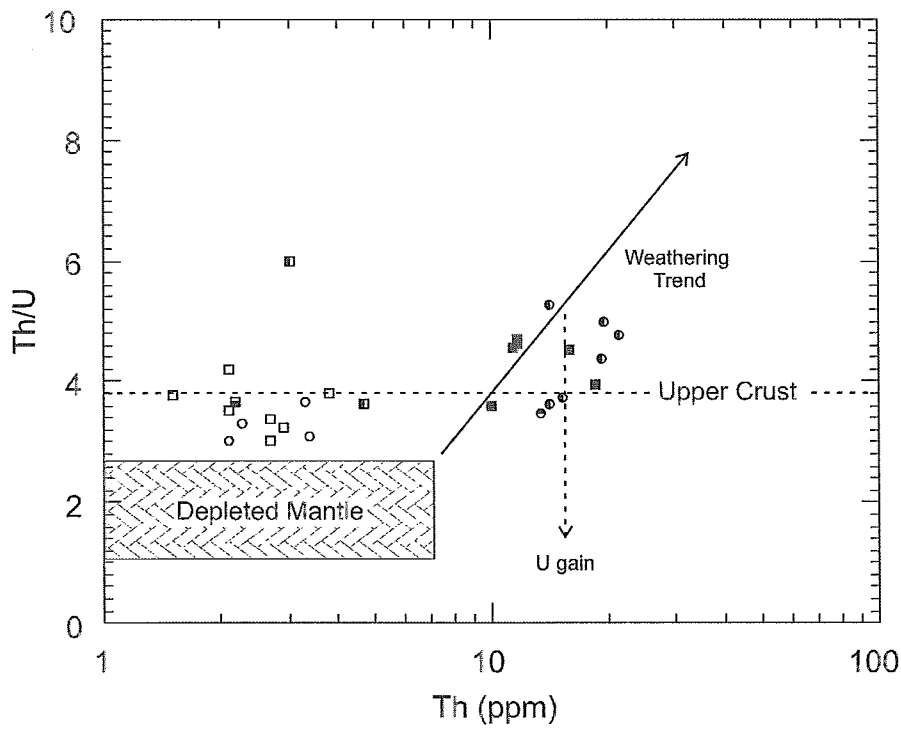

Figure 2: Th/U vs. Th plot. Fields and trends from Gu et al. (2002).

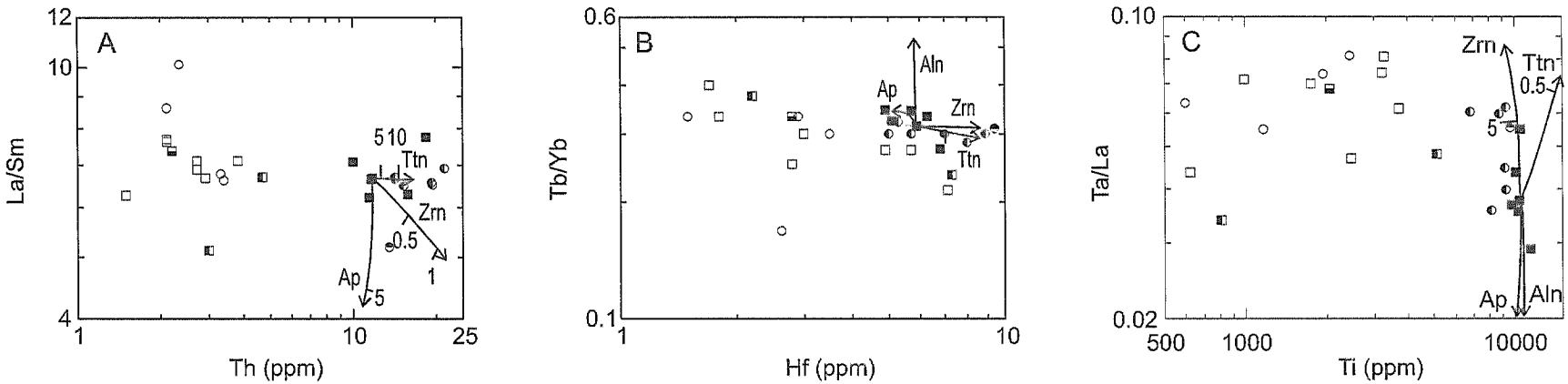

Figure 3: A: La/Sm vs. Th plot. B: Tb/Yb vs. Hf plot. C. Ta/La vs. Ti plot. Heavy mineral accumulation trends modified from Flèche and Camiré (1996).

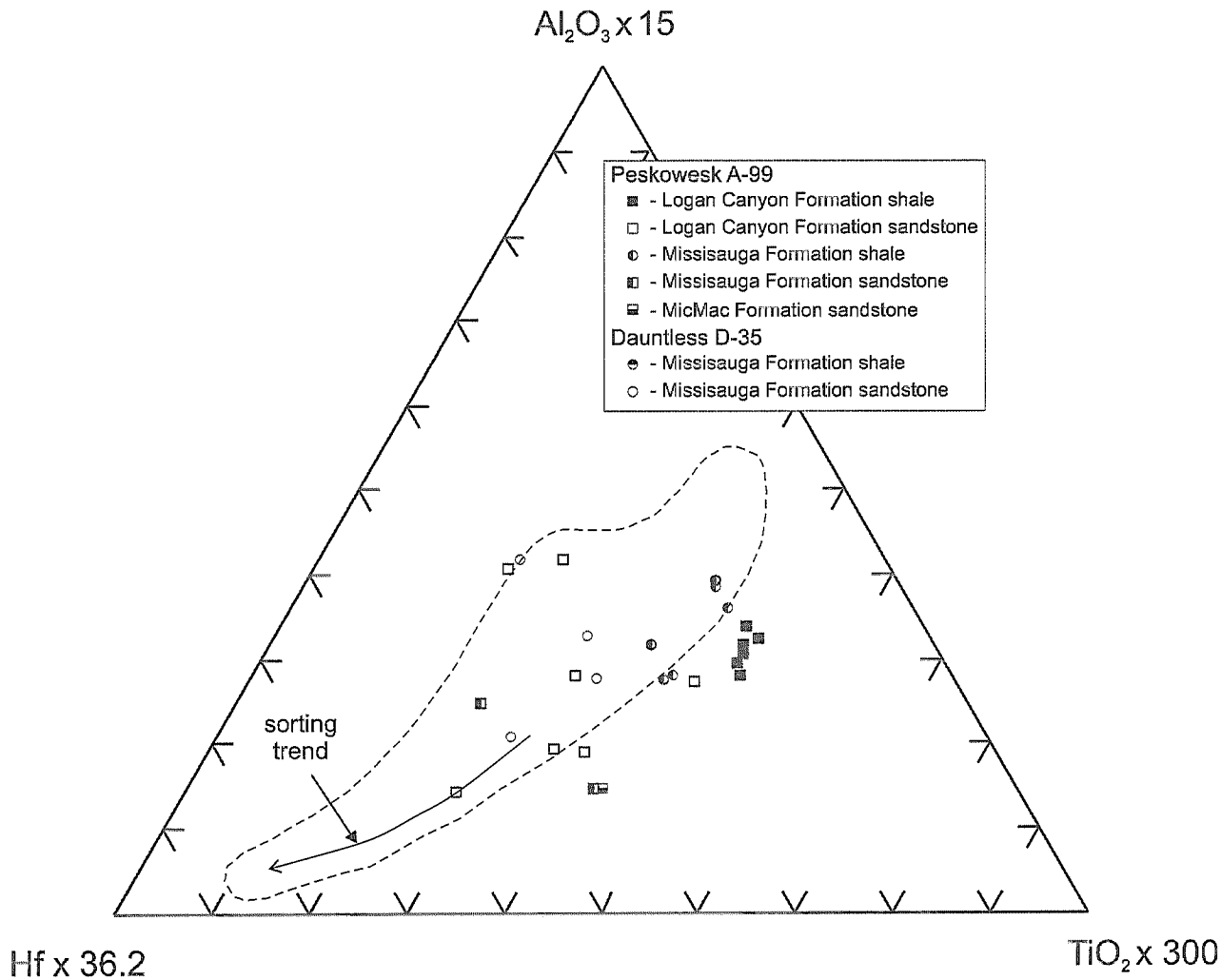

Figure 4: Al_2O_3*15 - Hf*36.2 - TiO_2*300 plot. Field after La Fleche and Camire (1996), and Garcia et al. (1994).

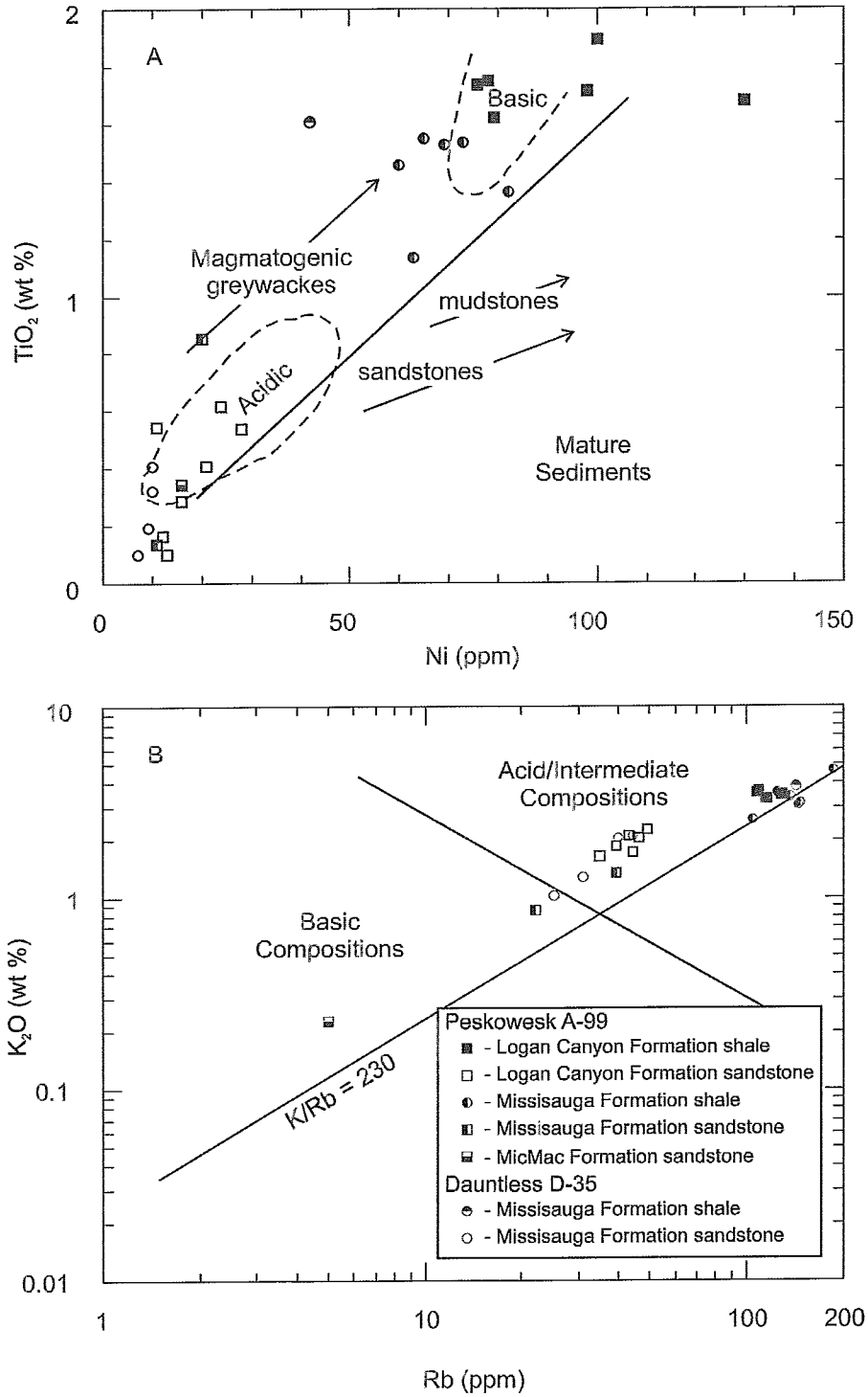

Figure 5 A: TiO_2 vs. Ni plot. Fields and trends after Gu et al., 2002 and Floyd et al. (1989). B: K_2O vs. Rb plot. Fields after Floyd and Leveridge (1987). Samples the same for both plots.

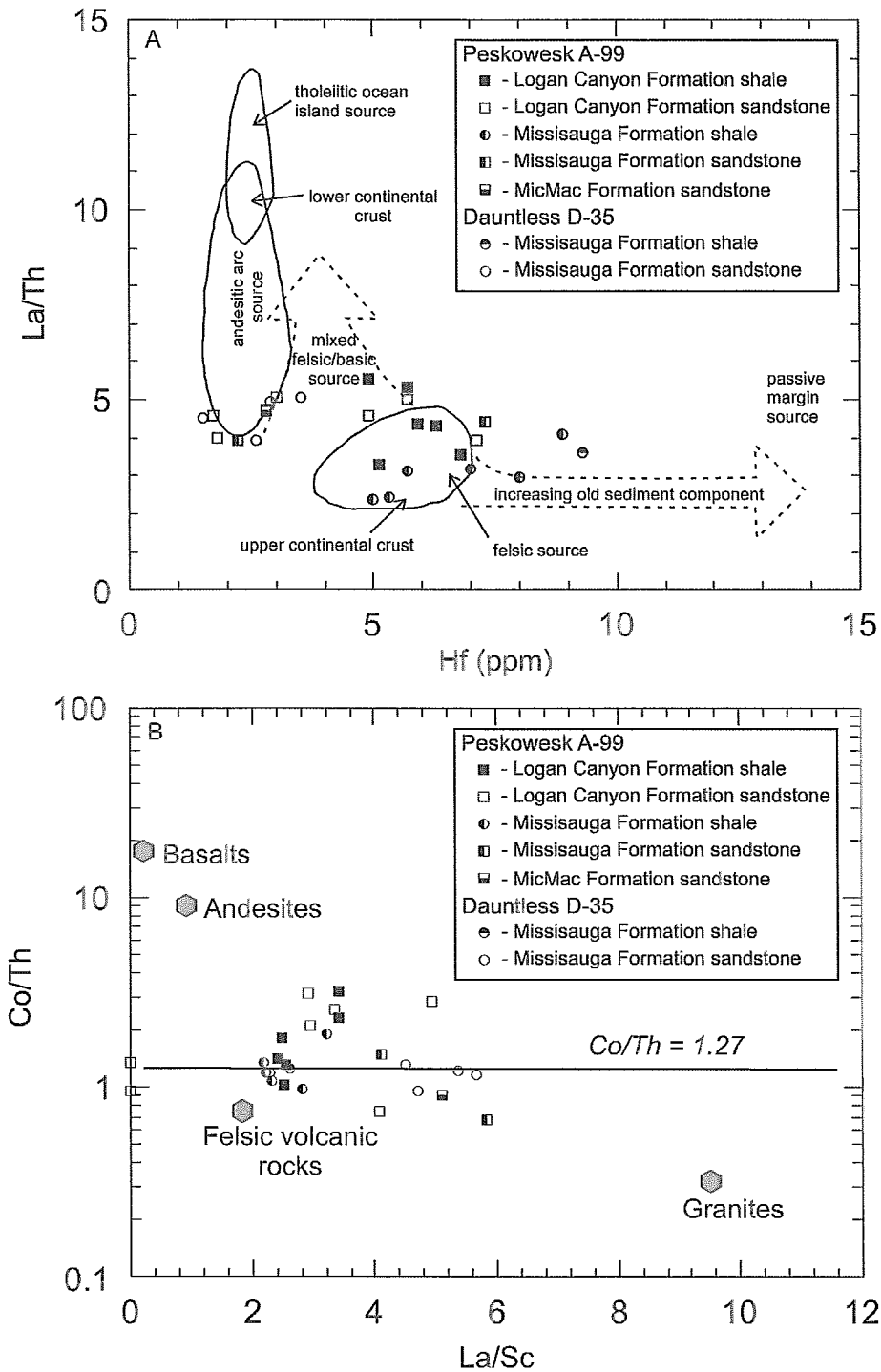

Figure 6 A: La/Th ratio vs. Hf plot. Fields after Floyd and Leveridge (1987), and Gu et. al (2002). B: Co/Th ratio vs. La/Sc ratio plot. Average compositions of igneous rocks from Condie (1993), and Gu et. al (2002).

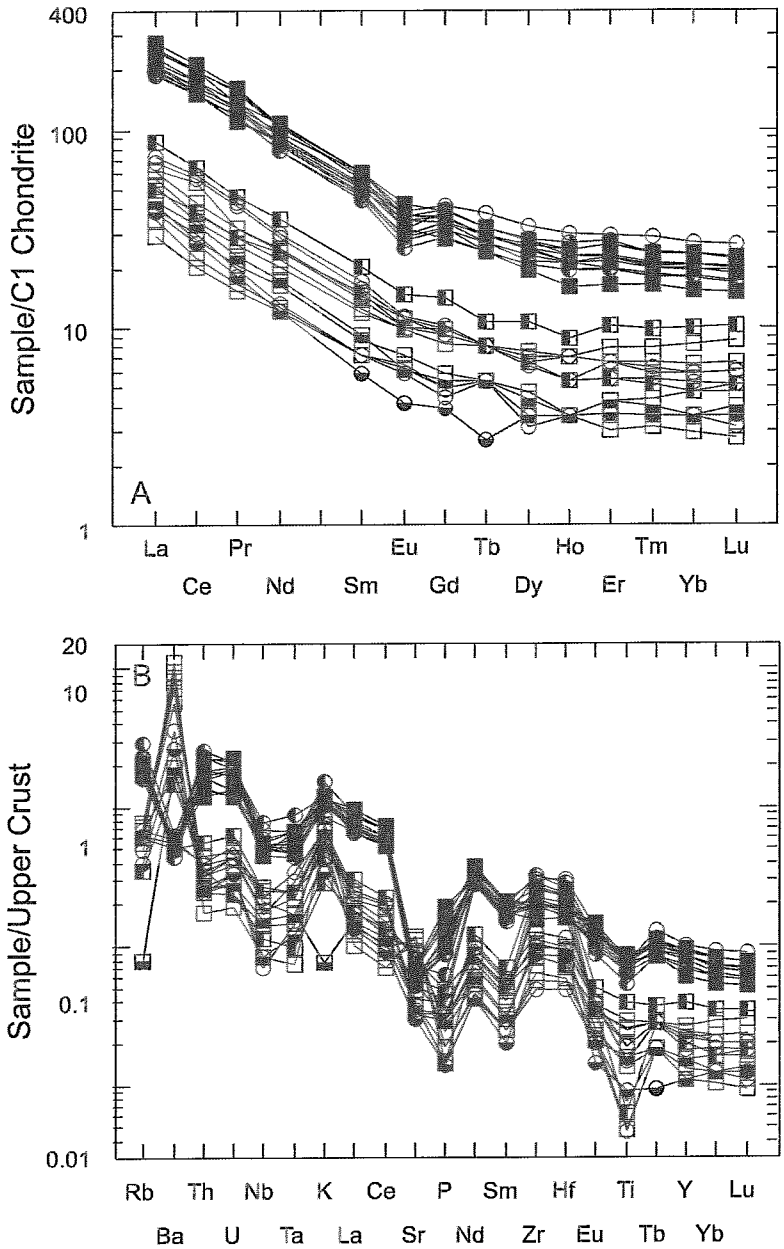

Figure 7A: Rare earth element plot normalized to C1 Chondrite values. B: Multi-element plots normalized to upper crustal values of Taylor and McLennan (1985). Same symbols are used in both plots.

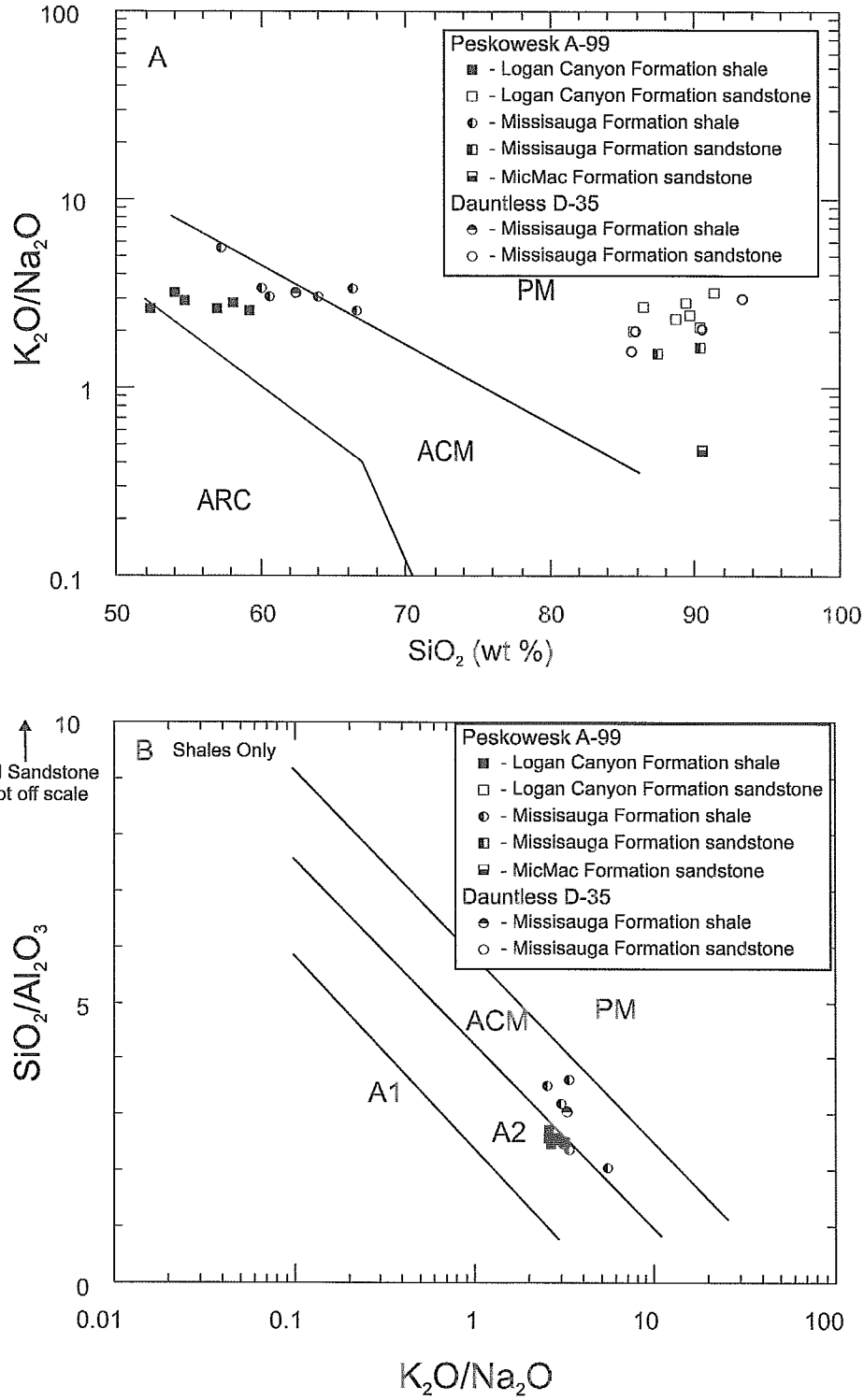

Figure 8 A: K_2O/Na_2O ratio versus SiO_2 plot. Fields after Roser and Korsch (1986): passive margin = PM, active continental margin = ACM and oceanic island arc =ARC. B: SiO_2/Al_2O_3 ratio versus K_2O/Na_2O ratio plot. Fields after Maynard et al. (1982) : passive margin = PM, active continental margin = ACM, arc setting, basaltic and andesitic detritus = A1 and evolved arc setting (felsic plutonic detritus) = A2.

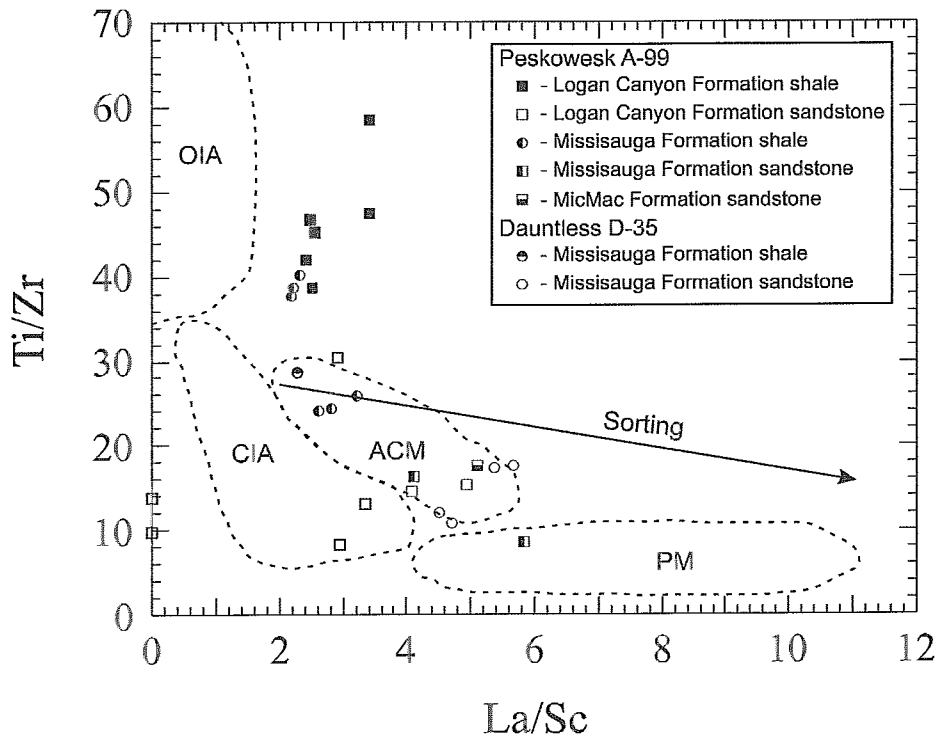

Figure 9: Ti/Zr ratio versus La/Sc ratio plot. Fields after Bhatia and Crook (1986): oceanic island arc = OIA, continental island arc = CIA, active continental margin = ACM and passive margin = PM. The sorting trend after Gu et al., 2002.

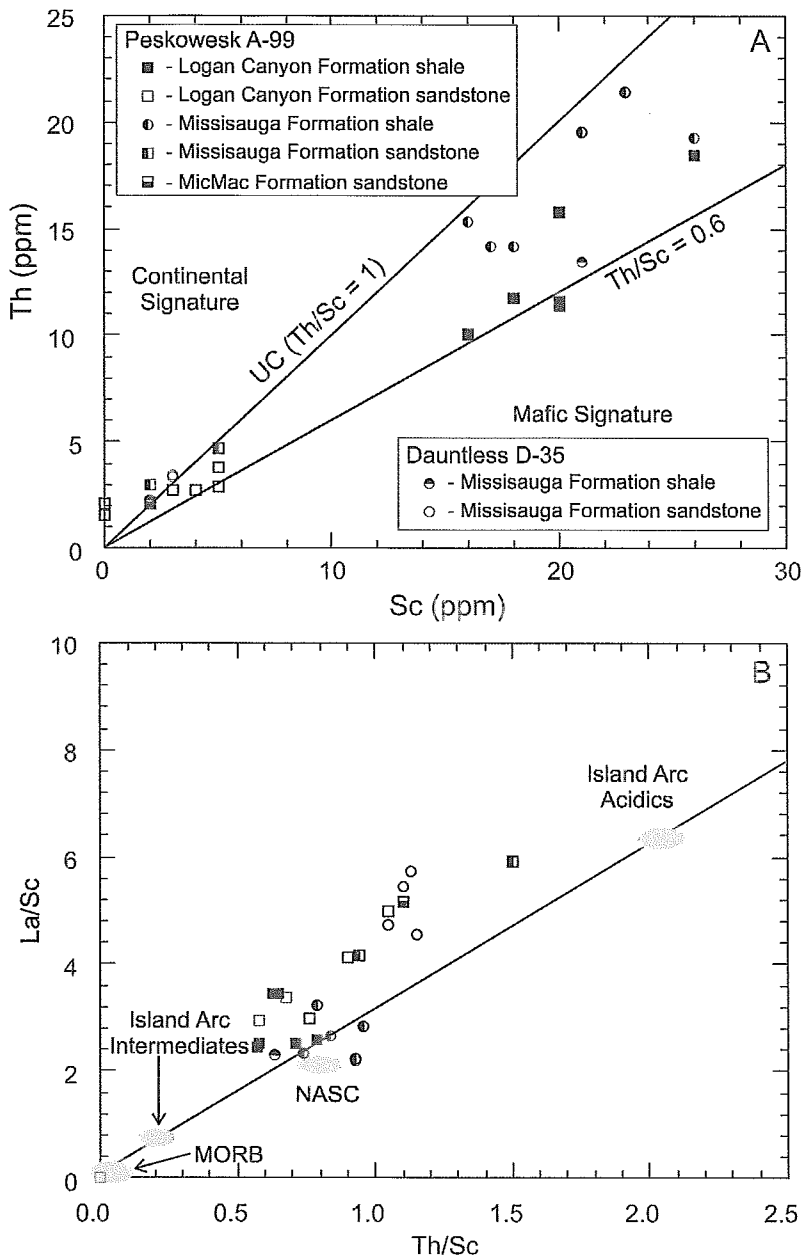

Figure 10A: Th vs. Sc plot. Fields and trends from Totten et al. (2000). B: La/Sc vs. Th/Sc ratio plot. Fields from Totten et al. (2000). Values of different igneous rock types and the North American shale composite (NASC) are included for reference (Taylor and McLennan,1985; Sun and McDonough, 1989; Gromet and Silver, 1983). Same symbols are used in both plots.

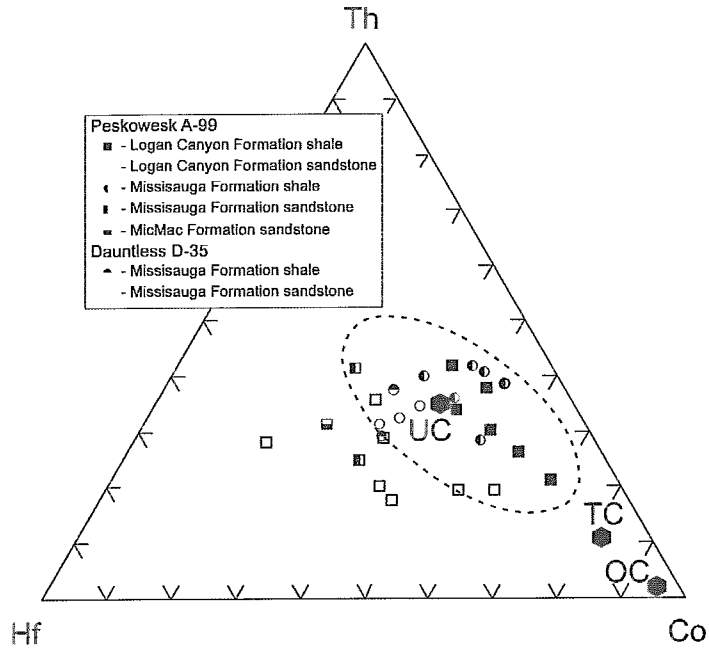

Figure 11: Th - Hf - Co plot. Fields after Taylor and McLennan, 1985. UC = Upper continental crust; TC = bulk continental crust; OC = average oceanic crust.

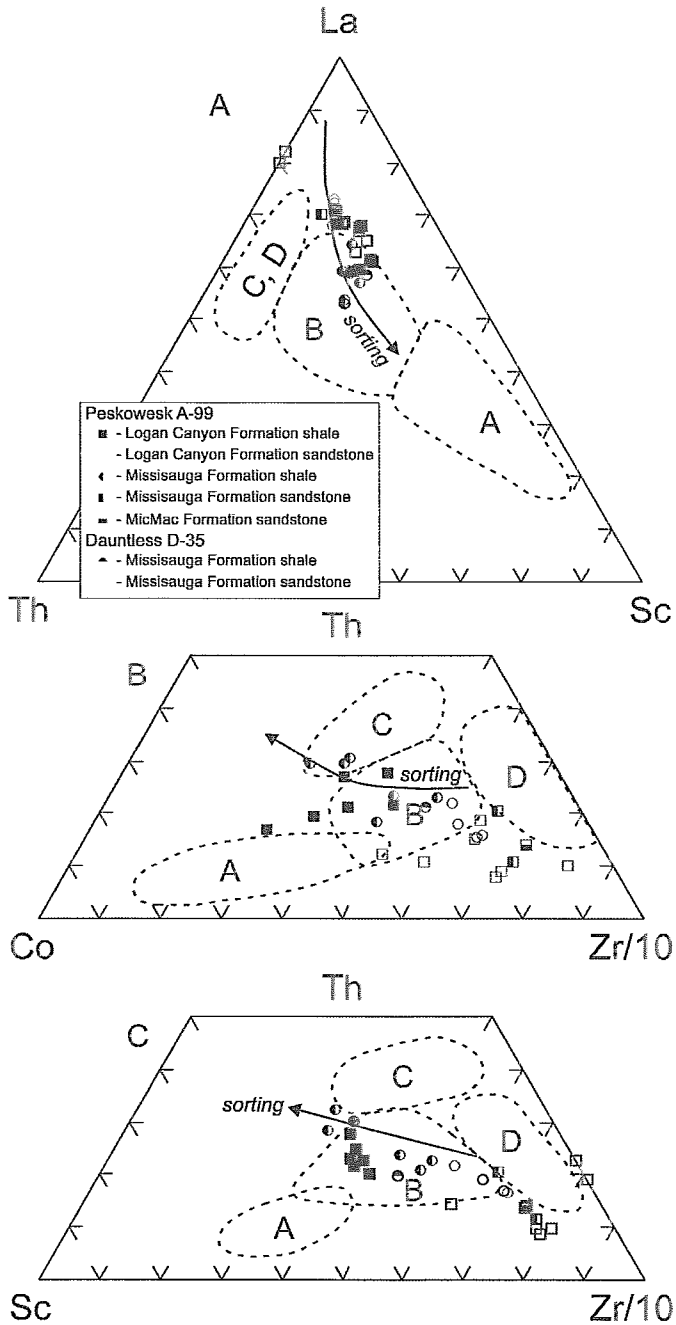

Figure 12 A: La - Th - Sc plot. B: Th - Co - Zr/10 plot. C: Th - Sc - Zr/10 plot. All fields from Bhatia and Crook (1986): A = oceanic island arc; B = continental island arc; C = active continental margin; D = passive margin. Sorting curves from Gu et al., 2002. Same symbols are used in all diagrams.

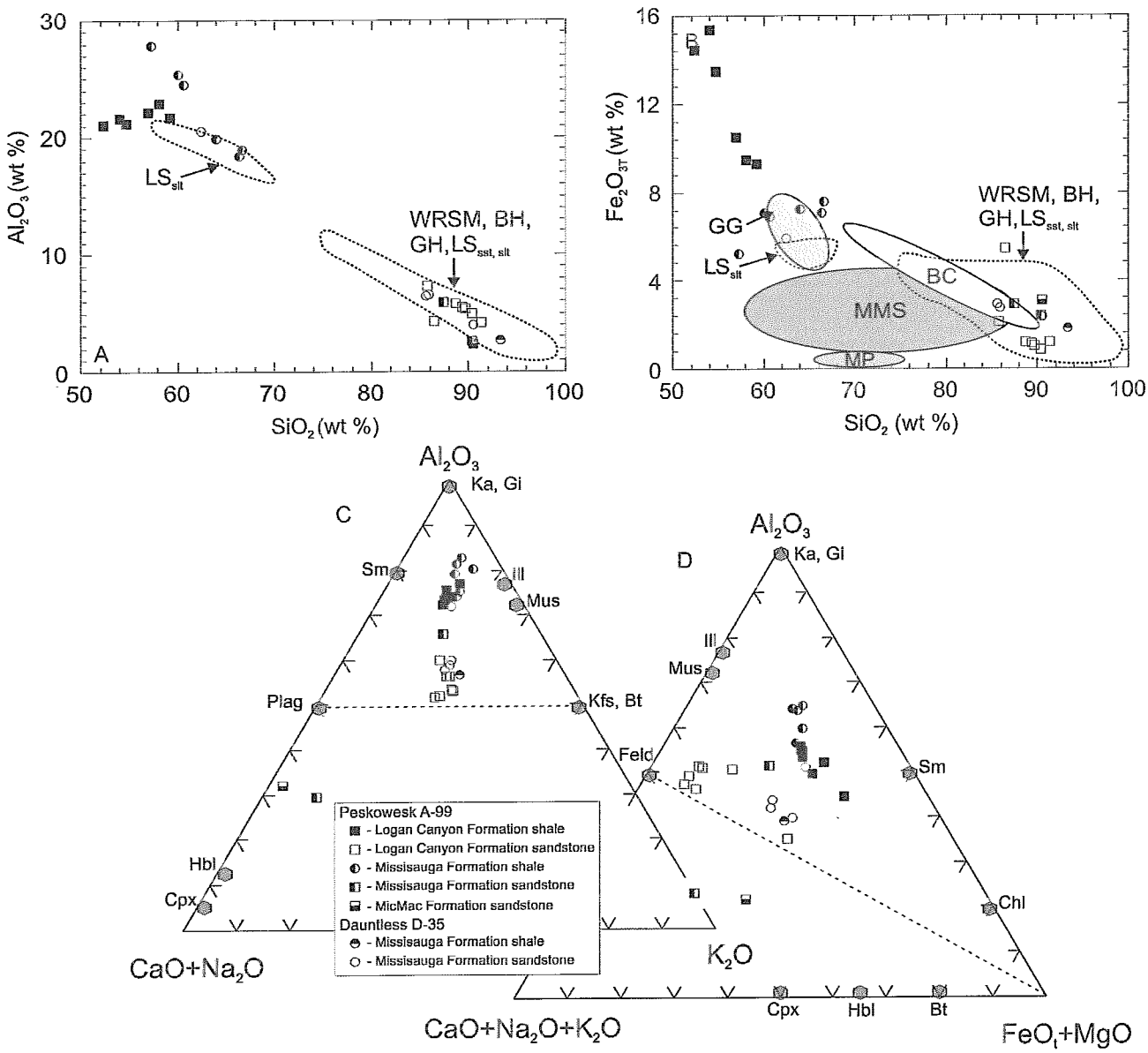

Figure 13: A: Al_2O_3 vs. SiO_2 wt % plot. LS_{sst} = Little Stewiacke sandstone, WRSM = West River St. Marys, BH = Barren Hills, GH = Graham Hill, LS_{slt} = Little Stewiacke siltstone (same for B.) B: Fe_2O_{3t} vs. SiO_2 wt % plot. Fields from Murphy (2000): GG = Neoproterozoic Georgeville Group, BC = Lower Silurian Beechill Cove Formation, MMS = Meguma Group metasedimentary rocks and MP = Meguma granitoid plutons. C: Al_2O_3 - $CaO+Na_2O$ - K_2O ternary plot and D: Al_2O_3 - $CaO+Na_2O+K_2O$ - FeO_t+MgO molar proportions (after Murphy, 2000; Nesbitt and Young, 1996; Nesbitt et al., 1995) ● ● mineral field abbreviations: Cpx = clinopyroxene, Hbl = hornblende, Bt = biotite, Chl = chlorite, Sm = smectite, Ka = kaolinite, Gi = gibbsite, Ill = illite, Mus = muscovite, Feld = feldspars, Kfs = K-feldspar, Plag = plagioclase. Same symbols used in all plots.

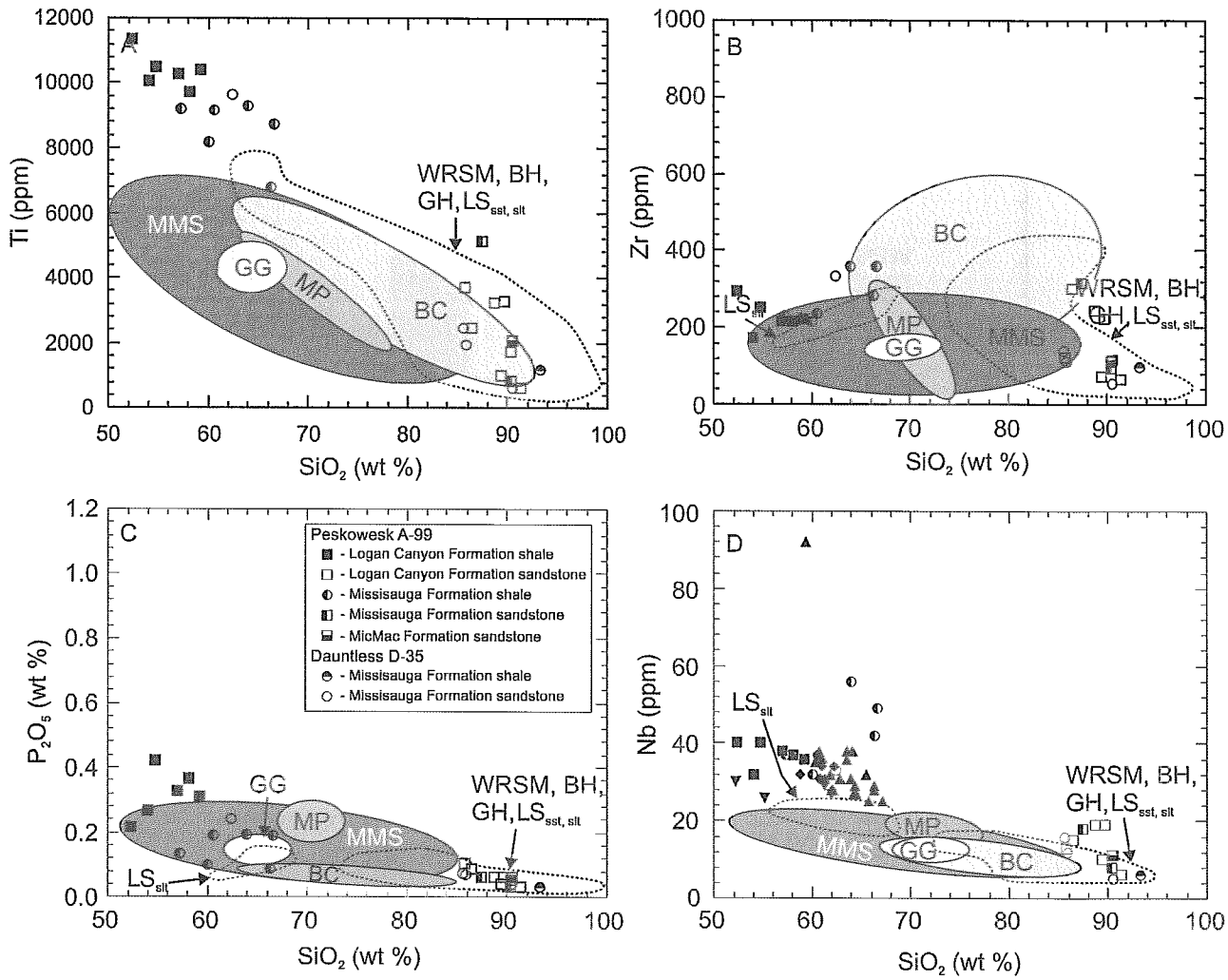

Figure 14: Selected Harker diagrams of major and trace elements. Fields are modified from Murphy (2000). A: Ti vs. SiO_2. B: Zr vs. SiO_2. LS_{sst} = Little Stewiacke sandstone, WRSM = West River St. Marys, BH = Barren Hills, GH = Graham Hill, Ls_{slt} = Little Stewiacke siltstone (same for all plots). C: P_2O_5 vs SiO_2. D: Nb vs SiO_2. MMS = Meguma Group metasedimentary rocks, MP = Meguma granitoid plutons, BC = Beechill Cove Formation and GG = Georgeville Group. Legend is the same for all plots.

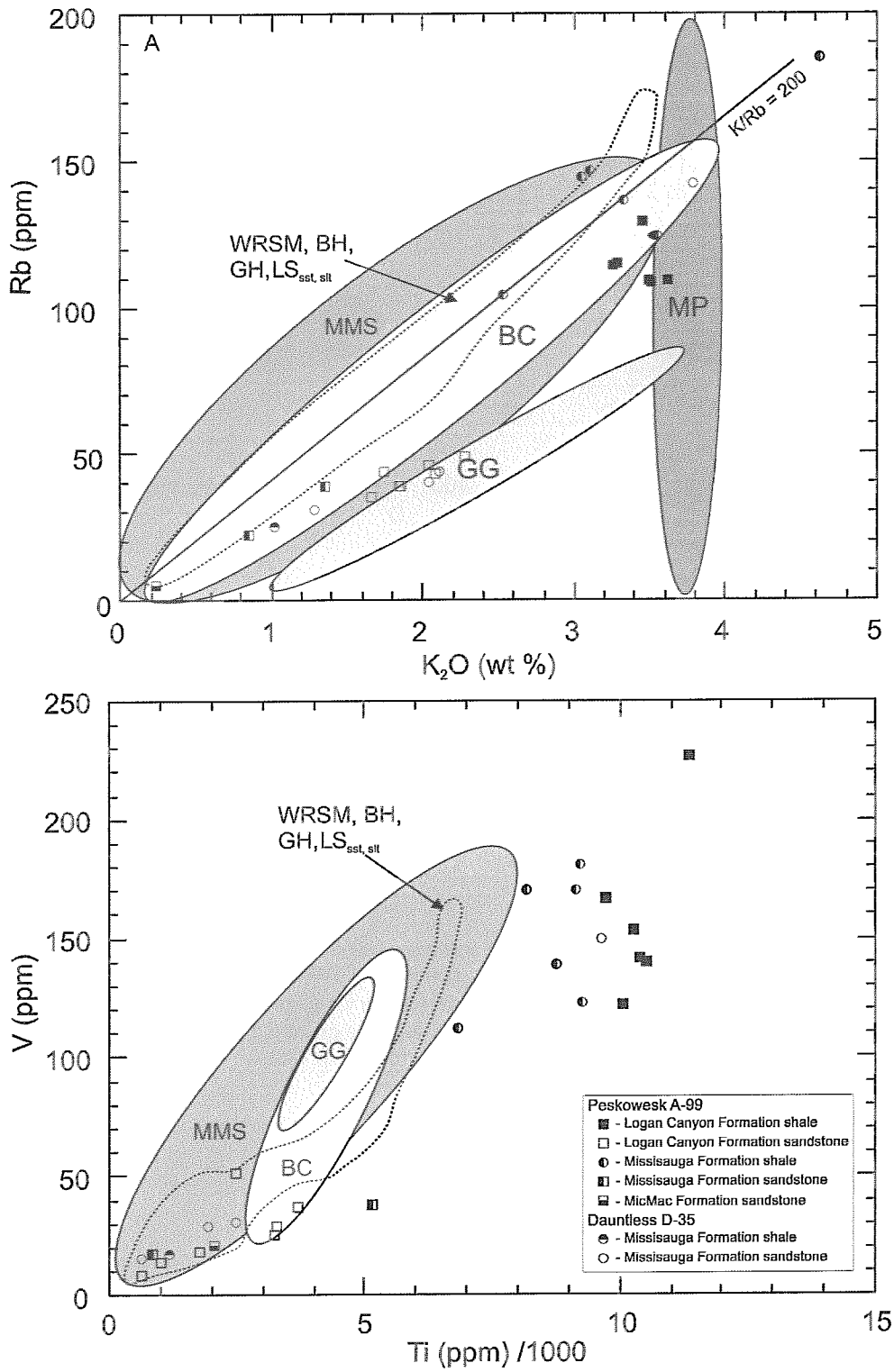

Figure 15: A: Rb vs. K_2O wt % plot. B: V vs. Ti/1000 ppm plot. Fields after Murphy (2000) MMS = Meguma Group metasedimentary rocks; MP = Meguma granitoid plutons; BC = Beechill Cove Formation; GG = Georgeville Group; LS_{sst} = Little Stewiacke sandstone; LS_{slt}, = Little Stewiacke siltstone; BH = Barren Hills; GH = Graham Hill; WRSM = West River St. Marys. Same legend for both plots.

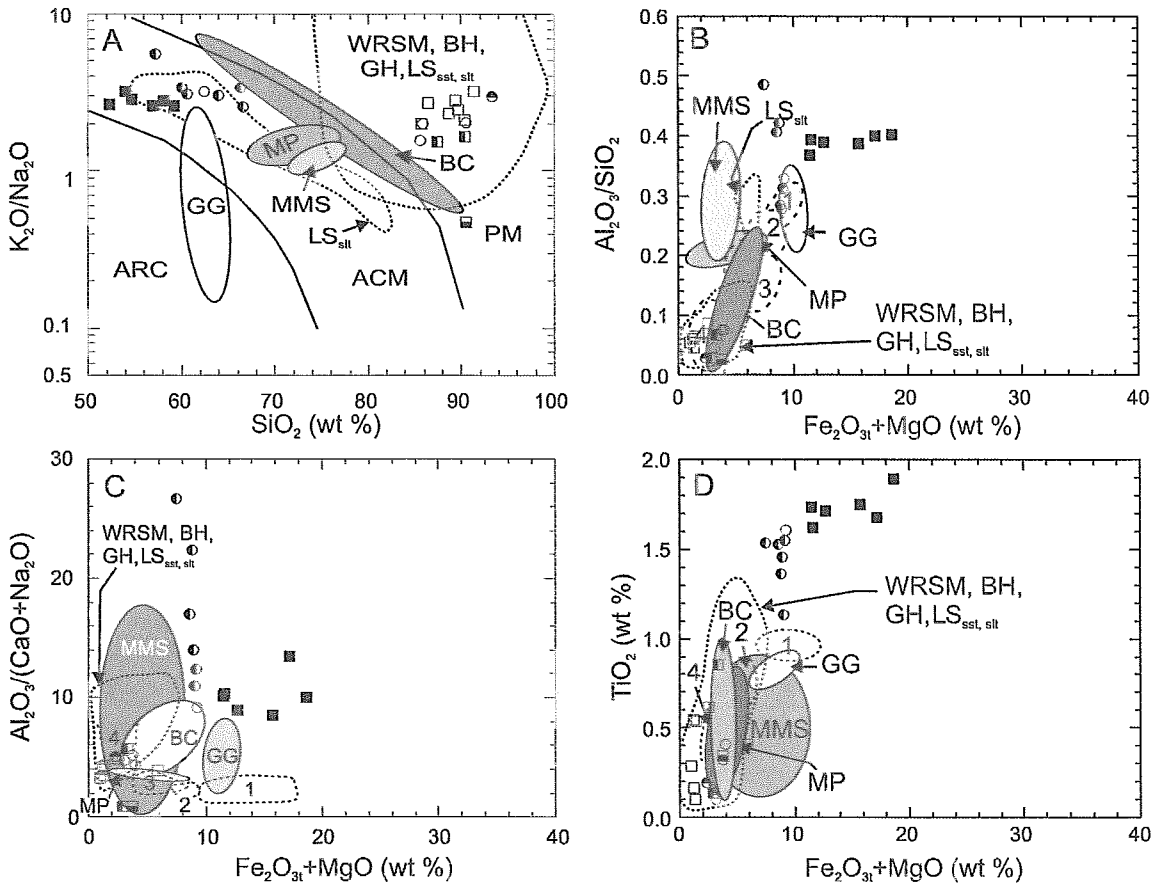

Peskowesk A-99
- Logan Canyon Formation shale
- Logan Canyon Formation sandstone
- Missisauga Formation shale
- Missisauga Formation sandstone
- MicMac Formation sandstone

Dauntless D-35
- Missisauga Formation shale
- Missisauga Formation sandstone

Figure 16: A: K_2O/Na_2O vs SiO_2 (wt %) plot. B: Al_2O_3/SiO_2 vs Fe_2O_{3t}+MgO (wt %) plot. C: $Al_2O_3/(CaO+Na_2O)$ vs Fe_2O_{3t}+MgO (wt %) plot. D: TiO_2 vs Fe_2O_{3t}+MgO (wt %) plot. Solid-line fields after Murphy (2000), doted-line fields have been drawn with data from Murphy (2000). MMS = Meguma Group metasedimentary rocks; MP = Meguma granitoid plutons; GG = Georgeville Group; and, BC = Beechill Cove Formation. In A discrimination fields modifiedfrom Roser and Korch, 1986: ARC = volcanic arc; ACM = active continental margin, and, PM = passive margin. In B, C and D tectonic setting fields after Bhatia, 1983: 1 = oceanic island arc, 2 = continental island arc, 3 = active continental margin, 4 = passive margin; LS_{sst} = Little Stewiacke sandstone, LS_{slt} = Little Stewiacke siltstone, BH = Barren Hills, GH = Graham Hill, WRSM = West River St. Marys. Legend is the same for all plots.

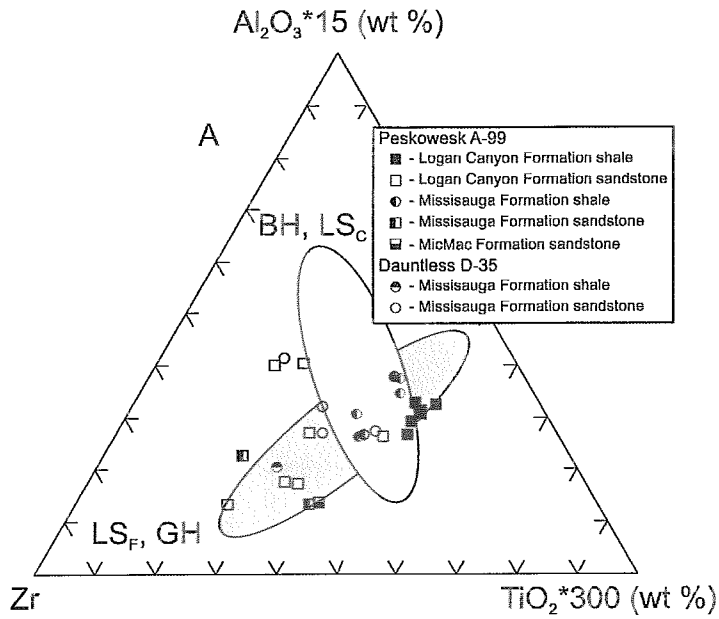

Figure 17: A: Al_2O_3*15 (wt %)- Zr (ppm)-TiO_2*300 (wt %) plot after Garcia et al. (1994) and La Flèche and Camiré (1995) comparing the fine-grained Little Stewiacke (LS_F) and Graham Hill (GH) rocks (ellipse pointing towards the Zr apex) as well as the coarse-grained Little Stewiacke (LS_C) and Barren Hills (BH) rocks (ellipse pointing towards the Al_2O_3 apex) with the Peskowesk (A-99) and Dauntless (D-35) well shales, and sandstones (modified from Murphy, 2000).